

The role of blowing snow in the hydrometeorology of the Mackenzie River Basin

by

Stephen J. Déry

Department of Atmospheric and Oceanic Sciences
McGill University
Montréal, Québec

A thesis submitted to the
Faculty of Graduate Studies and Research
in partial fulfillment of the requirements for the degree of
Doctor of Philosophy

© Stephen J. Déry, 2001

February 2001

Abstract

Despite being ubiquitous in the Mackenzie River Basin (MRB) of Canada, the role of snow in its energy and water budgets are still open to much speculation. This thesis presents a multi-scale analysis of the contribution of blowing snow to the hydrometeorology of the MRB. A climatology of adverse wintertime weather events is first presented and demonstrates that blowing snow events are rare within the forested sections of the MRB but become more frequent in the northern parts of the basin covered by Arctic tundra. It is these areas which experience the largest impacts of blowing snow transport and sublimation due to large-scale processes. To further assess the mesoscale and microscale effects of blowing snow to the northern regions of the MRB, the development of a bulk blowing snow model is then described. The single- and double-moment versions of the PIEKTUK blowing snow model are shown to produce equivalent results as a previous spectral version of the numerical model while operating about 100 times faster. The application of the double-moment PIEKTUK model (PIEKTUK-D) to a Canadian Arctic tundra site near the northern tip of the MRB reveals that blowing snow sublimation depletes ≈ 3 mm snow water equivalent (swe) from the snowpack over a period of 210 days during the winter of 1996/1997 at Trail Valley Creek, Northwest Territories. Various assumptions on the state of the background thermodynamic profiles and their evo-

lution during blowing snow, however, can yield significantly higher ($> 300\%$) rates of sublimation over the same period. PIEKTUK-D is then coupled to the Mesoscale Compressible Community (MC2) model for an interactive simulation of a ground blizzard at Trail Valley Creek. This coupled mesoscale simulation reveals that moistening and cooling of near-surface air associated with blowing snow sublimation is observed but mitigated in part by advective and entrainment processes. Combined, blowing snow sublimation and mass divergence are then shown to remove 1.4 mm swe per day during the Arctic ground blizzard at Trail Valley Creek. Nevertheless, blowing snow contributes to a lesser degree to the surface mass balance of the entire MRB by eroding 0.05 to 0.1 mm swe per year from the snowpack.

Résumé

Malgré son ubiquité dans le bassin du fleuve Mackenzie au Canada, le rôle de la neige dans ses budgets énergétiques et d'eau demeurent toujours des sujets de spéculation. Ce mémoire de thèse présente donc une analyse à échelle multiple de la contribution de la poudrerie dans l'hydrométéorologie du bassin du fleuve Mackenzie. En premier lieu, une climatologie de processus météorologiques hivernaux est présentée et démontre que les épisodes de poudrerie sont plutôt rares dans les régions boisées du bassin mais qu'elles deviennent plus abondantes sur la toundra arctique. Ce sont ces dernières régions qui subissent les effets les plus importants du transport et de la sublimation de la neige dans son déplacement éolien à grande échelle. Pour obtenir une évaluation à méso-échelle et à micro-échelle de la poudrerie dans les régions nordiques telles que celle du fleuve Mackenzie, une description d'un modèle numérique simplifié du processus est donc ensuite élaborée. Il est démontré que les versions à moment unique et double du modèle PIEKTUK reproduisent des solutions comparables à la version spectrale antécédente du modèle numérique mais opère environ 100 fois plus rapidement. L'application du modèle à double moments (PIEKTUK-D) à un site dans l'arctique canadien, près du bassin du fleuve Mackenzie, révèle que la sublimation durant des périodes de poudrerie, érode environ 3 mm équivalent en eau de la couverture neigeuse sur une période de 210 jours pendant

l'hiver de 1996/1997 à Trail Valley Creek, Territoires du Nord-Ouest. Une variété de suppositions au sujet de l'état des profils thermodynamiques ambiants durant l'évolution de la poudrerie peut cependant augmenter les taux de sa sublimation par 300% ou plus au cours de la même période. Le modèle PIEKTUK-D est ensuite uni au modèle à méso-échelle compressible communautaire (MC2) pour entretenir une simulation d'un blizzard à la surface de Trail Valley Creek. Cette simulation à méso-échelle révèle que le refroidissement et l'humidification de l'air dus à la sublimation de la poudrerie sont atténués en partie à cause du processus d'advection et d'entraînement dans la couche limite de l'atmosphère. Il est démontré que le transport éolien de la neige et sa sublimation érodent environ 1.4 mm équivalent en eau durant ce blizzard arctique à Trail Valley Creek. Néanmoins, la poudrerie volatilise tout au plus de 0.05 à 0.1 mm équivalent en eau annuellement de la couverture neigeuse du bassin du fleuve Mackenzie en entier.

Contents

Abstract	ii
Résumé	iv
Contents	vi
List of Figures	xi
List of Tables	xix
Acknowledgements	xxii
Manuscripts and Authorship	xxv
Co-Authored Manuscripts	xxvii
Statement of Originality	xxviii
Prologue	xxx
1 Introduction	1

1.1	Cold season processes in Canada	1
1.2	Past and Current Perspectives	5
1.3	Thesis Outline and Objectives	9
2	Climatology	12
2.1	Presentation of Article 1	12
2.2	Article 1	13
	Déry, S. J. and Yau, M. K., 1999: A climatology of adverse winter-type weather events, <i>J. Geophys. Res.</i> , 104 (D14), 16,657-16,672.	
3	Mass Balance	30
3.1	Presentation of Article 2	30
3.2	Article 2	31
	Déry, S. J. and Yau, M. K., 2001: The large-scale mass balance effects of blowing snow and surface sublimation, submitted to <i>J. Geophys. Res.</i>	
1	Introduction	33
2	Background	35
2.1	Mass Balance	35
2.2	Humidity	37
2.3	Surface Sublimation	38
2.4	Blowing Snow Sublimation	39
2.5	Blowing Snow Transport	40
3	Methodology	41
3.1	Data and Events	41

3.2	Biases and Limitations	42
4	Results	43
5	Sensitivity Tests	53
6	Comparison with Other Studies	62
6.1	Southern Hemisphere	62
6.2	Northern Hemisphere	64
7	Concluding Discussion	66
4	Blowing Snow Modelling	72
4.1	Presentation of Article 3	72
4.2	Article 3	73
	Déry, S. J. and Yau, M. K., 1999: A bulk blowing snow model, <i>Bound.-Layer Meteorol.</i> , 93 , 237-251.	
4.3	Presentation of Article 4	89
4.4	Article 4	89
	Déry, S. J. and Yau, M. K., 2001: Simulation of blowing snow in the Canadian Arctic using a double-moment model, <i>Bound.-Layer Meteorol.</i> , in press.	
5	Mesoscale Modelling	111
5.1	Presentation of Article 5	111
5.2	Article 5	112
	Déry, S. J. and Yau, M. K., 2001: Simulation of an Arctic ground blizzard using a coupled blowing snow-atmosphere model, submitted to <i>J. Hydrometeorol.</i>	

1	Introduction	114
2	Case Overview	120
3	Numerical Models	127
3.1	MC2 model	127
3.2	PIEKTUK model	128
3.3	Coupling of the models	129
3.4	Experimental Design and Strategy	132
3.5	Other Modifications	133
4	Uncoupled Simulation	136
4.1	Comparison with Observations	137
4.2	Precipitation and Humidity	139
4.3	Low-level Jet	142
5	Coupled Simulation	144
5.1	Blowing Snow Fluxes	146
5.2	Basic Meteorological Fields	152
5.3	Surface Energy Budget	154
6	Discussion	156
7	Summary and Conclusions	159
6	Conclusion	169
6.1	Thesis Summary	169
6.2	Suggestions for Future Work	172

Appendix 175

References 178

List of Figures

1.1	Geographical map of the Mackenzie River Basin. (Map produced by Eric Leinberger at the University of British Columbia for the Mackenzie Basin Impact Study [Cohen, 1997a, b]).	3
1.2	Schematic diagram of the components of the water and energy budgets of the Mackenzie River Basin (from Rouse, 2000).	4

Article 1

1	Geographical map of the Mackenzie River Basin. (Map produced by Eric Leinberger at the University of British Columbia for the Mackenzie Basin Impact Study [Cohen, 1997a, b].)	15
2	The contours of (a) the sea level pressure at 4 hPa intervals, (b) the 2-m air temperature at 5°C intervals, and (c) the 10-m wind speed at 2 m s ⁻¹ intervals, at 1200 UTC on March 14, 1993. Shaded areas indicate (a) regions experiencing a blowing snow event, (b) a high-windchill event, and (c) a blizzard event, as inferred from the ERA data. Refer to Table 1 for the locations numbered in Figure 2d.	17
3	Mean annual number of blowing snow events (as defined in the text) for the period 1979-1993 in (a) the Northern Hemisphere and (b) the Southern Hemisphere.	19
4	Mean annual number of high-windchill events (as defined in the text) for the period 1979-1993 in (a) the Northern Hemisphere and (b) the Southern Hemisphere.	19
5	Mean annual number of blizzard events (as defined in the text) for the period 1979-1993 in (a) the Northern Hemisphere and (b) the Southern Hemisphere.	20

6	Monthly (solid lines) and annual (dots) trends in the number of blowing snow events (BSE), high-windchill events (HWE), and blizzard events (BE) for (a) the Northern Hemisphere and (b) the Southern Hemisphere. Yearly values have been normalized by a factor of 12 for comparison with the monthly frequencies of events.	20
7	The positive (negative) monthly anomalies, shown by solid (dashed) lines, of (a) sea level pressure (intervals of 1 hPa), (b) 2-m air temperature (intervals of 1°C), and (c) 10-m wind speed (intervals of 0.5 m s ⁻¹) for February 1993 from the 15-year (1979-1993) means for February. Shaded (cross-hatched) regions indicate areas with positive (negative) deviations of two or more monthly (a) blowing snow, (b) high-windchill, and (c) blizzard events.	21
8	Mean annual frequency of (a) blowing snow, (b) high-windchill, and (c) blizzard events in the Mackenzie River Basin (denoted by the thick line) for the period 1979-1993.	22
9	Composites of the sea level pressure at 4 hPa intervals (a) 24 hours prior to (T-24), (b) during (T00), and (c) 24 hours after (T+24) 11 blowing snow events associated with winds from the SW quadrant near Yellowknife (denoted by "Y"). Shaded areas denote 10-m wind speeds >6 m s ⁻¹ . Positive (negative) deviations from the 15-year climatological mean sea level pressure (hPa) during the events (T00) are shown in Figure 9d in solid (dashed) lines with 2-m air temperature anomalies of >5°C (< -5°C) from the 15-year climatological mean shaded (cross-hatched).	23
10	As in Figure 9 except for 78 blowing snow events associated with winds from the NW quadrant near Yellowknife (denoted by "Y").	24
11	As in Figure 9 except for eight blowing snow events associated with winds from the NE quadrant near Yellowknife (denoted by "Y").	25
12	As in Figure 9 except for 37 blowing snow events associated with winds from the SE quadrant near Yellowknife (denoted by "Y").	26

Article 2

1	The mean relative humidity with respect to ice for the period 1979-1993 when $T_a < 0^\circ\text{C}$ in (a) the Northern Hemisphere and (b) the Southern Hemisphere. In this and subsequent figures, the Mackenzie River Basin is outlined in bold in the Northern Hemisphere.	45
---	--	----

2	The zonally-averaged relative humidity with respect to ice with and without blowing snow for the period 1979-1993 when $T_a < 0^\circ\text{C}$	46
3	The mean annual surface sublimation rate (mm swe) for the period 1979-1993 in (a) the Northern Hemisphere and (b) the Southern Hemisphere.	48
4	The mean annual blowing snow sublimation rate (mm swe) for the period 1979-1993 in (a) the Northern Hemisphere and (b) the Southern Hemisphere.	49
5	The mean annual blowing snow mass transport rate (Mg m^{-1}) for the period 1979-1993 in (a) the Northern Hemisphere and (b) the Southern Hemisphere.	50
6	The mean annual blowing snow mass transport vectors (Mg m^{-1}) for the period 1979-1993 in (a) the Northern Hemisphere and (b) the Southern Hemisphere.	51
7	The mean annual blowing snow divergence rate (mm swe) for the period 1979-1993 in (a) the Northern Hemisphere and (b) the Southern Hemisphere.	54
8	The mean annual total surface sublimation, blowing snow sublimation and divergence rates (mm swe) for the period 1979-1993 in (a) the Northern Hemisphere and (b) the Southern Hemisphere.	55
9	The zonally-averaged surface and blowing snow sublimation rates (mm swe) for the period 1979-1993.	58
10	The global relative frequency distribution of RH_i during blowing snow events for the period 1979-1993. The bin numbers refer to: 1) $\text{RH}_i \leq 0.7$, 2) $0.7 < \text{RH}_i \leq 0.8$, 3) $0.8 < \text{RH}_i \leq 0.9$, 4) $0.9 < \text{RH}_i \leq 1.0$, 5) $1.0 < \text{RH}_i \leq 1.1$, 6) $1.1 < \text{RH}_i \leq 1.2$, 7) $1.2 < \text{RH}_i \leq 1.3$, 8) $\text{RH}_i > 1.3$	58
11	The mean annual blowing snow sublimation rate (mm swe) for the period 1979-1993 in a) the Northern Hemisphere and b) the Southern Hemisphere, allowing for sublimation to occur when $\text{RH}_i > 1.0$	60
12	The mean annual blowing snow sublimation rate (mm swe) for the period 1979-1993 in a) the Northern Hemisphere and b) the Southern Hemisphere when steady-state background thermodynamic profiles are considered.	61

Article 3

- 1 The profiles of blowing snow mixing ratio as predicted by the bulk and spectral versions of the PIEKTUK model 10 minutes after blowing snow initiation for the control experiment. The analytical result without sublimation (“Analysis”) is also shown. 82
- 2 The temporal evolution of (a) the sublimation rate (Q_s) and (b) transport rate (Q_t) of blowing snow, predicted by the bulk and spectral versions of PIEKTUK for the control experiment. 83
- 3 The profiles of ambient air temperature and relative humidity with respect to ice predicted by the bulk and spectral versions of the PIEKTUK model 10 minutes after blowing snow initiation for the control experiment. 85
- 4 The temporal evolution of the sublimation rate Q_s of blowing snow for the control experiment and three sensitivity tests on the lower boundary conditions for humidity, (see text for a description of these tests.) 86

Article 4

- 1 The profiles of a) blowing snow mixing ratio, b) total particle number density and c) mean particle radius predicted by the double-moment and spectral versions of the PIEKTUK model 10 minutes after blowing snow initiation for the control experiment. The steady-state, analytical results without sublimation (“Analysis”) are also shown. In d), the implicit particle distributions within the double-moment scheme are compared to the explicit ones of the spectral model. Thick (thin) lines depict results at $z = 0.1$ m ($z = 2.5$ m). 96
- 2 The profiles of a) ambient air temperature and relative humidity with respect to ice and b) sensible (Q_h) and latent (Q_e) heat fluxes predicted by the double-moment (D.-M.) and spectral versions of the PIEKTUK model 10 minutes after blowing snow initiation for the control experiment. 97
- 3 The profiles of (a) the local and (b) cumulative sublimation rates of blowing snow, predicted by the double-moment and spectral versions of the PIEKTUK model 10 minutes after blowing snow initiation for the control experiment. 98

4	The temporal evolution of the vertically-integrated (a) sublimation rate and (b) transport rate of blowing snow, predicted by the double-moment and spectral versions of PIEKTUK for the control experiment.	99
5	The variation of the normalized sublimation rate Q'_s (a) with ξ for three values of U_{10} and (b) with U_{10} for two values of ξ . The variables are defined in the text.	101
6	Contours of Q'_s (at intervals of 2 mm d ⁻¹ swe) in terms of the 10-m wind speed U_{10} and the thermodynamic quantity ξ (as defined in the text).	102
7	The temporal evolution of half-hourly averaged values of the ambient air temperature (T_a), the relative humidity with respect to ice (RH_i), the 10-m wind speed (U_{10}), and the modelled sublimation (Q_s) and transport (Q_t) rates of blowing snow from 11 September 1996 to 8 April 1997 at Trail Valley Creek, Northwest Territories.	104
8	Comparison of the parametrized and modelled sublimation rates of blowing snow for Trail Valley Creek, Northwest Territories, during the winter of 1996/1997.	106

Article 5

1	Geographical map of the Mackenzie River Basin (MRB) and surrounding area of interest. The orography is depicted by shading at elevations of 0.5, 1.0, 2.0 and 3.0 km above sea level. Note that the following abbreviations are used: Tuktoyaktuk Peninsula (TP), Northwest Territories (NWT), Nunavut Territory (NVT), Yukon Territory (YT), Alaska (AK), Banks Island (BI) and Victoria Island (VI).	117
2	Close-up of the Trail Valley Creek (TVC) area. The orography is shaded at intervals of 50 m.	118
3	CMC analyses of sea-level pressure (hPa) at 1200 UTC on a) 16 November 1996, b) 17 November 1996 and c) 18 November 1996. The shading indicates areas where blizzard conditions are inferred from the analyses.	121
4	CMC analyses of 500 hPa geopotential heights (dam) at 1200 UTC on a) 16 November 1996, b) 17 November 1996 and c) 18 November 1996.	122

5	Infrared satellite imagery at 1655 UTC on 16 November 1996 over the area of interest. In the top panel, the image has a resolution of 4 km whereas in the bottom panel, the image has a 1 km resolution, both centred over Inuvik, NWT.	124
6	As in Figure 5 at 1125 UTC on 17 November 1996.	125
7	As in Figure 5 at 1114 UTC on 18 November 1996.	126
8	Distribution of grid points within the vertical domains of the MC2 (dots) and PIEKTUK-D (open circles) models.	130
9	a) The CMC snow depth (in mm swe) analysis valid at 1200 UTC on 16 November 1996, b) the aerodynamic roughness length for bare ground z_{0b} (m), c) the factor p and d) the ratio of z_{0b}/z_0 over the entire horizontal simulation domain.	135
10	The simulated sea-level pressure (hPa) at 1200 UTC on a) 17 November 1996 and b) 18 November 1996 from the UNC experiment. The shading indicates areas where blizzard conditions are inferred.	138
11	Simulated 500 hPa geopotential heights (dam) at 1200 UTC on a) 17 November 1996 and b) 18 November 1996 from the UNC experiment.	138
12	The observed and simulated conditions of air temperature (T_a), relative humidity with respect to ice (RH_i), 10-m wind speed (U_{10}) for Trail Valley Creek, NWT beginning at 1200 UTC on 16 November 1996 (JD 321.5) and ending at 1200 UTC on 18 November 1996 (JD 323.5).	140
13	The observed (solid lines) and simulated (dashed lines) upper air profiles of temperature (thick lines) and frostpoint temperature (thin lines) for Inuvik, NWT, at 1200 UTC on a) 17 and b) 18 November 1996. Profiles of the observed and simulated wind speeds and directions are shown along the vertical solid and dashed lines, respectively. Note here that a half (full) barb denotes wind speeds of 5 m s^{-1} (10 m s^{-1}).	141
14	a) The 48-h cumulative precipitation (mm) and b) the mean relative humidity (%) at $z = 449 \text{ m}$ for the UNC simulation.	143

15	Time-height cross sections of a) wind speed in m s^{-1} , b) air temperature in $^{\circ}\text{C}$, c) relative humidity expressed as a percentage and d) potential temperature in K at Trail Valley Creek, NWT, from 1200 UTC on 16 November 1996 (JD 321.5) to 1200 UTC on 18 November 1996 (JD 323.5). Note that relative humidities are with respect to water when $T_a > 0^{\circ}\text{C}$ and with respect to ice when $T_a < 0^{\circ}\text{C}$	145
16	a) The contours and vectors of blowing snow transport (Mg m^{-1}) and b) the associated mass divergence (mm swe) of blowing snow at the end of the CPL experiment.	148
17	a) The total sublimation of blowing snow (mm swe) and b) the combined effects of blowing snow divergence and sublimation at the end of the CPL experiment.	149
18	Hourly values of the observed and simulated surface air temperature (T_a), the surface relative humidity with respect to ice (RH_i), the 10-m wind speed (U_{10}), and the simulated sublimation (Q_s) and transport (Q_t) rates of blowing snow from 1200 UTC on 16 November 1996 (JD 321.5) to 1200 UTC on 18 November 1996 (JD 322.5) at Trail Valley Creek, NWT. The data are taken from observations (OBS), the uncoupled (UNC) and coupled (CPL) mesoscale simulations and the stand-alone (STA) blowing snow experiment.	151
19	The difference in the 48-h simulated a) surface air temperatures ($^{\circ}\text{C}$), b) surface relative humidities (%), c) sea-level pressure (hPa) and d) precipitation accumulation (mm) between the CPL and UNC experiments.	153
20	Temporal evolution of the observed (OBS) and simulated (UNC) surface pressure tendencies ($\partial P/\partial t$), 10-m wind directions (ϕ) and speeds (U_{10}), as well as the simulated surface Froude (Fr) and Richardson (Ri) numbers from 1200 UTC on 16 November 1996 (JD 321.5) to 1200 UTC on 18 November 1996 (JD 322.5) at Trail Valley Creek, NWT.	158
21	Schematic diagram of conditions for Trail Valley Creek at 1000 UTC on 17 November 1996 (JD 322.4). The elevation of the terrain above mean sea-level is plotted with negative distances upwind of Trail Valley Creek.	160

Appendix

A1 The observed values of relative humidity with respect to water (RH_w) versus temperature (T_a) during the winter of 1996/1997 at Trail Valley Creek, NWT. 176

A2 The observed values of relative humidity with respect to ice (RH_i) versus temperature (T_a) during the winter of 1996/1997 at Trail Valley Creek, NWT. 176

List of Tables

1.1	The vertically integrated sublimation rate of blowing snow (Q_s) for varying wind speeds predicted by the PBSM and PIEKTUK models 1 km downwind from the initiation of transport. The data are taken from Déry et al. (1998).	8
-----	---	---

Article 1

1	Surface Observations of Sea Level Pressure (SLP), 2-m Air Temperature (T_a), 10-m Wind Speed (U_{10}), Windchill (WC), and Precipitation and/or Weather Type (PWT) Recorded at Selected Canadian Meteorological Stations at 1200 UTC on March 14, 1993	18
2	The Observed Mean Annual 2-m Air Temperature $\overline{T_a}$ and 10-m Wind Speed $\overline{U_{10}}$ at Selected High-Latitude Climatological Stations Compared to the Values Obtained From the ERA Data	18
3	Average Annual Number of Blowing Snow Events (BSE), High-Windchill Events (HWE) and Blizzard Events (BE) in the Northern Hemisphere (NH), the Southern Hemisphere (SH), and the Globe for the Period 1979-1993	21

Article 2

1	The areally-averaged contribution of surface sublimation (Q_{surf}), blowing snow sublimation (Q_s) and divergence (D) to the surface mass balance within latitudinal bands of 10° in the Southern and Northern Hemispheres, as well as for Antarctica (ANT) and the Mackenzie River Basin (MRB). All units are in mm a^{-1} swe, with positive (negative) numbers indicating a sink (source) term in the surface mass balance.	56
---	---	----

-
- 2 Values of the blowing snow sublimation rate (in mm a^{-1} swe) areally-averaged over Antarctica (ANT) and the Mackenzie River Basin (MRB) for the control experiment and two sensitivity tests (described in the text). 62

Article 3

- 1 The sublimation rate (Q_s), in mm h^{-1} snow water equivalent (swe), and transport rate (Q_t) of blowing snow, for three wind speeds and two time integrations forecast by the spectral (S) and bulk (B) versions of PIEKTUK. Time-integrated values of sublimation (QT_s) and transport (QT_t) of blowing snow are also listed. 84

Article 4

- 1 The blowing snow sublimation (Q_s) and transport (Q_t) rates for 3 values of the 10-m wind speed (U_{10}) and 2 time integrations forecast by the spectral (S) and double-moment (D) versions of PIEKTUK. Time integrated values of sublimation (QT_s) and transport (QT_t) of blowing snow are also listed. 100
- 2 Coefficients for Equation (7). 102
- 3 Mean monthly values of observed air temperature (T_a), relative humidity with respect to ice (RH_i), 10-m wind speed (U_{10}), and total monthly values of estimated blowing snow transport (QT_t), sublimation (QT_s) and surface sublimation rates (QT_{surf}) at Trail Valley Valley Creek, Northwest Territories, between 11 September 1996 to 8 April 1997. Note that a negative value of QT_{surf} indicates net deposition at the snow surface. 105

Article 5

- 1 The complete listing of the vertical levels used in the numerical experiments. 133
- 2 The total simulated blowing snow sublimation and mass transport at Trail Valley Creek during the period 1200 UTC on 16 November 1996 to 1200 UTC on 18 November 1996 according to coupled (CPL) mesoscale and stand-alone (STA) blowing snow simulations. 152

3 Mean components of the surface energy and radiation budgets at Trail Valley Creek, NWT for the UNC and CPL experiments. Note that all fluxes are expressed in units of $W m^{-2}$ and that $Q_e = (Q_{surf} + Q_s)L_s$ 155

Acknowledgements

A large number of people have supported and aided me in my doctoral research. First and foremost, I would like to thank sincerely my supervisor, Dr. M. K. Yau, for allowing me to do work in a field we both find very compelling. His breadth of knowledge and professionalism have contributed greatly to the completion of this project. I thank also the other members of my supervisory committee, Drs. J. Gyakum and I. Zawadski for their helpful comments on this thesis.

My interest in cold-season processes arose from work previously done at York University where I must thank Dr. Peter Taylor for his continued moral support and insights into this project. I also wish to acknowledge the constructive discussions on polar and boundary-layer meteorology that I have entertained with Mrs. Jingbing Xiao (York University), Drs. Richard Bintanja and Michiel van den Broeke (University of Utrecht), Drs. Phil Anderson and John King (British Antarctic Survey, Cambridge), Drs. Graham Mann and Stephen Mobbs (University of Leeds) and Dr. Ron Stewart (Environment Canada, Downsview).

Field data from Trail Valley Creek was generously provided by Drs. Richard Essery, John Pomeroy, and Long Li at the Saskatoon branch of the NWRI. Dr. Mike

Branick (NSSL, Norman, Oklahoma) also kindly provided unpublished results of a climatology of severe winter-type weather events for the United States. A number of people at the Meteorology Service of Canada (MSC) of Environment Canada responded to my queries for information on forecasting and I am therefore grateful to Mr. Bevan Lawson (MSC, Winnipeg), Ms. Rosemary Tabory (MSC, Kelowna), Mr. Andrew Giles and Mrs. Sandra Buzzza (MSC, Edmonton). Numerous requests for observational data were always promptly responded to by Mr. Bob Crawford (MSC, Downsview). Satellite imagery was kindly provided by Mr. Patrick King (MSC, King City). Guidance on numerical modelling with the MC2 model was provided by Dr. Badrinath Nagarajan and Mr. Ron McTaggart-Cowan (McGill University), Dr. Steve Thomas (NCAR, Boulder, Colorado), Dr. Michel Desgagné and by Dr. Stéphane Bélair (RPN, Dorval). Mrs. Judy St. James and Mr. Stéphane Chamberland (RPN, Dorval) graciously constructed the geophysical fields required for the MC2 simulations. Dr. Bruce Brasnett (RPN, Dorval) also provided snow data used in the MC2 simulations.

Both the American Geophysical Union and Kluwer Academic Publishers are thanked for permitting the reproduction herein of papers published in one of their journals.

Special thanks are due to my office mate and friend Badrinath for answering promptly the many questions I have asked him. I also wish to acknowledge Jason and Marco for their excellent editing skills and perspicacity. Other colleagues and close friends in the department, such as Vasu, David, Ron and Natalie, only to name a few, were also most helpful in my research. Finally, I would like to acknowledge family and friends for their continued support during my long years as a student.

This work is respectfully dedicated to my grandmother Thérèse who passed away during the final stages of this work. Only through her sense of determination and courage have I learned that people do, in the end, get rewarded for hard work and personal sacrifices... I love you!

Manuscripts and Authorships

Candidates have the option, **subject to the approval of their Department**, of including, as part of their thesis, copies of the text of a paper(s) submitted for publication, or the clearly-duplicated text of a published paper(s), provided that these copies are bound as an integral part of the thesis.

If this option is chosen, **connecting texts, providing logical bridges between the different papers, are mandatory.**

The thesis must still conform to all other requirements of the “Guidelines Concerning Thesis Preparation” and should be in a literary form that is more a mere collection of manuscripts published or to be published. **The thesis must include, as separate chapters or sections:** (1) a Table of Contents, (2) a general abstract in English and French, (3) an introduction which clearly states the rationale and objectives of the study, (4) a comprehensive general review of the background literature to the subject of the thesis, when this review is appropriate, and (5) a final overall conclusion and/or summary.

Additional material (procedural and design data, as well as descriptions of equipment used) must be provided where appropriate and in sufficient detail (e.g., in

appendices) to allow a clear and precise judgement to be made of the importance of originality of the research reported in the thesis.

In the case of manuscripts co-authored by the candidate and others, **the candidate is required to make an explicit statement in the thesis of who contributed to such work and to what extent**; supervisors must attest to the accuracy of such claims at the Ph.D. Oral Defense. Since the task of the Examiners is made more difficult in these cases, it is in the candidate's interest to make perfectly clear the responsibilities of the different authors of co-authored papers.

The complete text of the above must be cited in full in the introductory sections of any theses to which it applies.

Co-Authored Manuscripts

Chapters 2 to 5, inclusive, of this thesis are in the form of articles published, in press or submitted for publication in scientific journals. The results presented in these manuscripts originate from the research I conducted within the context of my Ph.D. studies. The co-author of these papers, Dr. M. K. Yau, provided normal supervision of the research project as well as some text editing.

Statement of Originality

The main original aspects and findings of this dissertation are as follows:

1. A climatology of adverse wintertime events demonstrates that blowing snow events are frequent in the northern sections of the Mackenzie River Basin (MRB) covered by Arctic tundra, but rare in the forested regions of the basin.
2. It is found that the overall large-scale mass balance of the MRB is negligibly impacted by blowing snow transport and sublimation. However, these terms are more significant locally in regions susceptible to frequent blowing snow events such as the Arctic tundra.
3. An innovative methodology for the modelling of blowing snow is described. Single-moment and double-moment versions of a blowing snow model named PIEKTUK are shown to achieve high computational efficiency necessary for longterm integrations or coupled simulations with other atmospheric models.
4. Results of a unique coupled blowing snow/mesoscale model simulation of a remarkable ground blizzard which occurred over the northern sections of the MRB and adjacent Beaufort Sea in mid-November 1996 are discussed. The

simulation reveals that blowing snow sublimation and mass divergence erode 1.4 mm snow water equivalent from a typical Canadian Arctic tundra site during the ground blizzard. The sublimation of blowing snow is shown to be enhanced by $\approx 80\%$ when advective and entrainment processes in the atmospheric boundary layer are considered.

Prologue

She said, ‘Do you want one of those simoons, or blizzards, or mistrals, or whatever you call them? Do you want lumps of ice and falling water and blowing, whistling air?’

He lifted his eyebrows at her. ‘It’s not that bad. There are storms occasionally, but they can be predicted. Actually, they’re interesting-when they’re not too bad. It’s fascinating-a little cold, a little heat, a little precipitation. It makes for variation. It keeps you alive.’

-Isaac Asimov (*Nemesis*)

Chapter 1

Introduction

1.1 Cold season processes in Canada

Canadian weather is renowned for its long, frigid winters. Their persistent subfreezing conditions promote the accumulation of snow that is ubiquitous of the Canadian landscape and even lifestyle during the cold season. Despite their aesthetic and cultural aspects, winter and snow, unfortunately, also have negative impacts on Canadians. For instance, intense cold associated with high windchills remains Canada's most devastating natural hazard as about 100 people perish annually from exposure to the cold (Phillips, 1990). Severe winter weather that accompanies blizzards, snowdrifting or freezing rain storms also seriously disrupt, at times, the daily activities of millions of Canadians. A spectacular example is the 1998 "Ice Storm" in Eastern Canada which caused over a billion dollars of damage and was responsible for the deaths of dozens of people (Szeto et al., 1999; DeGaetano, 2000).

Despite their many impacts on Canadian society, processes responsible for the formation and evolution of winter storms and the seasonal snowpack are not fully understood. Speculation on such basic meteorological quantities as precipitation and evaporation remains due to the sparse observational network at high latitudes and altitudes in Canada. Concerns of a changing climate and a possible reduction in the snowcover, with implications to the hydrological cycle, have fortunately led to an escalation in the research of cold-season processes and storms in the past few years. One region in Canada subject to much ongoing investigation is the Mackenzie River Basin (MRB) of western Canada (Figure 1.1). The MRB drains approximately 1.8×10^6 km², making it the tenth largest worldwide by catchment area. It also provides a crucial northward import of fresh water into the Beaufort Sea and the Arctic Ocean. Subject to some of the strongest signatures of temperature increases over the past century in the Northern Hemisphere (Stewart et al., 1998), the MRB emerges as a key site for the study of ongoing high-latitude climate change. The Mackenzie GEWEX Study (MAGS) is one of the major research experiments held in part within the MRB (Stewart et al. 1998; Rouse, 2000). Its main objective is to observe, quantify and simulate the moisture and energy budgets of the MRB in its past, current and possible future states.

Given that the MRB remains snowcovered for a substantial part of the year (up to 250 days on the Arctic tundra according to Phillips (1990)), some of the processes influencing its surface mass balance are potentially linked to the transport of wind-driven snow that occurs during blizzards and other high wind events (see Figure 1.2). Drifting and blowing snow occur if winds surpass a certain threshold value and then erode snow from exposed surfaces to relocate it to zones of accumulation such as vegetated areas or depressions. A secondary process during advection is

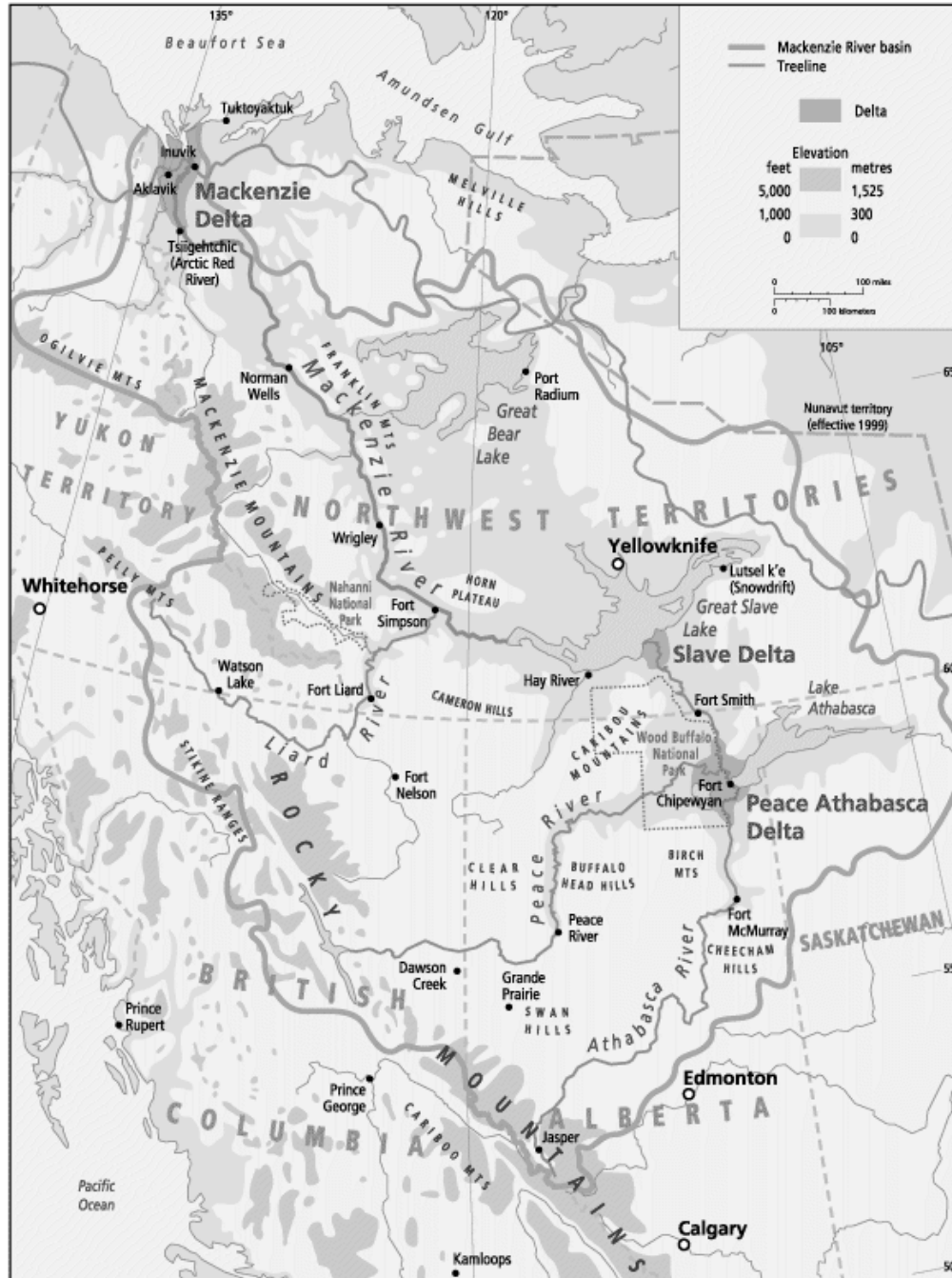


FIGURE 1.1: Geographical map of the Mackenzie River Basin. (Map produced by Eric Leinberger at the University of British Columbia for the Mackenzie Basin Impact Study [Cohen, 1997a, b]).

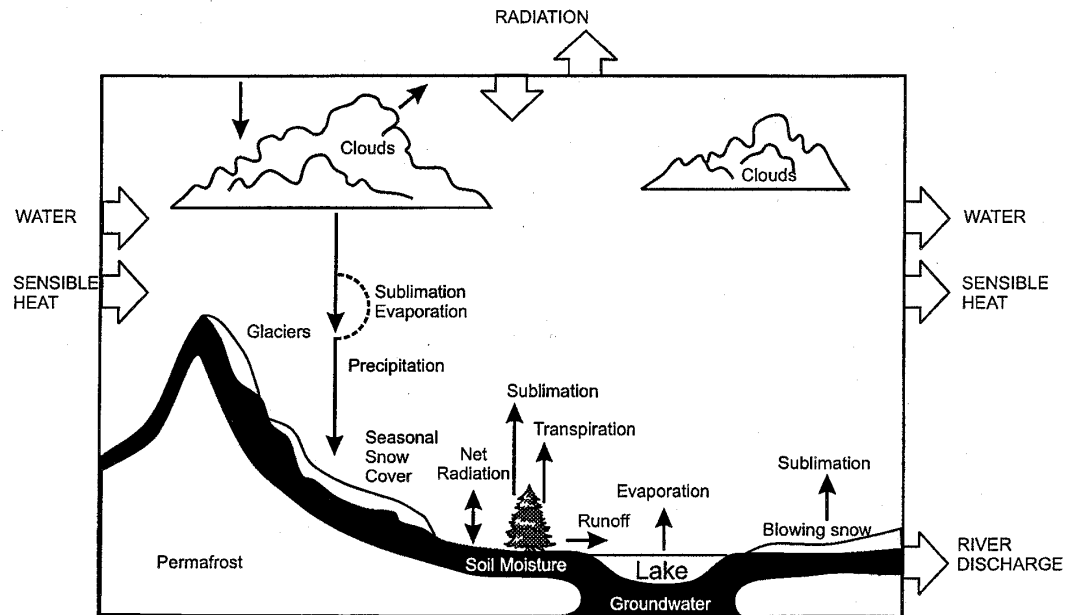


FIGURE 1.2: Schematic diagram of the components of the water and energy budgets of the Mackenzie River Basin (from Rouse, 2000).

sublimation (phase change of ice to water vapour), providing an additional source of moisture while acting as a sink of sensible heat to the atmospheric boundary layer (ABL; Déry and Taylor, 1996).

Despite the recent progress in the study of blowing snow, many questions remain regarding the role this process plays in the surface mass balance of high-latitude regions such as the MRB (Lawford, 1994). In the following section, a brief review of past and ongoing research in this field is presented as well as some of the questions that remain unanswered, followed by the motivation and goals of this thesis.

1.2 Past and Current Perspectives

In Canada, blowing snow has attracted growing attention in the past few decades from several disciplines including the engineering, meteorological and hydrological sciences. For instance, engineers have spent considerable efforts in mitigating the effects of snowdrifting on structures and transportation routes in Canada. A common example of such is the installation of snow fences along roads to reduce the effects of wind-blown snow (Verge and Williams, 1980). Wind tunnel measurements by Kind (1976) and others have also helped engineers understand the air flow that leads to the deposition of snow in drifts that smother buildings and highways with a thick blanket of snow even when precipitation is not occurring.

The hazardous aspects of blowing snow, including the formation of snowdrifts and the reduction of optical visibilities, has led Canadian meteorologists to forecast and to tabulate this phenomenon for decades following standard procedures (Atmospheric Environment Service, 1977, 1988). In Canada, blowing snow is recorded when horizontal optical visibilities are reduced to less than 1 km at eye level by suspended snow. On the other hand, drifting snow specifies the transport of snow that occurs very near the surface without a significant reduction of visibility at eye level. Based on these observations, limited climatologies of blowing snow have been compiled by Maxwell (1980) and Phillips (1990). Their works show, for instance, that blowing snow occurs upwards of 100 days per year in certain sections of the Canadian Arctic. These climatologies, however, do suffer from the sparse observational network at high latitudes and altitudes and do not explain thoroughly the mechanisms that lead to blowing snow events and their impacts to the surface mass balance.

A general lack of knowledge combined with a growing interest in cold climate processes led Canadian atmospheric scientists and their colleagues to initiate several extensive field campaigns in the 1980s and 1990s. The Canadian Atlantic Storms Program (CASP; Stewart, 1991) and the Beaufort and Arctic Seas Experiment (BASE) are two of the comprehensive observational experiments that spurred a flurry of activity in winter storm research. Although these field programmes did not necessarily focus on blowing snow, some authors have nonetheless investigated this process. In East Coast winter storms, for instance, Stewart et al. (1995a) found that blowing snow typically occurs ahead (behind) of a warm (cold) front passage and has a temporal scale typical of mesoscale processes. Unfortunately, no effort was made to establish the contribution of blowing snow to the water budget during these observational studies.

The Canadian hydrological community also began paying more attention to blowing snow in the early 1980s when the contributions of Male (1980) and Kind (1981) were published. The authors appropriately evoked the hazards of the blowing snow phenomenon as well as its potential impact to the surface mass balance. Subsequent to these works, Woo et al. (1983) examined the representativeness of snow gauge measurements on the actual snow accumulation in a high Arctic basin and found significant spatial heterogeneity due to snowdrifting. Spurred by these studies, Pomeroy (1988) established a field experiment in Saskatchewan to observe and model the snowdrifting phenomenon. His research provided some of the first detailed observations of blowing snow in both the saltation and suspension modes (Pomeroy and Gray, 1990; Pomeroy and Male, 1992). This led ultimately to the development of a numerical model of blowing snow called the Prairie Blowing Snow Model (PBSM) which has since been applied to other regions of Canada (Pomeroy

et al., 1993; Pomeroy et al., 1997). The PBSM is a physically-based, steady-state model designed to estimate the hydrological effects of blowing snow transport and sublimation. These results, conveniently summarized by Pomeroy and Gray (1995), indicate depletion rates of up to 75% of the seasonal snowcover by wind transport and sublimation for various locations in the Canadian Prairies.

In their exploration of the northern ABL, Déry and Taylor (1996) realized the potential effects of blowing snow on near-surface air and thus carried out some preliminary experiments with the PBSM. Unsatisfied with several aspects of the PBSM including its assumption of steady-state ambient meteorological conditions, Déry et al. (1998) constructed a column model of blowing snow of their own based nevertheless on the PBSM framework. The inclusion of evolving temperature and humidity fields in this new model entitled PIEKTUK, however, led to significant reductions in the blowing snow sublimation rates with time or fetch compared to the PBSM due to the associated cooling and moistening of near-surface air. Déry et al. (1998) referred to this sequence of events as the “self-limitation” mechanism arising from the negative thermodynamic feedbacks associated with blowing snow sublimation. Table 1.1 illustrates the substantial differences in the column-integrated blowing snow sublimation rates Q_s ($\text{mm h}^{-1} \text{ swe}$) forecast by these two numerical models despite their matching initial conditions.

Thus, a major conclusion reached by Déry et al. (1998) is that the assumption of fixed thermodynamic conditions in the numerical modelling of blowing snow can lead to a significant overestimation of its sublimation rate. Nevertheless, the 1-D idealized framework assumed in their study remains partly deficient since it does not consider other possible interactions of blowing snow with the ABL such as advective or entrainment processes that naturally occur in all dimensions. This implies that

TABLE 1.1: The vertically integrated sublimation rate of blowing snow (Q_s) for varying wind speeds predicted by the PBSM and PIEKTUK models 1 km downwind from the initiation of transport. The data are taken from Déry et al. (1998).

U_{10} (m s ⁻¹)	Q_s (mm h ⁻¹ swe)	
	PBSM	PIEKTUK
10	0.0693	0.0324
15	0.7552	0.1277
20	3.905	0.2938
25	12.32	0.5213

a more comprehensive modelling strategy is required to fully resolve the processes that affect the transition of suspended ice particles to water vapour.

Blowing snow is not the sole cold season process that is misunderstood in the Canadian scientific community. In fact, in their comprehensive review of winter storm research in Canada, Stewart et al. (1995b) came to the conclusion that:

“It is apparent that many aspects of winter storms in Canada have barely been examined at all. For example, downslope winds, orographically affected storms, snow bands, blowing snow, and blizzards need to be studied in much more detail.”

The timely implementation of MAGS in the 1990s has thus provided the research community with a unique opportunity to investigate thoroughly winter-type hydrometeorological processes that remain partially or completely unknown. With the help of enhanced observations conducted during MAGS, the present study will

hopefully provide a better understanding of some of these phenomena including blowing snow.

1.3 Thesis Outline and Objectives

The general goal of this thesis is to obtain a better understanding of the blowing snow phenomenon, its frequency, forcing mechanisms and role in the surface mass balance as well as its interactions with the atmosphere. Specific objectives of this research are:

- to determine the frequency of blowing snow and other adverse cold season processes and some of the meso- to synoptic-scale forcing mechanisms of these events;
- to establish the large-scale impacts of blowing snow in the surface mass balance;
- to improve and optimize the numerical modelling of blowing snow;
- to simulate an actual case study of a severe blizzard event using a complex mesoscale model coupled to a blowing snow model and then to examine some of the interactions between blowing snow, the atmosphere and the surface mass balance;
- to quantify the total contribution of snowdrifting to the water budget of the MRB.

To achieve these main goals, the following outline is proposed. In Chapter 2, we establish the criteria for 3 types of cold-season weather events using the European Centre for Medium-Range Weather Forecasts (ECMWF) Re-Analysis (ERA) data. We infer a climatology of these events for the MRB and the globe. Variability in the frequency and forcing mechanisms of these events are also explored.

In the third chapter, we examine the large-scale impacts of blowing snow sublimation and transport in the surface mass balance of the MRB and the globe. Emphasis is also given to the role of direct sublimation from snow and ice surfaces in comparison to the blowing snow terms in the water budget equation.

The development of a numerically efficient model of blowing snow is presented in Chapter 4. A transition from the spectral framework of the original PIEKTUK blowing snow model to a single-moment and then to a double-moment scheme is discussed. The application of the updated model to a small Arctic watershed provides additional results in the role blowing snow plays in the local wintertime mass balance. A comparison with a similar study at the same location yields possible explanations for some of the discrepancies found in the literature on the importance of blowing snow sublimation in the surface mass balance.

The subsequent chapter describes a remarkable blizzard and blowing snow event that occurred in the northern portion of the MRB during mid-November 1996. The event is simulated using the Mesoscale Compressible Community (MC2) model. The coupling of the MC2 and PIEKTUK models is described as well as results from the uncoupled and coupled simulations. Emphasis is given once again to the role of blowing snow in the surface mass balance. Interactions between blowing snow and the atmosphere are then investigated and discussed at length.

Chapters 2 to 5 inclusive comprise of papers published, in press or submitted for publication in either the *Journal of Geophysical Research*, *Boundary-Layer Meteorology* and *Journal of Hydrometeorology*. The appropriate permissions have been obtained to reproduce the papers herein. Chapter 6 presents a summary of the principal results obtained in the thesis and some suggestions for future work.

Chapter 2

Climatology

2.1 Presentation of Article 1

Given a lack of information on the frequency of cold-season processes within the MRB and other remote areas, we compile a climatology of these inferred from the European Centre for Medium-Range Weather Forecasts (ECMWF) Re-Analysis (ERA) data. The ERA data span 15 years (1979 to 1993 inclusive) and allow a long-term analysis of blowing snow, high windchill and blizzard events on a global scale. Variabilities in the number of occurrences and the mechanisms responsible for these are also investigated.

2.2 Article 1

A climatology of adverse winter-type weather events. By Stephen J. Déry and M. K. Yau, 1999: *J. Geophys. Res.*, **104**(D14), 16,657-16,672.

Copyright by the American Geophysical Union.

A climatology of adverse winter-type weather events

Stephen J. Déry and M. K. Yau

Department of Atmospheric and Oceanic Sciences, McGill University, Montréal, Québec

Abstract. Using the European Centre for Medium-Range Weather Forecasts Re-Analysis gridded data, a global climatology of blowing snow, blizzard, and high-windchill events is conducted for the period 1979–1993. The results show that these phenomena occur primarily over flat, open surfaces with long seasonal or perennial snow covers such as the Greenland and Antarctic ice fields as well as the Arctic tundra. On a regional scale, emphasis is given to the Mackenzie River Basin (MRB) of Canada, where fewer events take place within the boreal forest as opposed to the Arctic tundra. Interannual and monthly variabilities in the number of events are also evident and are due primarily to 10-m wind speed anomalies at high latitudes for blowing snow and blizzard events, while high-windchill events are more sensitive to air temperatures near the surface. We also find that high-windchill episodes are the more frequent events, since they occur at 9.3% of all possible grid points and times on a yearly basis, while blowing snow at 6.5% and blizzards at 1.4% are less common events. Compositing of principal meteorological fields show that anticyclones and lee cyclones are prominent features associated with blowing snow events in some sections of the MRB.

1. Introduction

Cold-season processes often dominate the weather of high-latitude regions. Winter storms combine high windchills and blowing snow that produce blizzard conditions over wide expanses, crippling human activity and leading to substantial economic and social losses.

Despite the recurrence of adverse wintertime weather over widespread areas of the world and inconvenience to people, little is known on the actual frequency of these events. Observations are particularly difficult and scarce in the remote polar areas and over sea ice. Although climatological works for the Antarctic and Arctic are not uncommon [e.g., Maxwell, 1980; Woo and Ohmura, 1997; King and Turner, 1997], few provide climatic data on adverse conditions. Others have examined winter storms and associated processes without assessing their yearly distributions [e.g., Stewart *et al.*, 1995a]; hence our goal is to provide an analysis of the frequency of these events.

This study is motivated in part by the Mackenzie GEWEX Study (MAGS) [Stewart *et al.*, 1998], the Canadian component of the Global Energy and Water Cycle Experiment (GEWEX). The ultimate goal of MAGS is to evaluate the energy and moisture fluxes for the entire Mackenzie River Basin (MRB) of western Canada (see Figure 1). Since some of the processes influencing the wintertime water and energy budgets of

the MRB are potentially associated with the transport of wind-driven snow and concurrent sublimation that occur during blizzards and other high-wind events [Lawford, 1993, 1994], a climatology of these events must be established. Given that the gridded data used in this study are global, an analysis is first presented for both hemispheres. We then proceed by examining the hemispheric trends and some causes of anomalous numbers in these events. Subsequently, we examine more closely the climatology as well as the synoptic-scale signatures of blowing snow events in the MRB, followed by a discussion of the results. The paper begins with some background information on the three significant wintertime processes of interest and a description of the methodology used to compile these events.

2. Background

2.1. Blowing Snow

A notable weather hazard associated with snowstorms is blowing and drifting snow. Intense blowing snow can decrease visibility to near zero and cause drifts several meters deep, making transportation extremely difficult [Kind, 1981]. Blowing and drifting snow occur when wind speeds exceed a certain threshold value and initiate the transport of snow that was formerly at the surface. Precipitating snow may also induce blowing snow, making the source of blown snow somewhat difficult to resolve in many instances. Two substantive processes are involved during blowing and drifting snow: saltation and suspension. Saltation is snow particles bouncing along the surface at heights of a few centimeters,

Copyright 1999 by the American Geophysical Union.

Paper number 1999JD900158.
0148-0227/99/1999JD900158\$09.00

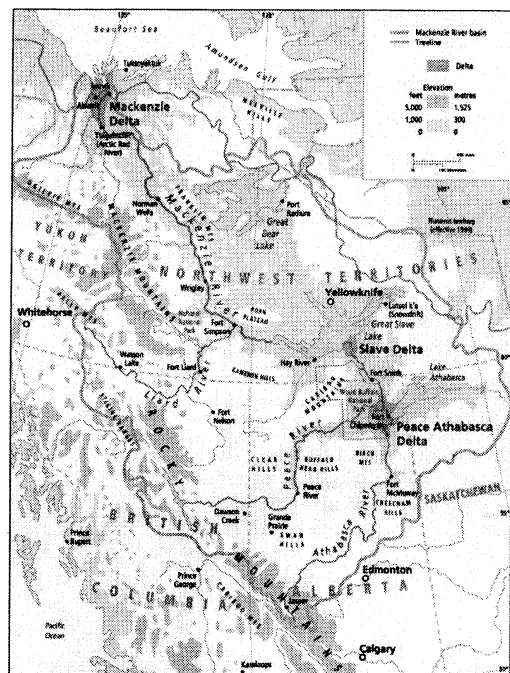


Figure 1. Geographical map of the Mackenzie River Basin. (Map produced by Eric Leinberger at the University of British Columbia for the Mackenzie Basin Impact Study [Cohen, 1997a, b].)

providing then a source for snow suspension [Pomeroy *et al.*, 1997]. Suspension occurs when snow particles are entrained by turbulent motions within the atmospheric boundary layer (ABL). In this mode, particles may rise to 100 m or more above the surface [Pomeroy and Goodison, 1997; King and Turner, 1997].

Although blowing snow usually refers to suspended snow that reduces visibility at eye level and drifting snow to snow transport below that height, we make no distinction between the two definitions in this work, and we will refer to the process as simply blowing snow. The 10-m wind speed threshold (U_t) for initiation of transport is usually in the vicinity of 5 to 10 m s^{-1} [King and Turner, 1997], depending on several environmental factors such as temperature and moisture conditions of the snowpack as well as the age of the snow [Schmidt, 1980]. Here we follow Li and Pomeroy [1997], who have found a dependence on the 2-m air temperature T_a ($^{\circ}\text{C}$) for U_t (m s^{-1}) as

$$U_t = U_{t_0} + 0.0033(T_a + 27.27)^2 \quad (1)$$

where the minimum value of the threshold 10-m wind speed, U_{t_0} , is equal to 6.98 m s^{-1} and is reached at about $T_a = -27^{\circ}\text{C}$. This parabolic equation predicts higher resistance to transport at very cold temperatures

and near the freezing point. Near 0°C , the snow tends to be wet, and the imbedded water leads to higher cohesion of the snowpack. On the other hand, at very cold temperatures, cohesion associated with strengthening elastic and frictional forces again reduce the capacity of the wind to displace snow from the surface. The intermediate range $-25^{\circ}\text{C} < T_a < -10^{\circ}\text{C}$ is defined by Li and Pomeroy [1997] as the cold cohesive regime in which wind transport of dry snow is generally most favorable.

2.2. Windchill

The combination of cold air and high winds leads to rapid loss of body heat, a process termed “windchill,” which was first examined by Siple and Passel [1945] and subsequently by Steadman [1971], among others. An empirical relationship for windchill (WC , W m^{-2}) was derived to be [Siple and Passel, 1945]:

$$WC = (10.7 - 0.323T_a)(37.62 + 36.0U_{10}^{0.5} - 3.6U_{10}) \quad (2)$$

with T_a in degrees Celsius and U_{10} the 10-m wind speed (m s^{-1}). As an example, for a wind of 11 m s^{-1} and $T_a = -20^{\circ}\text{C}$, equation (2) yields $WC = 2.0 \text{ kW m}^{-2}$, a common threshold at which windchill warnings are issued in Canada [Atmospheric Environment Service, 1988] and a value approximately at which exposed skin freezes in less than a minute.

2.3. Blizzards

“Blizzards” are winter storms that combine both high windchills and blowing snow, reducing visibilities markedly, as well as snowfall. “Ground blizzards” are winter storms with the same characteristics as blizzards but with no apparent snowfall. Although definitions may vary from region to region [e.g., Bluestein, 1993; Wild, 1995; Branick, 1997], a blizzard warning is usually issued in Canada when the following criteria are met for a period of at least 4 hours: (1) wind speeds $> 11 \text{ m s}^{-1}$ ($= 40 \text{ km h}^{-1}$), (2) windchills $> 1.6 \text{ kW m}^{-2}$, and (3) visibility $< 1 \text{ km}$ in snow and/or blowing snow [Stewart *et al.*, 1995a]. A temperature norm is at times utilized in place of windchill values, with $T_a < -12^{\circ}\text{C}$, along with the other stipulated elements, usually marking the onset of a blizzard [Phillips, 1990]. Omitting the time component, blizzard conditions can occur at any time, and “blizzard hours” or “days with blizzards” are the most often recorded climatological quantities.

Even though blizzards are common phenomena in many regions of the world, such as Antarctica [Alvarez and Lieske, 1960], Eurasia [Mikheev *et al.*, 1971] and North America [Stewart *et al.*, 1995a; Branick, 1997], few in-depth studies of blizzards exist in the literature. The climate studies of Burns [1973], Maxwell [1980], and Lawson [1987] provide some insight on typical conditions favoring the development of blizzards and the frequency of such events in Canada. Exceptional cases have also been described by, for instance, Babin [1975],

Graff and Strub [1975], *Burrows et al.*, [1979], *Salmon and Smith* [1980], *Eagleman* [1990], *Kocin and Uccellini* [1990], and *Wild et al.* [1996].

3. Methodology

3.1. Definitions

Since observations of adverse wintertime processes are scarce and conducted in very harsh conditions, we have compiled a climatology of these events using gridded reanalysis data. Thus a 15-year (from 1979 to 1993 inclusive) climatology of significant cold-season “events” for the MRB and the globe is obtained from 6-hourly European Centre for Medium-Range Weather Forecasts (ECMWF) Re-Analysis (ERA) data on a 2.5° latitude \times 2.5° longitude grid [*Gibson et al.*, 1997]. Subsequently, the results are converted to a polar stereographic projection, since the processes of interest occur mainly near the poles. The domains of the grids depicting the polar stereographic projections are composed of 50×50 points centered over the poles with a horizontal resolution of 250 km true at 60°N or S. The presence of snow is determined from the snow depth parameter of the ERA data that is based on station observations, but sea ice coverage is provided by the Canadian Meteorological Centre (CMC) at the same resolution as the former.

Definitions of the events are as follows. A blowing snow event is defined as any day when the surface was snow-covered land or sea ice (in concentration of 50% or more), the temperature was below 0°C , and the threshold velocity for transport was exceeded, as determined from equation (1), at any grid point. On the other hand, we consider a high-windchill event as any day when $WC > 2.0 \text{ kW m}^{-2}$ at any grid point. Finally, a blizzard event is interpreted as any day when blizzard conditions are met (see section 2.3) at any grid point, using the windchill and wind speed criteria, but necessarily omitting the time component given the temporal resolution of the ERA data. In addition, the visual range is not a parameter in the ERA data set and is therefore estimated from the following relationship [*Tabler*, 1979]:

$$VIS = AU_{10}^{-5} \quad (3)$$

where VIS is the approximate visibility (m) at eye level in blowing snow, A is a constant set to $10^8 \text{ m}^6 \text{ s}^{-5}$, and U_{10} is in m s^{-1} . When $VIS = 1 \text{ km}$, wind speeds are 10 m s^{-1} , corresponding essentially to the wind speed criterion for blizzard conditions. Although precipitation may also reduce the visual range, the wind speed threshold for blizzards ensures the incidence of blowing snow and ensuing deterioration in VIS below 1 km. A snow-covered surface (land or sea ice with concentration $> 50\%$) is a further requirement imposed for blizzard events. Note that unlike the case of a blowing snow event or a blizzard event, no temperature or wind speed

threshold appears in the definition of a high-windchill event. Therefore a high-windchill event can occur if the temperature is cold enough, even for a small wind speed, as long as $WC > 2.0 \text{ kW m}^{-2}$.

The ERA data are available four times daily (0000, 0600, 1200, and 1800 UTC). An event is considered to have occurred if the criteria for a specific event are satisfied at any one of the four times. However, for all grid points we limit the number of events to a maximum of one per day. This allows a comparison of our results with observations, since significant cold-season processes are often recorded only on a daily basis, i.e., a day with or without such an event.

3.2. Validation

To determine the validity of our analysis, tests were first conducted to verify the prediction of events with hourly surface observation (SA) reports at several Canadian meteorological stations during the month of March 1993. As an example, Figure 2 shows the near-surface fields of sea level pressure (SLP), temperature, and wind speed, as well as the areas experiencing some type of adverse wintertime weather at 1200 UTC on March 14, 1993. An intense low-pressure system, known as a “Superstorm” [e.g., *Huo et al.*, 1995], is battering the East Coast of North America. At the same time, an enhanced SLP gradient and strong winds are occurring over the Beaufort Sea in association with an anticyclone north of Alaska. Table 1 lists the surface observations recorded at six meteorological stations across Canada. The locations of the stations are shown in Figure 2d. In general, the surface parameters indicate reasonable agreement considering the resolution in our ERA data. Blowing snow is inferred from the ERA to occur along the Arctic coastline and in southern Québec and the Maritime provinces (Figure 2a) and is observed at four stations in the area, i.e., Inuvik, Montréal, Natashquan, and Stephenville (Table 1). Cold conditions prevail in the Nunavut Territory (NVT) and the Northwest Territories (NWT), with most areas surpassing the high-windchill threshold of 2.0 kW m^{-2} as observed in Baker Lake (Figure 2b). High windchill values and strong winds near the Gulf of St. Lawrence lead to blizzard conditions associated with the aforementioned Superstorm. Surface observations at the coastal stations of Natashquan and Stephenville in eastern Canada reveal the blizzard event that we infer from the ERA data (Figure 2c). Thus we are capturing accurately these synoptic-scale events from the reanalysis data set.

In addition to the above tests, we compared climatological observations of T_a and U_{10} in high-latitude regions to those of the ERA data and find generally good agreement (Table 2). As the data in Table 2 suggest, however, the ERA exhibits in some locations a significant negative 2-m air temperature bias. This bias occurs during winter and spring at high latitudes and is forced by the unrealistically high values of the surface albedo assigned to a snowcover [*Källberg*, 1997; *Slingo*

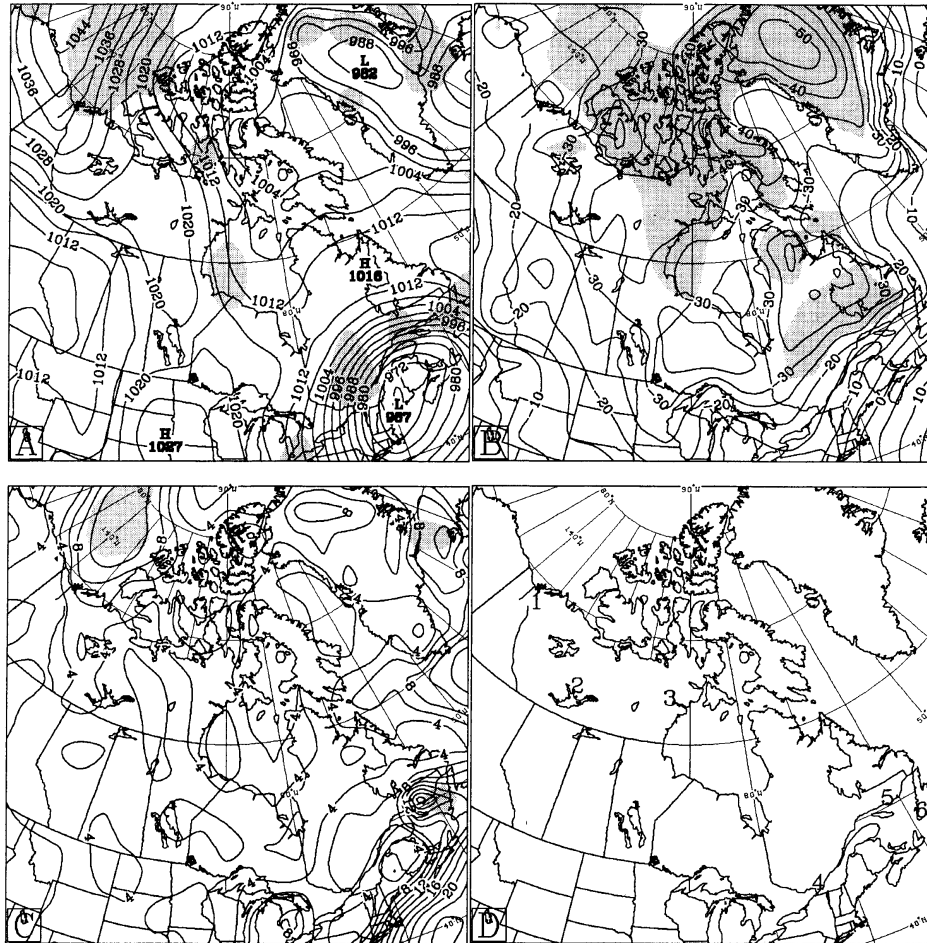


Figure 2. The contours of (a) the sea level pressure at 4 hPa intervals, (b) the 2-m air temperature at 5°C intervals, and (c) the 10-m wind speed at 2 m s⁻¹ intervals, at 1200 UTC on March 14, 1993. Shaded areas indicate (a) regions experiencing a blowing snow event, (b) a high-windchill event, and (c) a blizzard event, as inferred from the ERA data. Refer to Table 1 for the locations numbered in Figure 2d.

et al., 1998]. Wind speed biases in both hemispheres are also evident in Table 2. The ERA underestimates wind speeds in the Antarctic coastal areas (e.g., Mirny) susceptible to frequent katabatic wind episodes [King and Turner, 1997]. Intense katabatic winds are mesoscale phenomena which may not be properly resolved by the ERA data at a resolution of 2.5°. In the Northern Hemisphere, both positive and negative wind speed biases (± 1 m s⁻¹) are observed. Negative wind speed biases would lead to an underestimate in the number of all three types of events of interest. On the other hand, negative temperature biases will reduce the frequency of blowing snow events when $T_a < -27^\circ\text{C}$ but increase

the number of events in the range $-27^\circ\text{C} < T_a < 0^\circ\text{C}$, following our assumption for the threshold velocity for transport. For high-windchill and blizzard events, negative temperature biases will increase the frequencies of each. Note, however, that our sampling rate is limited to four times daily, whereas surface observations are often continuous in time. This may contribute to a lower number of days with a specific event as inferred from the ERA in comparison to actual observations.

For reasons of economy, we have used the ERA data at a resolution of 2.5°, which however, brings about limitations in detecting sub-synoptic-scale events. Both blowing snow and blizzard events are known to occur on

Table 1. Surface Observations of Sea Level Pressure (SLP), 2-m Air Temperature (T_a), 10-m Wind Speed (U_{10}), Windchill (WC), and Precipitation and/or Weather Type (PWT) Recorded at Selected Canadian Meteorological Stations at 1200 UTC on March 14, 1993

No. ^a	Station	SLP, hPa	T_a , °C	U_{10} , m s ⁻¹	WC , kW m ⁻²	PWT ^b
1	Inuvik	1036.3	-21	6.7	1.86	S-, BS
2	Yellowknife	1020.3	-24	3.6	1.71	S-
3	Baker Lake	1017.8	-37	9.3	2.58	IC, IF
4	Montréal	981.3	-13	9.3	1.69	S-, BS
5	Natashquan	992.2	-10	12.3	1.66	S-, BS
6	Stephenville	992.6	-6	18.0	1.58	IP-, S-, BS

^aThe station number (No.) refers to its location in Figure 2d.

^bThe precipitation and weather types and their abbreviations are snow (S), blowing snow (BS), ice crystals (IC), ice fog (IF), and ice pellets (IP). A “-” indicates light precipitation.

the mesoscale as well as the synoptic scale [e.g., *Stewart et al.*, 1995b; *Szeto and Stewart*, 1997], and we recognize that these may not be entirely accounted for in the present work. In addition, alpine events are unlikely to be detected at this grid resolution. Although mesoscale and mountainous events would increase the overall frequencies of occurrences, particularly on a regional basis, we will show in the following section that our compiled frequency of adverse winter-type weather events compares favorably with the few observations found in the literature.

4. Results

4.1. Global Climatology

Figure 3 depicts the number of blowing snow events for both the Northern and Southern Hemispheres (NH and SH, respectively). Blowing snow events are most prominent on the windy and snow-covered ice fields of Antarctica and Greenland, as well as over sea ice. A

high number of events also occurs on the Arctic tundra of Canada and Russia as well as the neighboring frozen seas and lakes. Forested areas increase surface friction and reduce wind speeds, limiting the number of occurrences there. This is evident in both North America and Asia, where the boreal forest endures fewer blowing snow events than the open plains south of the boreal forest (e.g., the Canadian prairies and steppes of Kazakhstan). Although climatological records of blowing snow are rare and definitions of events vary, we note a good correlation to that of *Phillips* [1990]. His blowing snow climatology for Canada portrays a similar local maximum in the prairies and a peak in the number of events in Hudson Bay, the NVT, and NWT, but with higher frequencies for the Arctic Islands and the prairies. The high number of events in Kazakhstan and along the Russian Arctic coastline also corresponds well to the regions of large volume transport reported by *Mikhel' et al.* [1971]. We remark, however, that alpine areas, prone to many blowing snow events [e.g., *Berg*, 1986; *Barry*, 1992], are not well represented here, except

Table 2. The Observed Mean Annual 2-m Air Temperature $\overline{T_a}$ and 10-m Wind Speed $\overline{U_{10}}$ at Selected High-Latitude Climatological Stations Compared to the Values Obtained From the ERA Data

Station	Latitude, Longitude	$\overline{T_a}$, °C		$\overline{U_{10}}$, m s ⁻¹		Source
		Observed	ERA	Observed	ERA	
<i>Northern Hemisphere</i>						
Inuvik, Canada	68°N, 133°W	-4.5	-7.5	2.8	3.3	1
Novosibirsk, Russia	55°N, 83°E	-0.2	1.7	3.8	3.7	2
Vilyuysk, Russia	64°N, 122°E	-9.2	-10.3	2.2	3.1	2
Yellowknife, Canada	62°N, 114°W	-5.4	-6.4	4.3	3.1	1
<i>Southern Hemisphere</i>						
Byrd, Antarctica	80°S, 119°W	-27.9	-32.0	8.6	2.9	3
Halley, Antarctica	76°S, 26°W	-18.5	-12.7	4.8	5.5	3
Mirny, Antarctica	67°S, 93°E	-11.5	-15.0	11.5	8.6	3
South Pole, Antarctica	90°S	-49.3	-52.7	4.8	5.0	3

Sources: 1, *Environment Canada* [1993]; 2, *Lydolph* [1977]; 3, *Schwerdtfeger* [1970].

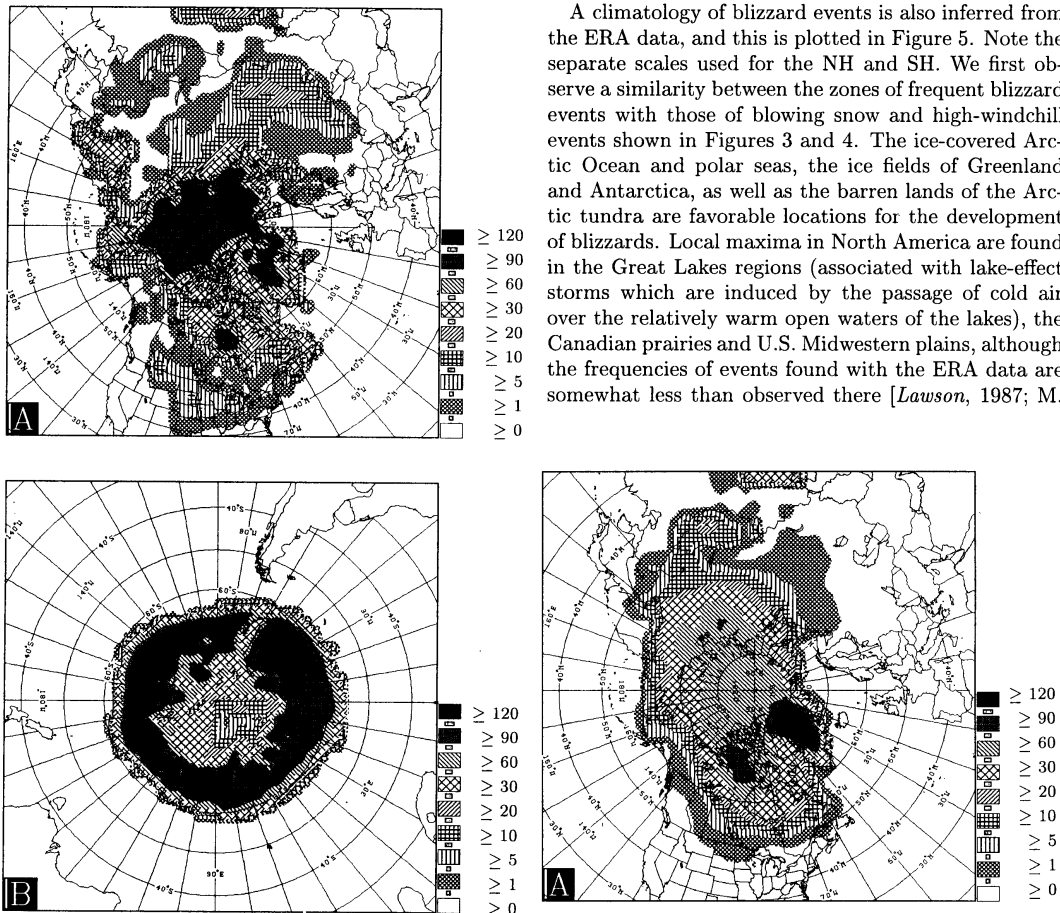


Figure 3. Mean annual number of blowing snow events (as defined in the text) for the period 1979-1993 in (a) the Northern Hemisphere and (b) the Southern Hemisphere.

perhaps the Tibetan Plateau, due to the resolution of the gridded data.

In the SH, a “ring” of maximum blowing snow events is associated with the stormy coastal regions of Antarctica and the circumpolar trough, with some areas experiencing blowing snow daily more than two thirds of the year (Figure 3b).

The annual number of days when WC surpasses 2.0 kW L^{-2} is presented in Figure 4. This shows that, on an annual basis, a greater number of blustery days occur in Antarctica as opposed to the ice-covered Arctic Ocean. However, the Asian and North American continents surrounding the Arctic Ocean promote a southward propagation of high-windchill events as far south as 40°N . In the SH these cold episodes rarely occur over open waters or even sea ice and do not extend much farther north than 70°S .

A climatology of blizzard events is also inferred from the ERA data, and this is plotted in Figure 5. Note the separate scales used for the NH and SH. We first observe a similarity between the zones of frequent blizzard events with those of blowing snow and high-windchill events shown in Figures 3 and 4. The ice-covered Arctic Ocean and polar seas, the ice fields of Greenland and Antarctica, as well as the barren lands of the Arctic tundra are favorable locations for the development of blizzards. Local maxima in North America are found in the Great Lakes regions (associated with lake-effect storms which are induced by the passage of cold air over the relatively warm open waters of the lakes), the Canadian prairies and U.S. Midwestern plains, although the frequencies of events found with the ERA data are somewhat less than observed there [Lawson, 1987; M.

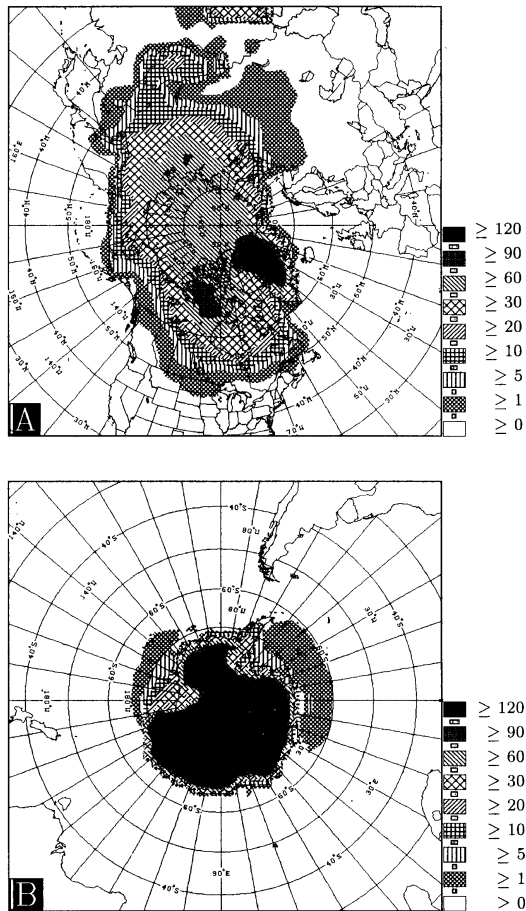


Figure 4. Mean annual number of high-windchill events (as defined in the text) for the period 1979-1993 in (a) the Northern Hemisphere and (b) the Southern Hemisphere.

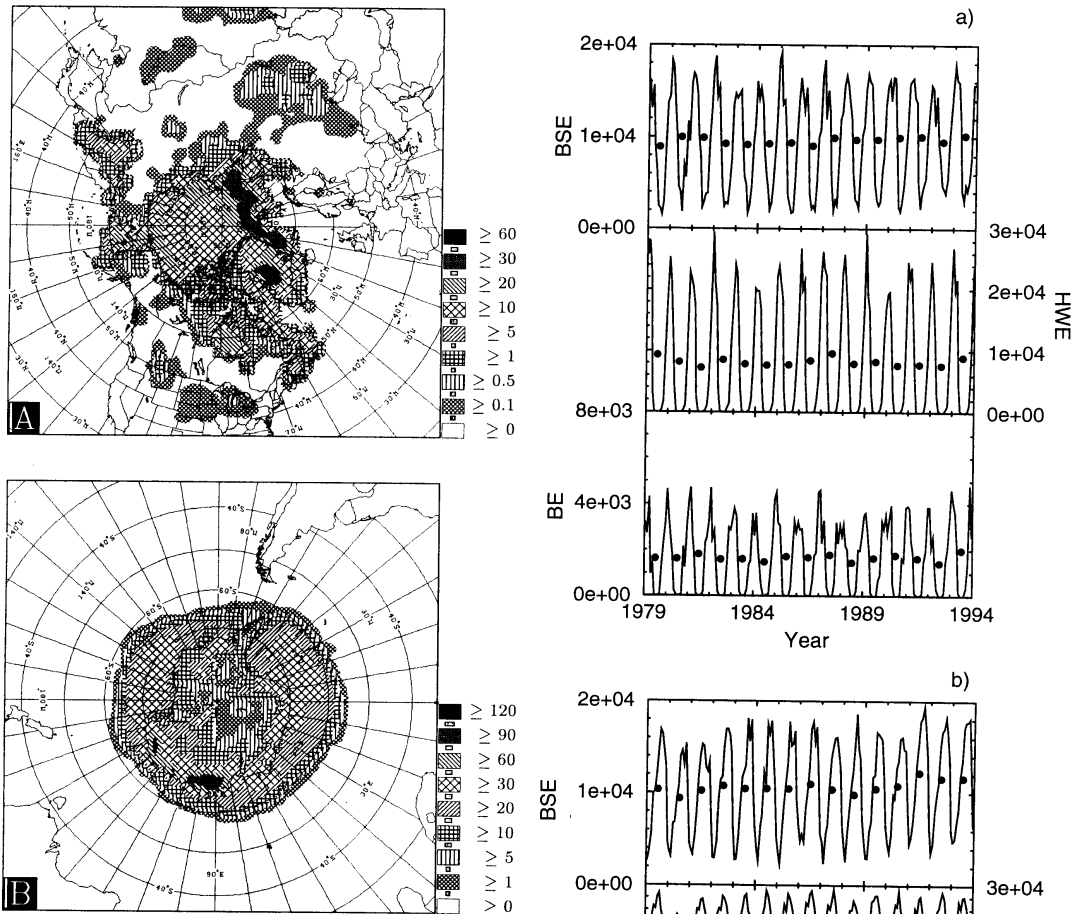


Figure 5. Mean annual number of blizzard events (as defined in the text) for the period 1979-1993 in (a) the Northern Hemisphere and (b) the Southern Hemisphere.

L. Branick, unpublished data, 1998]. Canada's East Coast is notorious for its frequent winter storms, many of which reach the status of blizzard. However, few blizzards are experienced where boreal forest prevails, again due to a significant reduction in high wind speed events there. In the SH, most events occur along the stormy coastal environment of eastern Antarctica, with some regions experiencing blizzards no less than 120 days annually.

4.2. Trends and Anomalies

Over the course of the 15 years investigated in this paper, monthly and annual variabilities in the number of adverse winter-type weather phenomena are evident from the time series of blowing snow, high-windchill, and blizzard events displayed in Figure 6. The time se-

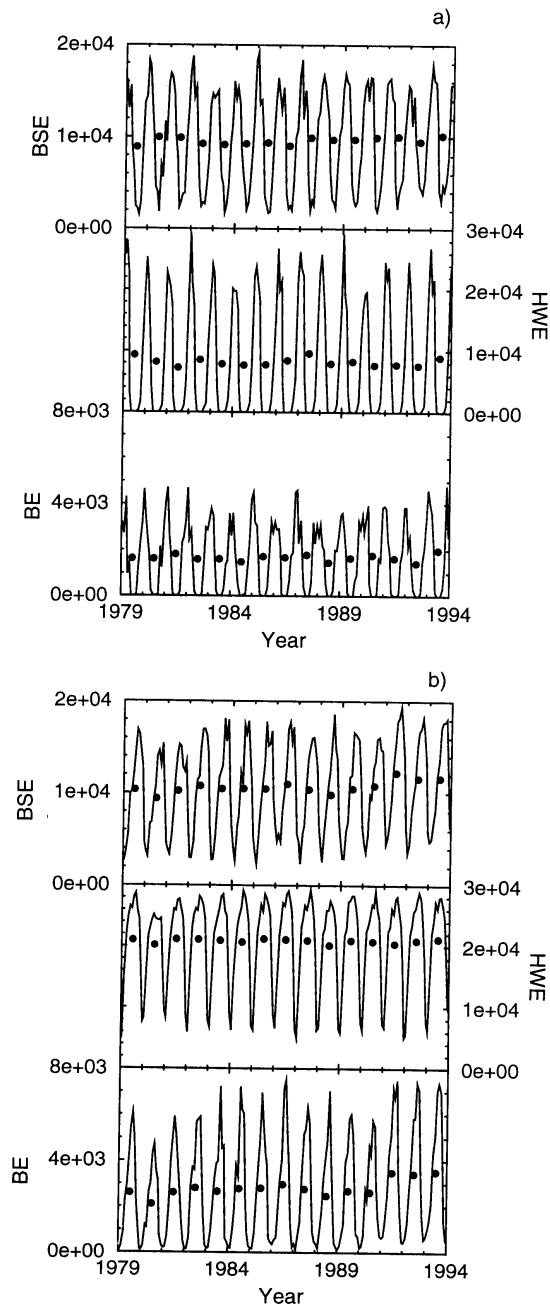


Figure 6. Monthly (solid lines) and annual (dots) trends in the number of blowing snow events (BSE), high-windchill events (HWE), and blizzard events (BE) for (a) the Northern Hemisphere and (b) the Southern Hemisphere. Yearly values have been normalized by a factor of 12 for comparison with the monthly frequencies of events.

Table 3. Average Annual Number of Blowing Snow Events (BSE), High-Windchill Events (HWE) and Blizzard Events (BE) in the Northern Hemisphere (NH), the Southern Hemisphere (SH), and the Globe for the Period 1979-1993

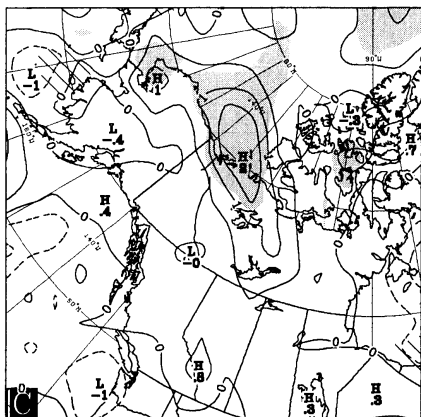
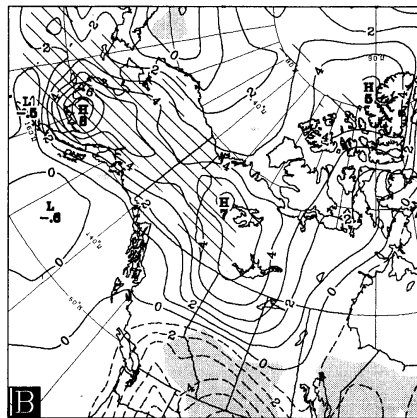
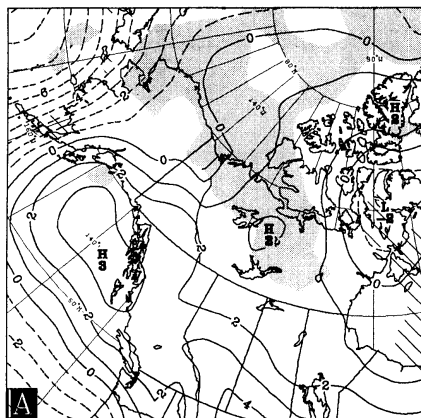
Type of Event	NH		SH		Globe	
	$\times 10^5$	%	$\times 10^5$	%	$\times 10^5$	%
BSE	1.152	6.17	1.279	6.85	2.432	6.51
HWE	0.983	5.27	2.502	13.40	3.485	9.33
BE	0.198	1.06	0.338	1.81	0.537	1.44

Percentile values indicate the frequency of events on a yearly basis over all grid points and times, i.e., the actual divided by the total possible number of events.

ries are presented for each hemisphere, and the monthly trends display peaks in the number of events during each hemispheric winter. In the NH, monthly frequencies attain a maximum typically between January and

March, while in the SH the maxima are reached usually between July and September. Note the absence of high-windchill and blizzard events in the NH during its summer, whereas the SH experiences these episodes year-round due to the colder summertime temperatures over Antarctica compared to those of the polar NH summer.

By observing the annual trends, we see that about an equal number of blowing snow events occurs in the NH and the SH but that considerably more high-windchill and blizzard events take place in the SH (Figure 6). Interannual variability is also evident in the yearly trends of blowing snow and blizzard events, but the number of high-windchill events is nearly constant in the SH. Table 3 lists some of the absolute and relative values of the frequencies of all three types of events. We see that, on average, the number of occurrences is of the order of 10^5 annually for the original latitude/longitude grid used in this study. High-windchill events are more common than blizzard events despite the higher *WC*



criterion for the former relative to the latter. This is due to the strict wind speed threshold imposed in the definition of a blizzard event, whereas a high-windchill event is not required to satisfy a critical value of either T_a or U_{10} , as long as $WC > 2.0 \text{ kW m}^{-2}$ (see section 2).

Anomalies in blowing snow, high-windchill, or blizzard events may be due to several factors, including SLP, air temperature, and wind speed fluctuations, all factors affecting these processes. Figure 7 depicts ar-

Figure 7. The positive (negative) monthly anomalies, shown by solid (dashed) lines, of (a) sea level pressure (intervals of 1 hPa), (b) 2-m air temperature (intervals of 1°C), and (c) 10-m wind speed (intervals of 0.5 m s^{-1}) for February 1993 from the 15-year (1979-1993) means for February. Shaded (cross-hatched) regions indicate areas with positive (negative) deviations of two or more monthly (a) blowing snow, (b) high-windchill, and (c) blizzard events.

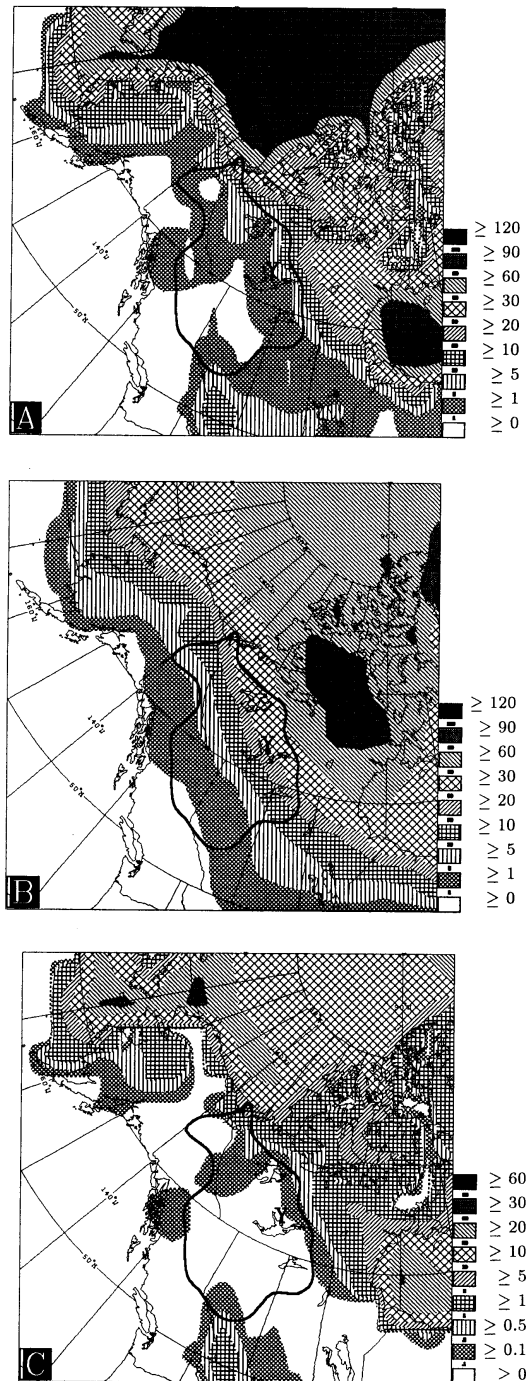


Figure 8. Mean annual frequency of (a) blowing snow, (b) high-windchill, and (c) blizzard events in the Mackenzie River Basin (denoted by the thick line) for the period 1979-1993.

areas that experienced in 1993 positive and negative deviations of at least two or more blowing snow, high-windchill, and blizzard events from the 15-year mean for the month of February in the vicinity of the MRB. Clearly associated with the positive blowing snow and blizzard event anomalies are significant deviations in U_{10} (up to 2 m s^{-1} from the monthly average) with noticeable positive T_a fluctuations nearby. This confirms that a strong correlation exists between wind speed and blowing snow and blizzard event anomalies. We also observe an SLP anomaly of 2 hPa from the climatological mean centered over the MRB. The near-surface air temperature is a more critical parameter for the number of high-windchill events as positive (negative) deviations in frequency are collocated with negative (positive) temperature fluctuations.

4.3. Climatology for the Mackenzie River Basin

4.3.1. Frequency of events. We now emphasize the climatology of significant winter-type weather events for the MRB, which is the area of interest of MAGS (Figure 1). The MRB drains approximately one fifth of the Canadian landmass and is situated in an area where wintertime processes are important [Lawford, 1993, 1994]. Although most of it is forested, the northeastern and northern sections of the basin lie within Arctic tundra. These barren lands are conducive to frequent blowing snow events (≥ 10 per year) which decline rapidly in number within the taiga, where fewer than five annual episodes occur (Figure 8a). The number of occurrences begins to increase southward as the boreal forest gives way to the open prairies. In comparison to Phillips [1990], we underestimate the frequency of blowing snow events in the forested regions of the MRB, where the ERA displays a negative wind speed bias (Table 2).

High-windchill events are also most common over the Arctic tundra (Figure 8b). Near the southernmost sections of the basin, no more than a few days per year with $WC \geq 2.0 \text{ kW m}^{-2}$ are expected. However, the number of events increases moving to the northeast such that as many as 60 high-windchill events occur over the cold Arctic tundra, which evidently coincides with the area of highest blizzard frequency (Figure 8c). Blizzards are uncommon in most sections of the MRB; nonetheless, perhaps one such storm may affect the lower Mackenzie Valley every 2 years, whereas the coastal regions may expect more than five events annually. These results confirm the conjecture by Stewart *et al.* [1995a] that two blizzard regimes exist in the NVT and NWT of Canada, with the areas of high and low frequencies delineated by the treeline.

4.3.2. Forcings of events. Compositing is an averaging technique used to reveal atmospheric patterns common to a meteorological event. The method has been applied, for instance, to detect synoptic- or planetary-scale signatures of widespread heavy precipi-

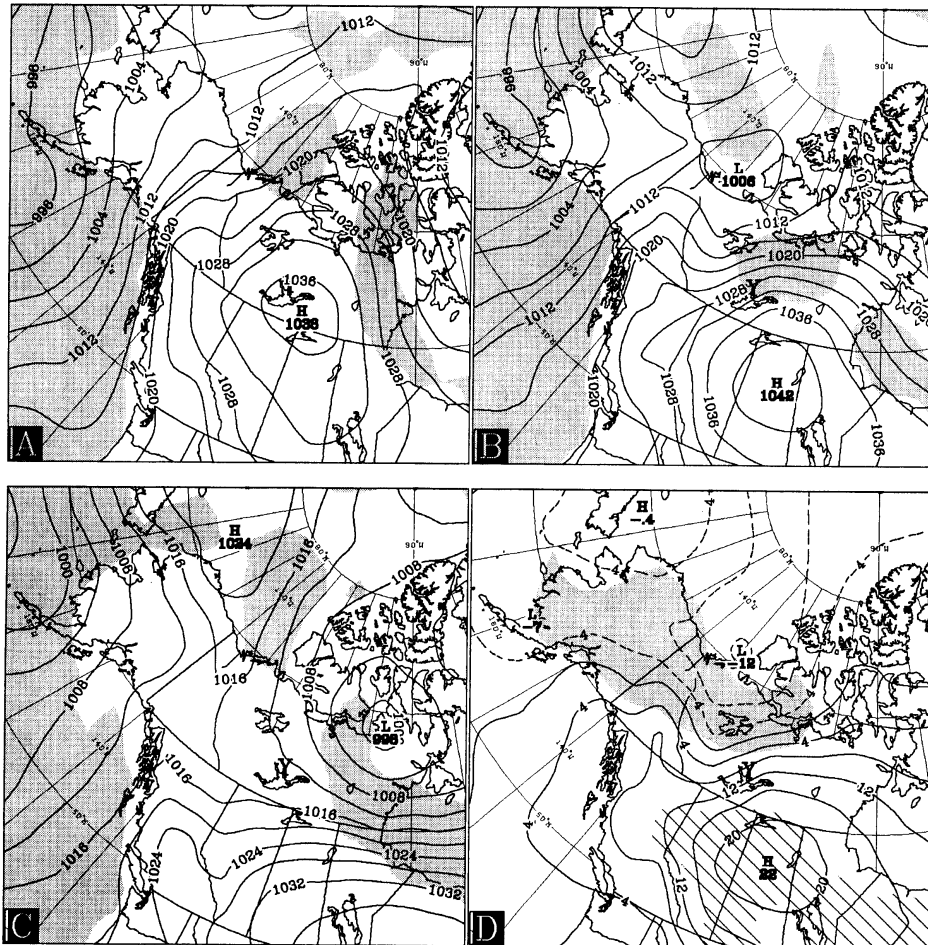


Figure 9. Composites of the sea level pressure at 4 hPa intervals (a) 24 hours prior to ($T-24$), (b) during ($T00$), and (c) 24 hours after ($T+24$) 11 blowing snow events associated with winds from the SW quadrant near Yellowknife (denoted by "Y"). Shaded areas denote 10-m wind speeds $>6 \text{ m s}^{-1}$. Positive (negative) deviations from the 15-year climatological mean sea level pressure (hPa) during the events ($T00$) are shown in Figure 9d in solid (dashed) lines with 2-m air temperature anomalies of $>5^\circ\text{C}$ ($<-5^\circ\text{C}$) from the 15-year climatological mean shaded (cross-hatched).

tation episodes in the MRB [Lackmann and Gyakum, 1996]. Given that our primary interest lies in snow transport, we apply the technique at a particular location by averaging the fields of SLP, surface temperature, and wind speed during blowing snow events. Some preliminary tests revealed that stratification of the events with respect to wind direction yielded superior results. We therefore classify blowing snow events into four categories, depending on the wind direction quadrant, i.e. (winds from the) SW, NW, NE, and SE quadrants. The results shown here are for blowing snow events that occurred during the months of January to March 1979 to 1993, inclusive, near Yellowknife, NWT ($62^\circ 28' \text{N}$,

$114^\circ 27' \text{W}$), chosen for its central location within the MRB (see Figure 1). To ensure the significance of the results, we applied a Student's t test [Wilks, 1995] to the data. This statistical test is commonly employed in the application of the compositing technique [e.g., Lackmann and Gyakum, 1996], with the threshold confidence level of 95% often used to assess the validity of the results. In our case, a confidence level $\geq 95\%$ limited our compositing to within ± 24 hours from the time of the events.

Figure 9 is a composite of the SLP field with superimposed regions where winds $\geq 6 \text{ m s}^{-1}$ when the event is occurring ($T00$), as well as 24 hours prior to and

after the event ($T-24$ and $T+24$, respectively), while Figure 9d represents deviations of SLP and T_a from the 15-year (1979-1993) monthly climatological means at T00. Thus Figures 9a-9c show the temporal evolution of SLP and wind fields that favor southwesterly blowing snow events near Yellowknife. At T00, we observe a composite anticyclone that has moved into the Canadian prairies with central SLP of 1042 hPa and a trough in the lee of the Mackenzie Mountains and an associated cyclone to the north that lead to an enhanced SLP gradient near Yellowknife. Mean wind speeds there are about 8.0 m s^{-1} with threshold for transport, again computed following equation (1), near 7.0 m s^{-1} . Associated with these strong southwesterly winds in the MRB are positive temperature deviations of about 5°C from the climatological mean northwest of

Yellowknife, while the prairies experience colder than normal conditions (Figure 9d). Subsequently, the cyclone moves eastward and intensifies along the Arctic coast of the NVT, whereas the high-pressure system has moved southeastward into the United States. Figure 9d reveals the SLP departures from the monthly climatological means at T00 responsible for the blowing snow events at Yellowknife. A decrease of up to 12 hPa in SLP to the northwest of Yellowknife, while to the southeast, an increase of up to 22 hPa in SLP from the climatological mean contributes to high wind speeds and blowing snow events near Yellowknife.

A developing anticyclone in Alaska is a dominant factor in producing blowing snow events occurring with northwesterly winds (Figure 10). This high-pressure system moves southeastward into the Yukon Territory

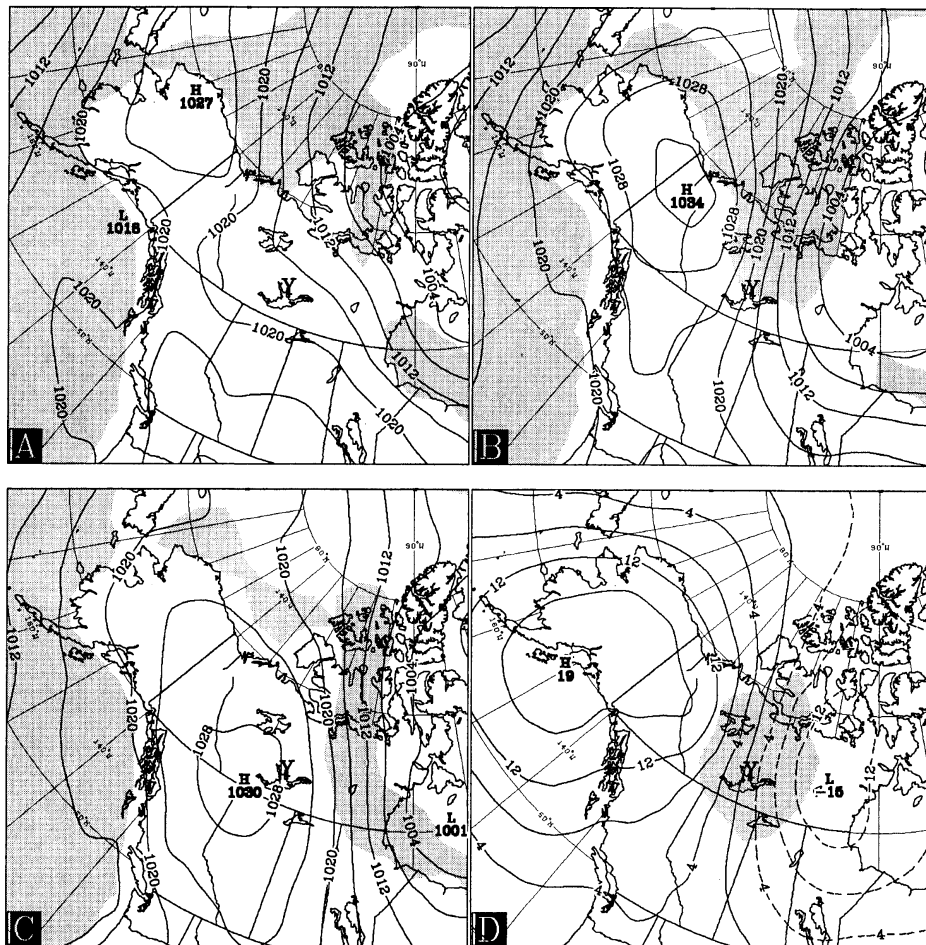


Figure 10. As in Figure 9 except for 78 blowing snow events associated with winds from the NW quadrant near Yellowknife (denoted by “Y”).

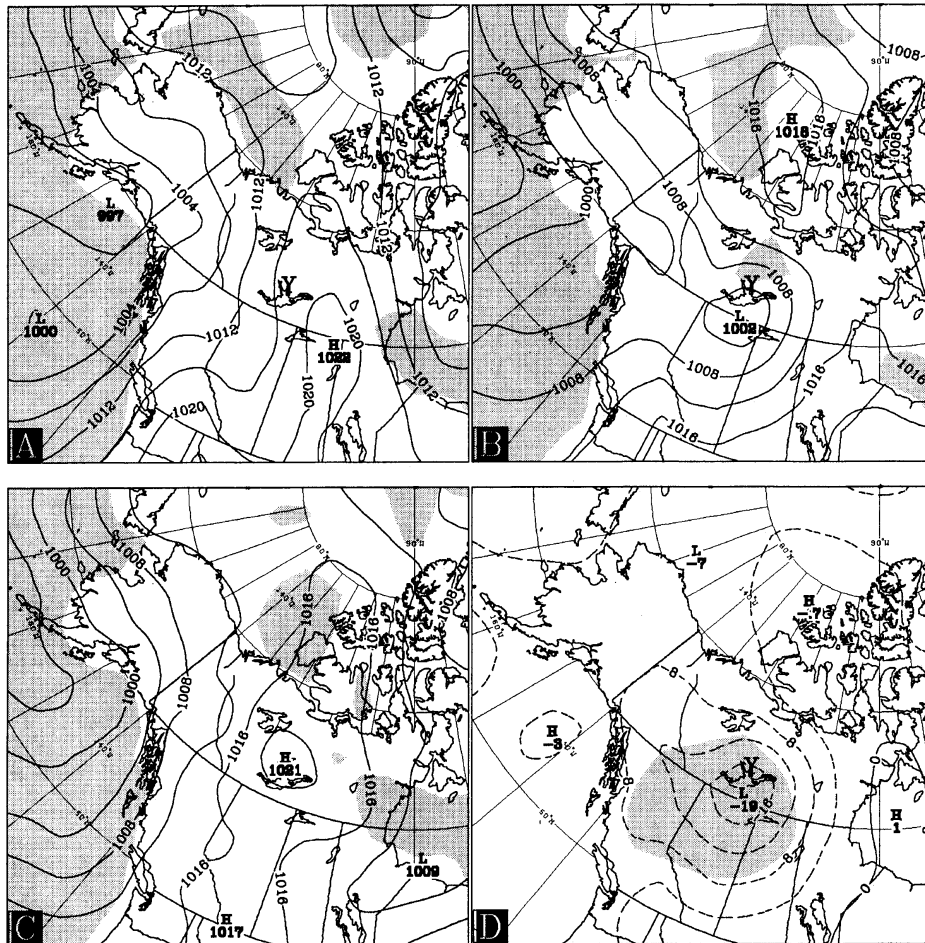


Figure 11. As in Figure 9 except for eight blowing snow events associated with winds from the NE quadrant near Yellowknife (denoted by “Y”).

(YT) at T00, while a quasi-stationary cyclone remains in the Hudson Bay area. Wind speeds reach values of 8.1 m s^{-1} , again 1.0 m s^{-1} on average above the threshold, while warmer conditions than normal prevail throughout the MRB. As in southwesterly events, there is both a maximum and minimum in SLP deviations from the climatological mean; however, positive changes in SLP are to the west of Yellowknife over Alaska and the YT, while negative changes in SLP are centered over the NVT. Warmer air than usual is also found during these blowing snow events.

Strong winds from the NE quadrant occur infrequently at Yellowknife. However, the few blowing snow events associated with northeasterly winds are associated with cyclogenesis in the lee of the Rocky Mountains in Alberta. Prior to genesis (T-24), a ridge of high

pressure dominates the SLP field over western Canada (Figure 11). However, a low in the Gulf of Alaska is also a prominent feature in this case as well. Troughing into the interior leads to cyclogenesis in central Alberta and blowing snow in Yellowknife. Subsequently, the low-pressure system moves quickly into Hudson Bay, allowing a high-pressure system to take its place near Great Slave Lake. In this case, only a strong decline in SLP with minimum of 19 hPa is notable, while surrounding areas experience little change in SLP from the climatological mean. The weaker SLP gradients signify that wind speeds are, on average, only 7.2 m s^{-1} for the northeasterly events, at least 0.5 m s^{-1} less than the other quadrants.

For the final sector, an anticyclone east of the Great Slave and Great Bear Lakes and an Aleutian low are

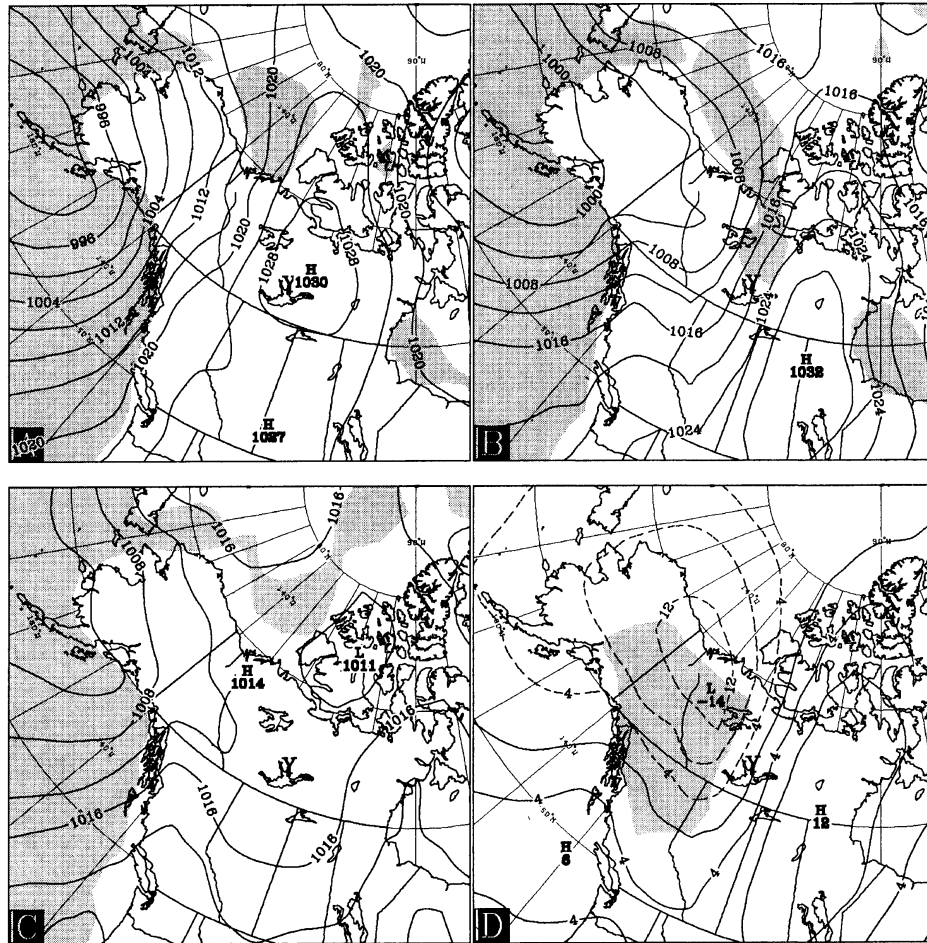


Figure 12. As in Figure 9 except for 37 blowing snow events associated with winds from the SE quadrant near Yellowknife (denoted by “Y”).

initial signatures of a blowing snow event with southeasterly winds near Yellowknife (Figure 12a). This high-pressure system propagates southeastward to lie over eastern Saskatchewan, with troughing along the Mackenzie Mountains yielding lower SLPs in the northwestern section of the basin. The strong SLP gradient results in mean wind speeds of 7.8 m s^{-1} in the Yellowknife area and warmer conditions than usual in the YT. Troughing into the MRB leads to cyclogenesis, and this low moves rapidly northeastward over the Arctic Islands at T+24 as it intensifies. As in the southwesterly cases, a decrease in SLP from the climatological mean exists to the northwest of Yellowknife, while an elongated region of positive deviations in SLP is centered to the east of Yellowknife.

For the four quadrants combined, 134 blowing snow events near Yellowknife are inferred for the 15 years of the ERA data. This is an average of about nine events annually, one less than the observed long-term climatology [Environment Canada, 1984]. Most blowing snow events at Yellowknife are observed to occur with northwesterly winds (A. C. Giles, personal communication, 1999), as we find in our climatology.

5. Concluding Discussion

Using the gridded ERA data, we have compiled a global 15-year climatology of blowing snow, blizzard, and high-windchill events. The results confirm that the blustery ice fields and ice shelves of Antarctica and

Greenland, the ice-covered Arctic Ocean and polar seas, as well as the Arctic tundra are high-frequency zones of significant winter-type weather processes. We find that the most common type of adverse cold-season processes are high-windchill episodes which occur at 9.3% of all possible grid points and times on a yearly basis, followed by blowing snow (6.5%), and then blizzard (1.4%) events. These are controlled primarily by geography (e.g., surface cover, latitude, altitude) and meteorological variables, most notably wind speed for blowing snow and blizzard events, and air temperature for high-windchill events. In the MRB, we find similar results, as fewer events occur within the boreal forest than the neighboring prairies or Arctic tundra. Trends in the frequency of events were examined and showed both monthly and interannual variability. Stormy periods at high latitudes are likely to be accompanied by higher frequencies of blowing snow and blizzard events, whereas colder than usual conditions will produce a higher number of windchill episodes.

The compositing of the near-surface fields of SLP, temperature, and wind speed has revealed some of the synoptic-scale signatures that produce blowing snow events near Yellowknife, NWT, located centrally within the MRB. The presence of strong SLP gradients producing wind speeds $>7 \text{ m s}^{-1}$ and subfreezing temperatures are the necessary ingredients to produce blowing snow over a snow-covered surface. For the four quadrants examined in section 4.3.2, we note that intensifying anticyclones are dominant features in all but one of the four composites. Additional strengthening of the SLP gradient is provided by troughing and cyclogenesis in the lee of the Mackenzie Mountains for SW and SE events and of the Rocky Mountains for NE events, while a quasi-stationary low over Hudson Bay is critical for NW events. These features lead to deviations in SLP from the monthly climatological means that show a "dipole" structure in three out of the four composites, with Yellowknife sandwiched between an area of positive and negative SLP departures. A similar dipole feature was also observed by Lackmann and Gyakum [1996] in 500 hPa geopotential height anomalies in their study of high-precipitation events in the MRB. Thus strong departures from the climatological mean SLP or 500 hPa geopotential heights in the vicinity of Yellowknife are conducive to adverse meteorological conditions there. We also noted positive temperature deviations from the climatological means near or at Yellowknife in all four composites. The prevalence of cold anticyclones and accompanying calm weather in this region during winter indicates that stormy periods are generally associated with warmer than average temperatures in the MRB.

The results in this paper have focused on the frequency of blowing snow events, since the water budget of nival regimes can be influenced by two related processes: (1) the redistribution of snow by wind can lead to significant erosion of mass in open, windswept areas and accumulation in others and (2) the concurrent

transfer of ice particles to water vapor during transport can lead to further snowpack depletion. A number of recent studies have assessed the contribution of these processes to the surface mass balance, with significant variation on the importance of the blowing snow sublimation component [King *et al.*, 1996; Pomeroy *et al.*, 1997; Bintanja, 1998]. To that effect, Déry and Taylor [1996] and Déry *et al.* [1998] have developed a blowing snow model named PIEKTUK that considers the negative thermodynamic feedbacks of the blowing snow sublimation process in the ABL. They conclude that in some circumstances this process is self-limiting, thus supporting studies that yield lower estimates of the blowing snow sublimation component to the surface water budget. With blowing snow occurring rarely over the forested areas of the MRB, the water budget for the basin will not likely be affected if storms and strong wind conditions are confined to the southern portion of the MRB. However, when storms and strong wind conditions affect the northern part of the basin occupied by Arctic tundra, the blowing snow component may not be negligible. We are presently coupling a modified version of PIEKTUK to the Mesoscale Compressible Community (MC2) model [Benoit *et al.*, 1997] to provide more accurate evaluations of the importance of blowing snow in the cold-season water budget of such regions.

Acknowledgments. We thank M. L. Branick (NOAA), A. C. Giles (AES), and J. R. Gyakum (McGill University) for providing us with unpublished data that enhanced this study. We are grateful to M. Carrera, J. Milbrandt (McGill University), and P. A. Taylor (York University) for their comments. This research was supported by the National Science and Engineering Research Council of Canada through a GEWEX collaborative research network grant.

References

- Alvarez, J. A., and B. J. Lieske, The little America blizzard of May 1957, in *Antarctic Meteorology*, edited by L. J. Dwyer, pp. 115-127, Pergamon, Tarrytown, N. Y., 1960.
- Atmospheric Environment Service, *MANPUB: Manual of Standard Procedures for Public Weather Service*, 5th ed., Environ. Can., Downsview, 1988.
- Babin, G., Blizzard of 1975 in Western Canada, *Weatherwise*, 28, 70-75, 1975.
- Barry, R. G., *Mountain Weather and Climate*, 2nd ed., 402 pp., Routledge, New York, 1992.
- Benoit, R., M. Desgagné, P. Pellerin, S. Pellerin, and Y. Chartier, The Canadian MC2: A semi-Lagrangian, semi-implicit wideband atmospheric model suited for finescale process studies and simulation, *Mon. Weather Rev.*, 125, 2382-2415, 1997.
- Berg, N. H., Blowing snow at a Colorado alpine site: Measurements and implications, *Arct. Alp. Res.*, 18, 147-161, 1986.
- Bintanja, R., The contribution of snowdrift sublimation to the surface mass balance of Antarctica, *Ann. Glaciol.*, 27, 251-259, 1998.
- Bluestein, H. B., *Synoptic-Dynamic Meteorology in Midlatitudes, Vol. 2: Observations and Theory of Weather Systems*, 594 pp., Oxford Univ. Press, New York, 1993.
- Branick, M. L., A climatology of significant winter-type

- weather events in the contiguous United States, 1982-94, *Weather Forecasting*, 12, 193-207, 1997.
- Burns, B. M., *The Climate of the Mackenzie Valley - Beaufort Sea*, vol. 1, *Climatol. Stud.* 24, 227 pp., Atmos. Environ. Ser., Environ. Can., Toronto, Ont., 1973.
- Burrows, W. R., R. A. Treidl, and R. G. Lawford, The Southern Ontario blizzard of January 26 and 27, 1978, *Atmos. Ocean*, 17, 306-320, 1979.
- Cohen, S. J., What if and so what in Northwest Canada: Could climate change make a difference to the future of the Mackenzie Basin?, *Arctic*, 50, 293-307, 1997a.
- Cohen, S. J. (Ed.), *Mackenzie Basin Impact Study (MBIS) Final Report*, 372 pp., Environ. Can., Downsview, 1997b.
- Déry, S. J., and P. A. Taylor, Some aspects of the interaction of blowing snow with the atmospheric boundary layer, *Hydrol. Proc.*, 10, 1345-1358, 1996.
- Déry, S. J., P. A. Taylor, and J. Xiao, The thermodynamic effects of sublimating, blowing snow in the atmospheric boundary layer, *Boundary Layer Meteorol.*, 89(2), 251-283, 1998.
- Eagleman, J. R., *Severe and Unusual Weather*, 2nd ed., 372 pp., Van Nostrand Reinhold, New York, 1990.
- Environment Canada, *Principal Station Data*, vol. 34, *Yellowknife A*, 48 pp., Atmos. Environ. Ser., Toronto, Ont., 1984.
- Environment Canada, *Canadian Climate Normals, 1961-1990*, vol. 3, *The North: Yukon and Northwest Territories*, 58 pp., Atmos. Environ. Ser., Toronto, Ont., 1993.
- Gibson, J. K., P. Källberg, S. Uppala, A. Hernandez, A. Nomura, E. Serrano, *ERA Description*, ECMWF Re-Analysis Project Report Series, vol. 1, 72 pp., Eur. Cent. for Medium-Range Weather Forecasts, Reading, England, 1997.
- Graff, J. V., and J. H. Strub, The Great Upper Plains blizzard of January 1975, *Weatherwise*, 28, 66-69, 1975.
- Huo, Z., D.-L. Zhang, J. Gyakum, and A. Staniforth, A diagnostic analysis of the Superstorm of March 1993, *Mon. Weather Rev.*, 123(6), 1740-1761, 1995.
- Källberg, P., *Aspects of the Re-Analysed Climate*, ECMWF Re-Analysis Project Report Series, vol. 2, 89 pp., Eur. Cent. for Medium-Range Weather Forecasts, Reading, England, 1997.
- Kind, R. J., Snowdrifting, in *Handbook of Snow - Principles, Processes, Management & Use*, edited by D. M. Gray and D. H. Male, pp. 338-359, Pergamon, Tarrytown, N. Y., 1981.
- King, J. C., and J. Turner, *Antarctic Meteorology and Climatology*, 409 pp., Cambridge Univ. Press, New York, 1997.
- King, J. C., P. S. Anderson, M. C. Smith, and S. D. Mobbs, The surface energy and mass balance at Halley, Antarctica during winter, *J. Geophys. Res.*, 101(D14), 19,119-19,128, 1996.
- Kocin, P. J., and L. W. Uccellini, *Snowstorms along the Northeastern Coast of the United States: 1955 to 1985*, *Meteorol. Monogr.* 44, 280 pp., Am. Meteorol. Soc., Washington, D. C., 1990.
- Lackmann, G. M., and J. R. Gyakum, The synoptic- and planetary-scale signatures of precipitating systems over the Mackenzie River Basin, *Atmos. Ocean*, 34(4), 647-674, 1996.
- Lawford, R. G., The role of ice in the global water cycle, in *Macroscopic Modelling of the Hydrosphere*, edited by W. B. Wilkinson, *IAHS Publ.*, 214, 151-161, 1993.
- Lawford, R. G., Knowns and unknowns in the hydroclimatology of the Mackenzie River Basin, in *Mackenzie Basin Impact Study (MBIS), Interim Rep.* 2, edited by S. D. Cohen, pp. 173-195, Yellowknife, NWT, 1994.
- Lawson, B., The climatology of blizzards in western Canada 1953-1986, *Cent. Reg. Rep. CAES 88-1*, Atmos. Environ. Ser., Environ. Can., Winnipeg, Man., 1987.
- Li, L., and J. W. Pomeroy, Estimates of threshold wind speeds for snow transport using meteorological data, *J. Appl. Meteorol.*, 36, 205-213, 1997.
- Lydolph, P. E., *Climates of the Soviet Union, World Surv. of Climatol.*, vol. 7, 443 pp., Elsevier, New York, 1977.
- Maxwell, J. B., *The Climate of the Canadian Arctic Islands and Adjacent Waters*, vol. 1, *Climatol. Stud.* 30, 532 pp., Atmos. Environ. Ser., Environ. Can., Winnipeg, Man., 1980.
- Mikhel', V. M., A. V. Rudneva, and V. I. Lipovskaya, *Snowfall and Snow Transport During Snowstorms over the USSR*, 174 pp., Engl. Transl., Main Admin. of the Hydrometeorol. Ser. of the Counc. of Minist. of the USSR, Leningrad, 1971.
- Phillips, D., *Climates of Canada*, 176 pp., Environ. Can., Ottawa, Ont., 1990.
- Pomeroy, J. W., and B. E. Goodison, Winter and snow, in *Surface Climates of Canada*, edited by W. G. Bailey, T. R. Oke, and W. R. Rouse, pp. 68-100, McGill Queen's Press, Montreal, Que., 1997.
- Pomeroy, J. W., P. Marsh, and D. M. Gray, Application of a distributed blowing snow model to the Arctic, *Hydrol. Proc.*, 11, 1451-1464, 1997.
- Salmon, E. M., and P. J. Smith, A synoptic analysis of the 25-26 January 1978 blizzard cyclone in the Central United States, *Bull. Am. Meteorol. Soc.*, 61, 453-460, 1980.
- Schmidt, R. A., Threshold wind-speeds and elastic impact in snow transport, *J. Glaciol.*, 26, 453-467, 1980.
- Schwerdtfeger, W., The climate of the Antarctic, in *Climate of the Polar Regions, World Surv. of Climatol.*, vol. 7, edited by S. Orvig, pp. 253-355, Elsevier, New York, 1970.
- Siple, P. A., and C. F. Passel, Measurements of dry atmospheric cooling in subfreezing temperatures, *Proc. Am. Philos. Soc.*, 89, 177-199, 1945.
- Slingo, A., J. A. Pamment, and M. J. Webb, A 15-year simulation of the clear-sky greenhouse effect using the ECMWF reanalyses: Fluxes and comparisons with ERBE, *J. Clim.*, 11, 690-708, 1998.
- Steadman, R. G., Indices of windchill of clothed persons, *J. Appl. Meteorol.*, 10, 674-683, 1971.
- Stewart, R. E., D. Bachan, R. R. Dunkley, A. C. Giles, B. Lawson, L. Legal, S. T. Miller, B. P. Murphy, M. N. Parker, B. J. Paruk, and M. K. Yau, Winter storms over Canada, *Atmos. Ocean*, 33, 223-247, 1995a.
- Stewart, R. E., D. T. Yiu, K. K. Chung, D. R. Hudak, E. P. Lozowski, M. Oleski, B. E. Sheppard, and K. K. Szeto, Weather conditions associated with the passage of precipitation type transition regions over Eastern Newfoundland, *Atmos. Ocean*, 33, 25-53, 1995b.
- Stewart, R. E., H. G. Leighton, P. Marsh, G. W. K. Moore, W. R. Rouse, S. D. Soulis, G. S. Strong, R. W. Crawford, and B. Kochtubajda, The Mackenzie GEWEX Study: The water and energy cycles of a major North American river basin, *Bull. Am. Meteorol. Soc.*, 79(12), 2665-2684, 1998.
- Szeto, K. K., and R. E. Stewart, Cloud model simulations of surface weather elements associated with warm frontal regions of winter storms, *Atmos. Res.*, 44, 243-269, 1997.
- Tabler, R. D., Visibility in blowing snow and applications in traffic operations, in *Snow Removal and Ice Control Research, Spec. Rep. 185*, pp. 208-214, Natl. Acad. of Sci., Washington, D. C., 1979.
- Wild, R., Definition of the British blizzard, *Weather*, 50, 327-328, 1995.
- Wild, R., G. O'Hare, and R. Wilby, A historical record of blizzards/major snow events in the British Isles, 1880-1989, *Weather*, 51, 82-91, 1996.

16,672

DÉRY AND YAU: CLIMATOLOGY OF WINTER-TYPE WEATHER EVENTS

Wilks, D. S., *Statistical Methods in the Atmospheric Sciences*, 467 pp., Academic, San Diego, Calif., 1995.

Woo, M.-K., and A. Ohmura, The Arctic Islands, in *Surface Climates of Canada*, edited by W. G. Bailey, T. R. Oke, and W. R. Rouse, pp. 172-197, McGill Queen's Press, Montreal, Que, 1997.

brooke Street West, Montréal, Québec, H3A 2K6, Canada.
(steph@zephyr.meteo.mcgill.ca;
yau@rainband.meteo.mcgill.ca)

S. J. Déry and M. K. Yau, Department of Atmospheric and Oceanic Sciences, McGill University, 805 Sher-

(Received November 18, 1998; revised March 4, 1999;
accepted March 4, 1999.)

Chapter 3

Mass Balance

3.1 Presentation of Article 2

The climatology presented in the previous chapter provides us with an idea as to the locations where blowing snow may have a significant impact to the surface mass balance. In this chapter, we extend these results by quantifying the role blowing snow sublimation and transport, as well as surface sublimation, exert in the water budget of high-latitude regions. Parametrizations describing the blowing snow transport and sublimation rates are applied during blowing snow events that are, once again, inferred from the European Centre for Medium-Range Weather Forecasts (ECMWF) Re-Analysis (ERA) data. For completeness, surface sublimation is computed at all other times when temperatures are subfreezing. Two sensitivity studies with regard to the background thermodynamic conditions during blowing snow are conducted and are followed by comparisons with other large-scale mass

balance studies.

3.2 Article 2

The large-scale mass balance effects of blowing snow and surface sublimation. By Stephen J. Déry and M. K. Yau, 2001: submitted to *J. Geophys. Res.*

The large-scale mass balance effects of blowing snow and surface sublimation

Stephen J. Déry and M. K. Yau

Department of Atmospheric and Oceanic Sciences, McGill University
Montréal, Québec

Submitted to *Journal of Geophysical Research*

Abstract

This study examines the effects of surface sublimation and blowing snow to the surface mass balance on a global and basin scale using the ECMWF Re-Analysis data at a resolution of 2.5° that span the years 1979-1993. Both surface and blowing snow sublimation play significant roles in the water budget of high-latitude regions. However, we find that near-surface air over large portions of the Northern Hemisphere and, to a lesser degree, the Southern Hemisphere, is often supersaturated with respect to ice, inhibiting these two processes. Nevertheless, the combined processes of surface (60%) and blowing snow (40%) sublimation are estimated to remove 20 mm a^{-1} snow water equivalent (swe) over Antarctica. In the Northern Hemisphere, these processes are generally less important in continental areas than over the frozen Arctic Ocean and polar seas where surface and blowing snow sublimation deplete

upwards of 10 mm a^{-1} swe. Areas with frequent blowing snow episodes such as the coastal regions of Antarctica and the Arctic Ocean are also prone to a mass transport $> 100 \text{ Mg m}^{-1} \text{ a}^{-1}$. Although important locally, values of the divergence of mass through wind redistribution are generally two orders of magnitude less than surface and blowing snow sublimation when averaged over large areas. For the entire Mackenzie River Basin of Canada, deposition overwhelms the effects of blowing snow as mass accumulates to the rate of 0.4 mm a^{-1} swe when the effects of these processes is summed.

1 Introduction

At high latitudes and altitudes, precipitation tends to fall in the form of snow that accumulates at the surface. A nival regime constitutes an important form of storage for water which may be released during melt to the environment or accumulated into an ice sheet if subfreezing conditions persist.

Movement of air above a snowpack impacts the surface mass balance in several ways. For instance, wind may remove snow from easily erodible surfaces to deposit it in accumulation areas such as depressions and bushes, leading to substantial heterogeneities in the snowcover with hydrometeorological implications. In subsaturated air with respect to ice, the sublimation (phase change of ice to water vapor) of suspended blowing snow particles may represent an additional sink of mass from the surface. In a process referred here to as surface sublimation, supplemental water vapor may be directly transferred between the atmospheric boundary layer (ABL) and the snowpack, even when wind speeds do not exceed the threshold for transport

of snow.

The Mackenzie River Basin (MRB) of Northwestern Canada is one region susceptible to long seasonal snowcovers, with some sections of the basin blanketed by snow more than 200 days a year (Phillips, 1990). Being ubiquitous in the MRB, processes involving snow and ice may therefore impact significantly its surface water budget (Stewart et al., 2000). For instance, Déry and Yau (1999a, 2001) showed that blowing snow occurs up to 60 days annually over the northern sections of the MRB. To examine the contribution of surface and blowing snow sublimation and transport to the MRB's water budget, we use gridded re-analysis data that are global and therefore present results for both hemispheres in addition to the MRB. The MRB is our principal area of interest as it is subject to an intensive field campaign titled the Mackenzie GEWEX Study (MAGS; Stewart et al., 1998; Rouse, 2000) launched to provide further information on the water and energy cycles of this large northern basin.

The paper begins with some background information on the processes affecting the surface mass balance of cold regions, with special attention given to the surface sublimation and blowing snow components. Subsequently, the methodology is described followed by some results, sensitivity tests, and then comparisons with other studies. The paper closes with a concluding discussion of our findings.

2 Background

2.1 Mass Balance

Several cold-season processes may influence the water budget of a snow-covered surface. Following King et al. (1996), the annual surface mass balance for a nival regime may be expressed as:

$$S = P - E - M - D - Q_s \quad (1)$$

where S is the storage or accumulation of snow at the surface (in mm a^{-1} snow water equivalent, swe), P is the precipitation rate (in mm a^{-1} swe, positive downward), E is the evaporation rate which includes the surface sublimation rate Q_{surf} (both in mm a^{-1} swe, positive upward), and M is the divergence of water after melt and runoff (in mm a^{-1} swe). The two terms associated with blowing snow are represented by D and Q_s , the divergence of snow by wind transport (in mm a^{-1} swe) and the sublimation of blowing snow, (in mm a^{-1} swe, positive upward) respectively.

There has been recently substantial effort in the literature to determine the amount of precipitation less evaporation ($P - E$) in the polar regions, notably for Antarctica (e.g., Giovinetto et al., 1992; Connelley and King, 1996; Cullather et al., 1998; Turner et al., 1999) as well as for the ice-covered Arctic Ocean (Walsh et al., 1994, 1998; Cullather et al., 2000). In most cases, these studies have neglected terms linked to blowing snow as they were considered negligible, at least on a continental scale (Connelley and King, 1996; Turner et al., 1999). Nevertheless, Giovinetto et al. (1992) estimate a net transport of about 120×10^{12} kg a^{-1} of mass northward

across 70°S through blowing snow, equivalent to the removal of 4.8 mm a⁻¹ swe over the area south of that latitude. Other authors have suggested that the sublimation of blowing snow may also erode substantial amounts of mass from the Antarctic continent (e.g., Bintanja, 1998; Gallée, 1998) or the Arctic tundra (Pomeroy et al., 1997; Essery et al., 1999). Few studies have examined the individual contribution of surface sublimation to the water budget of polar regions on a continental or basin scale, with perhaps the exception of van den Broeke (1997).

For the MRB, precipitation and evaporation estimates vary considerably, in part due to the lack of observations in the basin, most notably in the Mackenzie Mountains. Current estimates have the annual ($P - E$) averaged for the MRB to be at 180 mm a⁻¹ (Stewart et al., 1998). Although much attention has been recently given to the influx and efflux of atmospheric water vapour in the MRB domain (Bjornsson et al., 1995; Lackmann and Gyakum 1996; Lackmann et al., 1998; Smirnov and Moore, 1999; Misra et al., 2000), none of these authors have attempted to evaluate the impact of blowing snow to the surface mass balance of the MRB as a whole. Although Walsh et al. (1994) and Betts and Viterbo (2000) examine the role of surface sublimation in the MRB, the authors come to contradictory conclusions, with the former yielding significant deposition during wintertime over the MRB and the latter strong sublimation. The lack of accurate (if any) information on the role of blowing snow and surface sublimation in the water balance of cold climate regions including the MRB warrants this study.

2.2 Humidity

Before we proceed, a brief discussion on the issue of the ambient humidity is required since sublimation processes depend in part on the moisture content of the ABL. To derive the relative humidity with respect to ice RH_i from the dewpoint temperature, we may use the Magnus equation to compute the saturation mixing ratio over ice q_{si} (kg kg^{-1}) (Kong and Yau, 1997; Pruppacher and Klett, 1997):

$$q_{si} = \frac{3.8}{P_s} \exp\left(\frac{21.87(T_a - T_0)}{(T_a - 7.66)}\right), \quad (2)$$

where P_s is the surface atmospheric pressure (hPa), T_a the air temperature (K) and T_0 a constant with a value of 273.16 K. Similarly, the saturation mixing ratio over water q_s (kg kg^{-1}) is obtained by (Kong and Yau, 1997):

$$q_s = \frac{3.8}{P_s} \exp\left(\frac{17.27(T_a - T_0)}{(T_a - 35.86)}\right). \quad (3)$$

Given the dewpoint temperature T_d (K), we may then compute the specific humidity q_v (kg kg^{-1}) in the air by substituting T_a by T_d in Equation (3). Then the relative humidity with respect to ice is simply $\text{RH}_i = q_v/q_{si}$ while the relative humidity with respect to water $\text{RH}_w = q_v/q_s$. Since at subfreezing temperatures $q_{si} \leq q_s$ at all times, it is possible that air subsaturated with respect to water may be supersaturated with respect to ice, thereby promoting deposition rather than sublimation. This issue will be discussed at length later in the paper.

2.3 Surface Sublimation

Surface sublimation represents the continual exchange of water between the air (in the vapor phase) to or from the ice- or snowpack (in the solid phase). Here, we follow the methodology of van den Broeke (1997) by estimating Q_{surf} from

$$Q_{surf} = \rho' u_* q_*, \quad (4)$$

where u_* (m s^{-1}) is the friction velocity and ρ' (negative) is a conversion factor to units of mm a^{-1} swe. Assuming neutral stability near the surface and a logarithmic variation of wind speed with height, u_* can be obtained from (Garratt, 1992):

$$u_* = \frac{\kappa U}{\ln\left(\frac{z+z_0}{z_0}\right)}, \quad (5)$$

in which U (m s^{-1}) is the wind speed at a height z (m) above the surface, κ ($= 0.4$) depicts the von Kármán constant and z_0 (m) represents the aerodynamic roughness length for momentum. In a similar fashion, the humidity scale q_* (kg kg^{-1}) is deduced from a logarithmic moisture profile by assuming saturation with respect to ice near the surface such that (Garratt, 1992):

$$q_* = \frac{\kappa q_{si} (\text{RH}_i - 1)}{\ln\left(\frac{z+z_q}{z_q}\right)}, \quad (6)$$

in which z_q (m), taken here as equal to z_0 , denotes the roughness length for moisture over snow. Surface sublimation therefore depends critically on the gradients of

both humidity and wind speed near the surface. Note that when $\text{RH}_i > 1.0$ and q_* becomes positive, deposition to the surface (or negative sublimation) is said to occur. For simplicity, we neglect additional sublimation from snow-covered vegetation canopies which can enhance the overall sublimation rate (Schmidt, 1991).

2.4 Blowing Snow Sublimation

Blowing snow occurs when loose particles of snow are entrained by winds exceeding a certain threshold for transport. As particles become suspended in a subsaturated (with respect to ice) ABL, they sublime at relatively fast rates despite exhibiting certain self-limiting properties (D ery et al., 1998; D ery and Yau, 1999b; 2001). The modeling of blowing snow has recently attracted much interest in the hydro-meteorological community given its possible twofold impact to the water budget of snow-covered regions (e.g., Bintanja, 1998; Essery et al., 1999; Xiao et al., 2000).

Although Bintanja (1998) and Essery et al. (1999) provide parameterizations for the sublimation rate of blowing snow, D ery and Yau (2001) point out that neither considers the evolving and limiting thermodynamic conditions arising during snow transport. Therefore, to estimate blowing snow sublimation, we use here a parameterization for Q_s derived by D ery and Yau (2001) based on the development of a double-moment blowing snow model (PIEKTUK-D). The authors found that the relationship

$$Q_s = (a_0 + a_1\xi + a_2\xi^2 + a_3\xi^3 + a_4U_{10} + a_5\xi U_{10} + a_6\xi^2 U_{10} + a_7U_{10}^2 + a_8\xi U_{10}^2 + a_9U_{10}^3)/U', \quad (7)$$

provided very good estimates ($R^2 = 0.95$) of Q_s (here in units of mm d^{-1} swe) at a Canadian Arctic location (Déry and Yau, 2001). Equation (7) shows that the rate of blowing snow sublimation depends on the 2-m air temperature and humidity through a thermodynamic term ξ ($-1 \times 10^{-12} \text{ m}^2 \text{ s}^{-1}$) as well as on the 10-m wind speed U_{10} (m s^{-1}). Note also that the relationship is normalized by a factor U' (dimensionless) to remove a dependence on the saltation mixing ratio and that values for the coefficients $a_0 - a_9$ are given by Déry and Yau (2001).

2.5 Blowing Snow Transport

A number of empirical relationships describing the transport of blowing snow in terms of the wind speed can be found in the literature, as summarized by both Giovinetto et al. (1992) and Pomeroy and Gray (1995). Since the results of Pomeroy and Gray (1995) are based on measurements conducted in the Canadian prairies which extend into the southern sections of the MRB, we follow their results which express Q_t ($\text{kg m}^{-1} \text{ s}^{-1}$) as:

$$Q_t = B U_{10}^C, \quad (8)$$

where $B = 2.2 \times 10^{-6} \text{ kg s}^{3.04} \text{ m}^{-5.04}$ and $C = 4.04$. Once the blowing snow transport rate is known, its net contribution to the surface mass balance is found by

$$D = -\frac{\rho'}{\rho} \nabla \cdot Q_t, \quad (9)$$

with ρ (kg m^{-3}) being the air density. Note that positive values of D indicate divergence of mass through wind redistribution, and hence a sink in the mass balance equation.

3 Methodology

3.1 Data and Events

The gridded data used in this study are the 6-hourly European Centre for Medium-Range Weather Forecasts (ECMWF) Re-Analysis (ERA) data on a 2.5° latitude/longitude grid covering the period from 1979 to 1993 inclusive (Gibson et al., 1997). Before applying the relationships for the computations of blowing snow transport and sublimation, a “blowing snow event” must be inferred from the ERA data and here we follow the method of Déry and Yau (1999a) to detect these events. Briefly, they define a blowing snow event as any time when the near-surface temperature is subfreezing and a threshold wind speed for transport, computed following Li and Pomeroy (1997), are met at a grid point where the surface is snow-covered land or sea ice (in concentration of more than 50%). A “surface sublimation event” occurs when all the criteria for a blowing event are met except that winds must be less than the specified threshold for transport.

Once a surface sublimation or a blowing snow event has been detected, Q_{surf} , Q_s and Q_t are computed following the equations reported in the previous section. These rates are assumed constant for the 6-hour periods of the ERA data. However, we ensure that the mass eroded through any of these processes does not exceed that

present at the surface as deduced from the ERA data. Note that we compute RH_i only when air temperatures are below the freezing point. In the event that RH_i is > 1.0 , we set Q_s to zero despite the inference of a blowing snow event. According to Déry and Yau (2001), this can lead to the underevaluation of the total blowing snow sublimation rate. Therefore, an additional experiment is conducted in Section 5 to test the sensitivity of the results to this assumption. Nonetheless, deposition to the surface is computed when $RH_i > 1.0$. Once the data have been compiled for the 15 years that span the ERA data, we present our results using a polar stereographic projection since blowing snow and sublimation events occur most frequently in polar regions. The new grids are composed of 50×50 points centered over the poles and have a horizontal resolution of 250 km true at 60°N or S.

3.2 Biases and Limitations

As noted by Gibson et al. (1997), the ERA exhibits wind speed and temperature biases. Déry and Yau (1999a) examined these biases at several high-latitude climatological stations and observed the negative air temperature bias described by Gibson et al. (1997). This temperature bias will not affect much the calculations of Q_t but may reduce values of Q_{surf} and Q_s as both depend on T_a and RH_i . Wind speeds deduced from the ERA are generally less than observed for Antarctica (Déry and Yau, 1999a) and this feature tends to reduce the blowing snow transport and sublimation rates there. Note however that the temperature and wind speed biases also have an effect on the determination of the blowing snow events through the threshold wind speed for transport.

Despite the accuracy of the ERA to reproduce well the large-scale atmospheric

environment, using these near-surface data at a resolution of 2.5° and at 6 h intervals imposes certain limitations on the veracity of the results presented in the following section. Since the surface sublimation, blowing snow sublimation and transport rates vary nonlinearly with the ambient conditions of wind speed, temperature and humidity, the temporally and spatially averaged meteorological fields may mask natural variability and extreme events. For instance, katabatic winds over the Greenland and Antarctic ice fields are not necessarily well reproduced within the ERA and may lead to a possible underestimation of blowing snow fluxes in these regions (Déry and Yau, 1999a). Since the meteorological variables can vary substantially on the mesoscale, we caution the reader that the results presented herein depict solely the large-scale impacts of surface sublimation and blowing snow to the surface mass balance. Thus significant variations from the results can be expected on the subgrid-scale. This renders the validation of our results with point observations somewhat difficult. We therefore postpone to the final section comparisons of our findings with other continental-scale studies of the surface mass balance at high-latitude regions as a mean to validate the results herein.

4 Results

As was stated earlier, both blowing snow and surface sublimation depend highly on conditions of RH_i near the surface. We first present, therefore, average values of RH_i when $T_a < 0^\circ\text{C}$ in both hemispheres (Figure 1). This shows that in the Northern Hemisphere, on average for the period 1979 to 1993, saturated to supersaturated conditions (with respect to ice) exist over most of the ice-covered Arctic Ocean and the Greenland ice sheet (Figure 1a). Over snow-covered land surfaces of

Russia, Alaska and Northern Canada, including the MRB, the ERA also exhibits supersaturation with respect to ice. However, in more southern regions such as the Canadian prairies and United States Midwestern Plains, RH_i is on average less than unity. Despite the high frequency of blowing snow events reported by Déry and Yau (1999a) over the Arctic tundra and the ice-covered Arctic Ocean, the prevalence of supersaturated conditions will reduce the potential contribution of blowing snow sublimation there.

In the Southern Hemisphere, we find greater spatial variability of RH_i values over the Antarctic ice sheet, with some regions showing a yearly mean supersaturation with respect to ice as high as 20% (Figure 1b). Lower RH_i values are found along the Antarctic coastline and over sea ice.

Figure 2 depicts the zonal average of RH_i , with and without the occurrence of blowing snow events. We see that at high latitudes, conditions of supersaturation with respect to ice are persistent throughout the cold season, with higher values of RH_i observed during blowing snow events. In addition to the cold temperatures, these ambient humidity conditions will inhibit near-surface blowing snow sublimation.

Figure 3 confirms that surface sublimation is small over most continental regions such as the Arctic tundra of Canada and Siberia, and the Greenland and Antarctic ice fields. In the Northern Hemisphere, surface sublimation reaches values $> 10 \text{ mm a}^{-1}$ swe only over ice-covered regions. Deposition, rather than sublimation, predominates the area drained by the Mackenzie River. However a different scenario exists along coastal sections of Antarctica and neighboring sea ice as maximum values of Q_{surf} reach 50 mm a^{-1} swe or more. Significant deposition is nonetheless

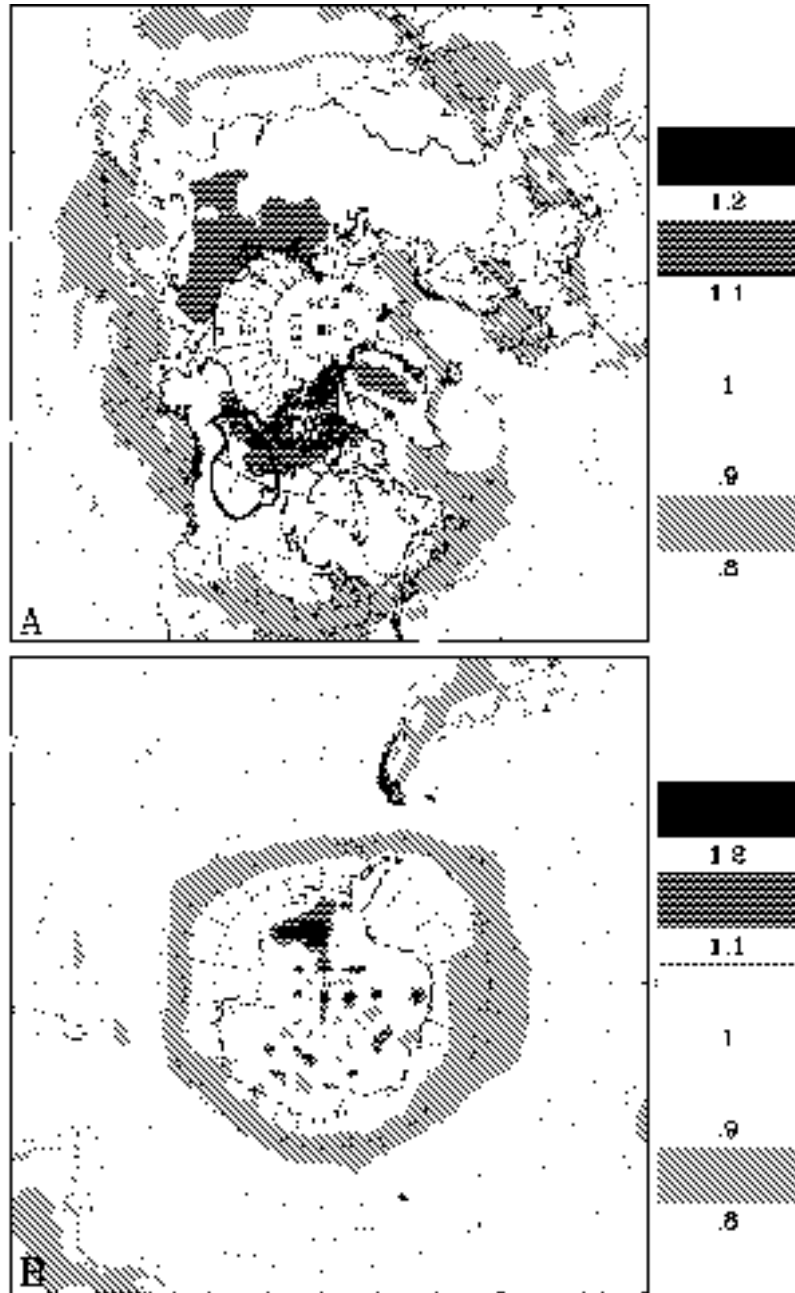


FIGURE 1: The mean relative humidity with respect to ice for the period 1979-1993 when $T_a < 0^\circ\text{C}$ in (a) the Northern Hemisphere and (b) the Southern Hemisphere. In this and subsequent figures, the Mackenzie River Basin is outlined in bold in the Northern Hemisphere.

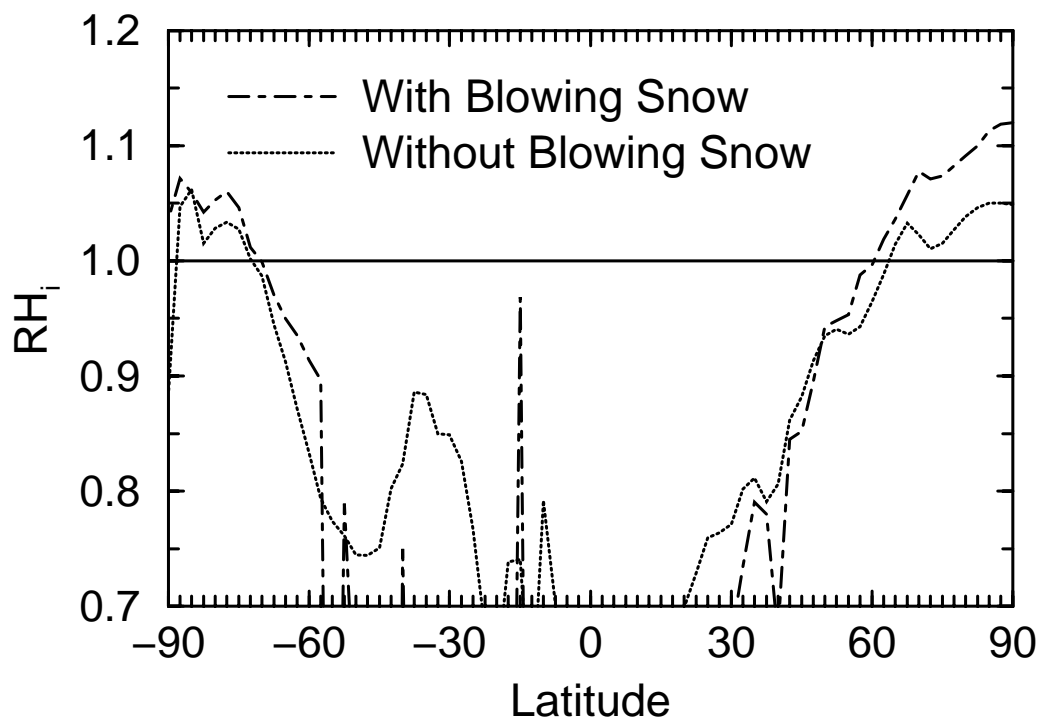


FIGURE 2: The zonally-averaged relative humidity with respect to ice with and without blowing snow for the period 1979-1993 when $T_a < 0^\circ\text{C}$.

inferred over the mountainous regions of the Antarctic Peninsula and Victoria Land west of the Ross Ice Shelf. Surface sublimation remains negligible over the interior of the Antarctic continent where conditions are much colder than in the boreal polar region (e.g., the mean annual temperature at the South and North Pole is $\approx -50^\circ\text{C}$ and -15°C , respectively).

The sublimation of blowing snow computed following Equation (7) is shown in Figure 4 to contribute significantly to the water budget of snow-covered sea ice in the Southern Hemisphere and, to a lesser extent, in the Northern Hemisphere. Continental regions such as the MRB are generally not influenced by blowing snow sublimation with the exception of northern areas where high winds enhance the sublimation process. Q_s reaches values $\geq 50 \text{ mm a}^{-1}$ swe along the western Antarctic coastline but attains values only $\geq 20 \text{ mm a}^{-1}$ swe between Greenland and Iceland in the Northern Hemisphere. The Arctic Ocean is more susceptible to blowing snow events (Déry and Yau, 1999a) and therefore experiences greater effects of snowdrift sublimation than the interior of Antarctica.

Since the criteria for a blowing snow event are met to apply the transport calculations, we find that, as expected, areas with the most blowing snow events (see Déry and Yau, 1999a) coincide with locations of large mass transport (Figure 5). Some sections of Greenland, the frozen Arctic Ocean and Antarctica are subject to the redistribution $100 \text{ Mg m}^{-1} \text{ a}^{-1}$ or more. Note also the local maximum in snow transport in the Canadian prairies and United States Great Plains where blowing snow is more frequent than in neighboring forested regions to the north such as the MRB. Only northern and northeastern sections of the MRB are prone to large mass redistribution (of the order of $5 \text{ Mg m}^{-1} \text{ a}^{-1}$) through wind transport.

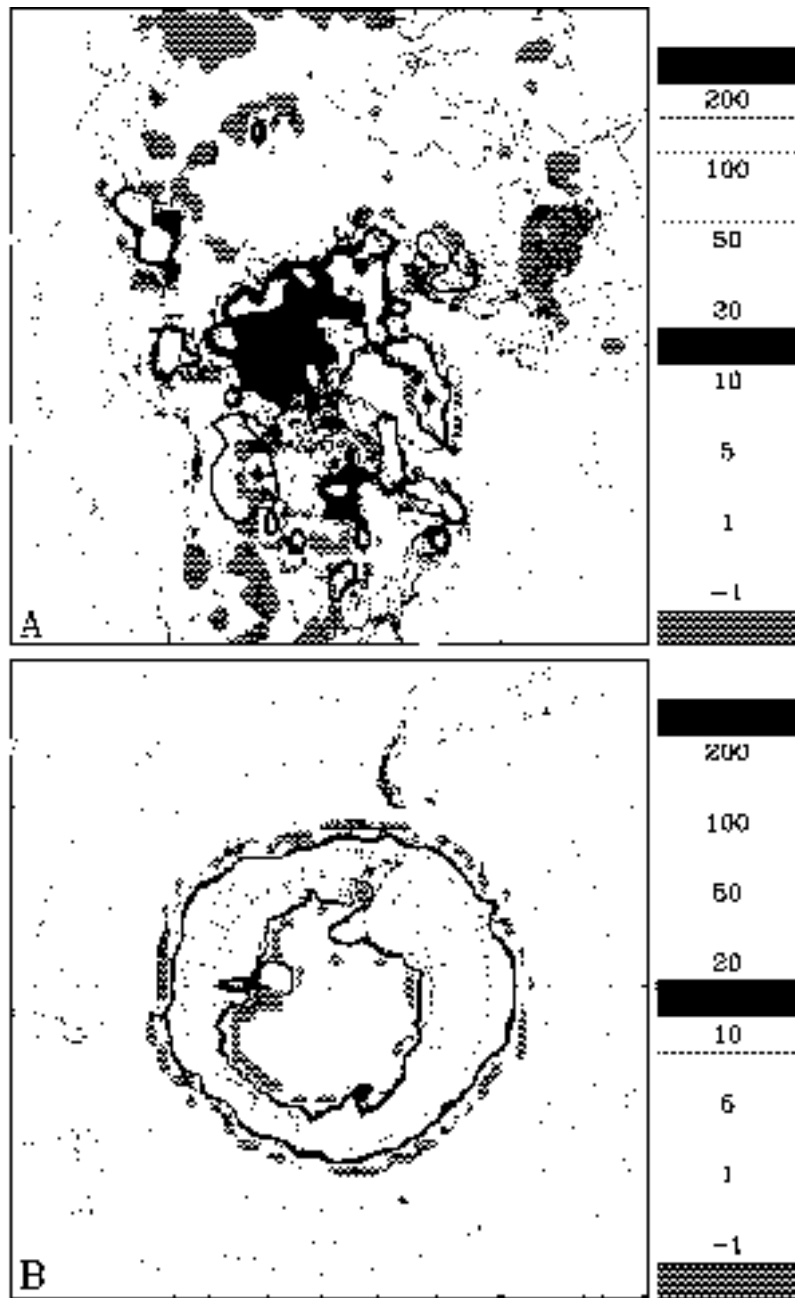


FIGURE 3: The mean annual surface sublimation rate (mm swe) for the period 1979-1993 in (a) the Northern Hemisphere and (b) the Southern Hemisphere.

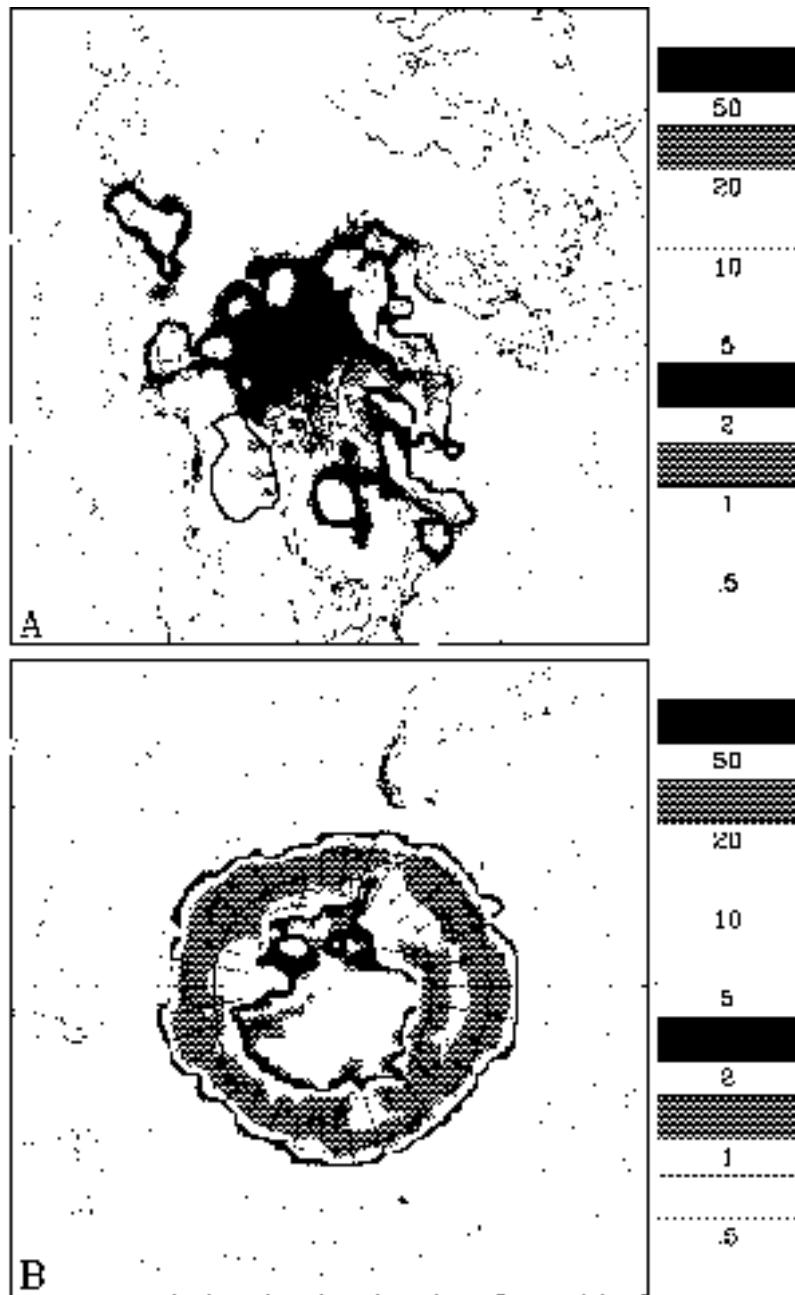


FIGURE 4: The mean annual blowing snow sublimation rate (mm swe) for the period 1979-1993 in (a) the Northern Hemisphere and (b) the Southern Hemisphere.

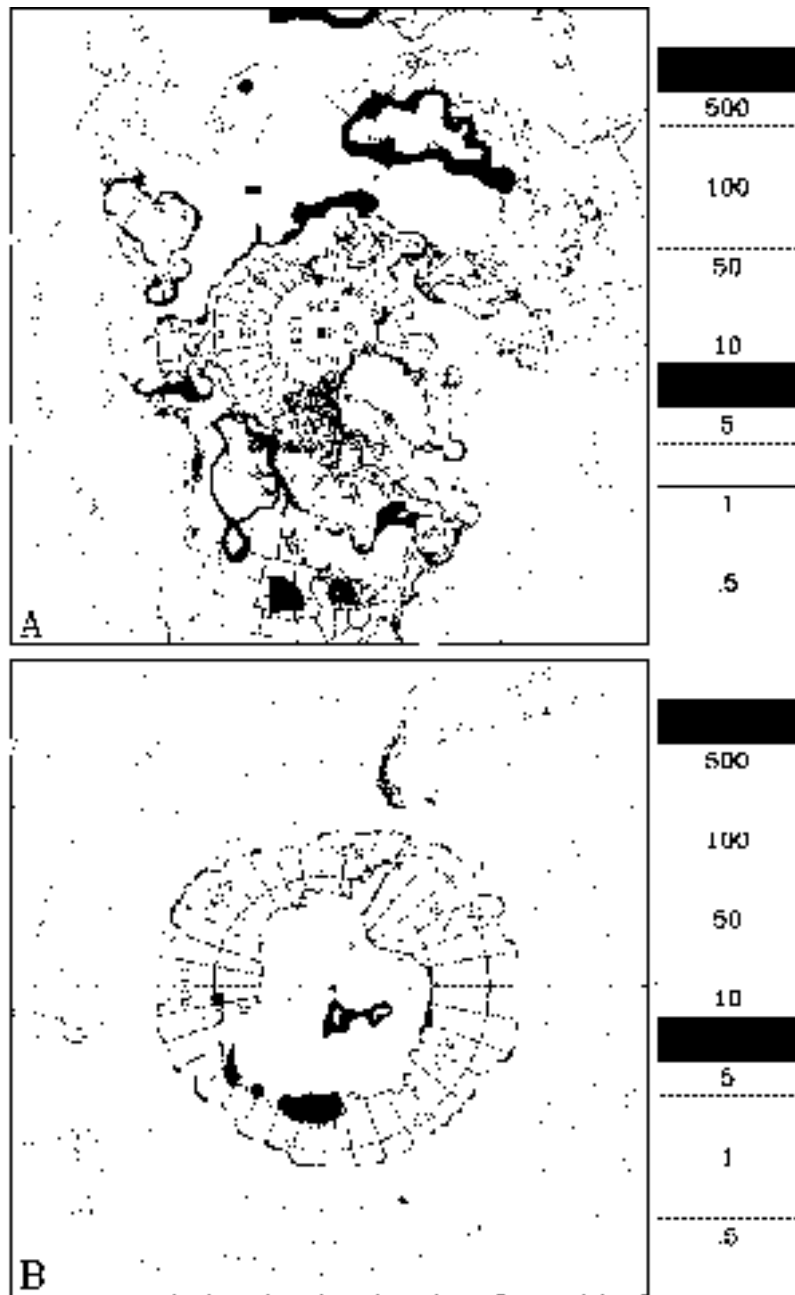


FIGURE 5: The mean annual blowing snow mass transport rate (Mg m^{-1}) for the period 1979-1993 in (a) the Northern Hemisphere and (b) the Southern Hemisphere.

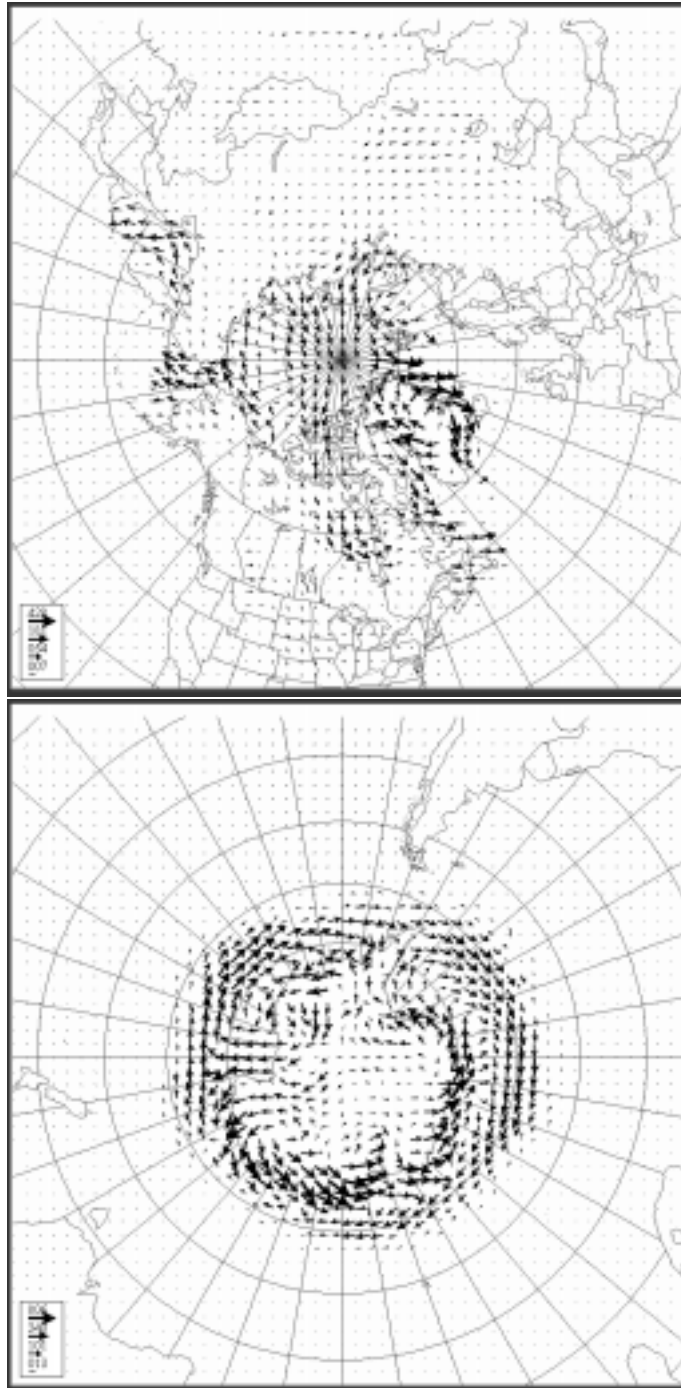


FIGURE 6: The mean annual blowing snow mass transport vectors (Mg m^{-1}) for the period 1979-1993 in (a) the Northern Hemisphere and (b) the Southern Hemisphere.

Taking into consideration the wind direction during the blowing snow events, we may represent the mass transport as vectors (Figure 6). Note here that the scales are different in each hemisphere and have units of $\text{Mg m}^{-1} \text{ a}^{-1}$. In the Northern Hemisphere, we observe once again the largest mass transport over the frozen Arctic Ocean and adjacent seas. For instance, on the eastern shores of Greenland, strong, northeasterly winds driven by the climatological Icelandic low force massive amounts of snow over the open waters of the North Atlantic Ocean. In western Greenland, winds have a strong southerly component and displace snow in a poleward direction. Note also the efflux of snow from the Bering Strait, the Sea of Okhotsk and the Labrador Sea into open waters. Near the MRB, the transport vectors are much smaller in magnitude, indicative of the lack of strong and frequent blowing snow events in the area.

In the Southern Hemisphere, mass transport vectors are generally higher in magnitude than in the Northern Hemisphere, especially in the windy coastal areas of Antarctica (Figure 6b). There is considerable efflux of mass from the continent to the open waters and frozen seas neighboring Antarctica. The transport vectors also reveal some of the climatological features of the austral polar region, most notably the circumpolar trough and the dominance of high pressure systems in the interior of Antarctica (King and Turner, 1997).

Computing the mass divergence from these transport vectors, we may then evaluate the net contribution of snow transport to the local water budget (term D in Equation 1). Figure 7 demonstrates that in the Northern Hemisphere, a single prominent zone of mass divergence is inferred over central Greenland with the loss of up to $1 \text{ mm a}^{-1} \text{ swe}$ due to drifting snow. Over Antarctica, katabatic winds tend to remove mass from the interior regions of the continent and displace it to coastal

areas or over sea ice. Note that negligible values of D are found within the MRB.

Figure 8 illustrates the combined large-scale effects of surface sublimation and blowing snow to the global surface mass balance. In both hemispheres, these terms have the largest impact over sea ice and the nearby coastal regions. In comparison, continental areas experience little effect from these cold climate processes. A summary of the contribution of the surface sublimation and blowing snow processes to the large-scale surface mass balance is presented in Table 1 for selected areas of interest. Areal-averaged over zonal bands of 10° , we observe the strong latitudinal variation of Q_{surf} and Q_s , with total contribution approaching $65 \text{ mm a}^{-1} \text{ swe}$ between 60 and 70°S . In the Northern Hemisphere, surface and blowing snow sublimation have a lesser impact to the surface mass balance as conditions are not as conducive for the occurrence of these processes (Table 1). Figure 9 reveals that, when zonally-averaged, Q_{surf} and Q_s reach peak values of ≈ 60 and $35 \text{ mm a}^{-1} \text{ swe}$, respectively at 65°S in the Southern Hemisphere and ≈ 16 and $5 \text{ mm a}^{-1} \text{ swe}$, respectively at 77.5°N in the Northern Hemisphere. The divergence of mass through wind transport is generally two orders of magnitude less than both Q_{surf} and Q_s in all regions (Table 1) and is therefore not included in Figure 9. In the MRB, all three terms combine to a negligible accumulation of $0.4 \text{ mm a}^{-1} \text{ swe}$ in the basin-scale water budget.

5 Sensitivity Tests

Although the sublimation of blowing snow has attracted much attention of late in the literature, there is significant variation on the results presented in these studies

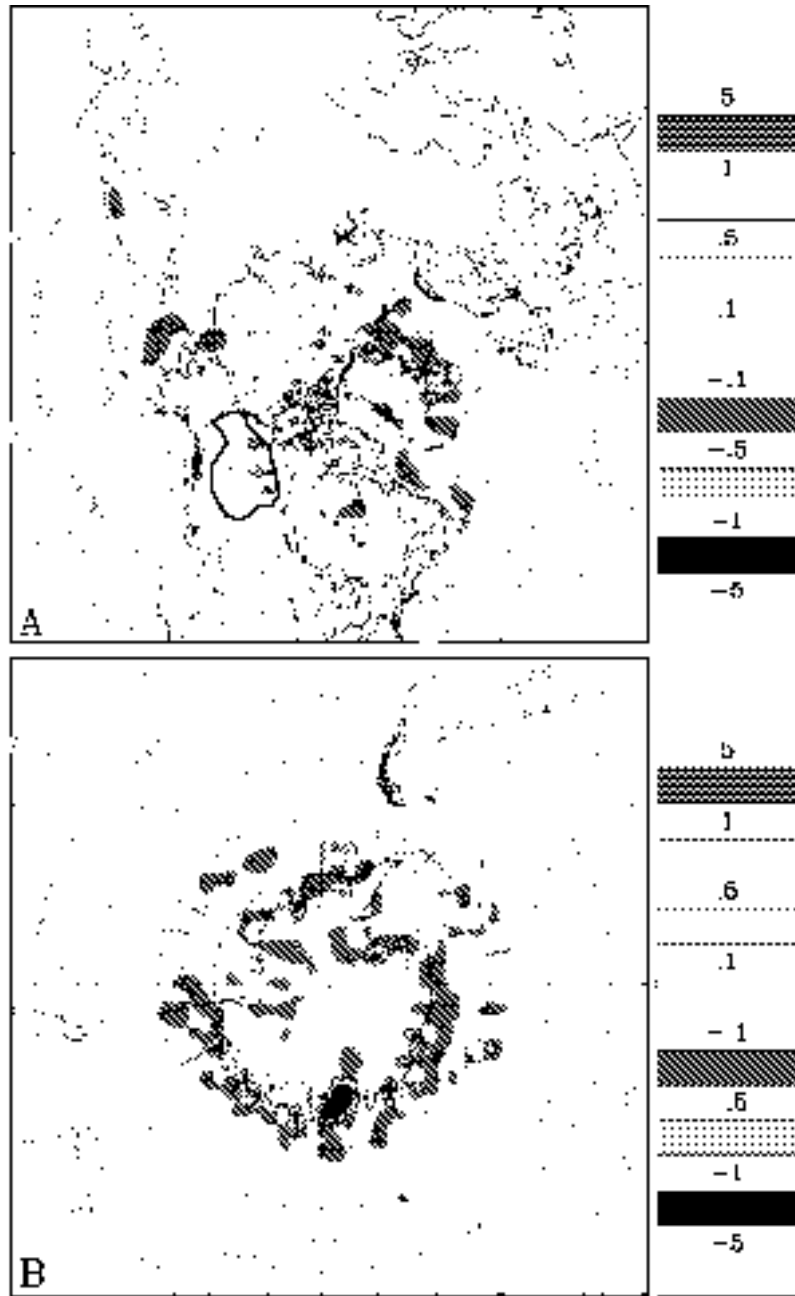


FIGURE 7: The mean annual blowing snow divergence rate (mm swe) for the period 1979-1993 in (a) the Northern Hemisphere and (b) the Southern Hemisphere.

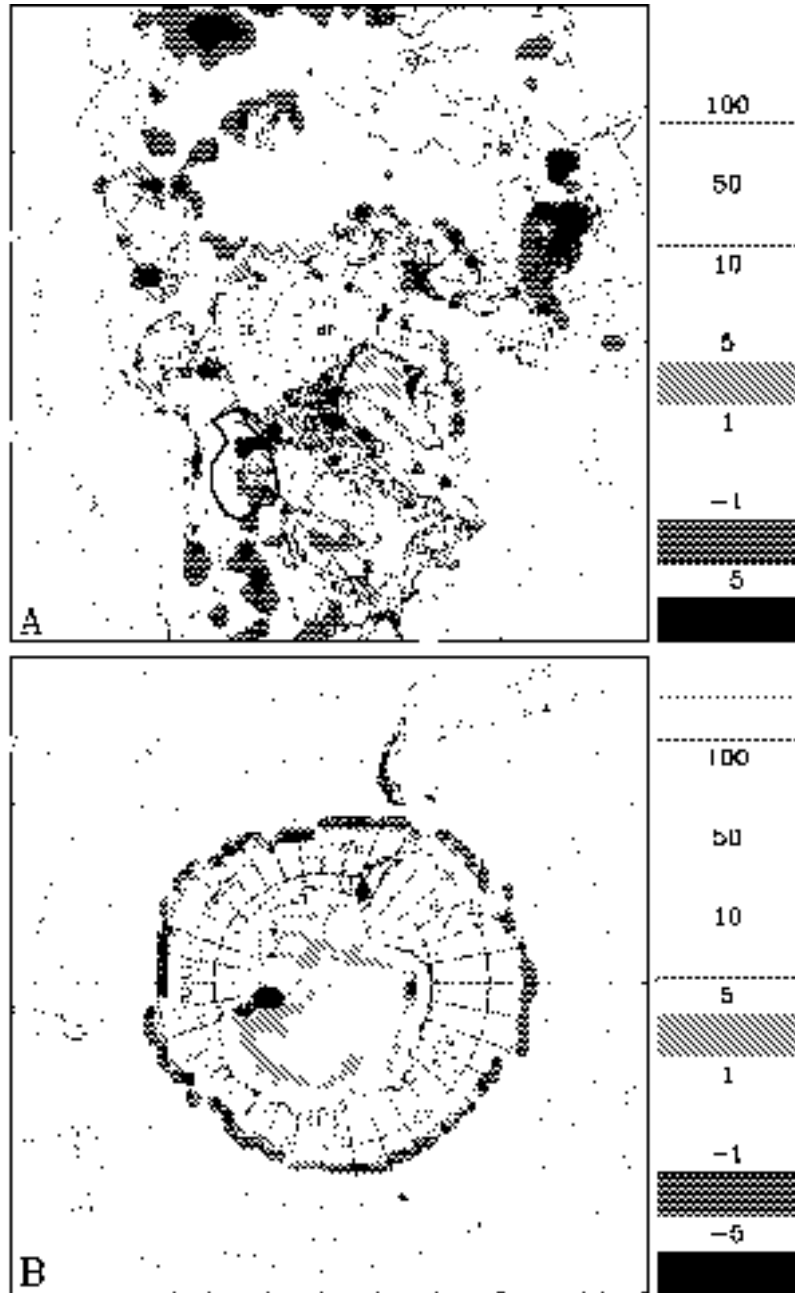


FIGURE 8: The mean annual total surface sublimation, blowing snow sublimation and divergence rates (mm swe) for the period 1979-1993 in (a) the Northern Hemisphere and (b) the Southern Hemisphere.

TABLE 1: The areally-averaged contribution of surface sublimation (Q_{surf}), blowing snow sublimation (Q_s) and divergence (D) to the surface mass balance within latitudinal bands of 10° in the Southern and Northern Hemispheres, as well as for Antarctica (ANT) and the Mackenzie River Basin (MRB). All units are in mm a^{-1} swe, with positive (negative) numbers indicating a sink (source) term in the surface mass balance.

Region	Q_{surf}	Q_s	D	Sum
80°S-90°S	2.573	1.762	-1.956×10^{-2}	4.315
70°S-80°S	20.60	10.60	5.486×10^{-2}	31.75
60°S-70°S	40.00	24.90	-3.855×10^{-2}	64.86
50°S-60°S	4.727	3.468	1.953×10^{-2}	8.215
ANT	11.71	8.099	4.294×10^{-2}	19.85
80°N-90°N	13.44	4.017	3.187×10^{-3}	17.46
70°N-80°N	10.12	3.958	5.222×10^{-3}	14.08
60°N-70°N	5.198	1.876	1.621×10^{-3}	7.076
50°N-60°N	2.212	0.849	-4.456×10^{-3}	3.057
MRB	-0.4857	0.05092	1.530×10^{-3}	-0.4195

with regard to its impact in the mass balance equation (e.g., King et al., 1996; Bintanja, 1998; Gallée, 1998; Essery et al., 1999). The calculations of blowing snow sublimation rates are particularly dependent on some of the chosen model parameters, initial and boundary conditions (Déry and Yau, 1999b, 2001). In order to obtain a range of the possible impact of blowing snow sublimation in the surface water budget of polar regions, two additional experiments are discussed in this section.

In the previous section, we have shown that, according to the ERA, wide expanses in the polar regions have climatological values of RH_i that are at or above the ice saturation point. Figure 2 confirms that such conditions are even more prominent during blowing snow events. In fact, no less than 62% of all blowing snow events inferred from the ERA occur when $RH_i \geq 1.0$ (Figure 10). Thus the assumption that the sublimation process completely shuts off in the entire column of blowing snow, which at times can extend up to several hundred meters above the ground (King and Turner, 1997), becomes important in evaluating its total contribution to the surface water budget. In this section, therefore, we first conduct an experiment which allows sublimation of blowing snow even when saturation with respect to ice occurs near the snow-covered surface.

Recent detailed humidity measurements by Mann et al. (2000) in the Antarctic confirm past observations by Schmidt (1982) that near-surface air becomes saturated with respect to ice during blowing snow. Thus model developers of blowing snow consistently use the constraint $RH_i = 1.0$ near or at the snow surface (e.g., Déry et al., 1998; Xiao et al., 2000; Bintanja, 2000). In this first sensitivity test (ST1), we relax that assumption by allowing $RH_i \geq 1.0$, but with a maximum value delineated by the saturation point with respect to water. The humidity profile is then initialized

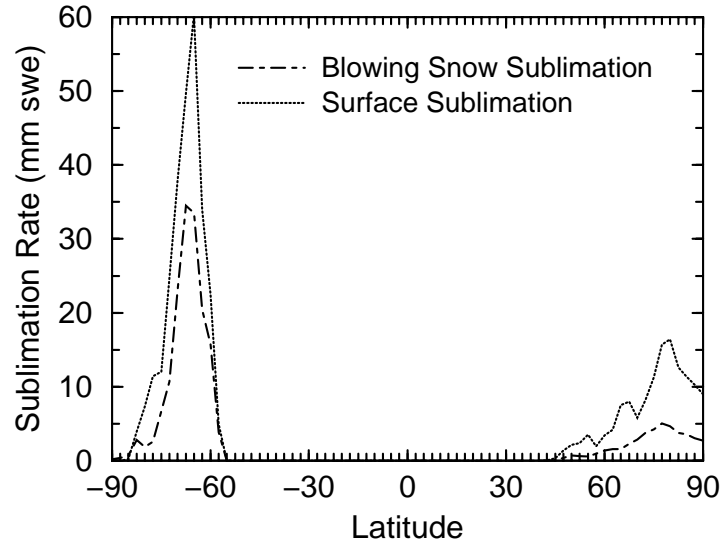


FIGURE 9: The zonally-averaged surface and blowing snow sublimation rates (mm swe) for the period 1979-1993.

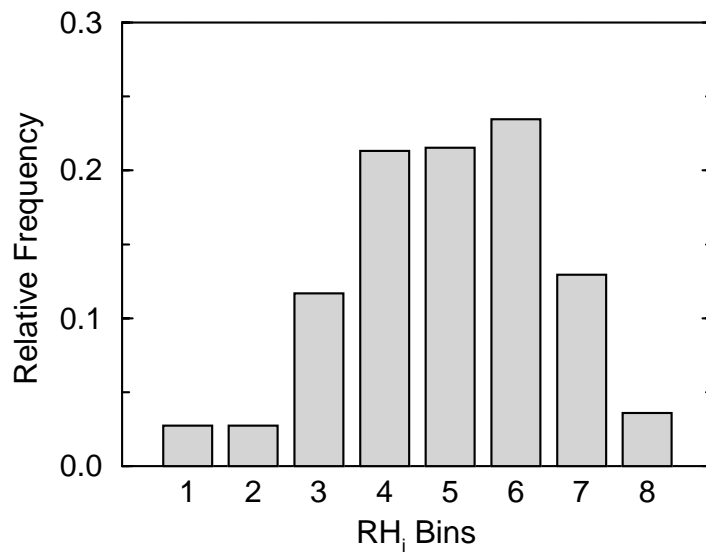


FIGURE 10: The global relative frequency distribution of RH_i during blowing snow events for the period 1979-1993. The bin numbers refer to: 1) $RH_i \leq 0.7$, 2) $0.7 < RH_i \leq 0.8$, 3) $0.8 < RH_i \leq 0.9$, 4) $0.9 < RH_i \leq 1.0$, 5) $1.0 < RH_i \leq 1.1$, 6) $1.1 < RH_i \leq 1.2$, 7) $1.2 < RH_i \leq 1.3$, 8) $RH_i > 1.3$.

using Equation (6) except that the moisture parameters are now with respect to water instead of with respect to ice. Applying this new parameterization to the 15-year ERA dataset, we observe in Figure 11 the expected increased contribution of blowing snow sublimation to the surface mass balance. Globally, sublimation rates increase by 35% from those presented in Figure 4. Although a large portion of blowing snow events occur when $RH_i \geq 1.0$, the relatively moist environment limits the total sublimation.

In the second sensitivity test (ST2), we assume that blowing snow sublimation has no impact on the background thermodynamic fields, i.e. that a certain mechanism exists to counter the heat and moisture perturbations induced by the phenomenon. Déry and Yau (2001) find that this assumption leads to a 329% increase of the seasonal blowing snow sublimation rates at an Arctic tundra location. Once again, successive integrations of PIEKTUK-D are performed for a variety of conditions and the results are expressed using a similar parameterization as before. As in our previous experiment, we allow blowing snow sublimation when $RH_i > 1.0$, as long as $RH_w < 1.0$. Figure 12 illustrates the importance of the above assumption as blowing snow sublimation rates increase globally by 334% when the self-limiting aspect of the process is removed. A summary of the impact of these sensitivity tests is presented in Table 2 for the Antarctic continent and the MRB. We see that the test in which the background environment is taken as constant represents the upper bound for values of Q_s whereas the control experiment depicts its lower bound.

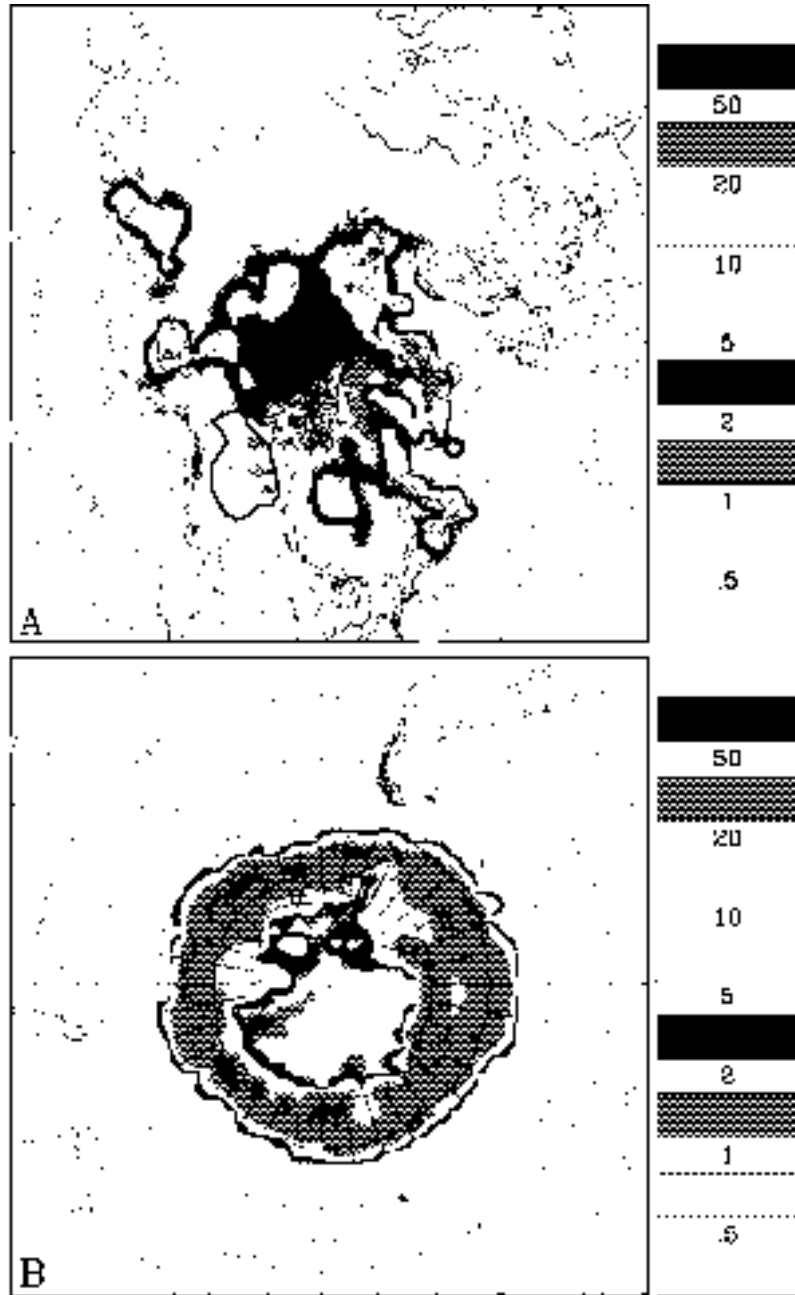


FIGURE 11: The mean annual blowing snow sublimation rate (mm swe) for the period 1979-1993 in a) the Northern Hemisphere and b) the Southern Hemisphere, allowing for sublimation to occur when $RH_i > 1.0$.

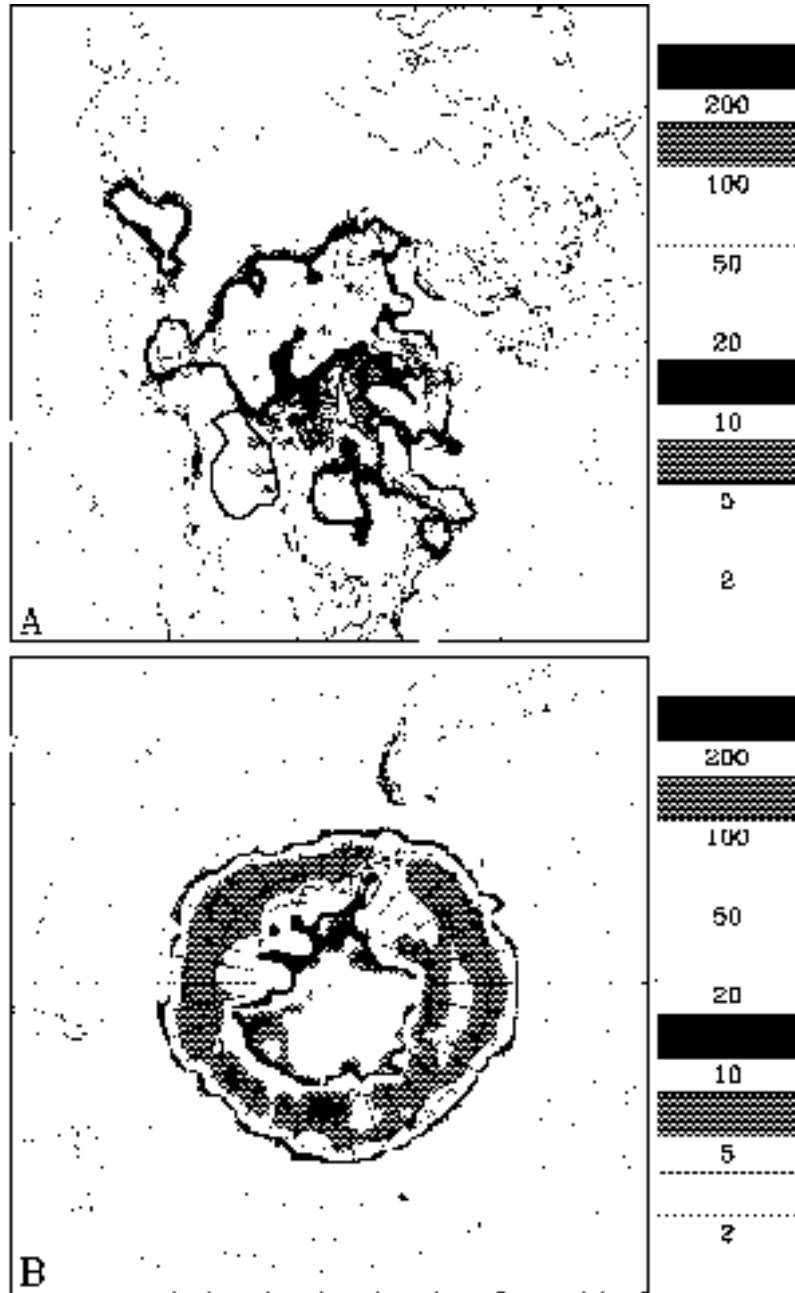


FIGURE 12: The mean annual blowing snow sublimation rate (mm swe) for the period 1979-1993 in a) the Northern Hemisphere and b) the Southern Hemisphere when steady-state background thermodynamic profiles are considered.

TABLE 2: Values of the blowing snow sublimation rate (in $\text{mm a}^{-1} \text{ swe}$) areally-averaged over Antarctica (ANT) and the Mackenzie River Basin (MRB) for the control experiment and two sensitivity tests (described in the text).

Location	Control	ST1	ST2
ANT	8.099	10.65	34.40
MRB	0.05092	0.07928	0.09326

6 Comparison with Other Studies

6.1 Southern Hemisphere

At first glance, the large values of near-surface RH_i in Antarctica may appear unrealistic. Due to its negative temperature bias (see Section 3.1), it is conceivable that the ERA data overestimate values of RH_i here. However, Schwerdtfeger (1984) and King and Anderson (1999) both report that conditions of saturation, and even supersaturation, with respect to ice are common in the austral polar region and may accompany “diamond dust”, a form of clear sky precipitation. Elevated values of RH_i in association with the onset of blowing snow have also been observed in Antarctica (Mann et al., 2000). Thus the climatology of RH_i presented herein suggests that saturation with respect to ice is quite common for the Antarctic ABL.

Our results for surface sublimation resemble those of van den Broeke (1997) for Antarctica, but with our study showing smaller values for this component of the water budget. We can attribute this in part to the cold temperature bias of the ERA, but we also need to take into account that we do not compute surface sublimation

during blowing snow events. In addition, van den Broeke (1997) considers evaporation from the surface even at temperatures above 0°C whereas we neglect this process. We do capture nonetheless the high sublimation rates experienced along the Antarctic coastal regions and sea ice as well as the reduced fluxes in the interior of the continent (see Figure 3 and c.f. Figure 9 of van den Broeke (1997)). In Table 1, we report that the total surface sublimation rate for Antarctica is about 12 mm a^{-1} swe, somewhat less than the 23 to 34 mm a^{-1} swe estimate of van den Broeke (1997). Part of this difference can be explained by the sublimation of blowing snow which, according to our results, removes an additional 8 mm a^{-1} swe from the surface mass balance of Antarctica. This value is much less than the 17 or 38 mm a^{-1} swe reported respectively by Bintanja (1998) and Gallée (1998). However, the sensitivity tests conducted in Section 5 reveal that by assuming steady-state background thermodynamic fields, we increase the total sublimation rate to 34 mm a^{-1} swe for Antarctica, matching relatively well Gallée’s (1998) estimates found under similar assumptions.

We have shown in addition that, as expected, regions subject to frequent blowing snow events are also susceptible to substantial mass transport. Giovinetto et al. (1992) compute a net transport of about $120 \times 10^{12}\text{ kg a}^{-1}$ of mass northward across 70°S through blowing snow. We estimate from our calculations the displacement of about $1 \times 10^{12}\text{ kg a}^{-1}$ across 70°S , about two orders of magnitude lower than that provided by Giovinetto et al. (1992). These differences can be explained in part by their use of a katabatic wind model to drive their transport fluxes versus our use of the ERA data which exhibits lower winds speeds than observed in Antarctica (Déry and Yau, 1999a). In addition, the high dependence of the mass transport equation on the wind speed means that slight disparities in the wind speed can yield

substantial differences in the transport estimates (Equation (8)). Finally, Giovinetto et al. (1992) assume that all mass transport at 70°S is equatorward although our results show that the mass transport vectors contain a large zonal component at this latitude (see Figure 7b). Our divergence computations for the Antarctic continent show the removal of no more than 0.005 mm a⁻¹ swe off the continent through this process. Averaging values of D over wide areas tends to reduce the impact of blowing snow transport to the mass balance as regions of mass convergence will oppose trends for divergent areas of mass. As stated by several other authors (e.g., Connelley and King, 1996; Turner et al., 1999), mass divergence through wind transport can be neglected for large-scale mass balance budgets of Antarctica.

Furthermore, the total contribution of surface sublimation and blowing snow to the surface mass balance inferred from the ERA in this study compares quite favorably with the evaporation (essentially the sublimation) rates found by Turner et al. (1999) using the same dataset for Antarctica. Specifically, they report the erosion of 21 mm a⁻¹ swe for Antarctica whereas our calculations show these processes remove about 20 mm a⁻¹ swe over the same area, with about 40% attributed to blowing snow. Thus the results presented here are generally consistent with other large-scale mass balance studies of the barren and frozen Antarctic continent.

6.2 Northern Hemisphere

In the Northern Hemisphere, there are relatively fewer large-scale, cold season mass balance studies to validate our own research. Fortunately, the works recently published by Walsh et al. (1994, 1998) and Cullather et al. (2000) have begun to fill this gap in the literature. However, to our knowledge, none have examined the

large-scale impacts of blowing snow to the surface mass balance in the boreal polar region. One possible exception is a monograph by Mikhel' et al. (1971) which presents volume transport estimates of snow in Russia. As opposed to our findings in Antarctica, our calculations of blowing snow transport are approximately one order of magnitude too large when compared to this Russian study. Our blowing snow transport and sublimation rates are somewhat less than those reported by Pomeroy and Gray (1995) and Essery et al. (1999) based on station measurements in the Canadian prairies and the Arctic tundra. A discussion of these discrepancies is found in Déry and Yau (2001) and revolves in part on the assimilation of humidity measurements and some assumptions in the model formulations. Relative humidity measurements with respect to ice in boreal regions are also scarce, although Vowinkel and Orvig (1970) report that saturation with respect to ice is often attained over the ice-covered Arctic Ocean. Déry and Yau (2001) have also shown that the mean wintertime value of RH_i is 97% at an Arctic tundra location situated near the MRB.

For the MRB as a whole, we demonstrated that the divergence and sublimation of blowing snow may not contribute significantly to the large-scale surface mass balance since blowing snow events are rare in the largely forested basin (Déry and Yau, 1999a). Only sections of the MRB lying in the Arctic tundra are susceptible to frequent blowing snow events, but according to the ERA data, ambient conditions of temperature and humidity tend to inhibit blowing snow sublimation there as well. Walsh et al. (1994) utilized rawinsonde observations to obtain as a residual the evaporation over the MRB. They found negative monthly values of surface sublimation (i.e. deposition) approaching in some cases -10 mm swe in the MRB for the period October to April for a total of about -45 mm swe. In contrast, our

estimates of surface sublimation for the same basin are much less than those of Betts and Viterbo (2000) who establish the evaporation from the snow surface to be on average 92 mm a^{-1} swe for the same area over two years using the ECMWF forecast model. However, the authors state that their study suffers from a large positive bias (of about 60%) in the evaporation rate arising in the ECMWF model such that this value should in fact be closer to 37 mm a^{-1} swe. Using the ERA, we determine that deposition adds $\approx 0.5 \text{ mm a}^{-1}$ swe over the entire MRB, a value midway between Walsh's (1994) observational study and Betts and Viterbo's (2000) study with the ECMWF model when its positive evaporation bias is removed. We do remind the reader, however, that our study neglects any sublimation from the canopy which can significantly enhance the evaporation of snow over the boreal forest that covers most of the MRB.

7 Concluding Discussion

To summarize, this paper provides a first step in establishing the combined climatological impacts of surface sublimation, blowing snow sublimation and divergence to the surface mass balance of polar regions. The budgets were computed using the ERA data for the years 1979-1993 inclusive at a horizontal resolution 2.5° . As outlined in Section 3.2, we recognize that using these data brings about certain limitations. The preceding chapter, however, demonstrates that our study compares favorably with other large-scale mass balance assessments in the polar regions. Nonetheless, we believe the results may be enhanced in several ways. First, the use of data at higher spatial and temporal resolutions may improve the computations by capturing more of the local to mesoscale variations of the snow processes of inter-

est. Information on the variability (e.g., standard deviation) of the meteorological fields implicit within the data may prove useful in distinguishing extreme events that are possibly masked in our study. Furthermore, we have coupled the PIEKTUK-D model (Déry and Yau, 2001) to the Mesoscale Compressible Community (MC2) model of Benoit et al. (1997) to better comprehend the process of blowing snow and its complex interactions with the environment. Preliminary evidence suggests that blowing snow sublimation is enhanced by almost a factor of two in the coupled simulations versus the stand-alone application of PIEKTUK-D. In future work, therefore, we will evaluate the impact of this finding on our current large-scale surface mass balance study by means of improved blowing snow parameterizations.

Acknowledgments

We wish to acknowledge the contributions of Dr. Graham Mann (University of Leeds), Dr. John King (British Antarctic Survey) and Dr. Michiel van den Broeke (University of Utrecht) during the preparation of this work. This research was supported by the Natural Sciences and Engineering Research Council of Canada through a GEWEX collaborative research network grant.

References

- Benoit, R., Desgagné, M., Pellerin, P., Pellerin, S., and Chartier, Y., 1997: The Canadian MC2: A semi-Lagrangian, semi-implicit wideband atmospheric model suited for finescale process studies and simulation, *Mon. Weather Rev.*, **125**, 2382-2415.
- Betts, A. K. and Viterbo, P., 2000: Hydrological budgets and surface energy balance of

-
- seven subbasins of the Mackenzie River from the ECMWF model, *J. Hydrometeorol.*, **1**, 47-60.
- Bintanja, R., 1998: The contribution of snowdrift sublimation to the surface mass balance of Antarctica, *Ann. Glaciol.*, **27**, 251-259.
- Bintanja, R., 2000: Snowdrift suspension and atmospheric turbulence. Part I: Theoretical background and model description, *Bound.-Layer Meteorol.*, **95**, 343-368.
- Bjornsson, H., Mysak, L. A., and Brown, R. D., 1995: On the interannual variability of precipitation and runoff in the Mackenzie drainage basin, *Clim. Dyn.*, **12**, 67-76.
- Connolley, W. M. and King, J. C., 1996: A modeling and observational study of East Antarctica surface mass balance, *J. Geophys. Res.*, **101**, 1335-1343.
- Cullather, R. I., Bromwich, D. H., and Van Woert, M. L., 1998: Spatial and temporal variability of Antarctic precipitation from atmospheric methods, *J. Climate*, **11**, 334-368.
- Cullather, R. I., Bromwich, D. H., and Serreze, M. C., 2000: The atmospheric hydrologic cycle over the Arctic Basin from reanalyses. Part I: Comparison with observations and previous studies, *J. Climate*, **13**, 923-937.
- Déry, S. J., Taylor, P. A., and Xiao, J., 1998: The thermodynamic effects of sublimating, blowing snow in the atmospheric boundary layer, *Bound.-Layer Meteorol.*, **89**, 251-283.
- Déry, S. J. and Yau, M. K., 1999a: A climatology of adverse winter-type weather events, *J. Geophys. Res.*, **104**(D14), 16,657-16,672.
- Déry, S. J. and Yau, M. K., 1999b: A bulk blowing snow model, *Bound.-Layer Meteorol.*, **93**, 237-251.
- Déry, S. J. and Yau, M. K., 2001: Simulation of blowing snow in the Canadian Arctic using a double-moment model, *Bound.-Layer Meteorol.*, in press.
- Essery, R., Li, L., and Pomeroy, J. W., 1999: A distributed model of blowing snow over complex terrain, *Hydrol. Proc.*, **13**, 2423-2438.
- Gallée, H., 1998: Simulation of blowing snow over the Antarctic ice sheet, *Ann. Glaciol.*, **26**, 203-206.

-
- Garratt, J. R., 1992: *The Atmospheric Boundary Layer*, Cambridge University Press, Cambridge, 316 pp.
- Gibson, J. K., Kållberg, P., Uppala, S., Hernandez, A., Nomura, A., and Serrano, E., 1997: *ERA Description*, ECMWF Re-Analysis Project Report Series, 1, 72 pp.
- Giovinetto, M. B., Bromwich, D. H., and Wendler, G., 1992: Atmospheric net transport of water vapor and latent heat across 70°S, *J. Geophys. Res.*, **97**, 917-930.
- King, J. C., Anderson, P. S., Smith, M. C., and Mobbs, S. D., 1996: The surface energy and mass balance at Halley, Antarctica during winter, *J. Geophys. Res.*, **101**, 19,119-19,128.
- King, J. C. and Anderson, P. S., 1999: A humidity climatology for Halley, Antarctica based on hygrometer measurements, *Antarctic Sc.*, **11**, 100-104.
- King, J. C. and Turner, J., 1997: *Antarctic Meteorology and Climatology*, Cambridge University Press, 409 pp.
- Kong, F. and Yau, M. K., 1997: An explicit approach to microphysics in the MC2, *Atmos.-Ocean*, **35**, 257-291.
- Lackmann, G. M. and Gyakum, J. R., 1996: The synoptic- and planetary-scale signatures of precipitating systems over the Mackenzie River Basin, *Atmos.-Ocean*, **34**(4), 647-674.
- Lackmann, G. M., Gyakum, J. R. and Benoit, R., 1998: Moisture transport diagnosis of a wintertime precipitation event in the Mackenzie River Basin, *Mon. Weather Rev.*, **126**, 668-691.
- Li, L. and Pomeroy, J. W., 1997: Estimates of threshold wind speeds for snow transport using meteorological data, *J. Appl. Meteorol.*, **36**, 205-213.
- Mann, G. W., Anderson, P. S., and Mobbs, S. D., 2000: Profile measurements of blowing snow at Halley, Antarctica, *J. Geophys. Res.*, **105**(19), 24,491-24,508.
- Mikhel', V. M., Rudneva, A. V., and Lipovskaya, V. I., 1971: *Snowfall and Snow Transport During Snowstorms over the USSR*, Main Admin. of the Hydrometeorological Service of the Council of Ministers of the USSR, Leningrad, 174 pp., [translated from Russian].
- Misra, V., Yau, M. K., and Badrinath, N., 2000: Atmospheric water species budget in

-
- mesoscale simulations of lee cyclones over the Mackenzie River Basin, *Tellus*, **52A**, 240-261.
- Phillips, D., 1990: *Climates of Canada*, Environment Canada, Ottawa, 176 pp.
- Pomeroy, J. W. and Gray, D. M., 1995: *Snowcover Accumulation, Relocation and Measurement*, NHRI Sci. Rep. 7, Environment Canada, Saskatoon, 144 pp.
- Pomeroy, J. W., Marsh, P., and Gray, D. M., 1997: Application of a distributed blowing snow model to the Arctic, *Hydrol. Proc.*, **11**, 1451-1464.
- Pruppacher, H. R. and Klett, J. D., 1997: *Microphysics of Clouds and Precipitation*, 2nd ed., Kluwer Academic Publishers, Dordrecht, 954 pp.
- Rouse, W. R., 2000: Progress in hydrological research in the Mackenzie GEWEX Study, *Hydrol. Proc.*, **14**, 1667-1685.
- Schmidt, R. A., 1982: Vertical profiles of wind speed, snow concentration, and humidity during blowing snow, *Bound.-Layer Meteorol.*, **23**, 223-246.
- Schmidt, R. A., 1991: Sublimation of snow intercepted by an artificial conifer, *Agri. and Forest Meteorol.*, **54**, 1-27.
- Schwerdtfeger, W., 1984: *Climate of the Antarctic*, Developments in Atmospheric Science 15, Elsevier, 261 pp.
- Smirnov, V. V. and Moore, G. W. K., 1999: Spatial and temporal structure of atmospheric water vapor transport in the Mackenzie River Basin, *J. Climate*, **12**(3), 681-696.
- Stewart, R. E., Leighton, H. G., Marsh, P., Moore, G. W. K., Rouse, W. R., Soulis, S. D., Strong, G. S., Crawford, R. W., and Kochtubajda, B., 1998: The Mackenzie GEWEX Study: The water and energy cycles of a major North American river basin, *Bull. Amer. Meteorol. Soc.*, **79**, 2665-2683.
- Stewart, R. E., Burford, J. E., and Crawford, R. W., 2000: On the meteorological characteristics of the water cycle of the Mackenzie River Basin, *Contr. Atmos. Phys.*, **9**, 103-110.
- Turner, J., Connolley, W. M., Leonard, S., Marshall, G. J., and Vaughan, G., 1999: Spatial and temporal variability of net snow accumulation over the Antarctic from ECMWF

- Re-Analysis project data, *Int. J. Climatology*, **19**, 697-724.
- van den Broeke, M. R., 1997: Spatial and temporal variation of sublimation on Antarctica: Results of a high-resolution general circulation model, *J. Geophys. Res.*, **102**(D25), 29,765-29,777.
- Vowinckel, E. and Orvig, S. 1970: The climate of the North Polar Basin, in *Climate of the Polar Regions*, World Survey of Climatology, vol. 7, edited by S. Orvig, Elsevier, pp. 129-252.
- Walsh, J. E., Zhou, X., Portis, D., and Serreze, M. C., 1994: Atmospheric contribution to hydrologic variations in the Arctic, *Atmos.-Ocean*, **32**, 733-755.
- Walsh, J. E., Kattsov, V., Portis, D., and Meleshko, V., 1998: Arctic precipitation and evaporation: Model results and observational estimates, *J. Climate*, **11**, 72-87.
- Xiao, J., Bintanja, R., Déry, S. J., Mann, G. W., and Taylor, P. A., 2000: An intercomparison among four models of blowing snow, *Bound.-Layer Meteorol.*, **97**(1), 109-135.

Chapter 4

Blowing Snow Modelling

4.1 Presentation of Article 3

The blowing snow numerical model used in this study is based on the “PIEKTUK” model of Déry et al. (1998). Before coupling PIEKTUK to a mesoscale model, the possibility of simplifying the algorithm and improve its running time is investigated. By solving a single diffusion/sedimentation equation for the blowing snow mixing ratio instead of a spectrum of particles, substantial savings in computer time (up to 100 times faster than the original spectral model) are achieved. Comparisons of the blowing snow fluxes and thermodynamic profiles simulated by both versions of PIEKTUK show few discrepancies.

4.2 Article 3

A bulk blowing snow model. By Stephen J. Déry and M. K. Yau, 1999: *Bound.-Layer Meteorol.*, **93**, 237-251.

Reproduced with kind permission from Kluwer Academic Publishers.

A BULK BLOWING SNOW MODEL

STEPHEN J. DÉRY and M. K. YAU

*Dept. of Atmospheric and Oceanic Sciences, McGill University, 805 Sherbrooke St. W.,
Montréal, Québec, H3A 2K6 Canada*

(Received in final form 6 May 1999)

Abstract. We present in this paper a simple and computationally efficient numerical model that depicts a column of sublimating, blowing snow. This bulk model predicts the mixing ratio of suspended snow by solving an equation that considers the diffusion, settling and sublimation of blowing snow in a time-dependent mode. The bulk model results compare very well with those of a previous spectral version of the model, while increasing its computational efficiency by a factor of about one hundred. This will allow the use of the model to estimate the effects of blowing snow to the mass balance and atmospheric boundary layer of such regions as the Mackenzie River Basin of Canada.

Keywords: Blowing snow, Bulk modelling, Mackenzie Basin, Sublimation, Suspension

1. Introduction

In addition to its hazardous aspects, the transport of snow and its sublimation are being recognized as important factors in the water and energy budgets of windswept regions such as the Arctic tundra. Erosion and accumulation of snow by wind can lead to substantial heterogeneities in the snowcover with hydrometeorological implications. In addition to supplying moisture to the atmospheric boundary layer (ABL), sublimation of blowing snow acts as a further sink of mass from the surface that can lead to erroneous estimates of the snow depth in numerical models which neglect these processes.

This work is conducted within the context of the ongoing Mackenzie GEWEX Study (MAGS; Stewart et al., 1998) since part of the territory drained by the Mackenzie River is susceptible to frequent blowing snow events (Déry and Yau, 1999). One of our future goals is to assess the contribution of blowing snow transport and sublimation to the water budget in this large northern drainage basin. Accurate and efficient numerical modelling of blowing snow is thus necessary in this context.

We therefore introduce in this paper a bulk version of a blowing snow model that provides the thermodynamic feedbacks of sublimating, blowing snow in the ABL while keeping track of its effects on the snowcover. The numerical model discussed here is based on the PIEKTUK blowing snow model of Déry et al. (1998) and the initial work of Déry and Taylor (1996) on blowing snow. The novelty of the bulk version is that it runs about 100 times faster than the spectral version but yields comparable results. Since the spectral PIEKTUK model is extensively described in Déry et al. (1998), we



first present only a brief review of its formulation before examining steps that lead to a so-called “bulk” version of the model. Subsequently, results, some sensitivity tests and a concluding discussion will be presented.

2. Model Description

2.1. SPECTRAL MODEL - (PIEKTUK-S)

The PIEKTUK model of Déry et al. (1998) is spectral in nature in that it depicts explicitly, in either a time or fetch-dependent framework, a spectrum of blowing snow particles that are gamma-distributed at the lower model boundary and are suspended through diffusion from a saltation layer just above the snow-covered surface. The spectral number density of suspended particles $F(r, z, t)$ (m^{-4}) for particles of radius r (m) is taken to satisfy:

$$\frac{\partial F(r)}{\partial t} = \frac{\partial}{\partial z} \left(K(r) \frac{\partial F(r)}{\partial z} + v(r) F(r) \right) - \frac{\partial}{\partial r} (\dot{r} F(r)), \quad (1)$$

for the time-dependent, horizontally homogeneous case. Here, time is denoted by t (s), the vertical coordinate by z (m), and \dot{r} denotes the rate of change of radius due to sublimation. We also abbreviated $F(r, z, t)$ by $F(r)$. Three active processes are depicted in the rhs of Equation (1): the vertical diffusion of blowing snow particles with eddy diffusivity $K(r)$ ($\text{m}^2 \text{s}^{-1}$), the sedimentation of particles with a terminal velocity $v(r)$ (m s^{-1}) obtained through a balance between the gravitational and drag forces (Déry et al., 1998), and the spectral shifting due to sublimation of blowing snow $\frac{\partial}{\partial r} (\dot{r} F(r))$ ($\text{m}^{-4} \text{s}^{-1}$).

Following the work of Rouault et al. (1991), the turbulent diffusion coefficient used by Déry et al. (1998) considered a reduction ζ from the eddy diffusivity for momentum K_m ($\text{m}^2 \text{s}^{-1}$) due to the inertia of the particles such that:

$$K(r) = \zeta K_m. \quad (2)$$

(Note that a detailed discussion of the interaction between the spectrum of particles and turbulence can also be found in Lee (1975).)

Values of ζ are size-dependent and are discussed at length by Déry et al. (1998). In near-neutral conditions, we may assume:

$$K_m = u_* l, \quad (3)$$

with the mixing length l (m) given by (e.g., Stull, 1988):

$$l = \kappa(z + z_0) [1 + \kappa(z + z_0)/l_{max}]^{-1}. \quad (4)$$

In these equations, u_* (m s^{-1}) is the friction velocity, κ ($=0.4$) is the von Kármán constant, and z_0 (m) the roughness length. Following Taylor (1969) and Mobbs and Dover (1993), an asymptotic value to l of 40 m is represented by l_{max} .

Neglecting for the moment the appropriate boundary conditions that are required to solve Equation (1), the above 3 relationships describe, in part, the suspension of blowing snow particles through the competing processes of diffusion, settling and sublimation in the spectral version of PIEKTUK (hereafter referred to as PIEKTUK-S). Déry et al. (1998) typically used 64 particle size bins to evaluate the blowing snow suspension and sublimation rates. For computational simplicity, we therefore investigate the possibility of using a bulk quantity, namely the blowing snow mixing ratio q_b (kg kg^{-1}), which is the ratio of the mass of suspended ice particles to that of dry air, to depict the amount of snow in suspension. The steps leading to this bulk approach are described in the following section.

2.2. BULK MODEL - (PIEKTUK-B)

2.2.1. Formulation

For the sake of computational efficiency, complex microphysical schemes have commonly employed a bulk method to derive certain hydrometeor species in atmospheric models (e.g., Kong and Yau, 1997). We apply here a similar technique for the computation of blowing snow suspension and sublimation.

Following Schmidt (1982) and others, we assume that blowing snow is composed of ice spheres such that the mixing ratio of blowing snow, q_b , can be related to the number density by

$$q_b = \frac{4\pi\rho_{ice}}{3\rho} \int_0^\infty r^3 F(r) dr, \quad (5)$$

with ρ_{ice} ($= 900 \text{ kg m}^{-3}$) and ρ (kg m^{-3}) denoting the constant densities of ice and air, respectively.

Multiplying Equation (1) by $(4\pi\rho_{ice}r^3/3\rho)$, followed by an integration with respect to r from 0 to ∞ and applying (5), we obtain

$$\frac{\partial q_b}{\partial t} = \frac{\partial}{\partial z} \left(K_b \frac{\partial q_b}{\partial z} + v_b q_b \right) + S_b, \quad (6)$$

where K_b (m^2) is some bulk diffusion coefficient and v_b (m s^{-1}) is some bulk fall velocity. The sink in q_b due to the sublimation of blowing snow, S_b ($\text{kg kg}^{-1} \text{ s}^{-1}$) is discussed in Section 2.2.2. To obtain v_b and K_b , we need to know the exact form of the number density function.

We begin by noting that Budd (1966) and Schmidt (1982) have showed that distributions of $F(r)$ typically follow those of a two-parameter gamma distribution such that:

$$F(r) = \frac{Nr^{(\alpha-1)} \exp^{-r/\beta}}{\beta^\alpha \Gamma(\alpha)}, \quad (7)$$

with N (m^{-3}) being the total number concentration of particles, α (dimensionless) and β (m) the shape and scale parameters of the gamma distribution Γ .

Substituting Equation (7) into (5), integrating and solving for N , we get:

$$N = \frac{3\rho q_b \Gamma(\alpha)}{4\pi\rho_{ice} \Gamma(\alpha+3)\beta^3}. \quad (8)$$

Several tests with PIEKTUK-S revealed that α varies little with height and is thus taken as constant (set to 2 following the analysis of King et al., 1996). Using $\alpha = 2$ in (8), we can solve for β as

$$\beta = \frac{1}{2} \left[\frac{\rho q_b}{4\pi\rho_{ice} N} \right]^{1/3}. \quad (9)$$

We now approximate N in Equation (9) by a special solution N_s of Equation (1) as follows. For a steady-state, saturated environment, (i.e., no sublimation), we may write:

$$K(r) \frac{\partial F(r)}{\partial z} = -v(r)F(r). \quad (10)$$

Integrating this equation from the top of the saltation layer z_s , assuming $l \approx \kappa(z+z_0)$ and neglecting any inertial effects, we retrieve the classical equation for suspended particle concentrations:

$$F(r, z) = F(r, z_s) \left[\frac{(z+z_0)}{(z_s+z_0)} \right]^{-v(r)/\kappa u_*}. \quad (11)$$

Integrating (11) from $r = 0$ to ∞ and assuming that $F(r)$ is given by a gamma distribution, we obtain

$$N_s = \int_0^\infty F(r, z_s) \left[\frac{(z+z_0)}{(z_s+z_0)} \right]^{-v(r)/\kappa u_*} dr. \quad (12)$$

We now set $N = kN_s$ in (9). It is found that $k = 3$ gives the best agreement between the solutions of the spectral and the bulk models.

As a final measure, we need to specify a bulk terminal velocity that characterizes the particle distribution and which will vary with height. Applying the method of Kong and Yau (1997), we get:

$$v_b = \frac{\int_0^\infty v(r)r^n F(r) dr}{\int_0^\infty r^n F(r) dr} \quad (13)$$

where n is a moment of the gamma distribution. As in Kong and Yau (1997), we tried setting n equal to 3 such that v_b represents the mass-weighted terminal velocity of the ice particle distribution. However, this approach predicts q_b profiles that are consistently too high compared to the results of PIEKTUK-S. After a number of tests, we find that the 5th moment of the distribution yields better approximations for q_b in PIEKTUK-B and, for this reason, set $n = 5$. These initial steps which use information on the assumed gamma-distributed spectra of blowing snow particles now allow us to proceed with the discussion of a bulk blowing snow model.

2.2.2. Diffusion and Sublimation

As mentioned previously, an alternative to the representation of the amount of suspended snow is the bulk quantity q_b , the blowing snow mixing ratio, governed by Equation (6). Note that although Equation (2) includes a reduction in the eddy diffusivity of the particles due to their inertia, we assume for the moment that ζ is unity such that $K_b = K_m$ as in Bintanja (1998a) and depicts the eddy diffusivity for q_b .

To conserve heat and moisture in the column of sublimating, blowing snow, we introduce two additional prognostic equations in the model for the ambient air temperature T_a (K) and water vapour mixing ratio q_v (kg kg^{-1}), which satisfy:

$$\frac{\partial T_a}{\partial t} = \frac{\partial}{\partial z} \left(K_h \frac{\partial T_a}{\partial z} \right) + Q \quad (14)$$

and

$$\frac{\partial q_v}{\partial t} = \frac{\partial}{\partial z} \left(K_v \frac{\partial q_v}{\partial z} \right) + E \quad (15)$$

with K_h and K_v being the heat and moisture eddy diffusivities, taken as equal to that for momentum (Equation (3)). The source term for water vapour, E ($\text{kg kg}^{-1} \text{ s}^{-1}$), is influenced by the sublimation process only and therefore is set equal to $-S_b$. The heating rate (negative here) due to sublimation is represented by Q (K s^{-1}) in Equation (14) and is computed from:

$$Q = \frac{S_b L_s}{c_p} \quad (16)$$

with the latent heat of sublimation and heat capacity for air denoted by L_s (J kg^{-1}) and c_p ($\text{J kg}^{-1} \text{K}^{-1}$), respectively. We neglect here additional heat from the particles as this component contributes negligibly to the phase change. Note however that both T_a and q_v are not subject to settling as is q_b such that we expect greater vertical redistribution of heat and moisture compared to ice particles.

The sublimation term S_b ($\text{kg kg}^{-1} \text{s}^{-1}$) is derived as follows. Ignoring any radiation transferred to a particle, the change in mass m (kg) of a single ice sphere due to sublimation is obtained through (Thorpe and Mason, 1966):

$$\frac{dm}{dt} = \frac{2\pi r Nu (q_v/q_{is} - 1)}{(F_k + F_d)}, \quad (17)$$

where q_{is} (kg kg^{-1}) denotes the saturation water vapour mixing ratio with respect to ice, Nu represents the Nusselt number and where the conduction and diffusion terms involved in the phase change are respectively given by F_k and F_d (m s kg^{-1}) (Rogers and Yau, 1989).

To obtain the total sublimation rate for a spectrum of particles, we multiply Equation (17) with the particle number concentration and perform an integration over all radii, i.e.

$$S_b = \frac{1}{\rho} \int_0^\infty F(r) \frac{dm}{dt} dr. \quad (18)$$

Assuming once again that the particles follow a gamma distribution (see Equation (7)), the integral yields the bulk sublimation rate:

$$S_b = \frac{q_b Nu (q_v/q_{is} - 1)}{2\rho_{ice} r_m^2 (F_k + F_d)}, \quad (19)$$

where the mean radius of the particle distribution, r_m (m), is defined as:

$$r_m = \frac{\int_0^\infty r F(r) dr}{\int_0^\infty F(r) dr} = \alpha\beta \quad (20)$$

Ventilation effects due to the settling of suspended particles are in effect introduced by Nu which is dependent on the Reynolds number Re through (Lee, 1975):

$$Nu = 1.79 + 0.606 Re^{0.5}, \quad (21)$$

where in still air

$$Re = \frac{2r_m v_b}{\nu}, \quad (22)$$

with ν being the kinematic viscosity of air ($1.53 \times 10^{-5} \text{ m}^2 \text{ s}^{-1}$). Thus to compute the diffusion and sublimation of blowing snow, it is clear that both r_m and ν_b must be known quantities.

2.2.3. Boundary and Initial Conditions

Setting proper initial and spatial boundary conditions is crucial to the modelling of blowing snow. Of particular difficulty here is assigning the lower boundary conditions on humidity and the blowing snow mixing ratio and hence, the particle distribution, (note that the boundary conditions discussed here are applied only when snow transport is predicted to occur). At the present time, we take the lower boundary height z_{lb} to be at the snow surface and the model lid z_{ub} to be 1 km above the surface where fluxes of particles, temperature and moisture are assumed zero.

At the lower boundary, we take the air to be saturated with respect to ice for the control case. However, supplementary experiments will be conducted to test the sensitivity of this critical assumption. Given a value of relative humidity with respect to ice RH_i at a certain level and neglecting stability effects, the vertical variation of humidity is deduced from a logarithmic profile (e.g., Garratt, 1992) as:

$$q_v = q_{is} + \frac{q_*}{\kappa} \ln \left[\frac{(z + z_0)}{z_0} \right] \quad (23)$$

where q_* (kg kg^{-1}) represents the humidity scale. For temperature, however, we assume initially no variation with height and that there is no heat flux at z_{lb} .

At the onset of blowing snow, we assume that the saltation layer instantaneously develops, but that no particles are in suspension above $z = 0.1 \text{ m}$, the first level above z_s . Thus we set a constant value for the saltation blowing snow mixing ratio $q_{b_{salt}}$ (kg kg^{-1}) in the saltation layer (Pomeroy et al., 1993):

$$q_{b_{salt}} = 0.385(1 - U_t/U_{10})^{2.59}/u_*, \quad (24)$$

where U_{10} and U_t are respectively the 10-m wind speed and its value at the cessation of blowing snow, in m s^{-1} . This quantity is then extrapolated and fixed at $z = 0.1 \text{ m}$ from $z = z_s$ based on the analytical profiles for $F(r)$ of Equation (11). Note that in our initial steps, we assess the vertical distribution of r_m by taking this parameter to be $100 \mu\text{m}$ at z_s following Pomeroy et al. (1993), although recent observations in Antarctica suggest r_m at z_s may be closer to $75 \mu\text{m}$ (King et al., 1996).

2.2.4. Other Modifications

Following the detailed sensitivity tests of Déry et al. (1998) with the PIEKTUK-S model, several other modifications have been incorporated into

PIEKTUK-B. For instance, they find little difference in assuming that the particles are at the ambient air temperature instead of the ice bulb temperature, and hence we take T_a as the particle temperature.

The threshold velocity for transport in PIEKTUK-B is estimated following the study of Li and Pomeroy (1997) such that:

$$U_t = U_{t_0} + 0.0033(T_a + 27.27)^2 \quad (25)$$

where T_a is in degrees Celsius and the minimum value of the threshold 10-m wind speed, U_{t_0} , is equal to 6.975 m s^{-1} and is reached at about $T_a = -27^\circ\text{C}$. Equation (25) shows increasing resistance to transport at temperatures near freezing and at very cold temperatures.

In addition, we do not assume at $t = 0$ that $\text{RH}_i = 1.0$ within the saltation layer. With our lower boundary set to the snow-covered surface, we can expect that this layer will contribute to the sublimation process and add water vapour to the ABL.

Given that the calculation of particle suspension is no longer constrained by the diffusion of small particles encountered in the spectral model, we are able to reduce significantly the vertical grid resolution while increasing the timestep. For the results presented in the following section, 24 vertical levels equidistant on a logarithmic scale and a timestep of 2 s are used in PIEKTUK-B. These changes, in addition to the elimination of the 64 particle size bins, augment the efficiency of PIEKTUK-B by a factor of about 100 over PIEKTUK-S.

3. Results

In the previous section, we described a simplified bulk algorithm for the depiction of the blowing snow process. We now perform a few tests to evaluate the model output of the bulk version of PIEKTUK in comparison to its spectral formulation. Both versions of the model have been modified following the discussion in Section 2.2.4, with the exception of the vertical and temporal resolutions in PIEKTUK-S which maintain those used in Déry et al. (1998). For our control experiment, we take here $U_{10} = 15 \text{ m s}^{-1}$ and initially that $T_a = -10^\circ\text{C}$, as background environmental conditions for a blowing snow period of 10 min. The initial humidity profile is obtained following Equation (23) by taking RH_i at $z = 100 \text{ m}$ to be 0.7 and constant above that level initially. Other parameters required for the integration, such as u_* and z_0 , are calculated following Déry et al. (1998). The vertical model boundaries are fixed at $z_{lb} = 0$ and $z_{ub} = 1 \text{ km}$, respectively.

To evaluate the ability of PIEKTUK-B to reproduce the results of PIEKTUK-S, we first examine in Figure 1 the profiles of blowing snow mixing ratio in the control experiment as predicted by both models 10 min. after

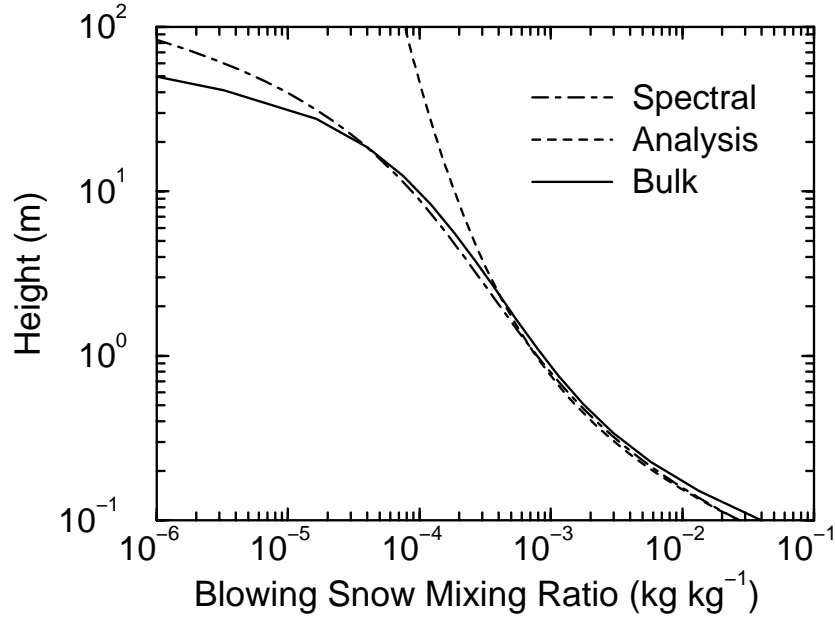


Figure 1. The profiles of blowing snow mixing ratio as predicted by the bulk and spectral versions of the PIEKTUK model 10 minutes after blowing snow initiation for the control experiment. The analytical result without sublimation (“Analysis”) is also shown.

the initiation of snow transport. The analytical profile of q_b that arises through a steady-state balance between diffusion and settling only is also shown in Figure 1. We see clearly that little accuracy is lost in using the bulk model to predict the variation of q_b with height.

For further tests, we examine the blowing snow sublimation and transport fluxes that affect the surface mass balance. The vertically integrated sublimation rate Q_s in units of mm h^{-1} snow water equivalent (swe) for a column of blowing snow is obtained from:

$$Q_s = -\rho' \int_{z_{lb}}^{z_{ub}} S_b dz, \quad (26)$$

where ρ' is the conversion factor from m s^{-1} to mm h^{-1} swe. For convenience, we introduce a negative sign in Equation (26) to report the sublimation rate as a positive quantity. The transport rate of blowing snow Q_t ($\text{kg m}^{-1} \text{s}^{-1}$) is given by

$$Q_t = \rho \int_{z_{lb}}^{z_{ub}} U q_b dz, \quad (27)$$

where U (m s^{-1}) is the wind speed. The evolution in time of Q_s and Q_t are shown in Figure 2 and again, we see that for both cases, good agreement

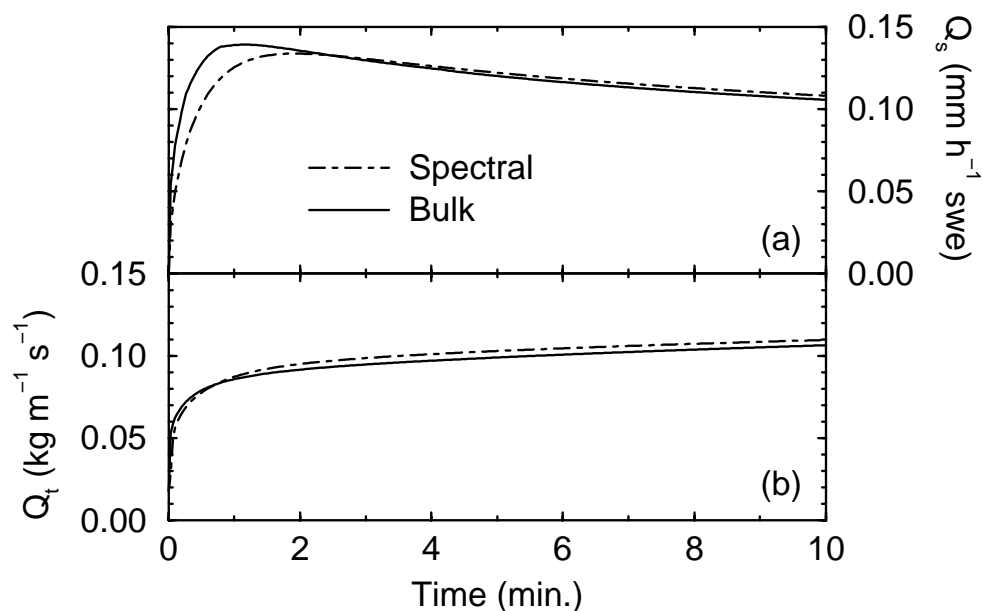


Figure 2. The temporal evolution of (a) the sublimation rate (Q_s) and (b) transport rate (Q_t) of blowing snow, predicted by the bulk and spectral versions of PIEKTUK for the control experiment.

between the bulk and spectral versions of PIEKTUK are found. Sublimation of blowing snow, as predicted by Déry et al. (1998), reaches a maximum within a few minutes of initiation, and then slowly decreases in time. This is related to the “self-limiting” property of blowing snow sublimation discussed by the authors. On the other hand, Q_t increases continually in time as higher humidities and diffusion act to augment the amount of suspended ice particles in a column of blowing snow.

Values of the blowing snow transport and sublimation rates predicted by both versions of PIEKTUK are shown in Table I for three values of the 10-m wind speed and two integration periods. The bulk model forecasts of the sublimation and transport rates match relatively well those of PIEKTUK-S, particularly at high wind speeds. For the control experiment, we find differences of approximately 5 and 3% between the integrated values of the sublimation and transport rates, respectively, as predicted by the bulk and spectral versions of PIEKTUK. For a one-hour period of blowing snow with $U_{10} = 15 \text{ m s}^{-1}$, the cumulative sublimation rate leads to a depletion of $0.09 \text{ mm h}^{-1} \text{ swe}$ from the surface, equivalent to the removal of $\approx 2 \text{ mm swe}$ per day. This is very similar to the sublimation rates reported by Schmidt (1982), King et al. (1996), and Bintanja (1998b).

Table I. The sublimation rate (Q_s), in mm h^{-1} snow water equivalent (swe), and transport rate (Q_t) of blowing snow, for three wind speeds and two time integrations forecast by the spectral (S) and bulk (B) versions of PIEKTUK. Time-integrated values of sublimation (QT_s) and transport (QT_t) of blowing snow are also listed.

U_{10} (m s^{-1})	Time (min.)	Model Version	Q_s (mm h^{-1} swe)	QT_s (mm swe)	Q_t ($\text{kg m}^{-1} \text{ s}^{-1}$)	QT_t (kg m^{-1})
10	10	S	0.02747	0.004726	0.01592	9.296
		B	0.03185	0.005570	0.01716	9.939
	60	S	0.02223	0.02491	0.01692	58.83
		B	0.02535	0.02877	0.01892	64.50
15	10	S	0.1081	0.01973	0.1097	59.89
		B	0.1045	0.01999	0.1065	58.09
	60	S	0.06874	0.08882	0.1390	439.7
		B	0.06511	0.08644	0.1421	438.1
20	10	S	0.2041	0.03972	0.4903	255.1
		B	0.1897	0.03951	0.4619	243.3
	60	S	0.1052	0.1550	0.6863	2071.
		B	0.09207	0.1434	0.6510	1962.

In Figure 3, the thermodynamic profiles are shown, 10 min. after the initiation of blowing snow, for the control experiment. These also show good correlation between the two versions of the model. Note how the sublimation of blowing snow leads to a weak temperature inversion in the ABL and a deviation from the logarithmic profile in humidity similar to the one proposed by Schmidt (1972) during blowing snow. Thus the temperature and humidity tendencies resulting from blowing snow sublimation predicted by PIEKTUK-B match those of PIEKTUK-S very well.

4. Sensitivity Tests

As discussed previously, the results presented in the previous section are highly dependent on the lower boundary conditions imposed on humidity. Maximum values of q_b are found in the saltation layer which is usually a layer several centimetres thick just above the snow surface. Observations by Schmidt (1982) suggest that RH_i approaches 1.0 in this region but diffusion of moisture outside of the saltation layer may promote further sublimation near the surface. We therefore conduct several additional experiments to test the sensitivity of the results to this parameter by modifying the lower boundary condition imposed on humidity in PIEKTUK-B.

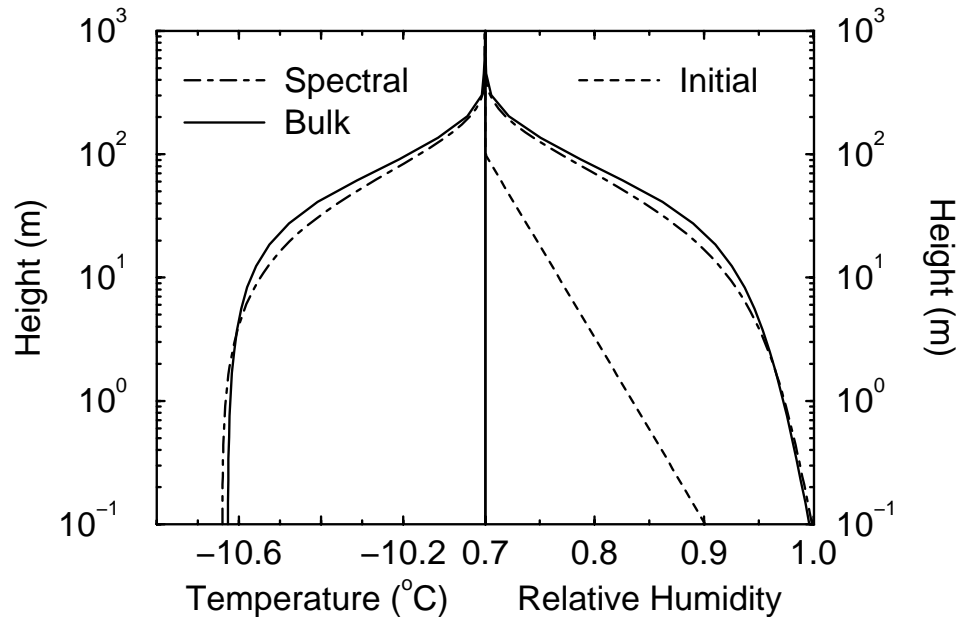


Figure 3. The profiles of ambient air temperature and relative humidity with respect to ice predicted by the bulk and spectral versions of the PIEKTUK model 10 minutes after blowing snow initiation for the control experiment.

In our previous integrations, we assumed saturation with respect to ice at the surface. In the first test, we fix RH_i at 0.95 at the surface during the integration. As expected, Q_s is higher than for the control run, with an increase of about 14% in QT_s for a 10 min. period of blowing snow (Figure 4). In two other experiments, we allow the lower boundary condition on humidity to vary in time (i.e., an “open” boundary condition) with limitation brought about by saturation with respect to ice. In one case, the initial humidity profile is as in the control run, while in the other one, we let $RH_i = 0.7$ initially throughout the column of air. We see that both show large increases in Q_s in comparison to the control experiment in the first few minutes that follow the initiation of blowing snow, but that both slowly tend towards the results of our control run in time as sublimation leads to increased moisture in the ABL. Differences incurred in QT_s in these additional experiments are of the order of 21 to 30% higher than the control run.

5. Concluding Discussion

The water budget of a snow-covered surface may be affected by blowing snow through the redistribution of snow by wind and the concurrent sublimation of

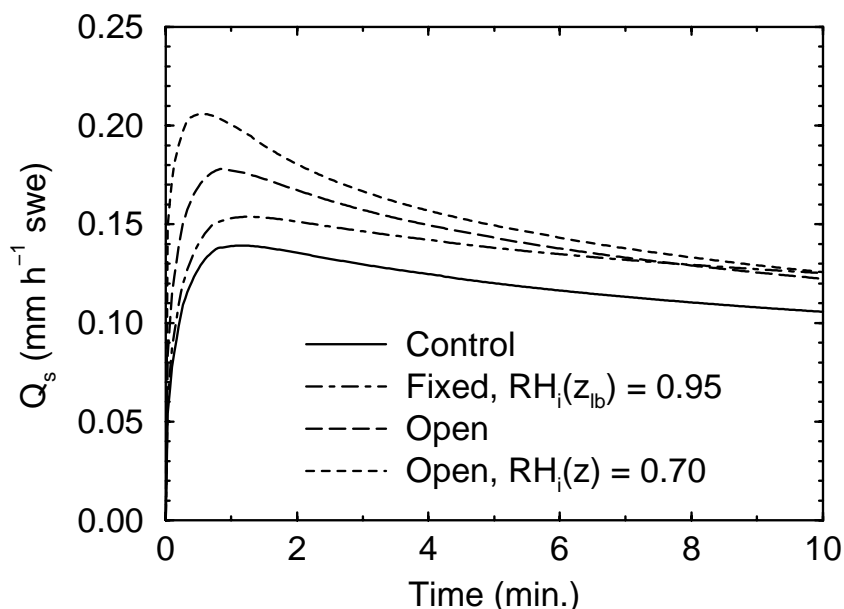


Figure 4. The temporal evolution of the sublimation rate Q_s of blowing snow for the control experiment and three sensitivity tests on the lower boundary conditions for humidity, (see text for a description of these tests.)

blowing snow. A number of studies have evaluated the contribution of these terms to the surface mass balance with notable variation on the significance of the sublimation component (e.g., Pomeroy et al., 1993, 1997; King et al., 1996; Bintanja, 1998b; Liston and Sturm, 1998). For instance, sublimation of blowing snow is evaluated to erode from a few millimetres swe at Halley, Antarctica over 6 months (King et al., 1996) to 37 mm swe during winter in a high-Arctic basin (Pomeroy et al., 1997). Considering the results presented in Table I for our control experiment in which $Q_s \approx 2 \text{ mm d}^{-1} \text{ swe}$, 17 days with continuous blowing snow would be required to erode the surface of the amount reported by Pomeroy et al. (1997). The climatology of cold-season processes compiled by Déry and Yau (1999) show an annual average ≥ 30 blowing snow events for this region, thus potentially leading to the snow removal rates assessed by Pomeroy et al. (1997).

As discussed by Tabler and Schmidt (1972), Tabler (1975), and others, the sublimation rate will tend to increase with fetch or time if environmental conditions remain unchanged. However, in their idealized experiments, Déry et al. (1998), as well as the results in this study, show that the thermodynamic feedbacks of blowing snow sublimation potentially lead to decreases in Q_s with time or fetch. As noted by King et al. (1996), Déry et al. (1998) and

others, however, the modelling of blowing snow depends critically on the lower boundary conditions imposed on humidity. We conducted several tests which showed an increase of 14 to 30% in the accumulated sublimation rate from the control run when varying the initial and boundary conditions on humidity. Mixing of dry air from aloft (> 1 km) with air in the ABL may also promote sublimation of blowing snow. It remains clear that further investigation of the blowing snow process, including the measurement of humidity and temperature in near-surface air, is required to assess more accurately the contribution of blowing snow sublimation and transport to the mass balance of snow-covered surfaces.

To summarize, we have presented in this paper a brief outline of a simple and efficient algorithm of sublimating, blowing snow. This blowing snow model, named PIEKTUK, uses a bulk approach to predict the temporal evolution of the blowing snow mixing ratio, temperature and moisture profiles, as well as the interactive feedbacks between these, for a column of air in the atmospheric boundary layer. In comparison with a previous spectral version of PIEKTUK, the bulk model successfully forecasts the evolution of the sublimation rate of blowing snow and its mixing ratio profiles with significant savings in computer time (by a factor of about one hundred).

Acknowledgements

This work has been supported by the Natural Science and Engineering Research Council of Canada through a collaborative research agreement as part of the Canadian GEWEX program. We also thank Mrs. Jingbing Xiao and Dr. Peter A. Taylor at York University for stimulating discussions on blowing snow modelling.

References

- Bintanja, R.: 1998a, 'The Interaction Between Drifting Snow and Atmospheric Turbulence', *Annals Glaciol.* **26**, 167-173.
- Bintanja, R.: 1998b, 'The Contribution of Snowdrift Sublimation to the Surface Mass Balance of Antarctica', *Annals Glaciol.* **27**, 251-259.
- Budd, W. F.: 1966, 'The Drifting of Non-Uniform Snow Particles', in Rubin, M. J. (ed.), *Studies in Antarctic Meteorology*, Antarctic Research Series Vol. 9, American Geophysical Union, Washington, DC, pp. 59-70.
- Déry, S. J. and Taylor, P. A.: 1996, 'Some Aspects of the Interaction of Blowing Snow with the Atmospheric Boundary Layer', *Hydrol. Proc.* **10**, 1345-1358.
- Déry, S. J., Taylor, P. A., and Xiao, J.: 1998, 'The Thermodynamic Effects of Sublimating, Blowing Snow in the Atmospheric Boundary Layer', *Boundary-Layer Meteorol.* **89**(2), 251-283.

- Déry, S. J. and Yau, M. K.: 1999, 'A Climatology of Adverse Winter-Type Weather Events', *J. Geophys. Res.*, in press.
- Garratt, J. R.: 1992, *The Atmospheric Boundary Layer*, Cambridge University Press, Cambridge, 316 pp.
- King, J. C., Anderson, P. S., Smith, M. C., and Mobbs, S. D.: 1996, 'The Surface Energy and Mass Balance at Halley, Antarctica during Winter', *J. Geophys. Res.* **101(D14)**, 19,119-19,128.
- Kong, F. and Yau, M. K.: 1997, 'An Explicit Approach to Microphysics in the MC2', *Atmos.-Ocean* **35**, 257-291.
- Lee, L. W.: 1975, *Sublimation of Snow in Turbulent Atmosphere*, Unpublished Ph. D. Dissertation, Dept. of Mechanical Engineering, University of Wyoming, Laramie WY, 82070, 162 pp.
- Li, L. and Pomeroy, J. W.: 1997, 'Estimates of Threshold Wind Speeds for Snow Transport using Meteorological Data', *J. Appl. Meteorol.* **36**, 205-213.
- Liston, G. E. and Sturm, M.: 1998, 'A Snow-Transport Model for Complex Terrain', *J. Glaciol.* **44**, 498-516.
- Mobbs, S. D. and Dover, S. E.: 1993, 'Numerical Modelling of Blowing Snow', in *Antarctic Special Topic*, British Antarctic Survey, Cambridge, pp. 55-63.
- Pomeroy, J. W., Gray, D. M., and Landine, P. G.: 1993, 'The Prairie Blowing Snow Model: Characteristics, Validation, Operation', *J. Hydrol.* **144**, 165-192.
- Pomeroy, J. W., Marsh, P. and Gray, D. M.: 1997, 'Application of a Distributed Blowing Snow Model to the Arctic', *Hydrol. Proc.* **11**, 1451-1464.
- Rogers, R. R. and Yau, M. K.: 1989, *A Short Course in Cloud Physics*, 3rd ed., Pergamon Press, 293 pp.
- Rouault, R. R., Mestayer, P. G., and Schiestel, R.: 1991, 'A Model of Evaporating Spray Droplet Dispersion', *J. Geophys. Res.* **96(C4)**, 7181-7200.
- Schmidt, R. A.: 1972, *Sublimation of Wind-Transported Snow - A Model*, USDA Res. Paper RM-90, USDA Forestry Service, Rocky Mountain Forest and Range Experimental Station, Fort Collins, Colorado, 24 pp.
- Schmidt, R. A.: 1982, 'Vertical Profiles of Wind Speed, Snow Concentrations, and Humidity in Blowing Snow', *Boundary-Layer Meteorol.* **23**, 223-246.
- Stewart, R. E., Leighton, H. G., Marsh, P., Moore, G. W. K., Rouse, W. R., Soulis, S. D., Strong, G. S., Crawford, R. W., and Kochtubajda, B.: 1998, 'The Mackenzie GEWEX Study: The water and energy cycles of a major North American river basin', *Bull. Amer. Meteorol. Soc.* **79(12)**, 2665-2684.
- Stull, R. B.: 1988, *An Introduction to Boundary Layer Meteorology*, Kluwer Academic Press, Dordrecht, 666 pp.
- Tabler, R. D. and Schmidt, R. A.: 1972, 'Weather Conditions that Determine Snow Transport Distances at a Site in Wyoming', in *UNESCO/WMO Symposia on the Role of Snow and Ice in Hydrology*, 118-127.
- Tabler, R. D.: 1975, 'Estimating the Transport and Evaporation of Blowing Snow', In *Proc. Symposium on Snow Management on the Great Plains*, Great Plains Agricultural Council Publ. 73, pp. 85-104.
- Taylor, P. A.: 1969, 'On Planetary Boundary Layer Flow Under Conditions of Neutral Thermal Stability', *J. Atmos. Sci.* **26**, 427-431.
- Thorpe, A. D. and Mason, B. J.: 1966, 'The Evaporation of Ice Spheres and Ice Crystals', *Brit. J. Appl. Phys.* **17**, 541-548.

4.3 Presentation of Article 4

This section proposes a further extension to the bulk version of the PIEKTUK blowing snow model described in Chapter 4.2. Although the adoption of a bulk scheme for blowing snow modelling provides accurate estimates of the temporal evolution of the transport and sublimation rates of blowing snow, it is deficient in describing the evolution of the total blowing snow particle numbers. We therefore add another prognostic variable for the total number density of particles, yielding a double-moment blowing snow model. It is shown that the double-moment scheme improves the predictions of the vertical profiles of the total number density of blowing snow particles and their implicit distributions. The double-moment version of PIEKTUK is then used to derive a parametrization of the sublimation rate of blowing snow that depends on the wind speed and a temperature- and moisture-dependent term. Both the model and parametrization are applied to the Canadian Arctic where blowing snow is estimated to remove several millimetres snow water equivalent from the surface mass balance at Trail Valley Creek, NWT. Since the conclusions reached in this study depend critically on the proper assimilation of the humidity measurements that were recorded at this Arctic tundra site, a thorough discussion on this matter is found in the Appendix.

4.4 Article 4

Simulation of blowing snow in the Canadian Arctic using a double-moment model.
By Stephen J. Déry and M. K. Yau, 2001: *Bound.-Layer Meteorol.*, in press.

Reproduced with kind permission from Kluwer Academic Publishers.

SIMULATION OF BLOWING SNOW IN THE CANADIAN ARCTIC USING A DOUBLE-MOMENT MODEL

STEPHEN J. DÉRY and M. K. YAU

*Dept. of Atmospheric and Oceanic Sciences, McGill University, 805 Sherbrooke St. W.,
Montréal, Québec, H3A 2K6 Canada*

Abstract. We describe in this paper the development of a double-moment model of blowing snow and its application to the Canadian Arctic. We first outline the formulation of the numerical model which solves a prognostic equation for both the blowing snow mixing ratio and total particle numbers, both moments of particles that are gamma-distributed. Under idealized simulations, the model yields realistic evolutions of the blowing snow particle distributions, transport and sublimation rates as well as the thermodynamic fields at low computational costs. A parametrization of the blowing snow sublimation rate is subsequently derived. The model and parametrization are then applied to a Canadian Arctic tundra site prone to frequent blowing snow events. Over a period of 210 days during the winter of 1996/1997, the near-surface relative humidity consistently approaches saturation with respect to ice. These conditions limit snowpack erosion by blowing snow sublimation to ≈ 3 mm snow water equivalent (swe) with surface sublimation removing an additional 7 mm swe. We find that our results are highly sensitive to the proper assimilation of the humidity measurements and the evolving thermodynamic fields in the atmospheric boundary layer during blowing snow. These factors may explain the lower values of blowing snow sublimation reported in this paper than previously published for the region.

Keywords: Arctic, Blizzard, Blowing snow, Double-moment, Mackenzie Basin, Sublimation

1. Introduction

In the Canadian Arctic, land and ice surfaces are predominantly covered by snow. Open and windswept areas thus become subject to frequent and hazardous blowing snow and blizzard events (Stewart et al., 1995; Déry and Yau, 1999a). As a consequence of these adverse meteorological conditions, the surface mass balance of the Canadian Arctic may be altered significantly by wind redistribution and concurrent sublimation.

The hydrometeorological implications of blowing snow have motivated a number of recent studies on the topic (e.g., King et al., 1996; Pomeroy et al., 1997; Bintanja, 1998; Essery et al., 1999; Mann et al., 2000). Nevertheless, questions remain on the importance of blowing snow sublimation in the surface water budget. For instance, Pomeroy et al. (1997) and Essery et al. (1999) estimate the seasonal removal of 37 to 85 mm snow water equivalent (swe) through blowing snow sublimation at a Canadian Arctic tundra site. In contrast, King et al. (1996) evaluate the erosion of no more than 4 mm swe over a period of 6 months from a snow-covered Antarctic ice shelf. The reported variations on the significance of blowing snow sublimation in



the surface mass balance are, in large part, a consequence of the numerical modelling strategies employed by the respective authors. Specifically, assumptions on the background thermodynamic profiles and their temporal and spatial evolutions are critical in evaluating the rates of snowdrift sublimation.

Déry and Yau (1999a) suggested that coupled simulations of a mesoscale model, such as the mesoscale compressible community (MC2) model (Benoit et al., 1997) and a blowing snow model, such as PIEKTUK (Déry et al., 1998) would improve our understanding of the snowdrift phenomenon and its interaction with the atmospheric boundary layer (ABL). However, to suit the requirements of the MC2 model, Déry and Yau (1999b, hereafter DY99b) derived a bulk formulation of the PIEKTUK model (PIEKTUK-B) that increased its computational efficiency by a factor of 100, allowing for coupled simulations of the two models at reasonable numerical costs.

In a recent intercomparison project of four blowing snow models (Xiao et al., 2000), it was found that PIEKTUK-B performed relatively well in predicting the blowing snow transport and sublimation rates and impact to the thermodynamic profiles. However, its predictions of the numbers and size distribution of particles appeared less realistic. This deficiency is understandable because the primary purpose of PIEKTUK-B was to predict accurately the transport and sublimation rates, and not the particle size spectra, of blowing snow. Since certain properties of blowing snow, such as its radar reflectivity and its impact to the horizontal visibility, are dependent on the numbers and size distribution of suspended ice particles, it is highly desirable to simulate realistically the total numbers of blowing snow particles in addition to its transport and sublimation fluxes. The first goal of this paper, therefore, is to remove this deficiency of PIEKTUK-B while maintaining the numerical efficiency of the model.

Although our ultimate objective for the development of a computationally inexpensive model of blowing snow is to perform coupled simulations with the MC2 model, we take advantage here of its efficiency by applying it to a lengthy and continuous meteorological dataset. These data were collected at an Arctic tundra site situated near the Mackenzie River Basin (MRB) in Northern Canada over a period of 210 days during the winter of 1996/1997 as part of the Mackenzie GEWEX Study (MAGS; Stewart et al., 1998). This intensive field programme aims to shed light on the water and energy budgets of the MRB, including the largely unknown role of blowing snow as a component of the surface mass balance (Lawford, 1994; Stewart et al., 1998). Although previous studies by Pomeroy et al. (1997) and Essery et al. (1999) have begun this process, their high values of blowing snow sublimation remain questionable. Therefore, our second objective is to assess the seasonal contribution of blowing snow to the Arctic tundra water budget using an updated numerical model with evolving thermodynamic fields. We will then consider some possible factors that lead to the high values of sublimation

reported by Essery et al. (1999) obtained from a steady-state numerical model applied to the same dataset.

A third and final goal of this work is the parametrization of blowing snow sublimation in terms of the ambient meteorological conditions. Even a simplified model of blowing snow can become computationally restrictive for long-term, basin-scale mass balance studies. The paper therefore introduces one such parametrization obtained from multiple integrations of the simplified blowing snow model and verified with the Canadian Arctic data.

The paper is structured as follows. In Section 2, we first describe the formulation and perform tests of the updated PIEKTUK model before the derivation of a parametrization of blowing snow sublimation rates. The model and parametrization are then applied to the Canadian Arctic to evaluate the possible role of blowing snow in the local surface mass balance. Section 4 contains a discussion of our results followed by a summary and some conclusions which close the paper in Section 5.

2. Numerical Model

The algorithm discussed in this section is an extension of the original spectral and bulk formulations of the PIEKTUK model which are already well documented in the literature (D ery and Taylor, 1996; D ery et al., 1998; DY99b). The spectral model (PIEKTUK-S) is referred to as such due to its explicit treatment of blowing snow particles using 64 or more size classes. On the other hand, the latter model expressed blowing snow in terms of a single (and hence “bulk”) quantity, thereby reducing significantly the computational requirements of the model. To maintain brevity, we now describe steps leading only from the single-moment, bulk blowing snow scheme to one where two moments of the size distribution of the particles are solved and encourage the reader to the aforementioned references for a more complete description of PIEKTUK. We then perform a few tests to evaluate the updated model in comparison to its spectral formulation.

2.1. MODEL FORMULATION

2.1.1. Bulk Model (PIEKTUK-B)

The single-moment formulation of PIEKTUK was developed by DY99b based on the premise that the evolution of the suspension and sublimation of blowing snow can be obtained through the solution of one prognostic equation for the mixing ratio of blowing snow q_b (kg kg^{-1}) instead of the spectral number density $F(r)$ (m^{-4}) of spherical particles of radius r (m). By definition, the two quantities are related through:

$$q_b = \frac{4\pi\rho_{ice}}{3\rho} \int_0^\infty r^3 F(r) dr, \quad (1)$$

where ρ (kg m^{-3}) and ρ_{ice} ($= 900 \text{ kg m}^{-3}$) denote the densities of air and ice, respectively.

Based on the field measurements of Budd (1966) and Schmidt (1982), DY99b assumed that the particle spectrum can be described by a two-parameter gamma distribution of the form

$$F(r) = \frac{Nr^{\alpha-1} \exp^{-r/\beta}}{\beta^\alpha \Gamma(\alpha)}, \quad (2)$$

with N (m^{-3}) representing the total number concentration of particles and α (dimensionless) and β (m) the shape and scale parameters of the gamma distribution Γ .

Substituting Equation (2) into (1), integrating and solving for β , we obtain

$$\beta = \left[\frac{3\rho q_b \Gamma(\alpha)}{4\pi\rho_{ice} \Gamma(\alpha+3)N} \right]^{1/3}. \quad (3)$$

Equation (3) states that α , β , N and q_b are all interrelated. To obtain the complete spectrum, we need to have knowledge of only three of the variables.

For the bulk model, DY99b specify α and N , but predict the evolution of q_b , the air temperature T_a (K), and the water vapour mixing ratio q_v (kg kg^{-1}) in a column of air from

$$\frac{\partial q_b}{\partial t} = \frac{\partial}{\partial z} \left(K_b \frac{\partial q_b}{\partial z} + v_b q_b \right) + S_b, \quad (4a)$$

$$\frac{\partial T_a}{\partial t} = \frac{\partial}{\partial z} \left(K_h \frac{\partial T_a}{\partial z} \right) + \frac{S_b L_s}{c_p}, \quad (4b)$$

and

$$\frac{\partial q_v}{\partial t} = \frac{\partial}{\partial z} \left(K_v \frac{\partial q_v}{\partial z} \right) - S_b, \quad (4c)$$

where t (s) denotes time, z (m) the vertical coordinate, L_s (J kg^{-1}) the latent heat of sublimation, and c_p ($\text{J kg}^{-1} \text{K}^{-1}$) the heat capacity for air. The terms K_b , K_h and K_v ($\text{m}^2 \text{s}^{-1}$) represent the turbulent eddy diffusivities for blowing snow, heat and moisture, respectively. Note that each equation has a source/sink term associated with the bulk sublimation rate S_b ($\text{kg kg}^{-1} \text{s}^{-1}$) of blowing snow. Unlike the heat and moisture variables, blowing snow is subject to sedimentation with a settling velocity denoted by v_b (m s^{-1}).

They further set $\alpha = \text{constant} = 2$ and $N = kN_s(z) = 3N_s(z)$, where $N_s(z)$ (m^{-3}) is a steady-state solution for the total particle number concentration in a saturated environment. DY99b showed that this bulk formulation predicts

well the sublimation and transport rates of blowing snow. However, N is only a function of height and is physically less realistic because it does not evolve in time.

2.1.2. Double-Moment Model (PIEKTUK-D)

To relax the assumption on N , we introduce an explicit equation for this quantity. Just as the other three prognostic variables, N is taken to satisfy

$$\frac{\partial N}{\partial t} = \frac{\partial}{\partial z} \left(K_N \frac{\partial N}{\partial z} + v_N N \right) + S_N. \quad (4d)$$

Here, K_N ($\text{m}^2 \text{s}^{-1}$) denotes the eddy diffusivity for N , v_N (m s^{-1}) a representative terminal velocity for the total number of blowing snow particles, and S_N ($\text{m}^{-3} \text{s}^{-1}$) denotes the rate of change of particle numbers due to the sublimation process. Note that other processes such as fractionation or coalescence of particles are included implicitly in Equation (4d) through the assumed form of the particle size distribution.

Equations (4a) - (4d) describe the double-moment model, so-called because the model predicts both the zeroth moment (N) and the third moment (q_b) of the size distribution function $F(r)$. As seen in the recent literature, double-moment schemes have been successfully applied to the modelling of microphysical processes (e.g., Harrington et al., 1995; Reisner et al., 1998).

Similarly to the other turbulent diffusion coefficients, we take K_N to be:

$$K_N = \zeta K_m = \zeta u_* l, \quad (5)$$

where u_* (m s^{-1}) is the friction velocity, K_m ($\text{m}^2 \text{s}^{-1}$) the turbulent diffusion coefficient for momentum, and l (m) the mixing length defined as in DY99b. Note that the quantity ζ ($\equiv K_N/K_m$), is taken as unity. Our methodology for the specification of v_N follows that of DY99b for v_b with the exception that v_N is weighed by the second moment n of the gamma distribution. We set $n = 2$ in their Equation (13) for the setting of v_N . This value is found experimentally to give the best comparisons with analytical solutions for profiles of N when blowing snow sublimation is inactive.

In Equation (4d), we also need to define the reduction in particle numbers due to blowing snow sublimation. In principle, computation of the number of particles that completely sublimate in one timestep can be obtained by the integration of an incomplete gamma function. Keeping in mind, however, that we are striving for a numerically efficient blowing snow model, it is in our best interest to avoid this computationally expensive step. Thus we employ here the method of Harrington et al. (1995) who express S_N in terms of the mass lost to sublimation. The assumption here is that S_N is proportional to a change in blowing snow mass, i.e.,

$$\frac{S_N \Delta t}{N} = \frac{S_b \Delta t}{q_b}, \quad (6)$$

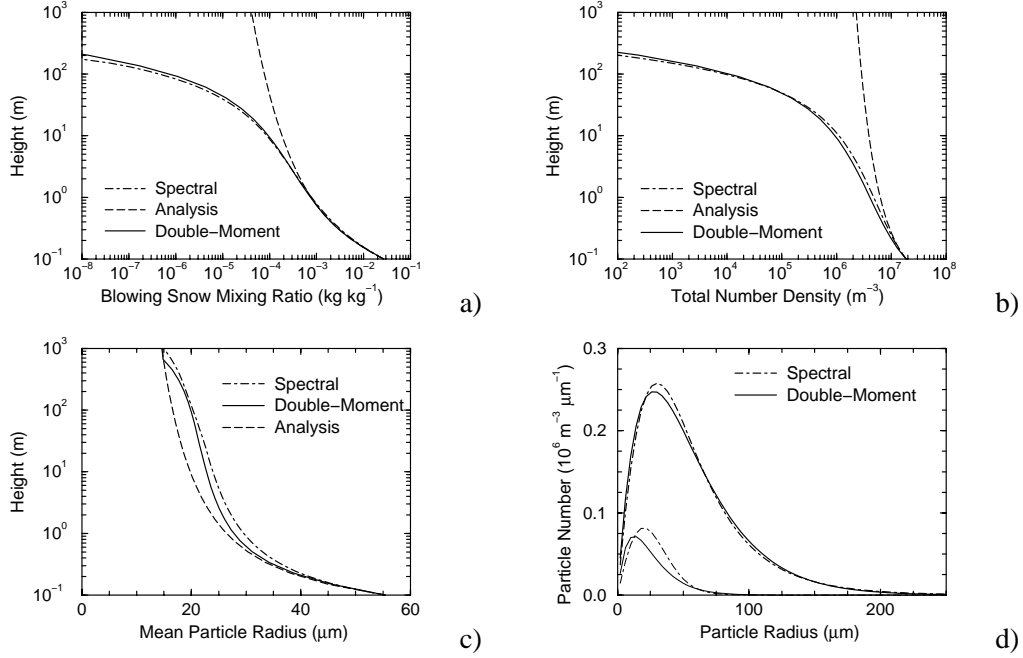


Figure 1. The profiles of a) blowing snow mixing ratio, b) total particle number density and c) mean particle radius predicted by the double-moment and spectral versions of the PIEKTUK model 10 minutes after blowing snow initiation for the control experiment. The steady-state, analytical results without sublimation (“Analysis”) are also shown. In d), the implicit particle distributions within the double-moment scheme are compared to the explicit ones of the spectral model. Thick (thin) lines depict results at $z = 0.1$ m ($z = 2.5$ m).

where Δt (s) denotes a model timestep. Model results are found to be quite sensitive to this assumption, but it is shown in the following section that this methodology yields realistic evolutions of N .

Boundary conditions on N are imposed as follows. At the model lid ($z_{ub} = 1$ km), we assume no vertical gradient in particle numbers. During blowing snow, we take the lower boundary (at $z_{lb} = 0.1$ m) on N to be invariable and given by:

$$N = \frac{3\rho q_b \alpha^3 \Gamma(\alpha)}{4\pi\rho_{ice} r_m^3 \Gamma(\alpha + 3)}, \quad (7)$$

where $r_m = \alpha\beta$ (m) is the mean radius of a spectrum of particles that are gamma-distributed. This constraint is obtained by solving for N in Equation (3) and then substituting $\beta = r_m/\alpha$. In Equation (7), values of r_m and q_b at z_{lb} are obtained by extrapolation from their respective values in the saltation layer. Through its dependence on the saltation mixing ratio, therefore, $N(z_{lb})$ is influenced by varying environmental factors such as wind speed,

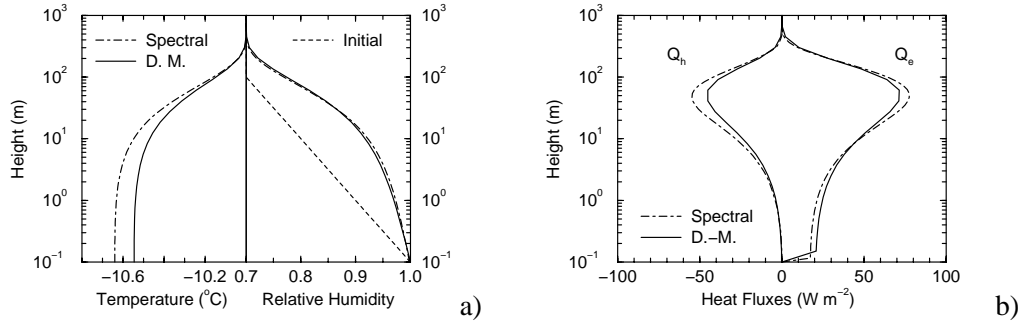


Figure 2. The profiles of a) ambient air temperature and relative humidity with respect to ice and b) sensible (Q_h) and latent (Q_e) heat fluxes predicted by the double-moment (D.-M.) and spectral versions of the PIEKTUK model 10 minutes after blowing snow initiation for the control experiment.

temperature and aerodynamic roughness length of the surface. Further details on the designation of these boundary conditions and values of the physical parameters can be found in DY99b.

2.2. MODEL TESTING

To verify the ability of PIEKTUK-D to reproduce the results of its antecedent spectral and bulk versions, we conduct similar numerical experiments to those of DY99b. For the control experiment, we take as initial conditions an isothermal ABL at $T_a = -10^\circ C$ and a relative humidity with respect to ice (RH_i) profile that varies logarithmically with height from $z = 100$ m where $RH_i = 0.70$ to z_{lb} where saturation with respect to ice is assumed. The wind speed profile also varies logarithmically with the 10-m wind speed $U_{10} = 15$ $m s^{-1}$. We also take $\alpha = 2$ at all heights and extrapolate a value for r_m at z_{lb} by taking $r_m = 100$ μm at the saltation layer height z_s (see DY99b for further details). Our use of $\Delta t = 5$ s yields an integration that is about 100 times faster than PIEKTUK-S.

Figure 1 shows the profiles of blowing snow mixing ratio, total particle number density, mean particle radius, as well as the distribution of particles at two levels above the surface, 10 minutes subsequent to the initiation of blowing snow. As shown in Figures 1a and 1b, agreement is very good between the spectral and double-moment models in terms of the vertical distribution of q_b and N .

The profiles of r_m predicted from both versions of PIEKTUK are also quite similar, with PIEKTUK-D matching more closely the analytical profile (Figure 1c). Values of r_m decrease with height as the suspension of heavier, larger particles becomes more difficult. Despite the constraint imposed on α in PIEKTUK-D, its implicit particle size distributions resemble closely the

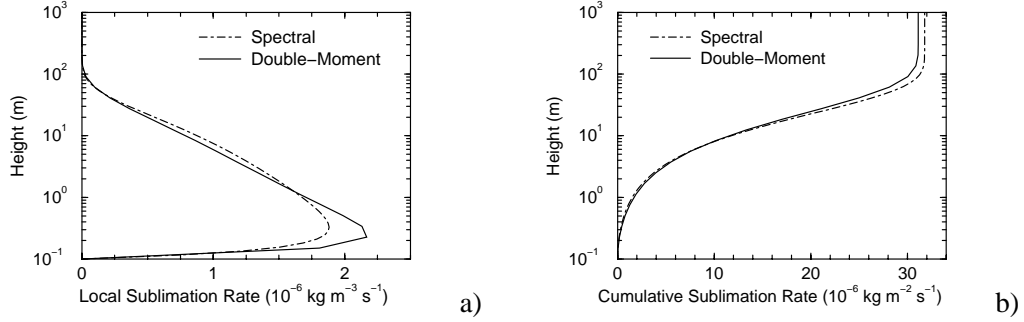


Figure 3. The profiles of (a) the local and (b) cumulative sublimation rates of blowing snow, predicted by the double-moment and spectral versions of the PIEKTUK model 10 minutes after blowing snow initiation for the control experiment.

explicit ones of PIEKTUK-S (Figure 1d). The observed differences can be explained in part by the fact that other spectral blowing snow models predict an increase in α with height from values of 2 near the surface to about 3 at higher elevations (Xiao et al., 2000).

Figure 2 illustrates the thermodynamic and heat flux profiles 10 minutes following the initiation of blowing snow. Although the changes in q_v and (especially) T_a profiles as a result of the sublimation process are less in PIEKTUK-D than in PIEKTUK-S, they do have similar shapes. Associated with the sublimation of blowing snow are perturbations in the sensible Q_h (W m^{-2}) and latent Q_e (W m^{-2}) heat fluxes, defined here as:

$$Q_h = -\rho c_p K_h \frac{\partial T_a}{\partial z}, \quad (8a)$$

and

$$Q_e = -\rho L_s K_v \frac{\partial q_v}{\partial z}, \quad (8b)$$

with positive (negative) heat fluxes directed towards the atmosphere (surface). The Q_h and Q_e profiles demonstrate the potentially large impact of blowing snow sublimation on ABL heat fluxes (Figure 2b). Although the largest temperature decreases occur near the surface at $t = 10$ min., the heat fluxes reach a maximum amplitude ($> 50 \text{ W m}^{-2}$) at $z \approx 50$ m. In the low-energy, wintertime environment of the Arctic, these heat flux perturbations can be quite significant (Déry et al., 1998).

The next illustration depicts the vertical profiles of the local sublimation rate $q_{subl} = -\rho S_b$ ($\text{kg m}^{-3} \text{ s}^{-1}$) and its cumulative value when integrated over height (using the trapezoidal rule), again 10 minutes subsequent to the start of blowing snow (Figure 3). Similar q_{subl} profiles are predicted by both models

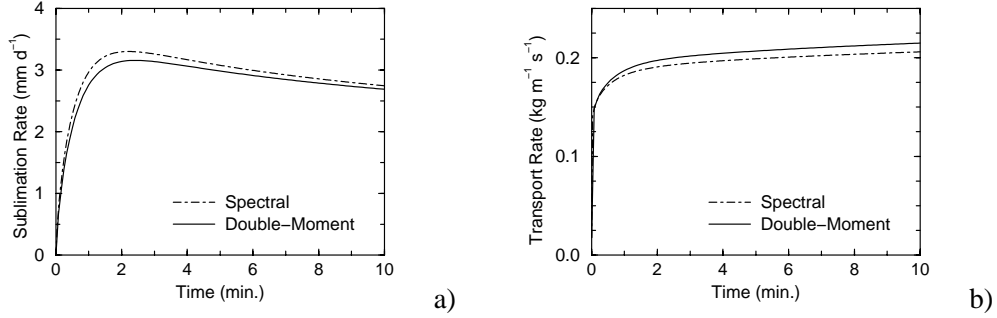


Figure 4. The temporal evolution of the vertically-integrated (a) sublimation rate and (b) transport rate of blowing snow, predicted by the double-moment and spectral versions of PIEKTUK for the control experiment.

but with the most notable differences near the lower model boundary. Since this region is relatively small compared to the overall model domain, it contributes negligibly to differences in the cumulative sublimation rate (Figure 3b). In addition, Figure 3b demonstrates that the region between $1 \text{ m} < z < 100 \text{ m}$ dominates the overall vertical integration of q_{subl} at this point in time.

We now present the temporal evolution of the total column-integrated sublimation Q_s (expressed here in units of $\text{mm d}^{-1} \text{ swe}$) and transport Q_t ($\text{kg m}^{-1} \text{ s}^{-1}$) rates of blowing snow for the two models. These quantities are defined as:

$$Q_s = -\rho' \int_{z_{lb}}^{z_{ub}} S_b dz, \quad (9a)$$

and

$$Q_t = \rho \int_{z_0}^{z_{ub}} q_b U dz, \quad (9b)$$

respectively. In these two equations, ρ' is a conversion factor from the units of m s^{-1} to $\text{mm d}^{-1} \text{ swe}$ and U (m s^{-1}) is the wind speed. We observe in Figure 4 slight underestimates of the transport and sublimation rates by PIEKTUK-D in comparison to PIEKTUK-S. Additional tests for three wind speeds and two time periods are conducted and show generally excellent agreement for both quantities (Table I).

2.3. PARAMETRIZATION OF THE BLOWING SNOW SUBLIMATION RATE

We have shown in the previous section that PIEKTUK-D yields, at a much lesser computational cost, similar results for the transport and sublimation rates of blowing snow as its spectral counterpart. We extend these results by conducting multiple integrations of PIEKTUK-D in order to parametrize the

Table I. The blowing snow sublimation (Q_s) and transport (Q_t) rates for 3 values of the 10-m wind speed (U_{10}) and 2 time integrations forecast by the spectral (S) and double-moment (D) versions of PIEKTUK. Time integrated values of sublimation (QT_s) and transport (QT_t) of blowing snow are also listed.

U_{10} (m s ⁻¹)	Time (min.)	Model Version	Q_s (mm d ⁻¹ swe)	QT_s (mm swe)	Q_t (kg m ⁻¹ s ⁻¹)	QT_t (kg m ⁻¹)
10	10	S	0.6847	0.004778	0.1076	64.32
		D	0.7155	0.004962	0.1095	65.32
	60	S	0.5632	0.02598	0.1086	388.9
		D	0.5915	0.02718	0.1113	396.9
15	10	S	2.746	0.02042	0.2059	117.4
		D	2.688	0.01971	0.2148	121.9
	60	S	1.767	0.09412	0.2374	789.7
		D	1.766	0.09286	0.2520	830.5
20	10	S	5.231	0.04168	0.5691	300.0
		D	5.145	0.04060	0.6167	326.6
	60	S	2.718	0.1654	0.7811	2380.
		D	2.648	0.1621	0.8253	2548.

blowing snow sublimation rate in terms of the meteorological conditions of wind speed, air temperature and humidity. First, we investigate the possibility of combining the two thermodynamic quantities into one. Recall from DY99b that the bulk sublimation rate of blowing snow is given by:

$$S_b = \frac{q_b Nu (q_v / q_{is} - 1)}{2\rho_{ice} r_m^2 (F_k + F_d)}, \quad (10)$$

where Nu depicts the Nusselt number, q_{is} (kg kg⁻¹) the saturation mixing ratio with respect to ice and F_k and F_d (m s kg⁻¹) the conductivity and diffusion terms associated with the sublimation process. By introducing a new variable ξ (m² s⁻¹) defined as:

$$\xi = \frac{(q_v / q_{is} - 1)}{2\rho_{ice} (F_k + F_d)}, \quad (11)$$

we may then express the bulk sublimation rate simply as:

$$S_b = \frac{q_b Nu \xi}{r_m^2}. \quad (12)$$

Hence, the effects of temperature and moisture on S_b are now combined into a single term ξ that is analogous to the condensation growth parameter discussed by Rogers and Yau (1989).

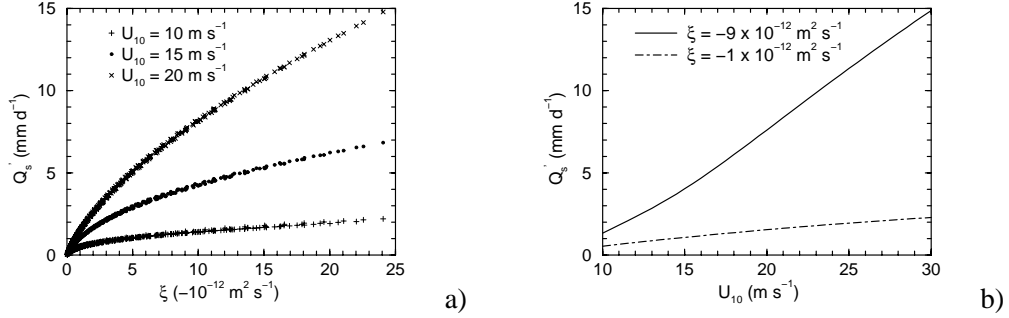


Figure 5. The variation of the normalized sublimation rate Q'_s (a) with ξ for three values of U_{10} and (b) with U_{10} for two values of ξ . The variables are defined in the text.

Before proceeding, we also introduce a new variable Q'_s (mm d^{-1} swe) which is a normalized column-integrated sublimation rate defined as:

$$Q'_s = Q_s q_{b_0} / q_{b_{salt}}, \quad (13)$$

where $q_{b_{salt}}$ (kg kg^{-1}) is the saltation mixing ratio and q_{b_0} (kg kg^{-1}) its value when the 10-m threshold wind speed for transport $U_t = 6.975 \text{ m s}^{-1}$. This removes a dependence of the sublimation rate on $q_{b_{salt}}$ which varies with U_t (see DY99b). Furthermore, we remark that values of RH_i and T_a for the computation of ξ are taken here to be 2 m above the surface. In this case, a logarithmic RH_i profile is assumed below $z = 2$ m (with $\text{RH}_i = 1.0$ at $z = z_{lb}$) but RH_i is taken as constant above this height. The distinct relationships for Q'_s in terms of ξ and U_{10} shown in Figure 5 confirm that a parametrization for the sublimation rate of blowing snow may only involve these two dependent variables.

After multiple integrations, we obtain the results shown in Figure 6. Values of Q'_s for half-hour periods, expressed in mm d^{-1} swe, demonstrate a strong dependence on both U_{10} and ξ . As the wind speed, temperature and subsaturation increase, so does the sublimation rate. We can then estimate Q'_s from an expression such as:

$$Q'_s = a_0 + a_1 \xi + a_2 \xi^2 + a_3 \xi^3 + a_4 U_{10} + a_5 \xi U_{10} + a_6 \xi^2 U_{10} + a_7 U_{10}^2 + a_8 \xi U_{10}^2 + a_9 U_{10}^3, \quad (14)$$

where U_{10} has units of m s^{-1} and ξ has units of $-1 \times 10^{-12} \text{ m}^2 \text{ s}^{-1}$. Values for the coefficients $a_0 - a_9$ are given in Table II. Note that Equation (14) is innovative compared to the parametrizations of Bintanja (1998) and Essery et al. (1999) in that it considers the unsteady effects of both temperature and humidity, in addition to the wind speed, up to heights of 1 km above the

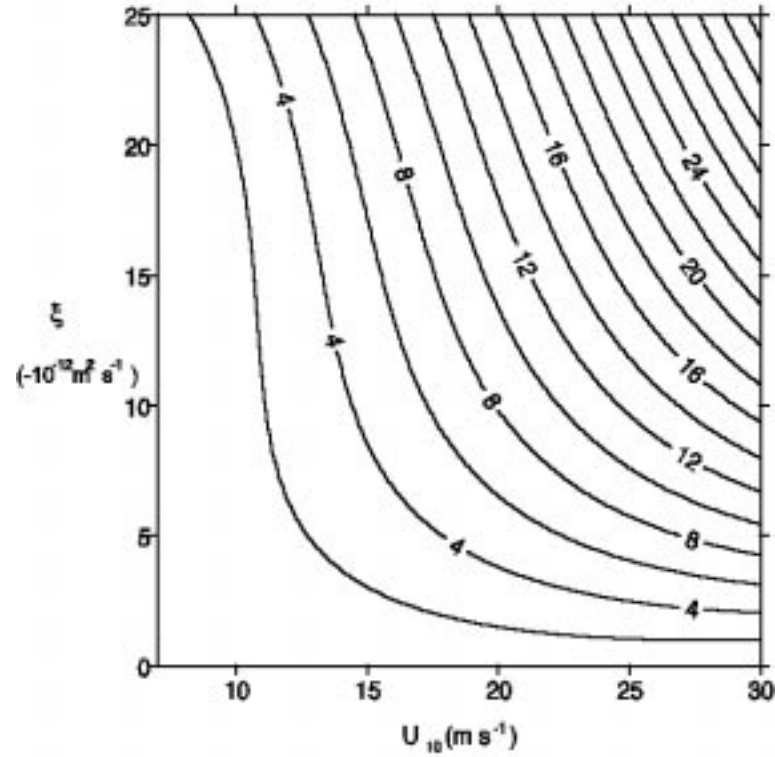


Figure 6. Contours of Q'_s (at intervals of $2 \text{ mm d}^{-1} \text{ swe}$) in terms of the 10-m wind speed U_{10} and the thermodynamic quantity ξ (as defined in the text).

Table II. Coefficients for Equation (14).

Coefficient	Value	Coefficient	Value
a_0	3.78407×10^{-1}	a_5	2.48430×10^{-2}
a_1	-8.64089×10^{-2}	a_6	-9.56871×10^{-4}
a_2	-1.60570×10^{-2}	a_7	1.24600×10^{-2}
a_3	7.25516×10^{-4}	a_8	1.56862×10^{-3}
a_4	-1.25650×10^{-1}	a_9	-2.93002×10^{-4}

surface, on the process of blowing snow sublimation. The parametrization is tested with model predictions in the following section.

3. Application to the Arctic

The windswept tundra regions of the Canadian Arctic are notorious for their adverse wintertime weather conditions. Given the high frequency of blowing snow and blizzard events in certain sections of the high-latitude MRB, its water and energy budgets are potentially susceptible to the effects of blowing snow (Déry and Yau, 1999a). As part of MAGS, special observations were conducted at Trail Valley Creek (68°45' N, 133°30' W), Northwest Territories (NWT), Canada, between 11 September 1996 to 8 April 1997 by researchers from the University of Saskatchewan and the National Hydrology Research Centre (NHRC; Essery et al., 1999). Although not within the MRB, the Trail Valley Creek research basin was determined to be a representative Arctic tundra site with undulating terrain and little vegetation (Pomeroy et al., 1997). Measurements of air temperature, wind speed and relative humidity were sampled every 30 seconds and averaged half-hourly. Details of the meteorological instruments can be found in Essery et al. (1999).

We have shown in the previous section that PIEKTUK-D yields comparable results to PIEKTUK-S in idealized situations with much lesser computational costs. We now take advantage of the updated model's efficiency by applying it to the meteorological dataset collected at Trail Valley Creek in 1996/1997. This allows us to make an assessment of the role of blowing snow in the local water budget when the "self-limiting" aspect of the sublimation process are considered. In addition, it will allow us to understand several factors that lead to the high sublimation rates reported by Essery et al. (1999) at the same location and time period.

For these simulations, PIEKTUK-D is initialized with the meteorological data and the model integrated forward in time for each half-hour period. The initial temperature profile is assumed constant within the ABL at the near-surface value but the initial humidity profile is taken to be logarithmic from the instrument height to the lower model boundary where saturation with respect to ice is assumed. A logarithmic wind profile is also inferred from the measured values. A uniform, snow-covered surface with no protruding vegetation, typical of the Arctic tundra during winter, is assumed within PIEKTUK-D. Note that the transport and sublimation rates of blowing snow are computed only when a blowing snow event, as defined by Déry and Yau (1999a), is detected, but that the sublimation rate is taken to be zero whenever $RH_i \geq 1.0$.

Over the course of this 210-day period, blowing snow conditions are inferred 10% of the total measurement times, with wind transport of snow occurring at least once daily on 71 days. This is consistent with the blowing snow climatology of Déry and Yau (1999a). Figure 7 shows the temporal evolution of the meteorological variables during the winter of 1996/1997 at Trail Valley Creek, including the modelled rates of blowing snow sublimation

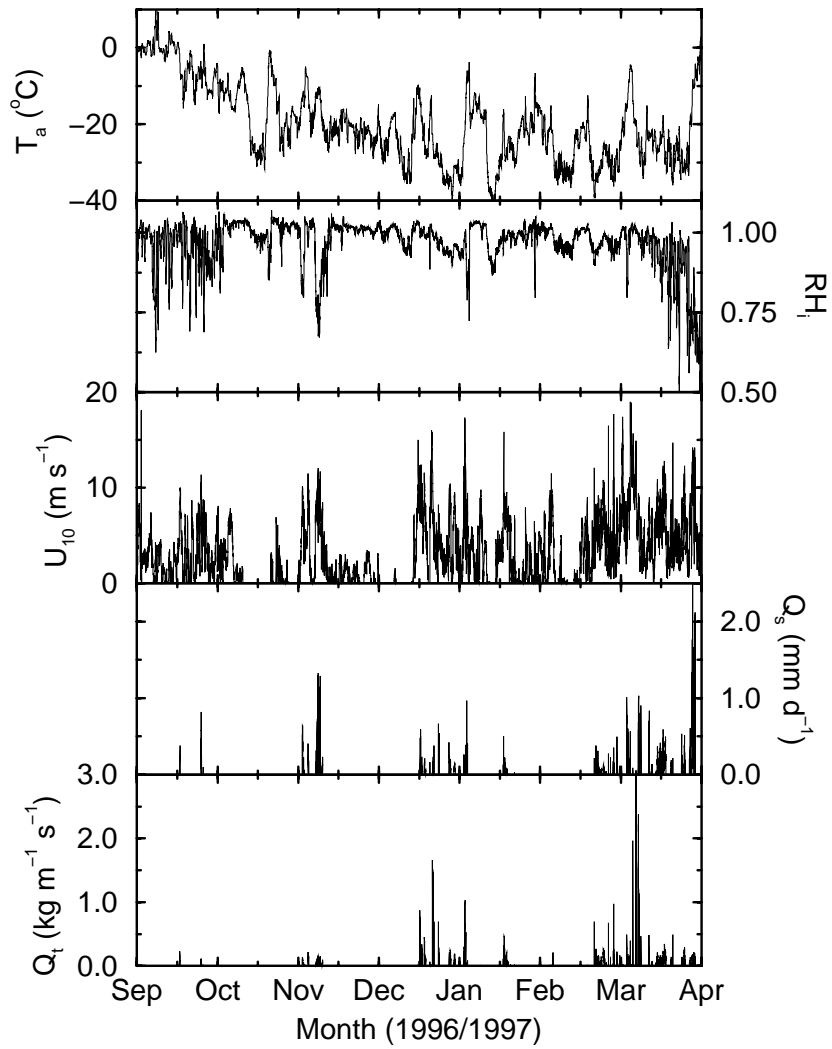


Figure 7. The temporal evolution of half-hourly averaged values of the ambient air temperature (T_a), the relative humidity with respect to ice (RH_i), the 10-m wind speed (U_{10}), and the modelled sublimation (Q_s) and transport (Q_t) rates of blowing snow from 11 September 1996 to 8 April 1997 at Trail Valley Creek, Northwest Territories.

SIMULATION OF BLOWING SNOW

15

Table III. Mean monthly values of observed air temperature (T_a), relative humidity with respect to ice (RH_i), 10-m wind speed (U_{10}), and total monthly values of estimated blowing snow transport (QT_t), sublimation (QT_s) and surface sublimation rates (QT_{surf}) at Trail Valley Valley Creek, Northwest Territories, between 11 September 1996 to 8 April 1997. Note that a negative value of QT_{surf} indicates net deposition at the snow surface.

Month	T_a (°C)	RH_i	U_{10} (m s ⁻¹)	QT_t (Mg m ⁻¹)	QT_s (mm swe)	QT_{surf} (mm swe)
Sep.	-1.1	0.98	2.5	0.632	0.0106	0.718
Oct.	-13.0	0.98	2.0	1.98	0.112	1.41
Nov.	-18.5	0.98	2.0	14.5	0.820	1.05
Dec.	-23.6	1.00	2.1	31.9	0.0896	-0.0731
Jan.	-26.8	0.97	3.2	41.4	0.299	0.488
Feb.	-24.7	0.99	2.0	1.69	0.00687	0.0560
Mar.	-25.1	0.95	5.4	87.9	0.776	0.677
Apr.	-18.4	0.79	5.3	21.0	1.27	2.71
Mean	-19.8	0.97	2.9			
Total				194.	3.38	7.04

and transport. We see clearly that during the cold winter months, air over the snow-covered Arctic tundra remains near the saturation point with respect to ice despite large wind and temperature fluctuations. These ambient humidity conditions, which limit *a priori* the sublimation of blowing snow at low levels, are often observed over ice- or snow-covered surfaces (Vowinckel and Orvig, 1970; Schwertdfeger, 1984; King and Anderson, 1999). Thus blowing snow events characterized by strong winds, and hence, large transport rates (e.g., 11 March 1997), do not necessarily lead to large sublimation fluxes. Significant blowing snow sublimation events occur more prominently during the early or late winter when drier (in a relative sense) and warmer (but nonetheless subfreezing) conditions exist, such as on 17 November 1996. This is clearly demonstrated in Table III which shows that 85% of the erosion of mass through blowing snow sublimation occurs during the months of November, March and April. For the entire winter of 1996/1997, PIEKTUK-D estimates the sublimation of about 3 mm swe whereas the wind displaces about 194 Mg m⁻¹ of snow.

The parametrization of Q_s discussed in the previous section yields reasonable estimates in comparison to the double-moment predictions for the sublimation rate of blowing snow, with the parametrization giving $QT_s = 3.2$ mm swe (Figure 8). The correlation coefficient between the two datasets

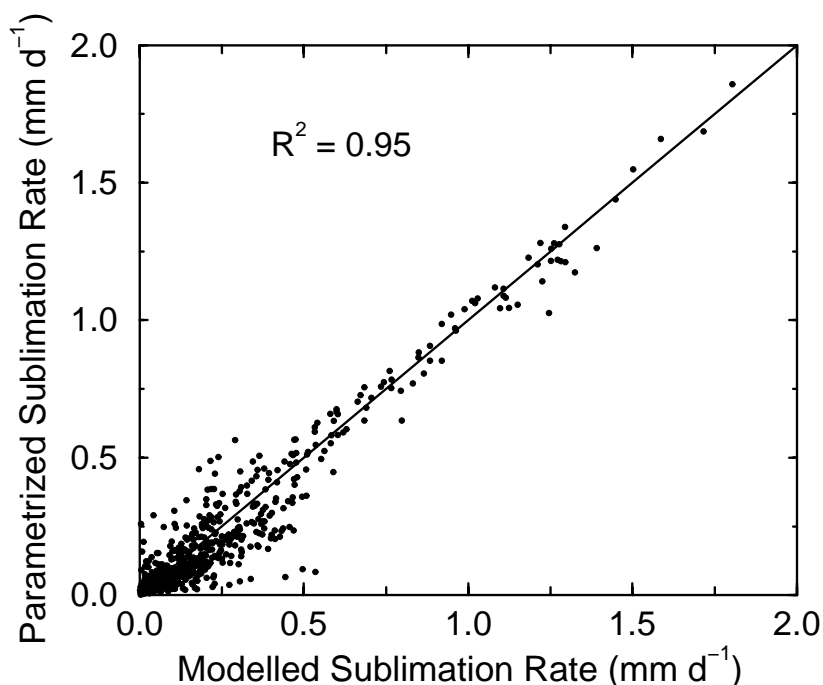


Figure 8. Comparison of the parametrized and modelled sublimation rates of blowing snow for Trail Valley Creek, Northwest Territories, during the winter of 1996/1997.

is about $R^2 = 0.95$, indicating that as a first approximation, sublimation of blowing snow can be determined from the parametrized expression.

4. Discussion

In the previous section, we estimated that blowing snow sublimation erodes ≈ 3 mm swe from the snowpack at Trail Valley Creek, NWT during winter. Similar values of the impact of blowing snow sublimation to the surface mass balance have been reported by King et al. (1996), Bintanja (1998), and Mann et al. (2000) for the Antarctic. However, in comparison with Essery et al. (1999), who assess losses of 44 to 85 mm swe due to blowing snow sublimation at Trail Valley Creek during the exact same 210-day period, we significantly underestimate its importance.

Considering that an order of magnitude separates our results with those of Essery et al. (1999), some possible factors accounting for these differences are now investigated. Following the methodology of Anderson (1994), we find that the relative humidity measurements presented by Essery et al.

(1999) are, in fact, with respect to water and not with respect to ice. Since the sublimation of blowing snow is constrained by ice saturation, we apply the parametrization of Essery et al. (1999) for Q_s to the relative humidity measurements at Trail Valley Creek following their conversion to RH_i . We then obtain a range between 11 and 22 mm swe for the total seasonal blowing snow sublimation, about a quarter of the original values reported by Essery et al. (1999) for this location.

In addition, we note that the parametrizations of Essery et al. (1999) are based on the steady-state Prairie Blowing Snow Model (PBSM; Pomeroy et al., 1993). The PBSM assumes a fully-developed column of sublimating, blowing snow up to z_{ub} and does not take into account self-limitation of the blowing snow sublimation process (Pomeroy et al., 1993; Déry et al., 1998). In the PBSM, z_{ub} is obtained through an iterative process and varies with both wind speed and fetch x (m) for blowing snow (Pomeroy et al., 1993; Déry and Taylor, 1996). Incorporating the PBSM assumptions into PIEKTUK-D and taking $x = 1$ km as in Essery et al. (1999), we then compute a seasonal blowing snow sublimation rate of 14.6 mm swe at Trail Valley Creek in 1996/1997. This is well within the range of values found above when the snowdrift sublimation rate of Essery et al. (1999) is derived from the observations of humidity with respect to ice. The increase of 11.2 mm in the total seasonal sublimation rate when a steady-state environment during blowing snow is assumed points to the fact that it is a critical assumption in assessing its role in the surface mass balance.

An additional component in the water budget of snow-covered regions not considered by Essery et al. (1999) consists of direct sublimation from the snowpack. Surface sublimation is known to remove locally substantial amounts of mass from the snowpack (e.g., van den Broeke 1997; Hoode et al., 1999). Following the method described by van den Broeke (1997), we computed the surface sublimation rate Q_{surf} (mm d^{-1} swe) for the winter of 1996/1997 at Trail Valley Creek from:

$$Q_{surf} = \rho' u_* q_*, \quad (15)$$

where q_* (kg kg^{-1}) is the humidity scale. Here, saturation with respect to ice at the snow surface is assumed for the computation of q_* . Surface sublimation is then estimated to erode an additional 7 mm swe from the snowpack during the winter of 1996/1997 at Trail Valley Creek, about twice as much as blowing snow sublimation (see Table III). Depending on the assumptions that govern the operation of PIEKTUK-D, the combined effects of surface and blowing snow sublimation deplete between 10 and 22 mm swe from the snowpack, in close agreement to the results of Essery et al. (1999) for sublimation based on the computations with RH_i .

Finally, we need to mention that the results of Section 3 clearly indicate that despite values of $RH_i \approx 1$ near the snow surface, substantial blowing

snow sublimation may occur aloft in the ABL. Thus the assumption that sublimation completely shuts off in these conditions is perhaps misleading. However, without detailed information about the vertical distributions of T_a and q_v , it is difficult to make conclusions about the total column-integrated sublimation rate in these circumstances.

5. Summary and Conclusions

An extension to a double-moment scheme of the bulk blowing snow (PIEKTUK-B) model of DY99b has been proposed. It is shown that predicting explicitly the profiles of total particle numbers of blowing snow, in addition to the temperature, water vapour and blowing snow mixing ratio profiles, provides consistent results with the spectral version of the model (PIEKTUK-S) for the evolution of particle concentrations and distributions. The double-moment model (PIEKTUK-D) also yields comparable blowing snow sublimation and transport rates as PIEKTUK-B at about the same computational cost since longer timesteps are employed in the integration of PIEKTUK-D. Thus, PIEKTUK-D provides a suitable alternative to the computationally expensive scheme of PIEKTUK-S without compromising some of the implicit characteristics of the blowing snow particle distributions as does PIEKTUK-B.

PIEKTUK-D is then used to derive a parametrization for the sublimation rate of blowing snow in terms of wind speed and a thermodynamic variable to include the effects of evolving temperature and humidity profiles on the sublimation process. The model and parametrization are then applied to experimental data collected in the Canadian Arctic and reveals that blowing snow sublimation may remove, particularly during the early or late stages of the cold season, several millimetres swe from the surface mass balance. The combined effects of surface and blowing snow sublimation are estimated to erode 10 mm swe from the surface during the winter of 1996/1997 at Trail Valley Creek, Northwest Territories. This total is at the lower end of values presented by Essery et al. (1999) exclusively for blowing snow sublimation at the same location and time period when their relative humidity measurements are reported with respect to ice.

Despite the emphasis on blowing snow sublimation in this paper, its precise role in the Arctic tundra water budget remains somewhat inconclusive. This is particularly evident given the sensitivity of the modelling results to various parameters as well as the lack of extensive, frequent *in situ* meteorological and snow stake measurements to confirm model predictions. Since blowing snow sublimation may significantly impact the heat flux profiles well above the surface, assumptions about the background thermodynamic profiles also become critical in evaluating the blowing snow sublimation and

transport rates. For instance, although RH_i may approach saturation near the surface, as is often the case in cold climate regimes, dry air aloft in the ABL could nonetheless sustain large blowing snow sublimation rates. Therefore, to obtain more realistic simulations of blowing snow and its interaction with the environment, we are currently coupling PIEKTUK-D to the MC2 model (Benoit et al., 1997). We anticipate that this work will provide more accurate estimates of the effects of blowing snow in the hydrometeorology of the MRB and, concurrently, yield improved parametrizations of blowing snow sublimation.

Acknowledgements

We thank Dr. Richard Bintanja (Utrecht University), Dr. Graham Mann (University of Leeds), Prof. Peter Taylor and Mrs. Jingbing Xiao (York University), for discussions which have led to improvements in our blowing snow model discussed in the paper. We are much grateful to Dr. Long Li, Dr. Richard Essery (NHRC) and Dr. John Pomeroy (University of Saskatchewan) who provided generously the field data used in this study and to Dr. P. S. Anderson (British Antarctic Survey) for support in its interpretation. We acknowledge the support of the Natural Sciences and Engineering Research Council of Canada who have funded this work through a collaborative research agreement as part of the Canadian GEWEX program.

References

- Anderson, P. S.: 1994, 'A Method for Rescaling Humidity Sensors at Temperatures Well Below Freezing', *J. Atmos. Oceanic Tech.* **11**, 1388-1391.
- Benoit, R., Desgagné, M., Pellerin, P., Pellerin, S., Chartier, Y., and Desjardins, S.: 1997, 'The Canadian MC2: A Semi-Lagrangian, Semi-Implicit Wideband Atmospheric Model Suited for Finescale Process Studies and Simulation', *Mon. Wea. Rev.* **125**, 2382-2415.
- Bintanja, R.: 1998, 'The Contribution of Snowdrift Sublimation to the Surface Mass Balance of Antarctica', *Annals Glaciol.* **27**, 251-259.
- Budd, W. F.: 1966, 'The Drifting of Non-Uniform Snow Particles', in M. J. Rubin (ed.), *Studies in Antarctic Meteorology*, Antarctic Research Series Vol. 9, American Geophysical Union, Washington, DC, pp. 59-70.
- Déry, S. J. and Taylor, P. A.: 1996: 'Some Aspects of the Interaction of Blowing Snow with the Atmospheric Boundary Layer', *Hydrol. Proc.* **10**, 1345-1358.
- Déry, S. J., Taylor, P. A., and Xiao, J.: 1998, 'The Thermodynamic Effects of Sublimating, Blowing Snow in the Atmospheric Boundary Layer', *Boundary-Layer Meteorol.* **89**(2), 251-283.
- Déry, S. J. and Yau, M. K.: 1999a, 'A Climatology of Adverse Winter-Type Weather Events', *J. Geophys. Res.* **104**(D14), 15,657-16,672.
- Déry, S. J. and Yau, M. K.: 1999b, 'A Bulk Blowing Snow Model', *Boundary-Layer Meteorol.* **93**(2), 237-251.

- Essery, R., Li, L. and Pomeroy, J. W.: 1999, 'A Distributed Model of Blowing Snow over Complex Terrain', *Hydrol. Proc.* **13**, 2423-2438.
- Harrington, J. Y., Meyers, M. P., Walko, R. L. and Cotton, W. R.: 1995, 'Parameterization of Ice Crystal Conversion Process Due to Vapor Deposition for Mesoscale Models Using Double-moment Basis Functions. Part I: Basic Formulation and Parcel Model Results', *J. Atmos. Sc.* **52**, 4344-4366.
- Hoode, E., Williams, M., and Cline, D.: 1999, 'Sublimation from a Seasonal Snowpack at a Continental, Mid-latitude Alpine Site', *Hydrol. Proc.* **13**, 1781-1797.
- King, J. C. and Anderson, P. S.: 1999, 'A Humidity Climatology for Halley, Antarctica based on Hygrometer Measurements', *Antarctic Sc.* **11**, 100-104.
- King, J. C., Anderson, P. S., Smith, M. C., and Mobbs, S. D.: 1996, 'The Surface Energy and Mass Balance at Halley, Antarctica during Winter', *J. Geophys. Res.* **101**(D14), 19,119-19,128.
- Lawford, R. G.: 1994, 'Knowns and Unknowns in the Hydroclimatology of the Mackenzie River Basin', in S. D. Cohen (ed.), *Mackenzie Basin Impact Study (MBIS)*, Interim Report #2, Yellowknife, NWT, pp. 173-195.
- Mann, G. W., Anderson, P. S., and Mobbs, S. D.: 2000, 'Profile Measurements of Blowing Snow at Halley, Antarctica', *J. Geophys. Res.* **105**(D19), 24,491-24,508.
- Pomeroy, J. W., Gray, D. M., and Landine, P. G.: 1993, 'The Prairie Blowing Snow Model: Characteristics, Validation, Operation', *J. Hydrol.* **144**, 165-192.
- Pomeroy, J. W., Marsh, P. and Gray, D. M.: 1997, 'Application of a Distributed Blowing Snow Model to the Arctic', *Hydrol. Proc.* **11**, 1451-1464.
- Reisner, J., Rasmussen, R. M. and Bruintjes, R. T.: 1998, 'Explicit Forecasting of Supercooled Liquid Water in Winter Storms Using the MM5 Mesoscale Model', *Q. J. R. Meteorol. Soc.* **124**, 1071-1107.
- Rogers, R. R. and Yau, M. K.: 1989, *A Short Course in Cloud Physics*, 3rd ed., Pergamon Press, 293 pp.
- Schmidt, R. A.: 1982, 'Vertical Profiles of Wind Speed, Snow Concentrations, and Humidity in Blowing Snow', *Boundary-Layer Meteorol.* **23**, 223-246.
- Schwerdtfeger, W.: 1984, *Climate of the Antarctic*, Developments in Atmospheric Science 15, Elsevier, 261 pp.
- Stewart, R. E., Bachard, D., Dunkley, R. R., Giles, A. C., Lawson, B., Legal, L., Miller, S. T., Murphy, B. P., Parker, M. N., Paruk, B. J., and Yau, M. K.: 1995, 'Winter Storms over Canada', *Atmos.-Ocean* **33**, 223-247.
- Stewart, R. E., Leighton, H. G., Marsh, P., Moore, G. W. K., Rouse, W. R., Soulis, S. D., Strong, G. S., Crawford, R. W., and Kochtubajda, B.: 1998, 'The Mackenzie GEWEX Study: The Water and Energy Cycles of a Major North American River Basin', *Bull. Amer. Meteorol. Soc.*, **79**(12), 2665-2684.
- van den Broeke, M. R.: 1997, 'Spatial and Temporal Variation of Sublimation on Antarctica: Results of a High-resolution General Circulation Model', *J. Geophys. Res.* **102**(D25), 29,765-29,777.
- Vowinckel, E. and Orvig, S.: 1970, 'The climate of the North Polar Basin', in S. Orvig (ed.), *Climate of the Polar Regions*, World Survey of Climatology, vol. 7, Elsevier, pp. 129-252.
- Xiao, J., Bintanja, R., Déry, S. J., Mann, G. and Taylor, P. A.: 2000, 'An Intercomparison among Four Models of Blowing Snow', *Boundary-Layer Meteorol.*, **97**, 109-135.

Chapter 5

Mesoscale Modelling

5.1 Presentation of Article 5

In the preceding chapters, we have established a climatology of blowing snow, its large-scale contribution to the surface mass balance as well as its efficient numerical modelling. However, we have yet to examine a specific case study in detail. In the present chapter, therefore, we discuss a ground blizzard that caused persistent blowing snow in the northern sections of the MRB in mid-November 1996. The case study is first simulated using the MC2 model without the blowing snow component followed by a second experiment where the MC2 and PIEKTUK models are coupled. Results on the effects of blowing snow to the surface mass balance, energy budget and background meteorological fields are investigated.

5.2 Article 5

Simulation of an Arctic ground blizzard using a coupled blowing snow-atmosphere model. By Stephen J. Déry and M. K. Yau, 2001: submitted to *J. Hydrometeorol.*

Simulation of an Arctic ground blizzard using a coupled blowing snow-atmosphere model

Stephen J. Déry and M. K. Yau

Department of Atmospheric and Oceanic Sciences, McGill University
Montréal, Québec

Submitted to *Journal of Hydrometeorology*

Abstract

A ground blizzard occurred from 16 to 18 November 1996 in the northern sectors of the Mackenzie River Basin (MRB) of Canada and adjacent Beaufort Sea. This hazardous event, accompanied by a low-level jet with wind speeds approaching 20 m s^{-1} and extensive blowing snow near the surface (but clear sky aloft), is forced by a strong sea-level pressure gradient that forms between a rapidly intensifying anticyclone over the Nunavut and Northwest Territories (NWT) of Canada and an intense depression over the frozen Arctic Ocean.

The event is first simulated at a horizontal grid size of 18 km using the uncoupled Canadian Mesoscale Compressible Community (MC2) model. This experiment is shown to capture the rapid anticyclogenesis event within 2 hPa of its central sea-

level pressure and the blizzard conditions near the Canadian Arctic coastline and the Beaufort Sea. Meteorological conditions observed at Trail Valley Creek (TVC), a small Arctic tundra watershed where ground blizzard conditions were experienced during the event, are also accurately reproduced by the uncoupled simulation with the notable exception of the blowing snow process. Thus, the mesoscale model is then coupled to the PIEKTUK blowing snow model and a second simulation is conducted. This additional experiment reveals the presence of extensive blowing snow associated with a strong low-level jet over TVC and the adjacent frozen Beaufort Sea. Our findings show that blowing snow affects the surface mass balance through sublimation and transport which combine to erode ≈ 1.4 mm snow water equivalent (swe) per day at TVC. The concurrent moistening and cooling of near-surface air due to blowing snow sublimation emerge during the blizzard, but to a lesser extent than in an idealized modelling framework as a consequence of entrainment and advective processes. Therefore, blowing snow sublimation rates are evaluated to be 1.8 times larger than in the stand-alone application of the PIEKTUK model to the same data.

1 Introduction

With mounting evidence that significant climate change is underway in northern high-latitudes (e.g., Dickson, 1999; Rothrock et al., 1999; Serreze et al., 2000), there is renewed interest in examining hydrometeorological processes in the Arctic. With its prevailing subfreezing conditions, processes involving snow and ice dominate the water and energy cycles of these regions (Stewart et al., 2000). As a surface, snow and ice have significant meteorological effects to the overlying air and underlying

ground due to their thermal and radiational properties. Any variation to the extent, thickness and/or duration of the snow and ice packs as a result of climate change may significantly alter the hydrometeorology of northern high-latitude regions.

As part of the Global Energy and Water Cycle Experiment (GEWEX), the Mackenzie GEWEX Study (MAGS) was established to examine the water and energy budgets and possible climate change impacts within the Mackenzie River Basin (MRB) of northwestern Canada (Stewart et al., 1998; Rouse, 2000). The site of notable temperature increases and concurrent snow depth decreases in the past 30 to 40 years (Stewart et al., 1998; Brown and Braaten, 1998), the MRB emerges as a prominent location for the study of ongoing high-latitude climate change. Despite evidence of an increased duration of snow-free days in the area, the MRB remains nonetheless blanketed by snow from 150 days annually in its southern sections to nearly 250 days annually on the Arctic tundra (Phillips, 1990). Its scarce vegetation and long seasonal snowcovers make the Arctic tundra especially susceptible to blowing snow and blizzard events (Déry and Yau, 1999a).

Apart from its hazardous aspects such as reduced optical visibilities, blowing snow associated with blizzards and other high wind events is of much interest due to its twofold contribution to the surface water and energy budgets through mass divergence or convergence in addition to concurrent in-transit sublimation (Déry and Yau, 1999b). The relative importance of these terms, however, remains uncertain given the wide range of values for blowing snow transport and, especially, sublimation, that are found in the literature (e.g., King et al., 1996; Pomeroy et al., 1997; Bintanja, 1998; Essery et al., 1999; Déry and Yau, 2001a, b). Déry and Yau (2001a) point out that the conclusions reached by each individual study was highly dependent on the modelling strategy employed by their respective authors, none

of which has included the full interaction between the atmospheric boundary layer (ABL) and the blowing snow process. Although Gallée (1998) and Liston and Sturm (1998) have included blowing snow parametrizations in their mesoscale modelling of high-latitude processes, neither of these studies considered interactive processes between blowing snow and ABL heat fluxes. For these reasons, these studies may overestimate significantly blowing snow sublimation rates since, in idealized settings, Déry et al. (1998) and Xiao et al. (2000) have demonstrated that this process has “self-limiting” characteristics. This is in response to the negative thermodynamic feedbacks associated with the sublimation process. Although preliminary observational evidence suggests that blowing snow sublimation does exhibit these qualities near the surface (Mann et al., 2000), a more comprehensive modelling strategy may help us understand some crucial aspects of the blowing snow phenomenon (in 4 dimensions) within the entire ABL, including its apparent self-limitation.

To that effect, we have chosen to examine a remarkable ground blizzard event that took place between 16 and 18 November 1996 on the Tuktoyaktuk Peninsula (TP) of the Northwest Territories (NWT) of Canada and adjoining Beaufort Sea (see Figures 1 and 2). Although rather commonplace in the Canadian Arctic, this particular event was unusual in its persistence and in that its forcing mechanism was rapid anticyclogenesis. These clear-sky storms are often labelled “ground blizzards” in Canada since their accompanying adverse weather conditions are usually constrained to the lowest tens of metres of the atmosphere (Stewart et al., 1995). High windchills ($WC > 1.6 \text{ kW m}^{-2}$), reduced horizontal optical visibilities ($VIS < 1 \text{ km}$) as well as strong 10-m winds ($U_{10} > 11 \text{ m s}^{-1}$) nonetheless render ground blizzards extremely dangerous in the Arctic.

Past studies on Arctic weather have generally focused on the evolution of cyclones

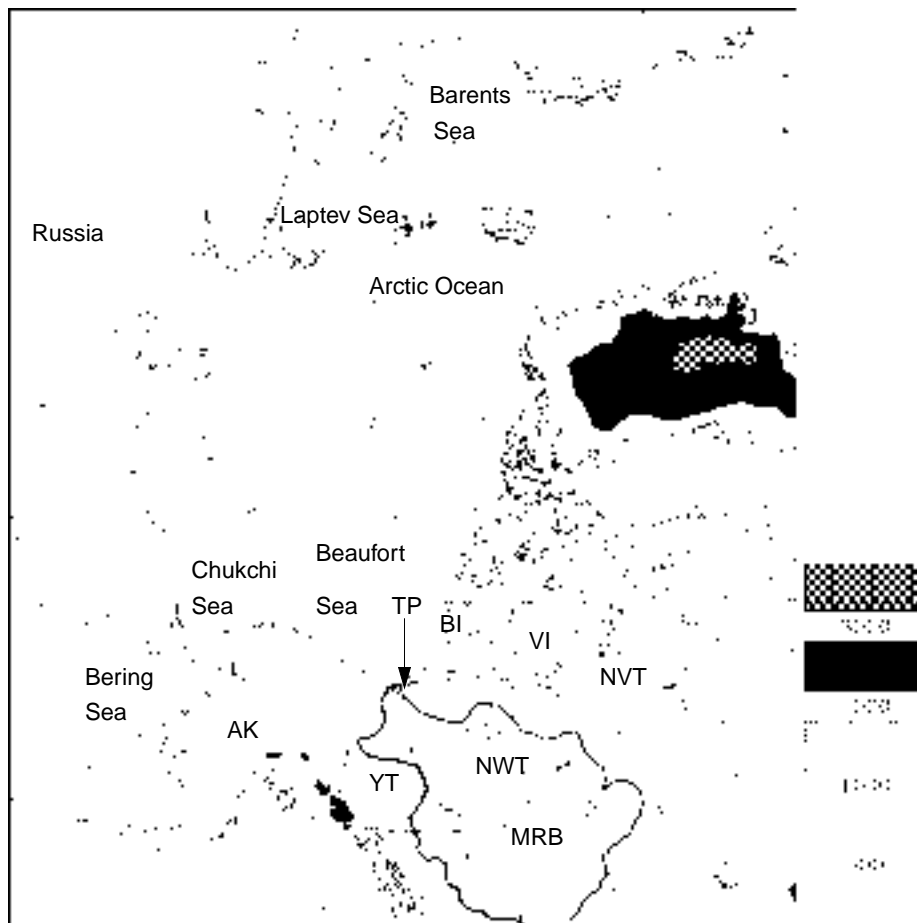


FIGURE 1: Geographical map of the Mackenzie River Basin (MRB) and surrounding area of interest. The orography is depicted by shading at elevations of 0.5, 1.0, 2.0 and 3.0 km above sea level. Note that the following abbreviations are used: Tuktoyaktuk Peninsula (TP), Northwest Territories (NWT), Nunavut Territory (NVT), Yukon Territory (YT), Alaska (AK), Banks Island (BI) and Victoria Island (VI).

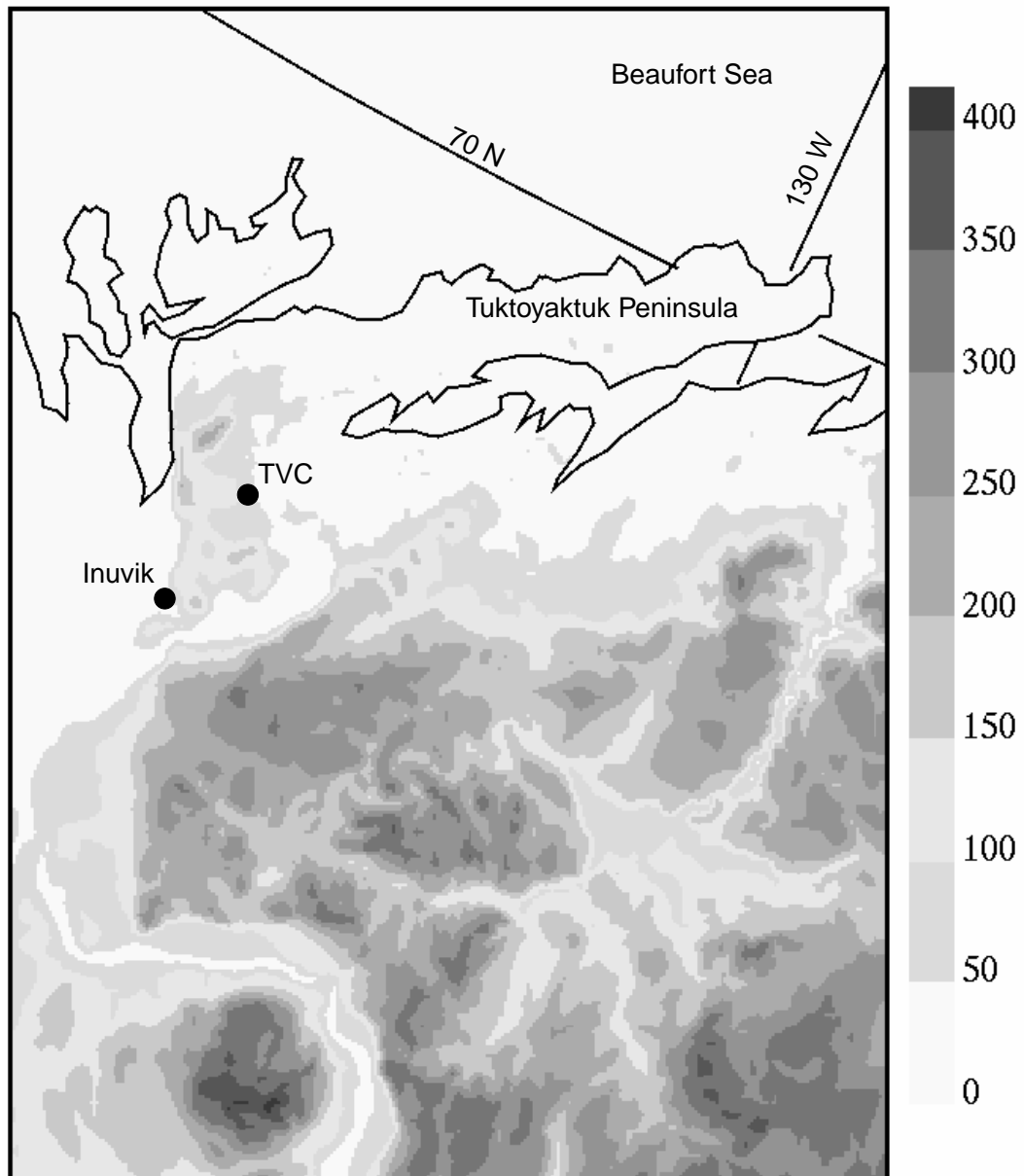


FIGURE 2: Close-up of the Trail Valley Creek (TVC) area. The orography is shaded at intervals of 50 m.

and associated frontal systems (e.g., Serreze, 1995; Hanesiak et al., 1997; Szeto et al., 1997) whereas anticyclones have attracted relatively less attention in the literature. Nonetheless, some exceptions include the studies of Curry (1983, 1987) who determined that radiative cooling is crucial to the development of these systems. Colucci and Davenport (1987), on the other hand, examined the synoptic-scale forcings of a number of rapid anticyclonogenesis cases, defined as an increase in the central sea-level pressure (SLP) of the system of 5 hPa per day, and found a relationship between these cases and rapid upwind cyclogenesis. Zishka and Smith (1980) and Colucci and Davenport (1987) also demonstrate that northwestern Canada is a prominent location for the development of high pressure systems. However, these authors have failed to examine the impact of surface processes such as blowing snow on the anticyclonogenesis, leading possibly to the forecast errors in the strength of high pressure systems observed in some NWP models (Colucci and Bosart, 1979; Grumm and Gyakum, 1986).

The objective of this study, therefore, is to conduct a mesoscale numerical study of a rapid anticyclonogenesis event and associated ground blizzard that occurred in mid-November 1996 near northern sections of the MRB. A lack of precipitation during this event facilitates the exploration of blowing snow, its interaction with the ABL and its role in the surface energy and mass balances at Trail Valley Creek (TVC), on the TP of the NWT for which enhanced observational data have been acquired. The paper begins with a brief description of the event of interest followed by some background information on the numerical models and the experimental strategy used in this study. Sections 4 and 5 present the results of the uncoupled and coupled experiments, respectively, followed by a discussion of results and conclusions.

2 Case Overview

In the 48 hours following 1200 UTC on 16 November 1996, severe wintertime conditions prevailed near the northern tip of the MRB. Public forecasts released for the area warned of blowing snow and high windchills combining to produce blizzard conditions along the Canadian Arctic coastline (Buzza, personal communication, 1999). Some important synoptic-scale features are shown to contribute to these adverse conditions as depicted by the Canadian Meteorological Centre (CMC) surface analyses (Figure 3). Prior to the development of blizzard conditions along the TP, calm weather prevailed as a surface ridge of high pressure approached the region from the west. As this system moved eastward of the TP, a strong SLP pressure gradient formed between the anticyclone and a 947 hPa cyclone situated over the Laptev Sea at 1200 UTC on 16 November 1996. During the next 48 h, blizzard conditions, defined as periods when $WC > 1.6 \text{ kW m}^{-2}$, $U_{10} > 11 \text{ m s}^{-1}$ and $VIS < 1 \text{ km}$ (Déry and Yau, 1999a), were sustained along the Arctic coastline and the Beaufort Sea as a surface anticyclone over Victoria Island intensified to 1050 hPa.

At 500 hPa, there are two dominant features over the boreal polar region (Figure 4). A strong upper level ridge propagates northeastward from Alaska on 16 November 1996 to reside over Banks Island 2 days later with a central geopotential height persistently near 565 dam. A deep, closed off 500 hPa low with central geopotential height reaching 468 dam at 1200 UTC on 17 November 1996 is associated with the strong surface cyclone over the frozen Arctic Ocean.

The infrared satellite imagery obtained for the period of interest reveals the generally clear conditions that prevail during the entire event in the vicinity of TVC (Figures 5-7). Note that in the region of the developing anticyclone, clouds cannot

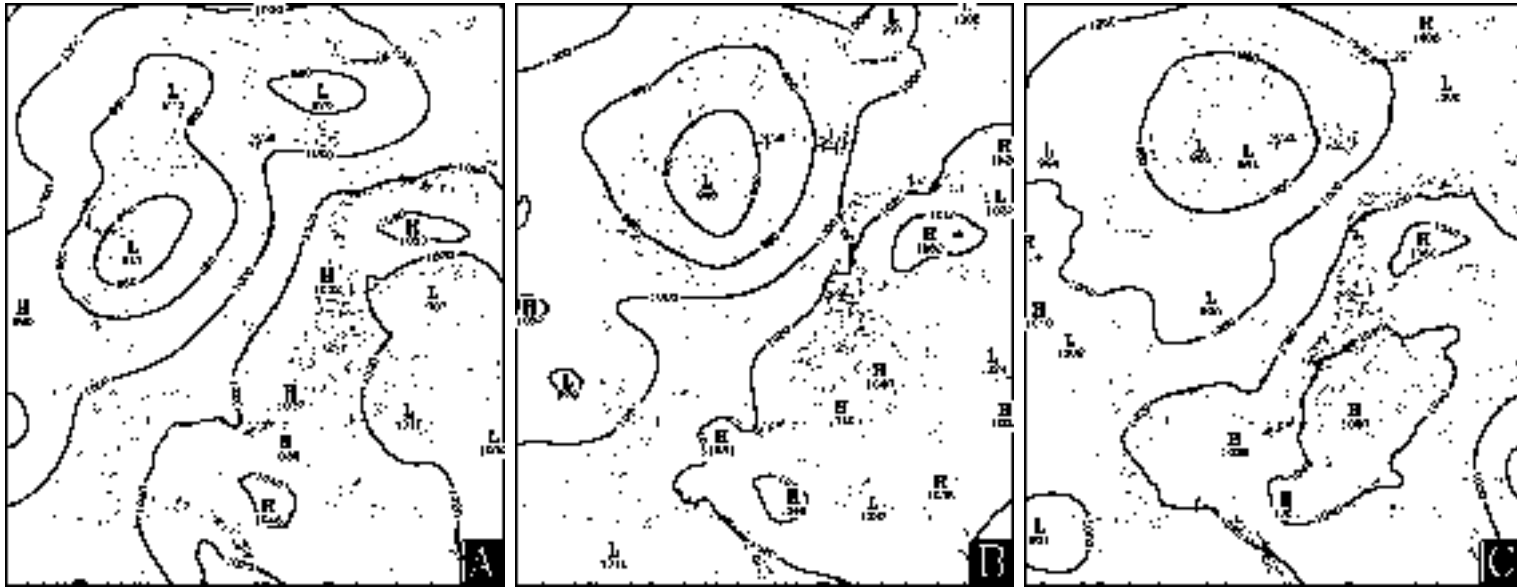


FIGURE 3: CMC analyses of sea-level pressure (hPa) at 1200 UTC on a) 16 November 1996, b) 17 November 1996 and c) 18 November 1996. The shading indicates areas where blizzard conditions are inferred from the analyses.

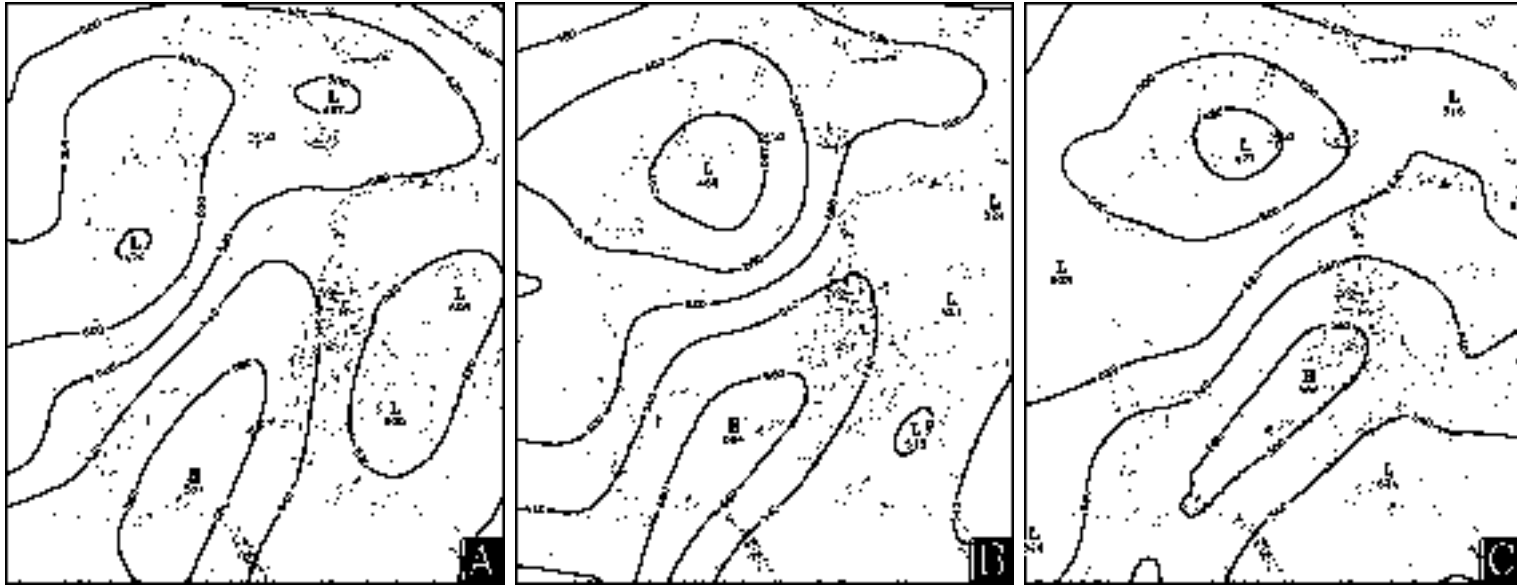


FIGURE 4: CMC analyses of 500 hPa geopotential heights (dam) at 1200 UTC on a) 16 November 1996, b) 17 November 1996 and c) 18 November 1996.

be discerned in these images. The high resolution images confirm the overwhelming presence of sea ice interspersed with leads in the Beaufort Sea. Note also the fuzziness and darker appearance of the subsequent images over the Beaufort Sea. This feature is likely due to the presence of suspended blowing snow particles composed entirely of ice that emit much more effectively in the infrared than water vapour. As discussed later, a strong thermal inversion is present during the event over the Beaufort Sea that significantly warms up the blowing snow particles. Due to their enhanced temperatures as well as scattering effects, the infrared satellite imagery takes on a darker and fuzzier appearance than in regions without blowing snow (Endoh et al., 1997). In addition, note that the Mackenzie River and its delta are clearly frozen at this time, but Great Bear and Great Slave Lakes remain partially open and eventually promote local cloudiness. Finally, observe the gradual northward retreat of sea ice forced by the strong southerly winds occurring over the area.

A few additional comments on the case described above are in order. The rise of 10 hPa d^{-1} in the central SLP of the high pressure system over Victoria Island on 17 November 1996 readily qualifies this as a rapid anticyclogenesis event (Colucci and Davenport, 1987). According to their study, the intensification of a high pressure system at rates of 5 hPa d^{-1} is sufficient to qualify the event as “implosive” anticyclogenesis. Consistent with their conclusions, upwind explosive deepening of the depression over the Arctic Ocean is observed prior to the Canadian anticyclogenesis event. Note also that the high pressure system builds in an area favourable to the development and passage of anticyclones (Zishka and Smith, 1980).

Using the CMC surface analyses, we were able to trace back the origins of the intense surface cyclone that contributed to the blizzard conditions over most of the Arctic Ocean in mid-November 1996. Interestingly, this system is associated with

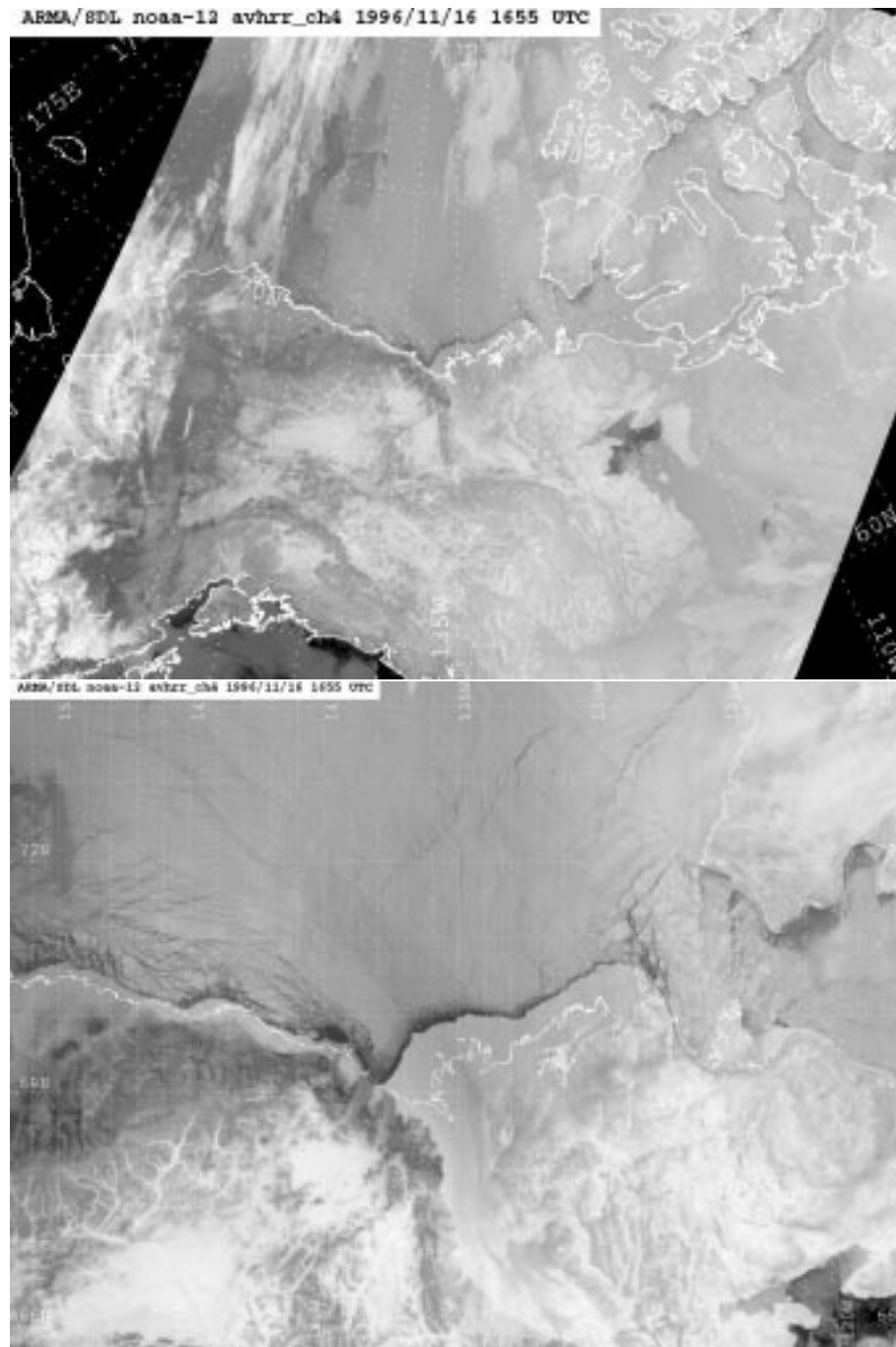


FIGURE 5: Infrared satellite imagery at 1655 UTC on 16 November 1996 over the area of interest. In the top panel, the image has a resolution of 4 km whereas in the bottom panel, the image has a 1 km resolution, both centred over Inuvik, NWT.

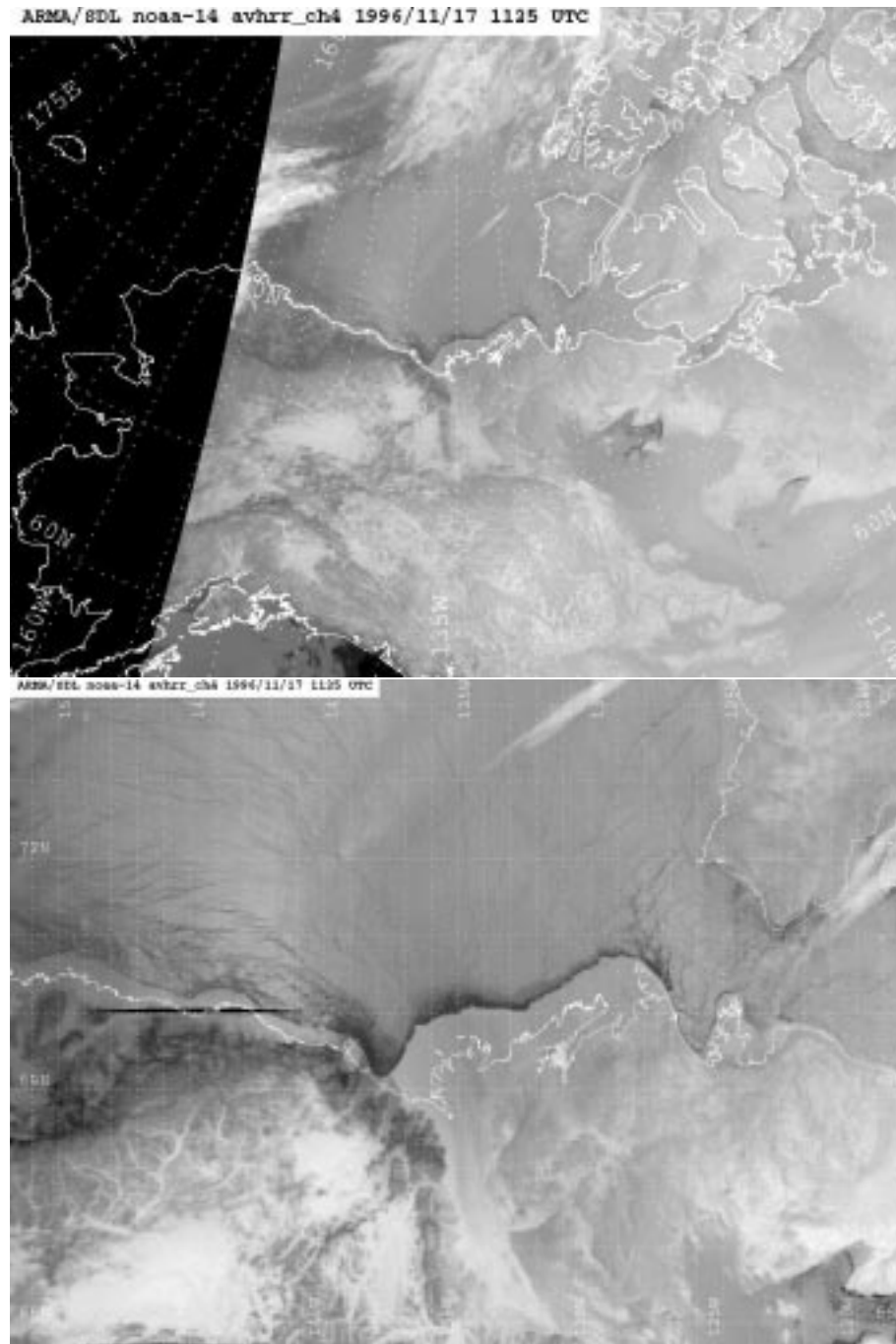


FIGURE 6: As in Figure 5 at 1125 UTC on 17 November 1996.

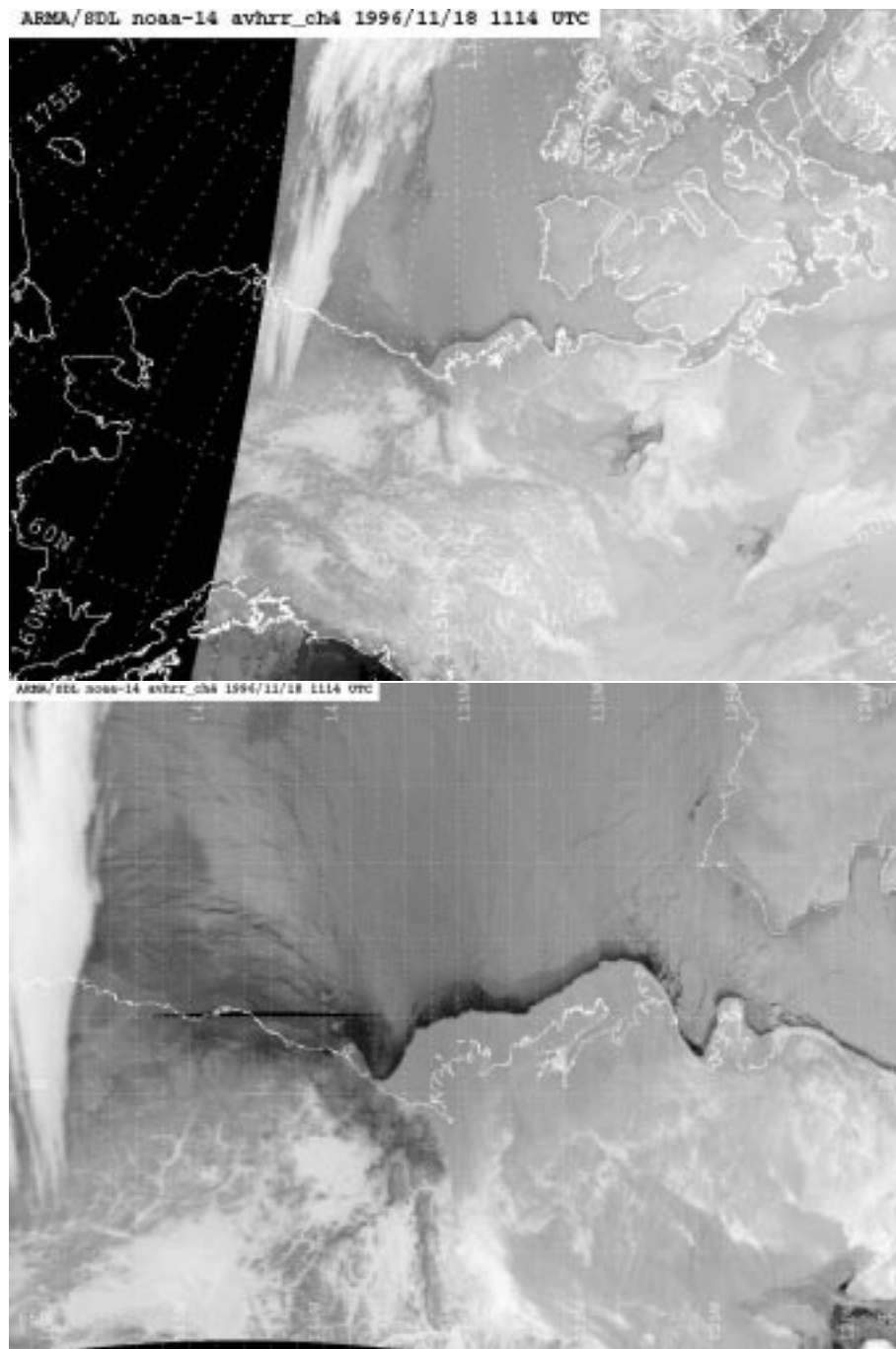


FIGURE 7: As in Figure 5 at 1114 UTC on 18 November 1996.

the extra-tropical re-intensification of the remnants of Supertyphoon Dale which formed just north of the Equator on 2 November 1996 (Lander et al., 1999). At one point during its evolution, Dale reached a central SLP of 898 hPa and had sustained winds of 72 m s^{-1} . As the weakening cyclone (with central SLP near 985 hPa) approached the Bering Sea, it rapidly re-intensified and propagated in a westward direction in what appears to be a wintertime secondary storm track for the area (Barry, 1989). According to the CMC analyses, the cyclone reached a minimum SLP of 944 hPa during its extra-tropical stage, a full 15 hPa lower than any of the 30 extra-tropical transition (ET) and re-intensification cases inventoried by Klein et al. (2000). Finally, it is noteworthy to mention that the Northern Hemisphere experienced an extremely large collapse of available potential energy (APE) during this time period (Wintels and Gyakum, 2000; Wintels, personal communication, 2000). Despite the uniqueness of these attendant large-scale features, for the time being our mesoscale study will focus on the rapid anticyclogenesis and ground blizzard events that occur in the vicinity of the MRB.

3 Numerical Models

3.1 MC2 model

The Mesoscale Compressible Community (MC2) model is a widely used prognostic and diagnostic tool within the Canadian atmospheric scientist community. It has been successfully applied to a wide range of locations, scales and cases, such as diagnostic studies of high wind, flood and explosive secondary cyclogenesis events at mid-latitudes (Benoit et al., 1997a; Carrera et al., 1999; Milbrandt and Yau,

2001). The MC2 model has also been extensively applied to the MRB as a short-term forecasting tool (Benoit et al., 1997b) and in the compilation of several water budget studies for the basin (Lackmann et al., 1998; Misra et al., 2000).

The dynamical core of the MC2 model relies on the integration of the Navier-Stokes equations using the semi-implicit, semi-Lagrangian numerical technique (see Benoit et al., 1997a). The MC2 model benefits from a comprehensive physics package that includes the treatment of surface fluxes based on the force-restore concept of Deardorff (1978) as well as the treatment of ABL processes in a turbulent kinetic energy (TKE) scheme developed by Mailhot and Benoit (1982) and Benoit et al. (1989). Although not expected to be a significant factor in this case, large-scale convection is parametrized following a Kuo-type scheme implemented by Mailhot and Chouinard (1989). The Kong and Yau (1997, hereafter KY) explicit microphysics package determines the stratiform precipitation through microphysical processes involving four types of water species: water vapour q_v , cloud water q_c , rain water q_r , and ice and snow q_i , with all mixing ratios expressed in units of kg kg^{-1} .

3.2 PIEKTUK model

Snow resuspension by wind is a process not taken into consideration in the standard MC2 model microphysics. To incorporate this process and its potential impact to the ABL, therefore, we make use of the PIEKTUK blowing snow model that was originally developed by Déry and Taylor (1996) and Déry et al. (1998). The version utilized in the present study is one based on the bulk adaptation of PIEKTUK (Déry and Yau, 1999b) that was later upgraded to a double-moment, but nonetheless computationally inexpensive, scheme (PIEKTUK-D; Déry and Yau, 2001a). Briefly,

PIEKTUK-D depicts the temporal evolution of a column of sublimating, blowing snow. The model has four prognostic variables: the mixing ratio q_b (kg kg^{-1}) and total number concentration N (m^{-3}) of blowing snow in addition to the air temperature T_a (K) and q_v . The model activates only at each point and time that a “blowing snow event” is detected from the ambient conditions. Following Déry and Yau (1999a), this is defined as any time when the surface is snow-covered, that $T_a < 0^\circ\text{C}$, and that U_{10} surpasses a certain threshold, estimated following Li and Pomeroy (1997).

3.3 Coupling of the models

Extensive work was required to interface the MC2 and PIEKTUK-D models. This section outlines some aspects of the coupling process and then describes the interactions between the two models. First, PIEKTUK-D was transformed into a subroutine and called within the MC2’s physics package. Since snow resuspension and sublimation are, in effect, microphysical processes (Déry and Yau, 1999b), we opted to call PIEKTUK-D within the KY scheme. Unlike other microphysical activities which occur at all levels, blowing snow generally reaches heights of tens to a few hundred metres at most (King and Turner, 1997). Therefore, we interface the MC2 and PIEKTUK-D models with partly matching vertical grids. Since PIEKTUK-D has 24 levels from its lower to upper boundaries and that the lowest prognostic thermodynamic level of the MC2 is at 18 m, only the grid points between 18 m and 1 km coincide with those of the MC2 (Figure 8).

With the vertical grids now fixed, the following describes the sequence of events that unfolds during a typical MC2 timestep $\Delta\tau$ (s) in a coupled simulation of the

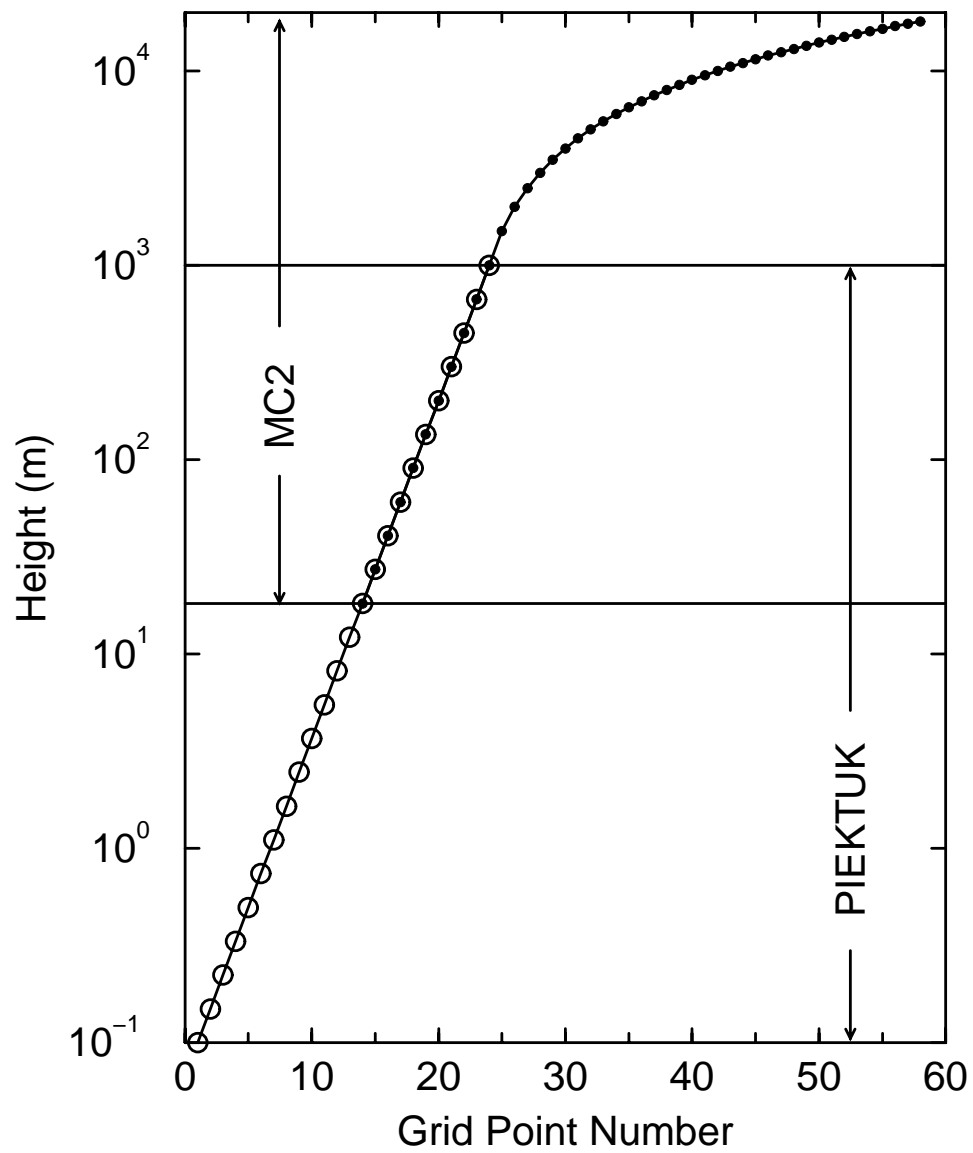


FIGURE 8: Distribution of grid points within the vertical domains of the MC2 (dots) and PIEKTUK-D (open circles) models.

two models. First, the MC2 model computes the 3-D semi-Lagrangian advection of predictive quantities including q_v , T_a , and the wind components U and V (both in m s^{-1}). The 3-D semi-Lagrangian advection of q_b and N is also performed by the MC2 for matching levels (i.e. $18 \text{ m} \leq z \leq 1 \text{ km}$). For vertical levels exclusive to PIEKTUK-D ($z < 18 \text{ m}$), we assumed that vertical advection is small and the MC2 performs only the horizontal advection of q_b and N . In addition, the wind components are prescribed a typical logarithmic profile below $z < 18 \text{ m}$. Next, the MC2 calculates the thermodynamic tendencies that arise due to microphysical activities before calling the PIEKTUK-D subroutine. Vertical profiles of q_v , T_a , U , V , q_b and N are thus transferred to the blowing snow model.

Upon receiving this information, PIEKTUK-D first checks whether the blowing snow criteria are met at each grid point. If the criteria are satisfied, PIEKTUK-D then initializes its dynamic and thermodynamic profiles using those of the MC2 for their coincident levels (i.e. $18 \text{ m} \leq z \leq 1 \text{ km}$). At other PIEKTUK-D levels ($z < 18 \text{ m}$), the initialization of the dynamic and thermodynamic profiles is conducted following Déry and Yau's (2001a) methodology. Briefly, they assume that the relative humidity with respect to ice RH_i follows a logarithmic profile from the measurement height of 2 m down to the snow surface where saturation with respect to ice is assumed. In the coupled simulation, we follow the same methodology to initialize RH_i with the exception that the "measurement height" is at $z = 18 \text{ m}$, the first matching vertical grid point of the two models. Similarly, using the surface ($z = 0$) and air ($z = 18 \text{ m}$) temperatures produced by the MC2 model, we prescribe an initial temperature profile that is also based on similarity theory for $z < 18 \text{ m}$. This differs from the constant T_a profiles taken by Déry and Yau (2001a) near the surface. Standard logarithmic profiles are also assumed for the wind components

below $z = 18$ m.

PIEKTUK-D then numerically integrates its four prognostic equations using a timestep Δt (s). Due to the small-scale microphysical processes and very high vertical resolution considered here, typically $\Delta t \leq \Delta\tau$. In PIEKTUK-D, blowing snow particles are susceptible to sublimation, diffusion and sedimentation, whereas q_v and T_a are only affected by diffusion and blowing snow sublimation. Since q_v and T_a have already undergone vertical diffusion within the MC2, we have opted to diffuse only the thermodynamic perturbations due to blowing snow sublimation within PIEKTUK-D. Having integrated to a full MC2 timestep (i.e. $n\Delta t = \Delta\tau$, where $n \equiv \Delta\tau/\Delta t$), PIEKTUK-D then outputs the column-integrated sublimation and transport rates of blowing snow. The associated thermodynamic tendencies for q_v and T_a from PIEKTUK-D are applied to the matching levels of the MC2. The MC2 model finally adjusts the T_a and q_v fields before repeating this sequence of events until the end of the integration.

3.4 Experimental Design and Strategy

Two distinct experiments are conducted in this study. In the first simulation, referred to as the uncoupled (UNC) experiment, the MC2 model is integrated without any blowing snow effects. In the subsequent model run, referred to as the coupled (CPL) experiment, the PIEKTUK-D model is interfaced with the MC2's microphysics to incorporate the thermodynamic effects of blowing snow in the ABL. Both simulations are conducted at a horizontal resolution of 18 km and are initialized at 1200 UTC on 16 November 1996 with meteorological and geophysical fields provided by CMC and the Centre de Recherche en Prévision Numérique (RPN). The

TABLE 1: The complete listing of the vertical levels used in the numerical experiments.

Model	Number of levels	Vertical levels (m)
PIEK- TUK-D	24	0.1000, 0.1492, 0.2228, 0.3324, 0.4962, 0.7406, 1.105, 1.650, 2.462, 3.675, 5.484, 8.185, 12.22, 18.23, 27.21, 40.62, 60.62, 90.47, 135.0, 201.5, 300.8, 448.9, 670.0, 1000.
MC2	46	2.000, 18.23, 27.21, 40.62, 60.62, 90.47, 135.0, 201.5, 300.8, 448.9, 670.0, 1000., 1500., 2000., 2500, 3000., 3500., 4000., 4500., 5000., 5500., 6000., 6500., 7000., 7500., 8000., 8500., 9000., 9500., 10000., 10500., 11000., 11500., 12000., 12500., 13000., 13500., 14000., 14500., 15000., 15500., 16000., 16500., 17000., 17500., 18000.

integrations span a period of 48 h and employ a timestep $\Delta\tau = 120$ s for the MC2 and $\Delta t = 5$ s for PIEKTUK-D. A total of 46 vertical levels are adopted for the MC2 vertical grid with 11 of these coinciding with PIEKTUK-D levels (see Figure 8 and Table 1). Note that the horizontal domain for both the UNC and CPL experiments, composed of 180×180 grid points, is illustrated in Figure 9. However, results of the numerical simulations are presented on a reduced horizontal mesh (160×160 grid points) to avoid the 10-point relaxation zone at the side boundaries.

3.5 Other Modifications

Apart from its coupling to PIEKTUK-D, several other modifications were incorporated into the MC2 model. Initial attempts to reproduce the observed conditions

at TVC resulted in near-surface air temperatures $\approx 5^\circ\text{C}$ too cold. As is shown in the following section, however, excellent results are obtained when the MC2 vertical diffusion coefficients for heat K_h ($\text{m}^2 \text{s}^{-1}$) are enhanced by a factor of 2 in the first and last 12 h of the simulation and by a factor of 6 during the remaining 24 h of the event. This suggests that the Mailhot and Benoit (1982) stability function for heat ϕ_h becomes too large for this stably stratified case (see Section 5). This is not surprising since Holtslag et al. (1990), in their formulation of an air mass transformation model, introduce a special stability function for heat in the case of a very stably stratified ABL. This prevents ϕ_h from becoming too large and allows the vertical diffusion of heat to persist in very stable conditions. Note however that the diffusion coefficients for moisture and momentum keep their original formulations (Mailhot and Benoit, 1982). In addition, we modified the calculation of the surface latent heat flux by using the latent heat of sublimation instead of that for evaporation when temperatures fall below 0°C .

Values of the roughness length for a bare surface z_{0b} (m) provided to us from RPN were altered to take into account the presence of snow at the surface. A snowcover generally exhibits smoother characteristics than bare ground or vegetated soils (see for instance, Oke, 1987). Following the methodology employed by Douville et al. (1995) in the Interaction between Soil, Biosphere and Atmosphere (ISBA) land-surface scheme of Noilhan and Planton (1989), the new roughness length z_0 (m) is given by:

$$z_0 = (1 - p)z_{0b} + pz_{0s} \quad (1)$$

where z_{0s} (m) is the roughness length for snow. The factor p is obtained from:

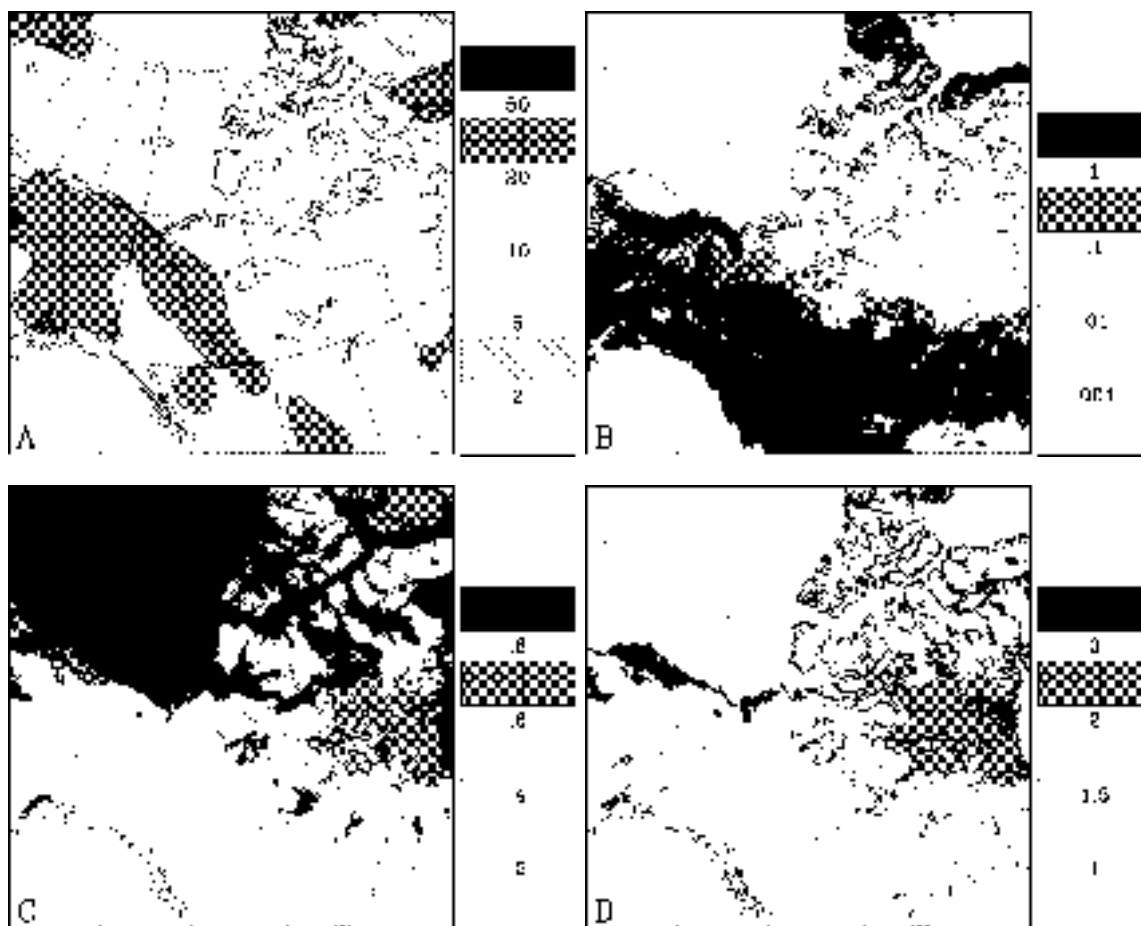


FIGURE 9: a) The CMC snow depth (in mm swe) analysis valid at 1200 UTC on 16 November 1996, b) the aerodynamic roughness length for bare ground z_{ob} (m), c) the factor p and d) the ratio of z_{ob}/z_0 over the entire horizontal simulation domain.

$$p = \frac{z_s}{(z_s + z_c + g\beta_s z_{0b})} \quad (2)$$

with z_s (m) denoting the snow depth, z_c ($= 0.01$ m) the critical snow depth, g ($= 9.81 \text{ m s}^{-2}$) gravitational acceleration, and β_s a constant equal to $0.408 \text{ s}^2 \text{ m}^{-1}$. Setting $z_{0s} = 0.001$ m in Equation (1) (Oke, 1987), any snow-covered surface with z_{0b} greater than this value will experience a decrease proportional to the snow depth in its overall roughness length.

To derive the new z_0 field, the high-resolution z_s analysis of Brasnett (1999) valid at the initial time of our simulations was employed. Figure 9 demonstrates that most of Northwestern Canada had considerable snow on the ground in mid-November 1996. High values of z_s combined with low values of z_{0b} over the Beaufort Sea and Arctic tundra yield elevated values of p in these regions. However, significant reductions in the roughness length occur only over the Arctic tundra where the ratio z_{0b}/z_0 reaches values from 2 to 3. No reduction to z_0 is observed over the Beaufort Sea since the roughness length is already at the value for snow in these regions.

4 Uncoupled Simulation

In this section, we present results from the uncoupled simulation that exclude the effects of blowing snow. Once we have compared the UNC experiment versus observational and analyzed data, we proceed to examine several aspects of the results including factors that favour the rapid anticyclogenesis and ground blizzard conditions in the Canadian Arctic. Blowing snow is then introduced into the MC2 model

and results from the CPL experiment are presented in the following section.

4.1 Comparison with Observations

The SLP fields predicted from the UNC simulation at intervals of 24 h are shown in Figure 10. These show that the MC2 model captures with accuracy the impulsive anticyclogenesis over the NVT and NWT. After 48 h of integration, the central SLP is predicted to be only 2 hPa lower and located slightly southeast of its position in the analysis (c.f. Figure 3c). Consistent with Figure 3, blizzard conditions are also inferred over the Beaufort Sea near the TP, albeit with reduced areal coverage.

The MC2 model also performs very well at higher levels in the atmosphere. Figure 11 shows the 500 hPa geopotential heights 24 and 48 h into the integration. The northeastward propagation of the strong upper-level ridge is well captured by the MC2 model with a difference of no more than 1 dam at all times in the forecast central geopotential height from those of the analyses. Note also that the location of the upper air features match very closely those from the CMC analyses, even after 48 h of integration.

To further evaluate the MC2 model simulations, we have obtained a time series of surface observations collected at TVC, NWT ($68^{\circ} 45'N$, $133^{\circ} 30'W$). These special measurements were conducted during the winter of 1996/1997 as part of the Mackenzie GEWEX Study (MAGS; Stewart et al., 1998). Readings of standard meteorological variables were sampled every 30 seconds and averaged over half-hourly periods (Essery et al., 1999). Emphasis here is given to the fields of T_a , relative humidity with respect to ice RH_i (%) and U_{10} since these 3 variables determine

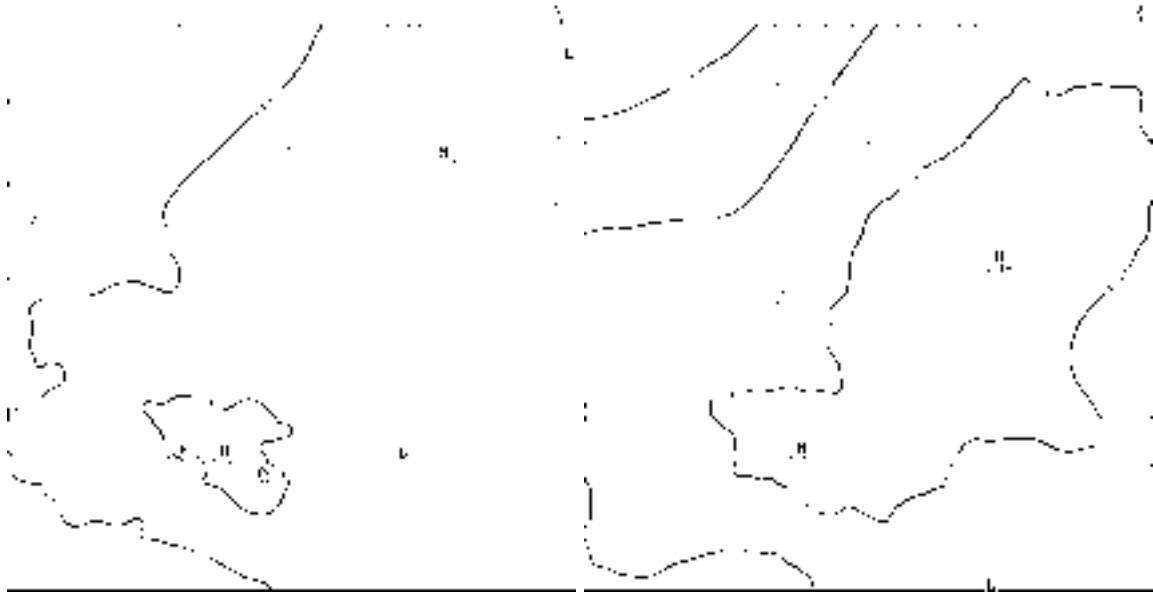


FIGURE 10: The simulated sea-level pressure (hPa) at 1200 UTC on a) 17 November 1996 and b) 18 November 1996 from the UNC experiment. The shading indicates areas where blizzard conditions are inferred.

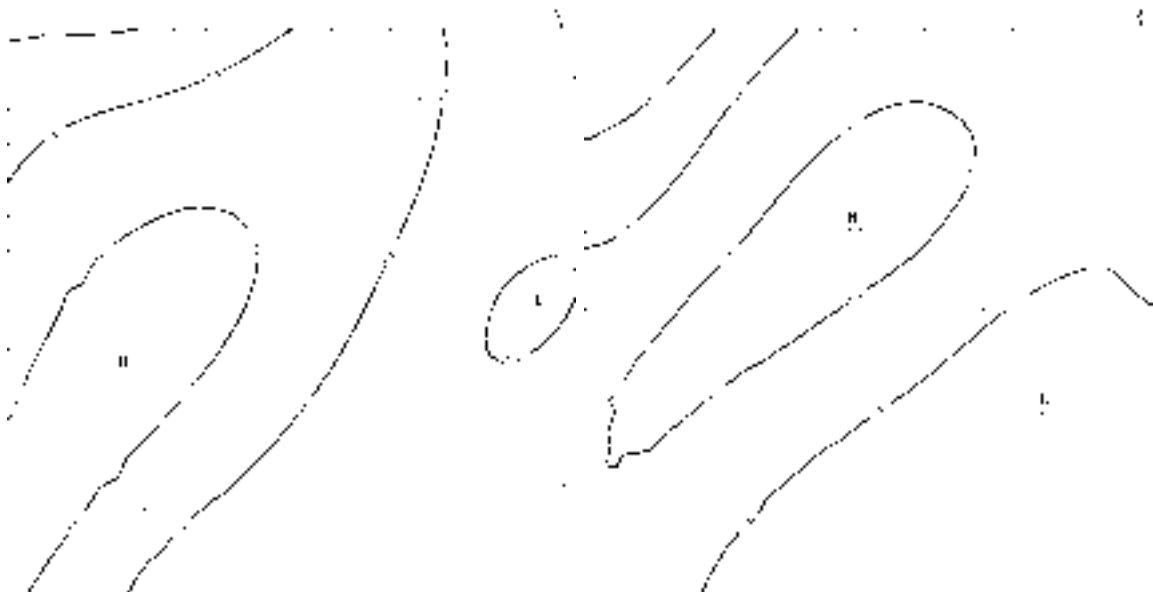


FIGURE 11: Simulated 500 hPa geopotential heights (dam) at 1200 UTC on a) 17 November 1996 and b) 18 November 1996 from the UNC experiment.

critically the blowing snow transport and sublimation rates (Déry and Yau, 2001a). Figure 12 demonstrates that the MC2 depicts reasonably well the time series of observed meteorological conditions at TVC during the 48-h event. However, the simulated conditions are slightly warmer and drier than observed, especially in the second half of the event. Some of the short-term fluctuations in all 3 fields are also missed by the MC2 model. Perhaps of greater concern is the overestimation of simulated wind speeds beginning just before JD 322.5. Some factors leading possibly to this deficiency in our simulation are discussed later.

Upper-air profiles for this event were also obtained for Inuvik ($68^{\circ} 18'N$, $133^{\circ} 29'W$), a sounding station ≈ 50 km to the south of Trail Valley Creek. Note that, for the skew-T diagrams shown in Figure 13, we plot the frostpoint temperature profile instead of the usual dewpoint temperature profile to reveal any subsaturation with respect to ice above the surface. The observed temperature profiles exhibit a sharp inversion ($\approx 15^{\circ}C$) below 900 hPa which the model depicts accurately. Some notable discrepancies in the frostpoint temperature profiles are evident at the end of the 48-h simulation, with the model maintaining more water vapour than observed below 600 hPa. Note that subsaturation with respect to ice is prevalent throughout the column of air with RH_i reaching values $< 10\%$ at some levels. Winds are generally well represented by the MC2 model but display lower wind speeds above 500 hPa than those reported by the rawinsonde measurements.

4.2 Precipitation and Humidity

Even though we observe the occurrence of rapid anticyclogenesis over the NVT and NWT, the KY scheme predicts the accumulation of some solid precipitation

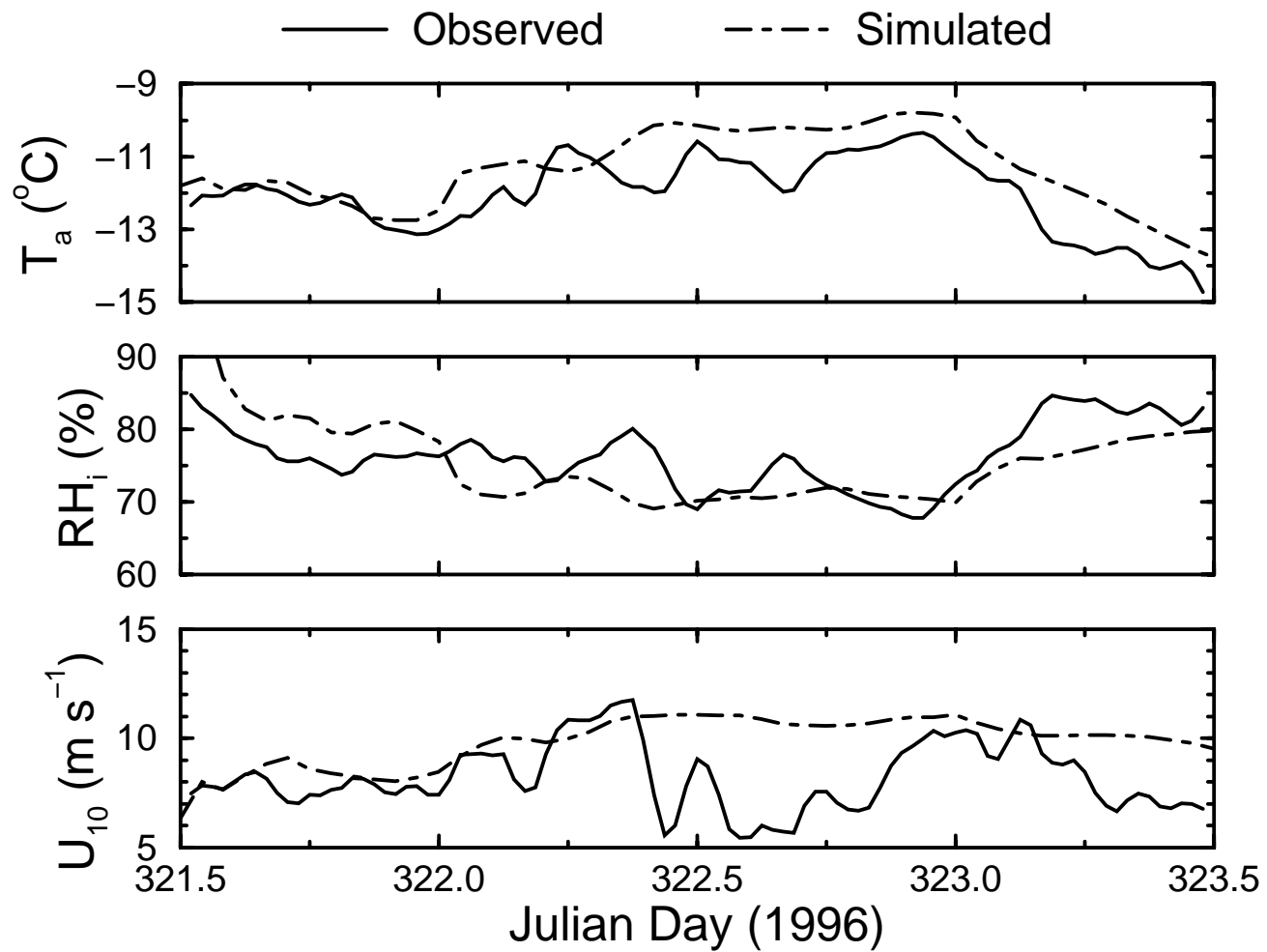


FIGURE 12: The observed and simulated conditions of air temperature (T_a), relative humidity with respect to ice (RH_i), 10-m wind speed (U_{10}) for Trail Valley Creek, NWT beginning at 1200 UTC on 16 November 1996 (JD 321.5) and ending at 1200 UTC on 18 November 1996 (JD 323.5).

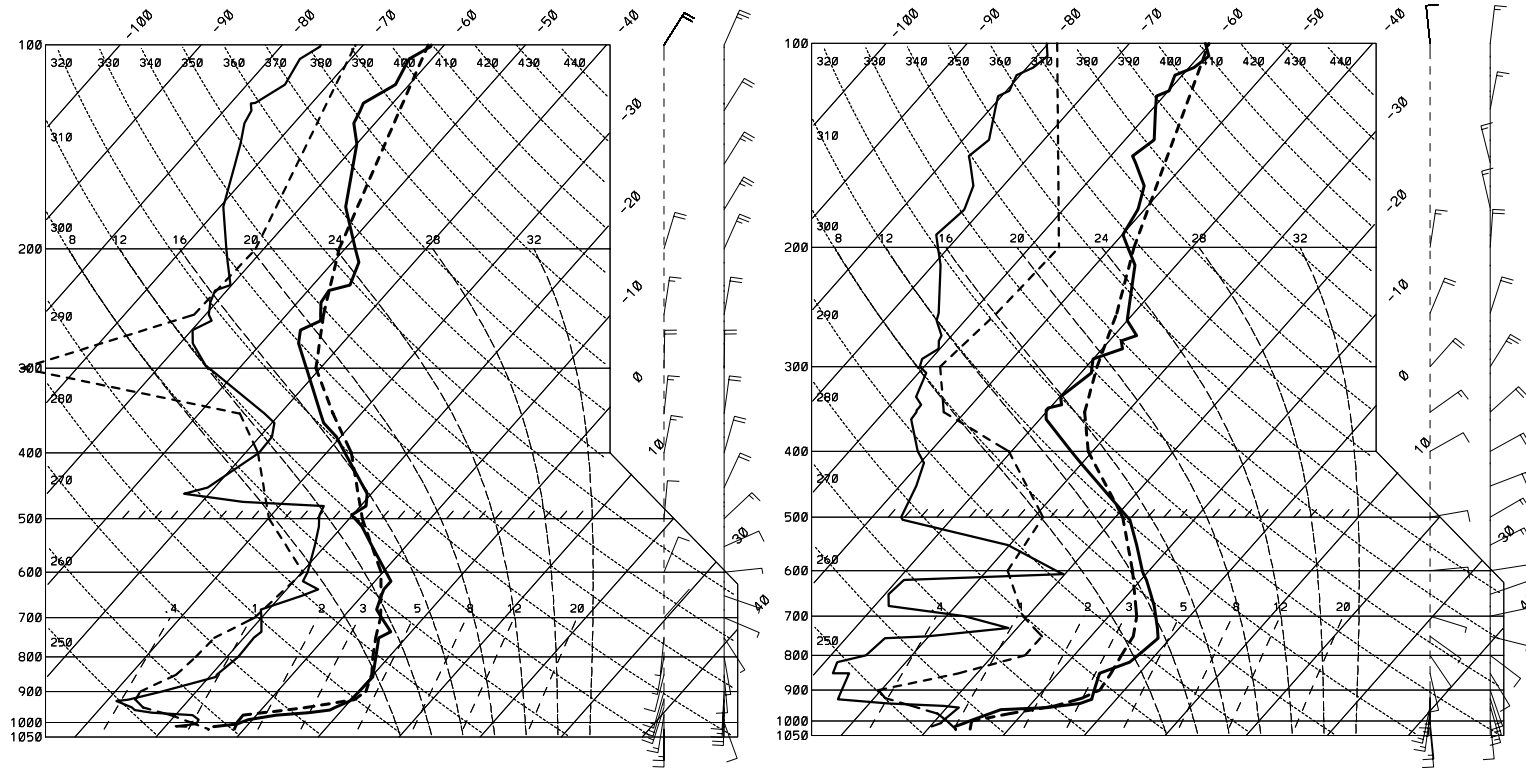


FIGURE 13: The observed (solid lines) and simulated (dashed lines) upper air profiles of temperature (thick lines) and frostpoint temperature (thin lines) for Inuvik, NWT, at 1200 UTC on a) 17 and b) 18 November 1996. Profiles of the observed and simulated wind speeds and directions are shown along the vertical solid and dashed lines, respectively. Note here that a half (full) barb denotes wind speeds of 5 m s^{-1} (10 m s^{-1}).

over large portions of the area where the event occurs (Figure 14a). The apparent lack of clouds over the area suggests that this is clear-air precipitation. Such precipitation is often termed “diamond dust” and occurs when relative humidities are saturated with respect to ice such that strong atmospheric cooling promotes deposition (Ohtake, 1982). Figure 14b confirms that low-level conditions of saturation and near-saturation with respect to ice is maintained over the central and eastern portions of the developing anticyclone. These results are consistent with those of Curry (1983, 1987) who demonstrated that anticyclogenesis is favoured by radiational cooling associated with the presence of clear air ice particles.

Lower SLPs are forecast over the Great Bear and Great Slave Lakes which remain open at the time of the event (recall Figures 3 and 5-7). Enhanced surface fluxes promote low-level convection and precipitation over and in the lee of the lakes. These conditions appear to be in the form of “lake-effect” snowsqualls that occur when cold air aloft travels over the much warmer large open bodies of water (e.g., Stewart et al., 1995). The convection tends to be banded in structure along the low-level flow which is enhanced over the lakes due to lower frictional effects. Intense lake-effect storms pose significant hazards to coastal inhabitants of the Great Northern Lakes during the month of November (Buzza, personal communication, 2000).

4.3 Low-level Jet

The presence of a low-level jet (LLJ) over TVC is clearly visible in the time-height cross-sections shown in Figure 15. Winds at $z = 449$ m reach speeds above 19 m s^{-1} throughout the latter half of the event. Just above this low-level wind maximum, the air remains relatively warm and very dry. This picture is in accordance with

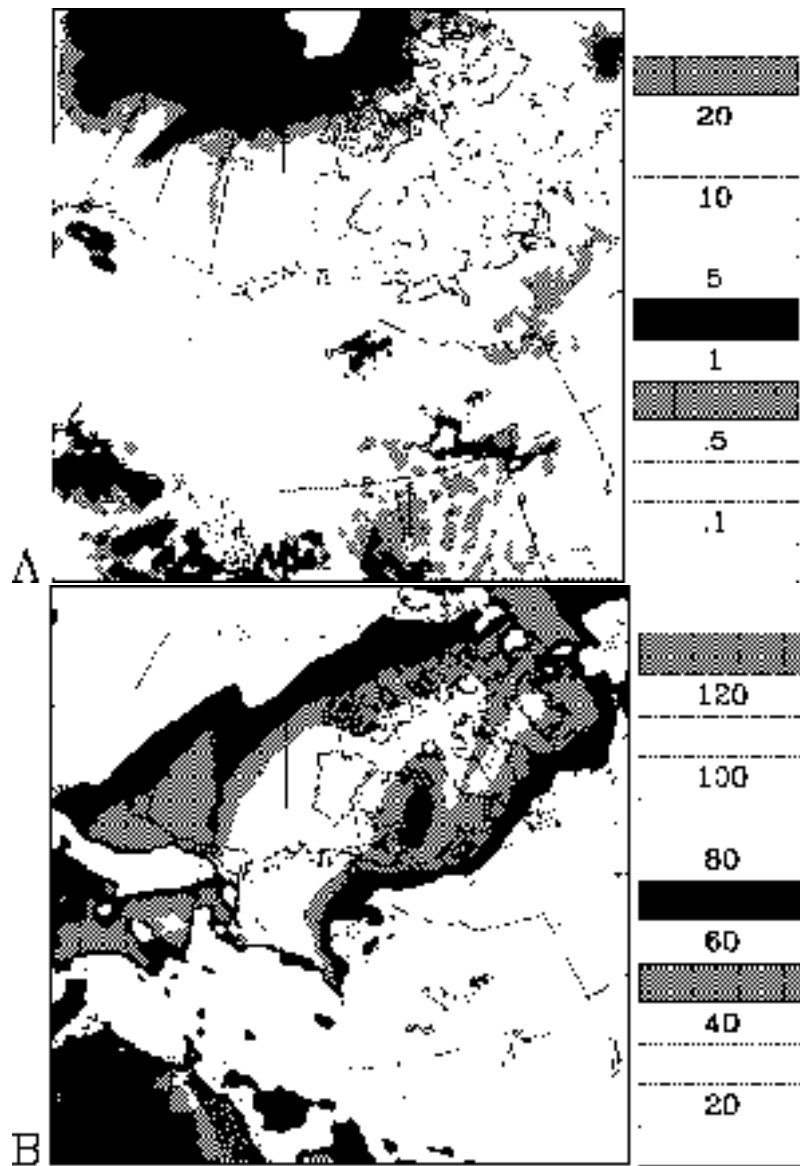


FIGURE 14: a) The 48-h cumulative precipitation (mm) and b) the mean relative humidity (%) at $z = 449$ m for the UNC simulation.

the Inuvik sounding data (Figure 13). The time-height cross-section for potential temperature θ (K) demonstrates that the ABL remains very stably stratified during the event although the surface layer exhibits near neutral stability between JD 322.5 and JD 323.0 (Figure 15d). As expected, strong descending motion in association with the high pressure system is inferred from the model data for TVC (not shown).

Note that it is not the first time a LLJ has been reported in the area since Kosović and Curry (2000) based their large eddy simulation of the ABL on a similar, albeit weaker, situation over the Beaufort Sea. Mechanisms leading to the formation of LLJs vary considerably in nature. Stull (1988), for instance, suggests that LLJs may occur in association with frontal systems, advective accelerations or the nocturnal ABL. In this case, however, it appears that the acceleration of low-level winds is simply a consequence of the favourable synoptic setting. Reviewing Figure 2 and considering the persistent southerly winds during the event, topographical effects may also come into play in the LLJ's formation.

5 Coupled Simulation

As mentioned before, motivation to examine this case arose from the need to explore the blowing snow phenomenon without contamination from precipitation. Thus, the ground blizzard described in this paper is the ideal situation to investigate any interaction between resuspended snow and the ABL. In addition, Déry and Yau (2001a) demonstrated that conditions of near-saturation with respect to ice are prevalent close to the surface during wintertime at TVC. In examining other potential cases during the winter of 1996/97, we found few instances where significant subsaturation

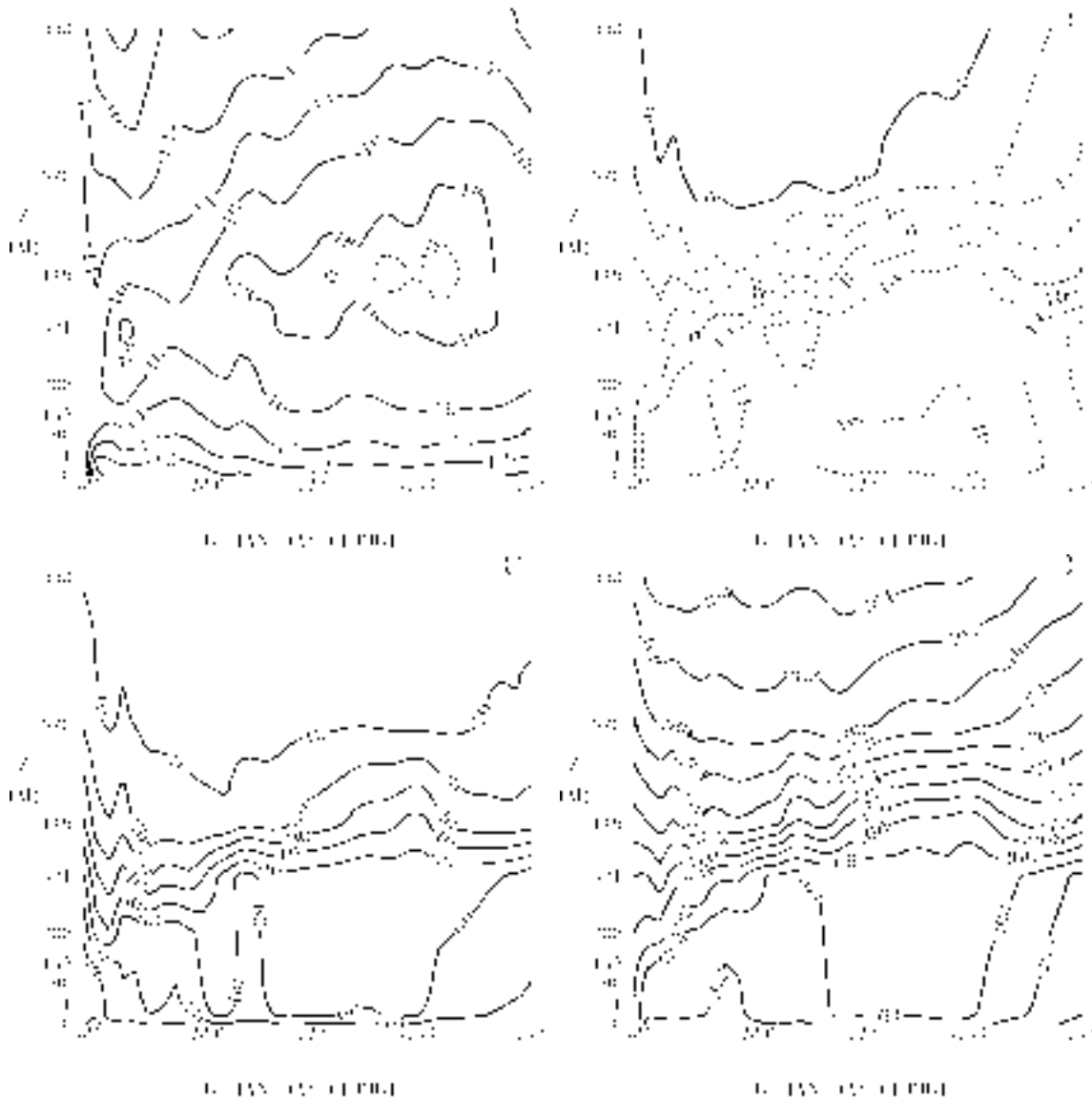


FIGURE 15: Time-height cross sections of a) wind speed in m s^{-1} , b) air temperature in $^{\circ}\text{C}$, c) relative humidity expressed as a percentage and d) potential temperature in K at Trail Valley Creek, NWT, from 1200 UTC on 16 November 1996 (JD 321.5) to 1200 UTC on 18 November 1996 (JD 323.5). Note that relative humidities are with respect to water when $T_a > 0^{\circ}\text{C}$ and with respect to ice when $T_a < 0^{\circ}\text{C}$.

with respect to ice, a necessary condition for the promotion of blowing snow sublimation, were present near the surface at TVC. The chosen case (16 to 18 November 1996) stood out as the strongest sublimation event in the stand-alone application of PIEKTUK-D (forced by the observational data) with an estimated 0.64 mm swe removed from the surface for the 2-day period. Additional erosion through mass divergence was not computed but wind transport displaced no less than 8.8 Mg m^{-1} during this event according to the stand-alone experiments of Déry and Yau (2001a).

Following the exact same methodology applied for the UNC experiment, a second simulation is conducted whereby the MC2 model is coupled to PIEKTUK-D. In the CPL experiment, PIEKTUK-D activates when the criteria for a blowing snow event are satisfied at any specific grid point and time. Thus regions experiencing high winds are also likely to be susceptible to blowing snow transport and sublimation. Subsequent to the presentation of the blowing snow fluxes, we will examine how this process affects the basic meteorological fields as well as the surface energy budget with respect to the UNC experiment.

5.1 Blowing Snow Fluxes

With its twofold impact to the surface mass balance, blowing snow emerges as a potentially significant hydrometeorological process in the Canadian Arctic. Hence, we first examine in Figure 16 results for the transport of blowing snow QT_t (Mg m^{-1}) and the associated mass divergence D (mm swe). Observe the large transport rates over the Beaufort Sea in association with the strong southerly winds occurring there. Values of QT_t peak at $\approx 30 \text{ Mg m}^{-1}$ just off the coast of the TP. For the duration of the ground blizzard, the strong southerly winds transport $1 \times 10^9 \text{ kg}$ of

snow across 70°N in the longitudinal band between 130 and 140°W . This is equivalent to a volume flux of $58 \text{ m}^3 \text{ s}^{-1}$ or about 1% of the Mackenzie River's discharge into the Beaufort for this time of the year (Stewart et al., 1998). Divergence (convergence) of mass, however, has large values in regions only where winds accelerate (decelerate) or diverge (converge). In this case, for instance, mass is eroded from the Mackenzie delta area and displaced northward into the Beaufort Sea. The TP thus loses upwards of 0.1 mm swe during the event.

Now let us consider Figure 17 which depicts the sublimation of blowing snow QT_s (mm swe) accumulated at the end of the 48-h CPL integration. We see high values of this blowing snow flux over the TP and the Beaufort Sea accompanying the ground blizzard conditions there. QT_s reaches a maximum value of 3 mm swe or more in about the same area where the largest transport rates are observed. The results presented in Figures 16 and 17 therefore suggest that during this ground blizzard, regions along the Canadian Arctic coastline provide a significant net source of fresh water (in both the solid and vapour phases) to the Beaufort Sea. Since the divergence of mass is typically one order of magnitude smaller than sublimation, the total blowing snow fluxes generally combine to erode mass in all locations experiencing snowdrifting (Figure 17b).

Figure 18 depicts the temporal evolution of the hourly blowing snow sublimation and transport rates at TVC from the CPL experiment as well as the corresponding observed and simulated meteorological conditions. First, note the improvement in the simulated weather conditions as a consequence of the cooling and moistening of near-surface air by blowing snow sublimation. On the other hand, wind speeds are negligibly affected by the inclusion of blowing snow in the numerical experiment. We also see that the blowing snow fluxes are closely tied with the modelled wind

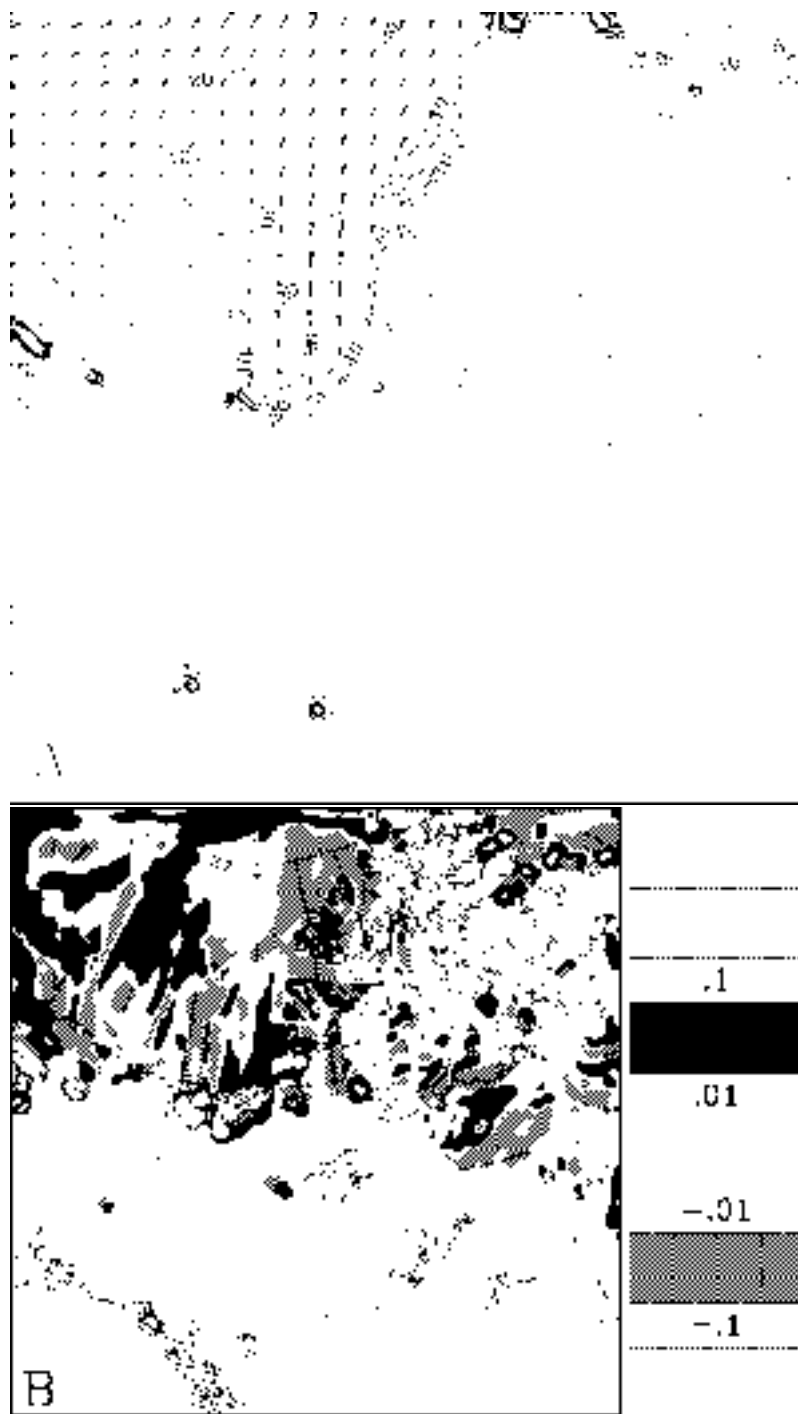


FIGURE 16: a) The contours and vectors of blowing snow transport (Mg m^{-1}) and b) the associated mass divergence (mm swe) of blowing snow at the end of the CPL experiment.

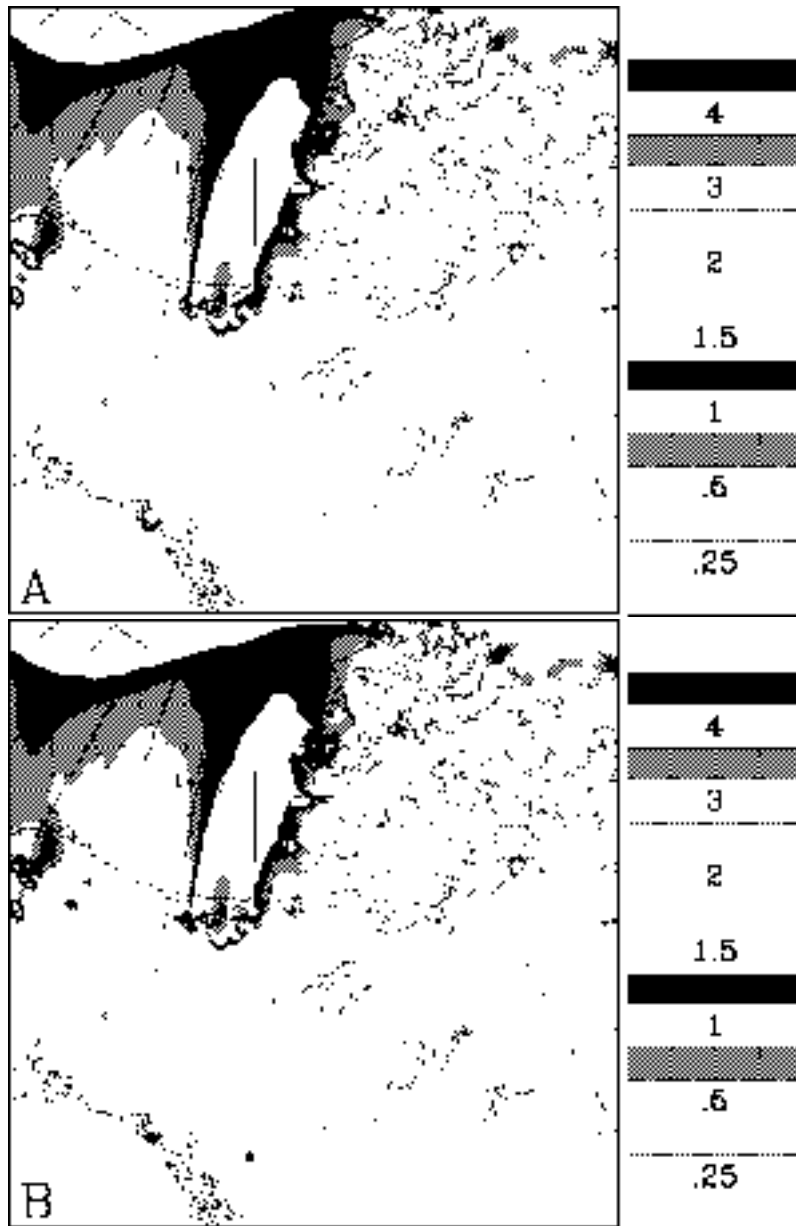


FIGURE 17: a) The total sublimation of blowing snow (mm swe) and b) the combined effects of blowing snow divergence and sublimation at the end of the CPL experiment.

speeds as peaks in these quantities coincide. Observe how decreasing temperatures and subsaturation with respect to ice tend to suppress the blowing snow sublimation rate in the final 12 h of the event whereas the transport rate remains nearly constant. For the duration of the ground blizzard, blowing snow sublimation and divergence erode 2.3 and 0.4 mm swe respectively from the snowpack at TVC according to the CPL experiment. Given that the simulation does not depict the sudden and persistent wind decrease in the second half of the period, our computed values of the blowing snow fluxes are likely to be overestimates of the actual conditions experienced at TVC.

In order to determine the effects of advection and entrainment on the snowdrift sublimation and transport rates, an additional experiment is now performed. We will refer to this as the stand-alone (STA) blowing snow experiment whereby the near-surface dynamic and thermodynamic variables in PIEKTUK-D are updated offline by the MC2 output for TVC. Here, the profiles of temperature, water vapour and wind speed are initialized by the methodology outlined in Déry and Yau (2001a). In this case, therefore, PIEKTUK-D depicts a single column of sublimating, blowing snow for TVC that excludes the effects of advective and entrainment processes. As shown in Figure 18, values of Q_s from the CPL simulation are generally 1.8 times larger than those in the STA experiment (see also Table 2). In contrast, Q_t remains larger in the STA simulation than in the CPL experiment. This suggests that entrainment and advection, processes not fully considered in the stand-alone simulations, import relatively dry air into the column of blowing snow over TVC that sustains the phase transition of ice particles to water vapour. Correspondingly, the advection and sublimation of particles reduce the amount of blowing snow and hence the transport rates as well.

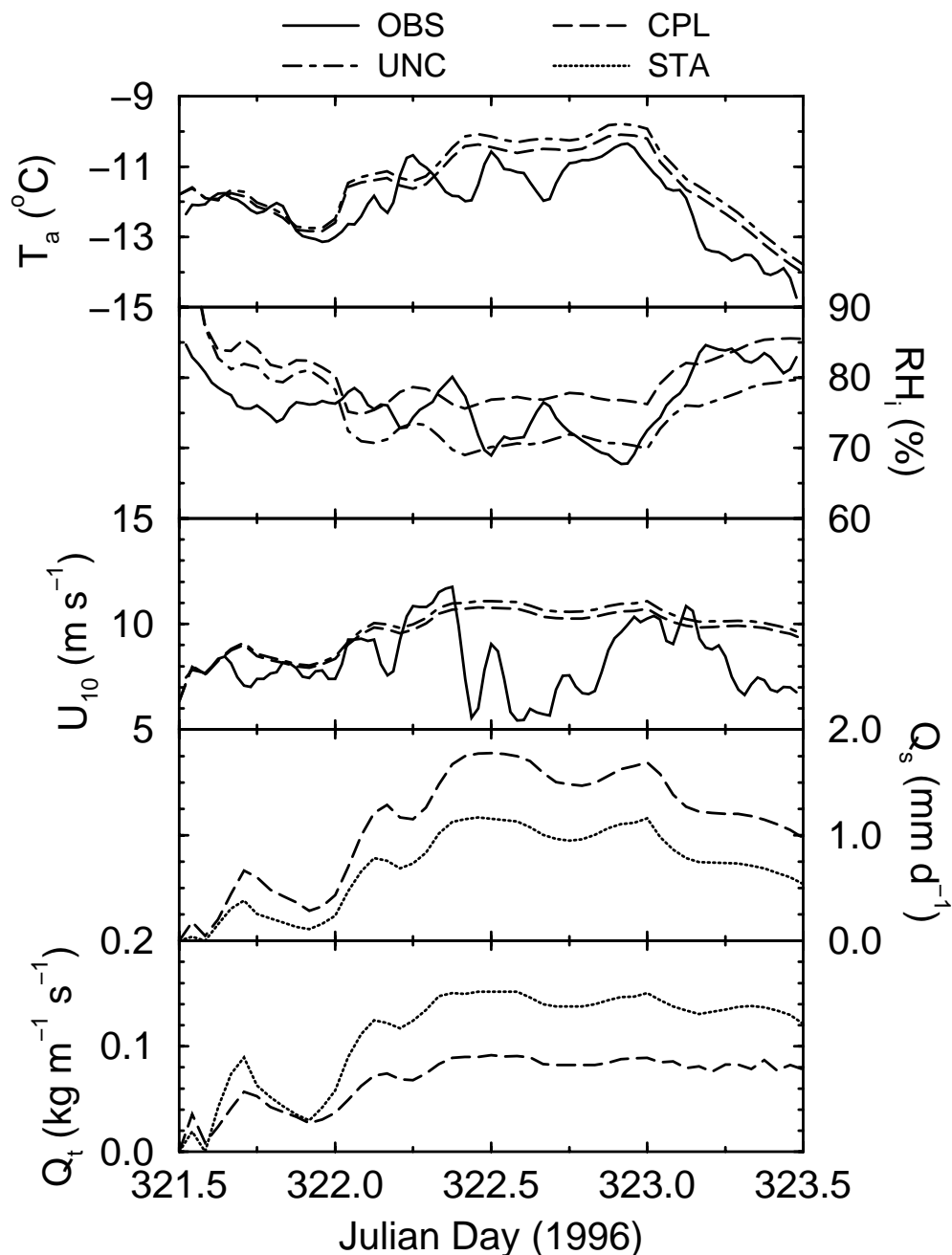


FIGURE 18: Hourly values of the observed and simulated surface air temperature (T_a), the surface relative humidity with respect to ice (RH_i), the 10-m wind speed (U_{10}), and the simulated sublimation (Q_s) and transport (Q_t) rates of blowing snow from 1200 UTC on 16 November 1996 (JD 321.5) to 1200 UTC on 18 November 1996 (JD 322.5) at Trail Valley Creek, NWT. The data are taken from observations (OBS), the uncoupled (UNC) and coupled (CPL) mesoscale simulations and the stand-alone (STA) blowing snow experiment.

TABLE 2: The total simulated blowing snow sublimation and mass transport at Trail Valley Creek during the period 1200 UTC on 16 November 1996 to 1200 UTC on 18 November 1996 according to coupled (CPL) mesoscale and stand-alone (STA) blowing snow simulations.

Experiment	QT_s (mm swe)	QT_t (Mg m ⁻¹)
CPL	2.27	13.9
STA	1.27	19.9

5.2 Basic Meteorological Fields

Due to its thermodynamic effects, the inclusion of the blowing snow process may have an impact on the other predictive fields within the MC2. As demonstrated for TVC in Figure 18, reduced near-surface air temperatures and enhanced relative humidities accompany the blowing snow process. Expanding these results to the entire simulation domain, we generally observe a decrease in T_a and an increase in RH_i where blowing snow occurs, although maximum changes in these two fields do not coincide (Figure 19). In addition, regions subject to blowing snow experience an increase in SLPs of up to 1 hPa. Differences in the accumulated precipitation vary in sign with notable decreases in areas where blowing snow cools air temperatures whereas other locations experience an enhanced precipitation total. Figure 18 therefore implies that the absence of blowing snow originating from the surface in conventional numerical weather prediction (NWP) models may explain some of the recurring biases encountered in the forecasts of near-surface meteorological fields at high latitudes (Colucci and Bosart, 1979; Grumm and Gyakum, 1986).

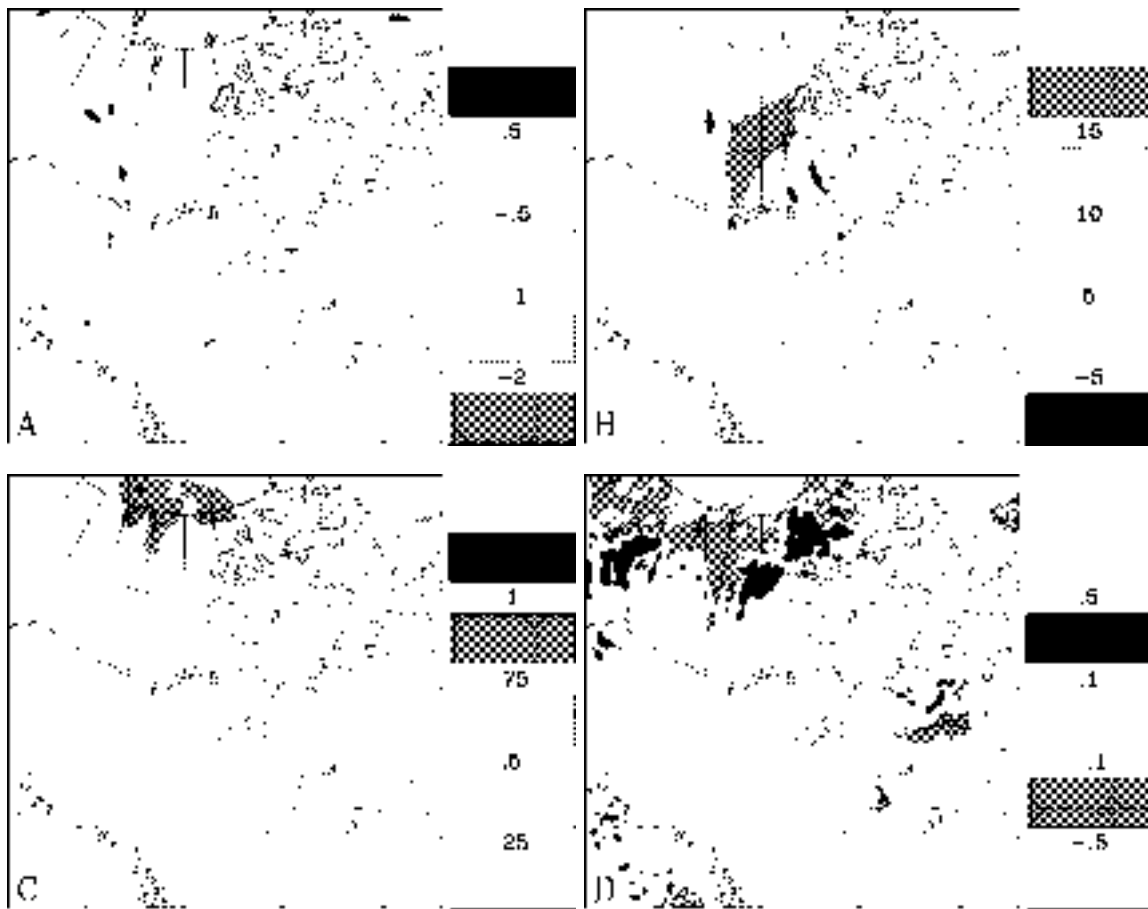


FIGURE 19: The difference in the 48-h simulated a) surface air temperatures ($^{\circ}\text{C}$), b) surface relative humidities (%), c) sea-level pressure (hPa) and d) precipitation accumulation (mm) between the CPL and UNC experiments.

5.3 Surface Energy Budget

In response to the thermodynamic effects of blowing snow sublimation, the surface energy budget will also be modified. Enhanced perturbations in the surface sensible and latent heat fluxes (Q_h and Q_e , respectively, in W m^{-2}) induced by blowing snow have previously been reported in the idealized modelling framework of Déry et al. (1998) and observed in the Canadian Prairies by Pomeroy and Essery (1999). Considering that polar night conditions exist at this time at TVC, the surface radiation and energy budgets are not influenced by incoming solar radiation and the net heat flux at the surface Q_* (W m^{-2}) may therefore be expressed as (Oke, 1997):

$$Q_* = L^\uparrow + L^\downarrow + Q_g + Q_h + Q_e \quad (3)$$

where L^\uparrow and L^\downarrow (W m^{-2}) are respectively the outgoing and incoming longwave radiation fluxes, and Q_g (W m^{-2}) denotes the heat flux into the ground. By convention, we indicate a loss (gain) of energy at the earth/atmosphere interface by a positive (negative) value in any of the fluxes. Table 3 reveals the predominance of radiational cooling with a net outgoing longwave flux near 60 W m^{-2} in the two experiments. Loss of surface heat results in large downward values of Q_h but slightly positive values of Q_e .

In the CPL simulation, blowing snow provides an additional source of water vapour to the ABL. In this situation, Q_e may then be partitioned in terms of the surface sublimation rate Q_{surf} ($\text{kg m}^{-2} \text{ s}^{-1}$) and the blowing snow sublimation rate Q_s ($\text{kg m}^{-2} \text{ s}^{-1}$) such that:

TABLE 3: Mean components of the surface energy and radiation budgets at Trail Valley Creek, NWT for the UNC and CPL experiments. Note that all fluxes are expressed in units of W m^{-2} and that $Q_e = (Q_{surf} + Q_s)L_s$.

Experiment	L^\uparrow	L^\downarrow	Q_g	Q_h	$Q_{surf}L_s$	Q_sL_s	Q_e	β_r
UNC	244	-183	22	-101	18	0	18	-5.6
CPL	243	-182	21	-128	10	36	46	-2.8

$$Q_e = (Q_{surf} + Q_s)L_s, \quad (4)$$

where L_s ($= 2.835 \times 10^6 \text{ J kg}^{-1}$) is the latent heat of sublimation. Note that although a column of blowing snow may extend up to 1 km above the surface, Q_s usually reaches a maximum very near the surface such that this component may also be considered as a surface heat flux. Table 3 presents the contribution of each of these terms to the surface energy budget. In the CPL experiment, we see that, on average, the surface sublimation component is reduced due to the presence of blowing snow. Nevertheless, the overall latent heat flux emanating from the surface is more than doubled with respect to the UNC simulation. The sensible heat required for the phase conversion of blowing snow particles is taken from the air itself and leads to a gradual cooling of the ABL. Also consistent with the results of Déry et al. (1998), the Bowen ratio β_r , defined as the ratio of Q_h/Q_e , remains negative during the event but decreases due to the heat flux perturbations attributed to blowing snow.

6 Discussion

Although the MC2 model simulations reproduce quite accurately the meteorological conditions experienced at TVC, they fail to detect the sudden abatement of high near-surface winds that occurs about midway during the period of interest. To explain this model deficiency, a thorough investigation of this peculiar feature is now undertaken.

As established in Section 4.1, the MC2 model depicts very well the initial sequence of events observed at TVC including the gradual strengthening of near-surface winds. At JD 322.4, however, there are a number of abrupt changes in the observed meteorological conditions at TVC which the model does not resolve. Accompanying the near-surface wind cessation, the observations display a 30° backing of the winds (note that when the wind direction $\phi = 180^\circ$, winds are southerly) and a significant surface pressure P rise > 1 hPa in one hour (Figure 20). Although the MC2 model fails to represent at this time these significant features, it does suggest a change in the stratification of the ABL (Figure 15). To evaluate the stability of the ABL, we introduce the surface Richardson number Ri that is expressed in terms of the vertical gradients of potential temperature and wind shear such that (Blackadar, 1957):

$$Ri = \frac{\frac{g}{\theta} \left(\frac{\partial \theta}{\partial z} \right)}{\left(\frac{\partial U}{\partial z} \right)^2 + \left(\frac{\partial V}{\partial z} \right)^2}. \quad (5)$$

The vertical gradients are computed between the surface and $z = 449$ m which is the approximate height of the LLJ (Figure 15a). As such, Ri provides in this case

an integrated measure of the ABL's stability. Figure 20 reveals that Ri gradually diminishes in time such that it attains its critical value of 0.25 when wind speeds rapidly decline and θ becomes well-mixed in the surface layer (see Figure 15d).

For further analysis, we introduce the Froude number Fr , computed here following King and Turner (1997):

$$Fr = |V| \left(\frac{\rho_s - \rho}{\rho_s} g z \right)^{-0.5}, \quad (6)$$

where $|V|$ (m s^{-1}) denotes the wind speed at height z , and ρ_s and ρ (kg m^{-3}) are the near-surface and ABL air densities, respectively. Again, we take $z = 449$ m to obtain a value of Fr that is representative of the entire ABL. Physically, Fr represents the ratio of the inertial to gravitational forces of the flow (Arya, 1988). It is interesting to note that according to the UNC simulation, Fr also undergoes a transition from subcritical ($Fr < 1$) to supercritical ($Fr > 1$) conditions as the simulated winds accelerate on JD 322.

This sequence of events thus suggests the passage of a “hydraulic jump” at TVC (e.g., Arya, 1988; Stull, 1988). This phenomenon has often been observed with the sudden cessation of strong katabatic winds in Antarctica (e.g., King and Turner, 1997; Gallée and Pettré, 1998) or as in this case, the reduction of wind speeds downstream of elevated topographical features (Stull, 1988). A cross-section of the orography along the flow demonstrates the elevated relief upwind of TVC (Figure 21). In its approach to TVC, therefore, the flow becomes constrained in a shallow layer between the elevated terrain and the very stably stratified air aloft that lead to the acceleration of the flow. Downwind of this feature, the terrain flattens once again

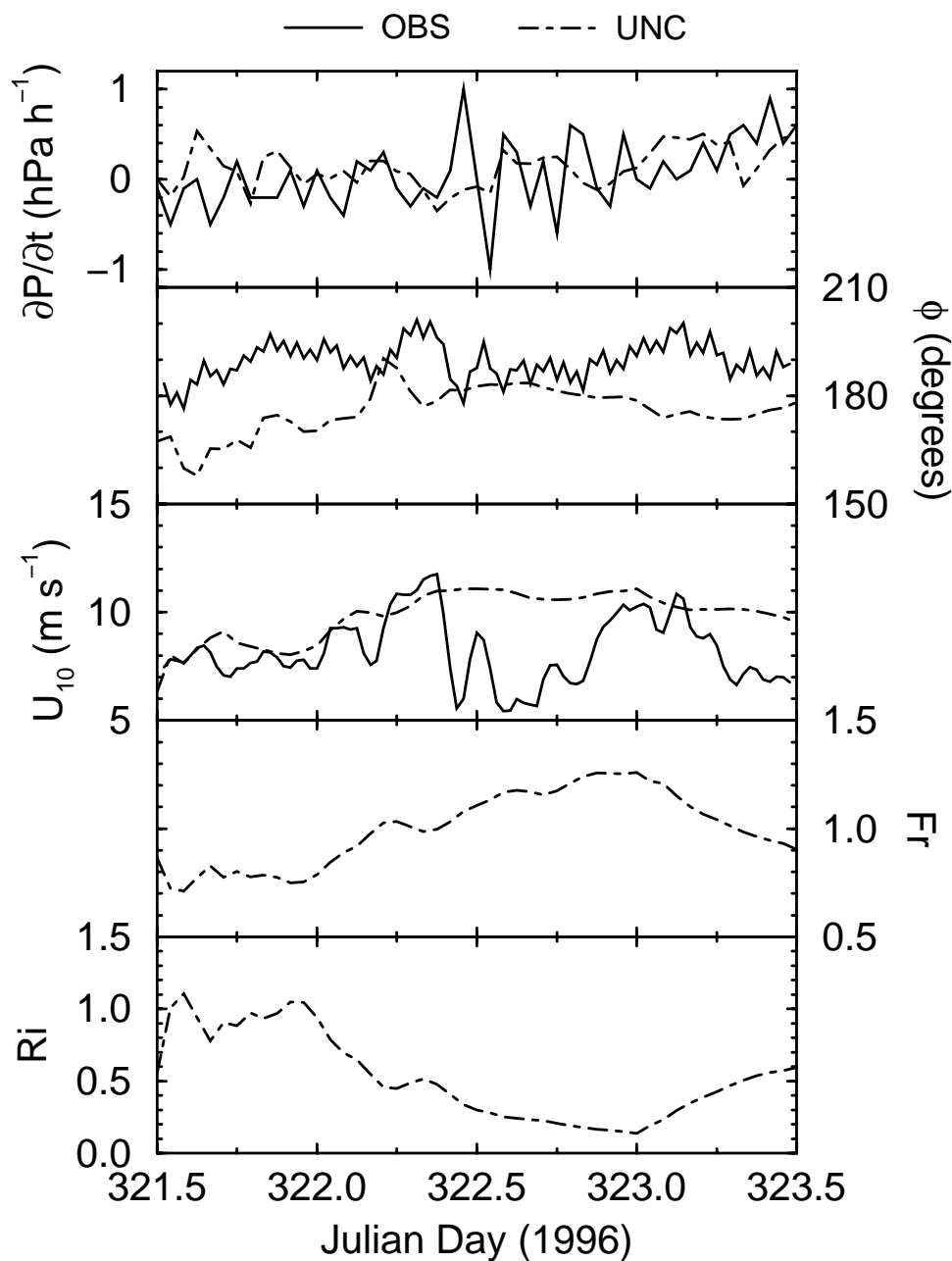


FIGURE 20: Temporal evolution of the observed (OBS) and simulated (UNC) surface pressure tendencies ($\partial P/\partial t$), 10-m wind directions (ϕ) and speeds (U_{10}), as well as the simulated surface Froude (Fr) and Richardson (Ri) numbers from 1200 UTC on 16 November 1996 (JD 321.5) to 1200 UTC on 18 November 1996 (JD 322.5) at Trail Valley Creek, NWT.

allowing a deceleration (and perhaps even a separation) of the flow in a less stable surface layer. The hydraulic jump itself, marked by a value of $Fr \approx 1$, delineates the two regimes as it retreats towards the upwind topography. Its passage is marked by the large surface pressure perturbation and the sudden abatement of near-surface winds.

In an attempt to simulate similar events, other researchers such as Benoit et al. (1997a) and Gallée and Pettré (1998) have used horizontal grids with resolutions of ≤ 2 km. Since the hydraulic jump itself may manifest itself over distances of only a few hundred metres (King and Turner, 1997), the grid spacing of 18 km employed in our simulations clearly becomes restrictive in this case. For future work, therefore, we propose to cascade the UNC and CPL experiments to higher horizontal resolutions to resolve this peculiar feature of the ground blizzard event.

7 Summary and Conclusions

We have investigated a ground blizzard which inflicted high windchills and blowing snow over the Tuktoyaktuk Peninsula (TP) of the Northwest Territories (NWT) of Canada and adjacent Beaufort Sea from 16 to 18 November 1996. It is demonstrated that synoptic forcing of the event is dominated by a rapidly intensifying anticyclone to the east of the TP. Satellite imagery verifies the absence of clouds in the area but reveals the presence of snow on the ground.

The ground blizzard is probed using a sequence of numerical simulations with the Mesoscale Compressible Community (MC2) model. The uncoupled experiment is conducted at a horizontal grid spacing of 18 km and captures with accuracy

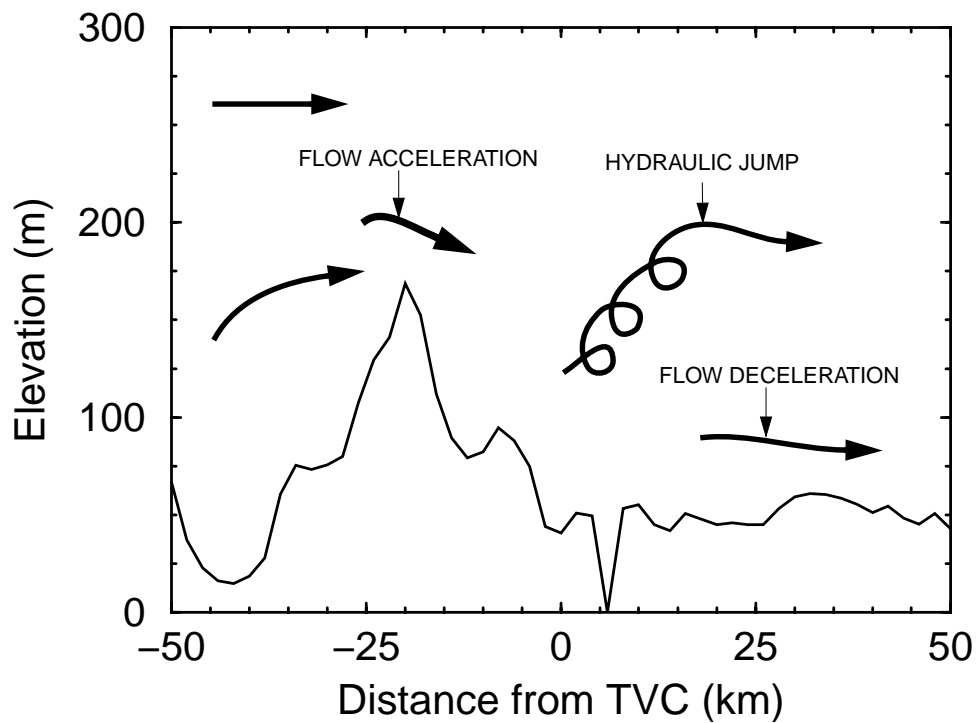


FIGURE 21: Schematic diagram of conditions for Trail Valley Creek at 1000 UTC on 17 November 1996 (JD 322.4). The elevation of the terrain above mean sea-level is plotted with negative distances upwind of Trail Valley Creek.

the anticyclogenesis event within 2 hPa. The uncoupled simulation also provides a satisfactory depiction of the meteorological conditions observed on the TP during the ground blizzard excluding, however, the presence of blowing snow. Having compared the uncoupled simulation to observations, we then proceed to a second experiment whereby the MC2 model is coupled to the PIEKTUK-D blowing snow model. This supplemental integration, conducted in a similar fashion as in the uncoupled case, reveals the presence of abundant blowing snow (but no precipitation) in the vicinity of TVC and the Beaufort Sea in association with strong low-level winds. Combined, blowing snow sublimation and transport are estimated to erode about 1.4 mm snow water equivalent (swe) per day from the snowpack at TVC. Sublimation rates in the coupled simulation are found to increase by about 80% with respect to the stand-alone application of PIEKTUK-D to the same case study. Qualitatively, this is in accordance with the results found by Bintanja (2001) who observed increases in simulated sublimation rates when columns of blowing snow were prescribed a certain entrainment rate of dry air.

The coupled simulation also reveals some interesting aspects of the blowing snow phenomenon and its interaction with the atmospheric boundary layer. For instance, the inclusion of blowing snow in the numerical simulation leads to some modifications of the basic meteorological fields such as cooling and moistening of the air that in turn affect the sea-level pressure and precipitation fields. The negative thermodynamic feedbacks of snowdrift sublimation arise in the coupled simulation but are less prominent than in an idealized modelling framework because of the comprehensive treatment of advective and entrainment processes. Nevertheless, the neglect of blowing snow and its sublimation in numerical weather prediction models may therefore explain some of the systematic errors in the forecasts of near-surface meteorological

fields at high latitudes.

With the prospect of climate change reducing the duration and depth of the seasonal snowpack within the Mackenzie River Basin, there is speculation that blowing snow will diminish even more in importance as an agent of its water and energy budgets. However, if high wind events and storminess become more frequent during the cold season (as is suggested by several studies), a larger portion of the snowfall may be returned to the atmosphere as water vapour, leading to further depletion of the snowpack. Considering that blowing snow transport and sublimation are highly dependent on wind speeds, the intensity of the events will also be a crucial factor in estimating its future contributions to the surface mass balance of the basin and the fresh water input into the Beaufort Sea. The present study, however, suggests that blowing snow impacts marginally the water budget of the MRB in its current state.

Acknowledgements

We sincerely thank Dr. Stéphane Bélair and Dr. Michel Desgagné (RPN, Dorval), Dr. Steve Thomas (NCAR), Dr. Badrinath Nagarajan and Mr. Ron McTaggart-Cowan (McGill University) for their assistance in the operation of the MC2 model and Mr. Stéphane Chamberland, Mrs. Judy St-James and Dr. Bruce Brasnett (RPN, Dorval) for providing the required geophysical and snow depth fields in the MC2 simulations. We wish to express our sincere gratitude to Dr. John Pomeroy and his colleagues at the NWRI (Saskatoon) who generously provided the Trail Valley Creek field data. Inuvik sounding data were kindly supplied by Mr. Bob Crawford (MSC, Downsview), public forecasts for the Northwest Territories by Mrs.

Sandra Buzza (MSC, Edmonton) and satellite imagery by Mr. Patrick King (MSC, King City). This research was financially supported by the Natural Sciences and Engineering Research Council of Canada through a GEWEX collaborative research network grant.

References

- Arya, S. P. S., 1988: *Introduction to Micrometeorology*, Academic Press, 307 pp.
- Barry, R. G., 1989: The present climate of the Arctic Ocean and possible past and future states, in Herman, Y. (Ed.), *The Arctic Seas: Climatology, Oceanography, Geology and Biology*, Van Nostrand Reinhold, pp. 1-46.
- Benoit, R., Côté, J., and Mailhot, J., 1989: Inclusion of a TKE boundary layer parameterization in the Canadian regional finite-element model, *Mon. Weather Rev.*, **117**, 1726-1750.
- Benoit, R., Desgagné, M., Pellerin, P., Pellerin, S., and Chartier, Y., 1997a: The Canadian MC2: A semi-Lagrangian, semi-implicit wideband atmospheric model suited for finescale process studies and simulation, *Mon. Weather Rev.*, **125**, 2382-2415.
- Benoit, R., Pellerin, S. and Yu, W., 1997b: MC2 model performance during the Beaufort and Arctic Storms Experiment, in Lin, C. A., Laprise, R., and Ritchie, H. (Eds.) *Numerical Methods in Atmospheric and Oceanic Modelling: The André Robert Memorial Volume*, NRC Research Press, Ottawa, Ontario, pp. 195-220.
- Bintanja, R., 1998: The contribution of snowdrift sublimation to the surface mass balance of Antarctica, *Ann. Glaciol.*, **27**, 251-259.
- Bintanja, R., 2001: Modelling snowdrift sublimation and its effect on the moisture budget of the atmospheric boundary layer, *Tellus*, **53A**, 215-232.
- Blackadar, A. K., 1957: Boundary layer wind maxima and their significance for the growth of nocturnal inversions, *Bull. Amer. Meteorol. Soc.*, **38**, 283-290.

-
- Brasnett, B., 1999: A global analysis of snow depth for numerical weather prediction, *J. Appl. Meteorol.*, **38**, 726-740.
- Brown, R. D., and Braaten, R. O., 1998: Spatial and temporal variability of Canadian monthly snow depths, *Atmos.-Ocean*, **36**, 37-54.
- Carrera, M. L., Gyakum, J. R., and Zhang, D.-L., 1999: A numerical case study of secondary marine cyclogenesis sensitivity to initial error and varying physical processes, *Mon. Weather Rev.*, **127**, 641- 660.
- Colucci, S. J. and Bosart, L. F., 1979: Surface anticyclone behavior in NMC prediction models, *Mon. Weather Rev.*, **107**, 377-394.
- Colucci, S. J. and Davenport, J. C., 1987: Rapid surface anticyclogenesis: synoptic climatology and attendant large-scale circulation changes, *Mon. Weather Rev.*, **115**, 822-836.
- Curry, J. A., 1983: On the formation of continental polar air, *J. Atmos. Sc.*, **40**, 2278-2292.
- Curry, J. A., 1987: The contribution of radiative cooling to the formation of cold-core anticyclones, *J. Atmos. Sc.*, **44**, 2575-2592.
- Deardorff, J. W., 1978: Efficient prediction of ground surface temperature and moisture with inclusion of a layer of vegetation, *J. Geophys. Res.*, **83**, 1889-1904.
- Déry, S. J. and Taylor, P. A., 1996: Some aspects of the interaction of blowing snow with the atmospheric boundary layer, *Hydrol. Proc.*, **10**, 1345-1358.
- Déry, S. J., Taylor, P. A., and Xiao, J., 1998: The thermodynamic effects of sublimating, blowing snow in the atmospheric boundary layer, *Bound.-Layer Meteorol.*, **89**, 251-283.
- Déry, S. J. and Yau, M. K., 1999a: A climatology of adverse winter-type weather events, *J. Geophys. Res.*, **104**(D14), 16,657-16,672.
- Déry, S. J. and Yau, M. K., 1999b: A bulk blowing snow model, *Bound.-Layer Meteorol.*, **93**, 237-251.
- Déry, S. J. and Yau, M. K., 2001a: Simulation of blowing snow in the Canadian Arctic using a double-moment model, *Bound.-Layer Meteorol.*, in press.
- Déry, S. J. and Yau, M. K., 2001b: The large-scale mass balance effects of blowing snow

and surface sublimation, submitted to *J. Geophys. Res.*

- Dickson, B., 1999: All change in the Arctic, *Nature*, **397**, 389-391.
- Douville, H., Royer, J.-F., and Mahfouf, J.-F., 1995: A new snow parameterization for the Météo-France climate model, Part I: Validation in stand-alone experiments, *Clim. Dyn.*, **12**, 21-35.
- Endoh, T., Yamanouchi, T., Ishikawa, T., Kakegaw, H., and Kawaguchi, S., 1997: Dark streams observed on NOAA satellite images over the katabatic wind zone, Antarctica, *Ant. Record*, **41**(1), 447-457.
- Essery, R., Li, L., and Pomeroy, J. W., 1999: A distributed model of blowing snow over complex terrain, *Hydrol. Proc.*, **13**, 2423-2438.
- Gallée, H., 1998: Simulation of blowing snow over the Antarctic ice sheet, *Ann. Glaciol.*, **26**, 203-206.
- Gallée, H. and Pettré, P., 1998: Dynamical constraints on katabatic wind cessation in Adélie Land, Antarctica, *J. Atmos. Sci.*, **55**, 1755-1770.
- Grumm, R. H. and Gyakum, J. R., 1986: Systematic surface anticyclone errors in NMC's limited area fine mesh and spectral models during the winter of 1981/82, *Mon. Weather Rev.*, **114**, 2329-2343.
- Hanesiak, J. M., Stewart, R. E., Szeto, K. K., Hudak, D. R., and Leighton, H. G., 1997: The structure, water budget, and radiational features of a high-latitude warm front, *J. Atmos. Sc.*, **54**, 1553-1573.
- Holtslag, A. A. M., de Bruijn, E. I. F., and Pan, H.-L., 1990: A high resolution air mass transformation model for short-range weather forecasting, *Mon. Weather Rev.*, **118**, 1561-1575.
- King, J. C. and Turner, J., 1997: *Antarctic Meteorology and Climatology*, Cambridge University Press, 409 pp.
- King, J. C., Anderson, P. S., Smith, M. C., and Mobbs, S. D., 1996: The surface energy and mass balance at Halley, Antarctica during winter, *J. Geophys. Res.*, **101**, 19,119-19,128.

-
- Klein, P. M., Harr, P. A., and Elsberry, R. L., 2000: Extratropical transition of western north Pacific tropical cyclones: An overview and conceptual model of the transformation stage, *Wea. Forecasting*, **15**, 373-395.
- Kong, F. and Yau, M. K., 1997: An explicit approach to microphysics in the MC2, *Atmos.-Ocean*, **35**, 257-291.
- Kosović, B. and Curry, J. A., 2000: A large eddy simulation of a quasi-steady, stably stratified atmospheric boundary layer, *J. Atmos. Sci.*, **57**, 1052-1068.
- Lackmann, G. M., Gyakum, J. R., and Benoit, R., 1998: Moisture transport diagnosis of a wintertime precipitation event in the Mackenzie River Basin, *Mon. Weather Rev.*, **126**, 668-691.
- Lander, M. A., Trehubenko, E. J., and Guard, C. P., 1999: Eastern hemisphere tropical cyclones of 1996, *Mon. Weather Rev.*, **127**, 1274-1300.
- Li, L. and Pomeroy, J. W., 1997: Estimates of threshold wind speeds for snow transport using meteorological data, *J. Appl. Meteorol.*, **36**, 205-213.
- Liston, G. E. and Sturm, M., 1998: A snow-transport model for complex terrain, *J. Glaciol.*, **44**, 498-516.
- Mailhot, J. and Benoit, R., 1982: A finite-element model of the atmospheric boundary layer suitable for use with numerical weather prediction models, *J. Atmos. Sci.*, **39**, 2249-2266.
- Mailhot, J. and Chouinard, C., 1989: Numerical forecasts of explosive winter storms: Sensitivity experiments with a meso- α model, *Mon. Weather Rev.*, **117**, 1311-1343.
- Mann, G. W., Anderson, P. S., and Mobbs, S. D., 2000: Profile measurements of blowing snow at Halley, Antarctica, *J. Geophys. Res.*, **105**(19), 24,491-24,508.
- Milbrandt, J. and Yau, M. K., 2001: A mesoscale modeling study of the 1996 Saguenay flood, *Mon. Weather Rev.*, in press.
- Misra, V., Yau, M. K., and Badrinath, N., 2000: Atmospheric water species budget in mesoscale simulations of lee cyclones over the Mackenzie River Basin, *Tellus*, **52A**, 140-161.

-
- Noilhan, J. and Planton, S., 1989: A simple parameterization of land surface processes for meteorological models, *Mon. Weather Rev.*, **117**, 536-549.
- Ohtake, T., Jayaweera, K., and Sakurai, K.-I., 1982: Observation of ice crystal formation in lower Arctic atmosphere, *J. Atmos. Sci.*, **39**, 2898-2904.
- Oke, T. R., 1987: *Boundary Layer Climates*, 2nd ed., Methuen, 435 pp.
- Oke, T. R., 1997: Surface climate processes, in Bailey, W. G., Oke, T. R., and Rouse, W. R. (Eds.), *Surface Climates of Canada*, McGill Queen's Press, 21-43.
- Phillips, D., 1990: *Climates of Canada*, Environment Canada, Ottawa, Ont., 176 pp.
- Pomeroy, J. W., Marsh, P., and Gray, D. M., 1997: Application of a distributed blowing snow model to the Arctic, *Hydrol. Proc.*, **11**, 1451-1464.
- Pomeroy, J. W. and Essery, R. L. H., 1999: Turbulent fluxes during blowing snow: Field tests of model sublimation predictions, *Hydrol. Proc.*, **13**, 2963-2975.
- Rothrock, D. A., Yu, Y., and Maykut, G. A., 1999: Thinning of the Arctic sea-ice cover, *Geophys. Res. Lett.*, **23**, 3469-3472.
- Rouse, W. R., 2000: Progress in hydrological research in the Mackenzie GEWEX study, *Hydrol. Proc.*, **14**, 1667-1685.
- Serreze M., 1995: Climatological aspects of cyclone development and decay in the Arctic, *Atmos.-Ocean*, **33**, 1-23.
- Serreze, M. C., Walsh, J. E., Chapin III, F. S., Osterkamp, T., Dyurgerov, M., Romanovsky, V., Oechel, W. C., Morison, J., Zhang, T., and Barry, R. G., 2000: Observational evidence of recent change in the northern high-latitude environment, *Clim. Change*, **46**, 159-207.
- Stewart, R. E., Bachan, D., Dunkley R. R., Giles, A. C., Lawson, B., Legal, L., Miller, S. T., Murphy, B. P., Parker, M. N., Paruk, B. J., and Yau, M. K., 1995: Winter storms over Canada, *Atmos.-Ocean*, **33**, 223-247.
- Stewart, R. E., Leighton, H. G., Marsh, P., Moore, G. W. K., Rouse, W. R., Soulis, S. D., Strong, G. S., Crawford, R. W., and Kochtubajda, B., 1998: The Mackenzie GEWEX Study: The water and energy cycles of a major North American river basin, *Bull. Amer.*

Meteorol. Soc., **79**, 2665-2683.

Stewart, R. E., Burford, J. E., and Crawford, R. W., 2000: On the meteorological characteristics of the water cycle of the Mackenzie River Basin, *Contr. Atmos. Phys.*, **9**, 103-110.

Stull, R. B., 1988: *An Introduction to Boundary Layer Meteorology*, Kluwer Academic Publishers, 666 pp.

Szeto, K. K., Stewart, R. E., and Hanesiak, J. M., 1997: High latitude cold season frontal cloud systems and their precipitation efficiency, *Tellus*, **49**, 439-454.

Wintels, W. and Gyakum, J. R., 2000: Synoptic climatology of Northern Hemisphere available potential energy collapses, *Tellus*, **52A**, 347-364.

Xiao, J., Bintanja, R., Déry, S. J., Mann, G. W., and Taylor, P. A., 2000: An intercomparison among four models of blowing snow, *Bound.-Layer Meteorol.*, **97**(1), 109-135.

Zishka, K. M. and Smith, P. J., 1980: The climatology of cyclones and anticyclones over North America and surrounding ocean environs for January and July 1955-77, *Mon. Weather Rev.*, **108**, 387-401.

Chapter 6

Conclusion

6.1 Thesis Summary

In this thesis, the role of blowing snow in the hydrometeorology of the Mackenzie River Basin has been investigated. Using the ERA data, a climatology of these events and their impact to the surface mass balance was compiled for the basin and the globe. The development of a numerically efficient model of blowing snow was then described as well as its application to an Arctic tundra location in order to quantify the role of blowing snow sublimation in the wintertime surface mass balance. A case study during which extensive blowing snow occurred was then simulated by means of a mesoscale model that was coupled to the blowing snow model to determine the role of blowing snow in the surface mass balance in the Canadian Arctic. A description of the principal results of this study follows.

The climatology of blowing snow, high windchill and blizzard events inferred

from the ERA data demonstrates the prominence of these phenomena at high latitudes where cold temperatures and persistent snowpacks dominate the local climate. In the MRB, these events occur predominantly in the northern portions of the basin where long seasonal snowcovers, high winds and cold temperatures are most common. For instance, blowing snow occurs on average up to 60 times annually along the Arctic coastline whereas the Yellowknife region of the NWT experiences fewer than 10 events on a yearly basis. In a composite analysis, it is demonstrated that blowing snow events near Yellowknife, NWT, are often forced in part by strong anticyclones and/or lee cyclogenesis.

In the following chapter, the results from the blowing snow climatology are extended to establish the large-scale effects of this process to the surface mass balance. Regions susceptible to frequent high wind events are most vulnerable to the impact of blowing snow sublimation and transport. In the MRB, only regions lying in the Arctic tundra incur significant effects from snowdrifting. It is shown that direct sublimation from the surface is also non-negligible over the basin with deposition counteracting any sublimation associated with blowing snow in some areas. In total, the surface sublimation component overwhelms the blowing snow terms such that mass accumulates to the rate of 0.4 mm snow water equivalent annually over the MRB.

Chapter 4 concerns the development of a computationally efficient blowing snow model. By analytically integrating the particle distribution and sublimation rates, we manage to reduce the determination of the blowing snow mixing ratio to a single equation. The model therefore performs at a rate approximately 100 times faster than its spectral formulation while providing very similar output. This single-moment approach to blowing snow modelling, however, yields unrealistic evolutions

of the blowing snow particle distributions and total numbers. To remedy this weakness of the bulk version of PIEKTUK, an additional equation for total particle numbers is introduced. The resulting double-moment model (PIEKTUK-D) then provides realistic evolutions of both the blowing snow mixing ratio and the particle size distribution. The application of the updated model to a meteorological dataset collected at Trail Valley Creek, NWT, provides some initial estimates of the seasonal blowing snow sublimation rates for the area. For the winter of 1996/1997, PIEKTUK-D predicts the erosion of about 3 mm swe from the snowpack at Trail Valley Creek, much less than values previously reported in the literature for the same area. A discussion revolving around model assumptions and the assimilation of humidity data reveals that these two features are critical in evaluating the contribution of blowing snow sublimation in the Arctic.

To investigate the blowing snow process more thoroughly, a case study spanning two days in mid-November 1996 is examined using the MC2 model at a horizontal resolution of 18 km. The uncoupled experiment captures the rapid anticyclogenesis which causes ground blizzard conditions along the Tuktoyaktuk Peninsula and the Beaufort Sea. A second experiment following the same methodology is then conducted whereby the MC2 is coupled to the PIEKTUK-D model. This simulation reveals the presence of extensive blowing snow in association with the ground blizzard. Total blowing snow sublimation and divergence rates reach several millimetres snow water equivalent over certain areas. At Trail Valley Creek, the coupled simulations indicate that $\approx 1.4 \text{ mm d}^{-1}$ swe is eroded through the combined effects of blowing snow mass divergence and sublimation. Evidence of the self-limiting characteristic of blowing snow sublimation is observed, but the comprehensive treatment of advective and entrainment processes mitigate the negative thermodynamic feed-

backs associated with the phase transition. In the coupled simulation, the overall sublimation rate of blowing snow increases by a factor of 1.8 from the stand-alone application of PIEKTUK-D forced by the same meteorological data.

Although the full consideration of 3-D processes in the coupled modelling yields blowing snow sublimation rates that nearly double in magnitude, this process remains negligible in the surface mass balance of the MRB as a whole. For instance, if we adjust the values of the mass balance study described in Chapter 3 by a similar factor, the total basin loses no more than 0.1 mm swe a^{-1} due to blowing snow sublimation. At Trail Valley Creek, however, the blowing snow sublimation component remains nonetheless more important since it represents an annual sink of about 6 mm swe when the results of Chapter 4 are adjusted for the consideration of the additional entrainment and advective processes.

6.2 Suggestions for Future Work

Despite the advancement in our understanding of the blowing snow phenomenon through the research conducted in this thesis, some of its aspects remain partially incomplete or unknown. For instance, the climatology and mass balance studies presented in Chapters 2 and 3 were performed using the ERA data at a horizontal resolution of 2.5° and at intervals of 6 h. Thus the results presented herein may lack some of the blowing snow events that occur on the mesoscale. Using a dataset with increased horizontal resolution and additional information on the temporal and spatial variability of the meteorological fields would enhance the results of these two chapters.

The optimized blowing snow models described in Chapter 4 could be easily applied in operational weather forecast offices across Canada and elsewhere. Given their numerical efficiency, the single- and double-moment versions of PIEKTUK could be fed either observed or forecast meteorological data in order to determine the presence and intensity of a blowing snow event. This would provide, for instance, crucial information on optical visibilities and snowdrifting rates for current transportation conditions.

The mesoscale modelling discussed in Chapter 5 of the thesis has focused on a single event in mid-November 1996. To generalize some of its conclusions, further case studies with varying mesoscale settings should be investigated. Specifically, the exploration of the role of blowing snow in a cyclone versus an anticyclone would yield an interesting comparison of its overall importance in varying meteorological conditions. By resolving some of the smaller-scale features of a blowing snow event, results of the mesoscale simulations would certainly improve at higher horizontal resolutions. Even in these circumstances, the simulations would also benefit from the consideration of subgrid scale topographical effects, such as gullies and vegetation. Finally, a number of applications can be suggested with regard to the coupled models. For instance, PIEKTUK-D could easily be modified to represent the aeolian suspension of other types of particles. As such, the MC2 and PIEKTUK-D models could simulate dust and sandstorms or even the evaporation from sea spray.

On longer timescales, the consideration of climate change and its impact on the high-latitude snow and ice covers are of great concern. Will the role of blowing snow diminish or increase in a warmer environment? Will increased storminess return a greater percentage of the seasonal snowfall back to the atmosphere? Such questions remain open to much speculation and ensure that the topic of blowing snow

will attract continued interest during the coming years in the hydrometeorological community.

Appendix

The observational data used in Chapter 4 of the thesis were recorded at Trail Valley Creek (TVC), Northwest Territories (NWT). They were graciously provided to us by Dr. John Pomeroy who collected these data with the help of colleagues at the Saskatoon Branch of the National Water Research Institute (NWRI). Upon receipt of these data, an uncertainty existed on whether the relative humidity measurements were with respect to water (RH_w) or with respect to ice (RH_i). This is indeed a crucial point since blowing snow usually occurs in subfreezing conditions such that the sublimation of suspended ice particles remains constrained by saturation with respect to ice.

Following Anderson's (1994) methodology, a plot of the relative humidity versus temperature was performed (Figure A1). This clearly demonstrates that the relative humidity measurements recorded at TVC during the winter of 1996/1997 are with respect to water since the observed maximum values decrease almost linearly with temperatures. For all temperatures, we would expect the maximum value of RH_i to approach 100%. This is especially true at frigid temperatures where the amount of moisture the air can sustain is very low such that saturation with respect ice is readily attained.

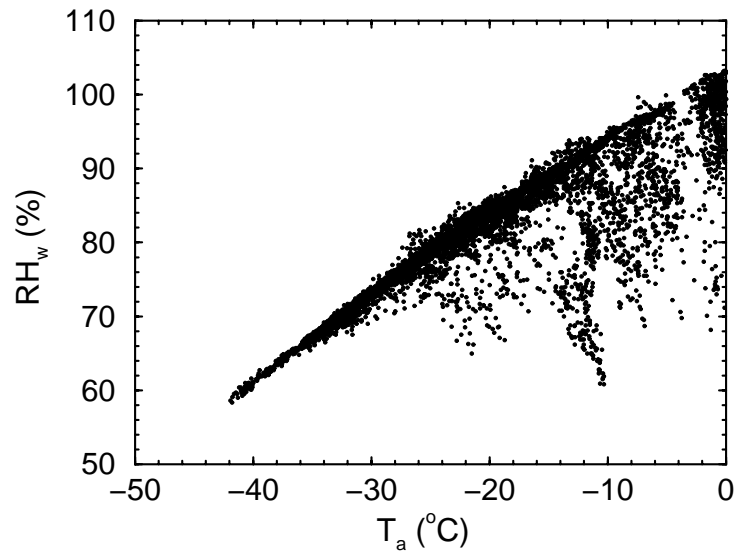


FIGURE A1: The observed values of relative humidity with respect to water (RH_w) versus temperature (T_a) during the winter of 1996/1997 at Trail Valley Creek, NWT.

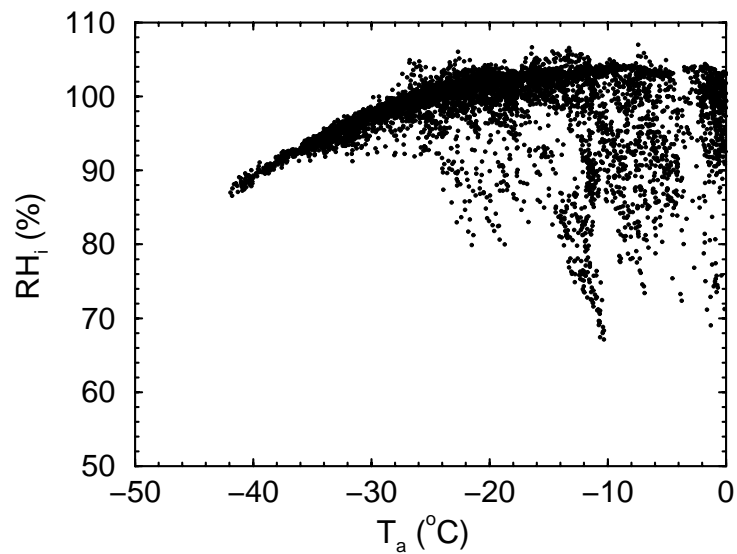


FIGURE A2: The observed values of relative humidity with respect to ice (RH_i) versus temperature (T_a) during the winter of 1996/1997 at Trail Valley Creek, NWT.

By converting the relative humidity measurements to with respect to ice using the equations outlined in Chapter 3, we now observe the expected maxima in their values near 100% at all temperatures (Figure A2). As discussed by Anderson (1994), there are limitations with the instrument that yield a slightly curved profile in the approximate maxima in RH_i . Note however that we have made no attempt to recalibrate the humidity measurements despite the instrument biases shown here.

Based on this evidence, we converted all of the RH_w measurements collected at TVC during the winter of 1996/1997 to RH_i . As demonstrated in Chapter 4, this has significant consequences to the evaluation of the seasonal blowing snow sublimation rates at this Arctic tundra location. The results of Essery et al. (1999) must also be re-evaluated in light of the above since their conclusions were obtained by assuming that the initial humidity measurements were with respect to ice and not with respect to water.

Nevertheless, caution must be used in interpreting these adjusted RH_i values. Makkonen (1996) and Pomeroy (personal communication, 2001) both attest that hygrometers often become coated with ice at subfreezing temperatures. This can lead to erroneous measurements of humidities that consistently and artificially approach the saturation point with respect to ice. Anderson (1996), however, claims that hygrometers are especially deficient when $RH_i > 1$, but relatively good below the ice saturation point. In any case, without continuous human maintenance of the recording instruments during the winter of 1996/97 at TVC, some doubts remain on the accuracy of the humidity values recorded there. Therefore, the contribution of blowing snow sublimation to the surface mass balance may be underestimated in Chapter 4.4. On the other hand, surface sublimation may be either overestimated or underestimated at the same location.

References

- Alvarez, J. A., and Lieske, B. J., 1960: The little America blizzard of May 1957, in Dwyer, L. J. (Ed.), *Antarctic Meteorology*, Pergamon Press, pp. 115-127.
- Anderson, P. S., 1994: A method for rescaling humidity sensors at temperatures well below freezing, *J. Atmos. Oceanic Tech.*, **11**, 1388-1391.
- Anderson, P. S., 1996: Reply, *J. Atmos. Oceanic Tech.*, **13**, 913-914.
- Arya, S. P. S., 1988: *Introduction to Micrometeorology*, Academic Press, 307 pp.
- Atmospheric Environment Service, 1977: *MANOBS: Manual of surface weather observations*, Environment Canada.
- Atmospheric Environment Service, 1988: *MANPUB: Manual of standard procedures for public weather service*, 5th ed., Environment Canada.
- Babin, G., 1975: Blizzard of 1975 in Western Canada, *Weatherwise*, **28**, 70-75.
- Barry, R. G., 1989: The present climate of the Arctic Ocean and possible past and future states, in Herman, Y. (Ed.), *The Arctic Seas: Climatology, Oceanography, Geology and Biology*, Van Nostrand Reinhold, pp. 1-46.
- Barry, R. G., 1992: *Mountain Weather and Climate*, 2nd ed., Routledge, 402 pp.
- Benoit, R., Côté, J., and Mailhot, J., 1989: Inclusion of a TKE boundary layer parameterization in the Canadian regional finite-element model, *Mon. Weather Rev.*, **117**, 1726-1750.
- Benoit, R., Desgagné, M., Pellerin, P., Pellerin, S., and Chartier, Y., 1997a: The Canadian MC2: A semi-Lagrangian, semi-implicit wideband atmospheric model suited for finescale process studies and simulation, *Mon. Weather Rev.*, **125**, 2382-2415.
- Benoit, R., Pellerin, S., and Yu, W., 1997b: MC2 model performance during the Beaufort and Arctic Storms Experiment, in Lin, C. A., Laprise, R. and Ritchie, H. (Eds.) *Numerical Methods in Atmospheric and Oceanic Modelling: The André Robert Memorial Volume*, NRC Research Press, pp. 195-220.

-
- Berg, N. H., 1986: Blowing snow at a Colorado alpine site: measurements and implications, *Arctic and Alpine Res.*, **18**, 147-161.
- Betts, A. K. and Viterbo, P., 2000: Hydrology of seven sub-basins of the Mackenzie River from the ECMWF model, *J. Hydrometeorol.*, **1**, 47-60.
- Bintanja, R., 1998a: The contribution of snowdrift sublimation to the surface mass balance of Antarctica, *Ann. Glaciol.*, **27**, 251-259.
- Bintanja, R., 1998b: The interaction between drifting snow and atmospheric turbulence, *Annals Glaciol.* **26**, 167-173.
- Bintanja, R., 2000: Snowdrift suspension and atmospheric turbulence. Part I: Theoretical background and model description, *Bound.-Layer Meteorol.*, **95**, 343-368.
- Bintanja, R., 2001: Modelling snowdrift sublimation and its effect on the moisture budget of the atmospheric boundary layer, *Tellus*, **53A**, 215-232.
- Bjornsson, H., Mysak, L. A., and Brown, R. D., 1995: On the interannual variability of precipitation and runoff in the Mackenzie drainage basin, *Clim. Dyn.*, **12**, 67-76.
- Blackadar, A. K., 1957: Boundary layer wind maxima and their significance for the growth of nocturnal inversions, *Bull. Amer. Meteorol. Soc.*, **38**, 283-290.
- Bluestein, H. B., 1993: *Synoptic-Dynamic Meteorology in Midlatitudes, Vol. 2: Observations and Theory of Weather Systems*, Oxford University Press, 594 pp.
- Branick, M. L., 1997: A climatology of significant winter-type weather events in the contiguous United States, 1982-94, *Wea. Forecasting*, **12**, 193-207.
- Brasnett, B., 1999: A global analysis of snow depth for numerical weather prediction, *J. Appl. Meteorol.*, **38**, 726-740.
- Brown, R. D., and Braaten, R. O., 1998: Spatial and temporal variability of Canadian monthly snow depths, *Atmos.-Ocean*, **36**, 37-54.
- Budd, W. F., 1966: The drifting of non-uniform snow particles, in Rubin, M. J. (Ed.), *Studies in Antarctic Meteorology*, Antarctic Research Series Vol. 9, American Geophysical Union, pp. 71-134.
- Burns, B. M., 1973: *The Climate of the Mackenzie Valley - Beaufort Sea*, vol. 1, Climatol.

-
- Studies No. 24, Atmos. Env. Ser., Environment Canada, 227 pp.
- Burrows, W. R., Treidl, R. A., and Lawford, R. G., 1979: The Southern Ontario blizzard of January 26 and 27, *Atmos.-Ocean*, **17**, 306-320.
- Carrera, M. L., Gyakum, J. R., and Zhang, D.-L., 1999: A numerical case study of secondary marine cyclogenesis sensitivity to initial error and varying physical processes, *Mon. Weather Rev.*, **127**, 641- 660.
- Cohen, S. J., 1997a: What if and so what in Northwest Canada: Could climate change make a difference to the future of the Mackenzie Basin, *Arctic*, **50**, 293-307.
- Cohen, S. J. (Ed.), 1997b: *Mackenzie Basin Impact Study (MBIS) Final Report*, Environment Canada, 372 pp.
- Colucci, S. J. and Bosart, L. F., 1979: Surface anticyclone behavior in NMC prediction models, *Mon. Weather Rev.*, **107**, 377-394.
- Colucci, S. J. and Davenport, J. C., 1987: Rapid surface anticyclogenesis: synoptic climatology and attendant large-scale circulation changes, *Mon. Weather Rev.*, **115**, 822-836.
- Connolley, W. M. and King, J. C., 1996: A modeling and observational study of East Antarctica surface mass balance, *J. Geophys. Res.*, **101**, 1335-1343.
- Cullather, R. I., Bromwich, D. H., and Van Woert, M. L., 1998: Spatial and temporal variability of Antarctic precipitation from atmospheric methods, *J. Climate*, **11**, 334-368.
- Cullather, R. I., Bromwich, D. H., and Serreze, M. C., 2000: The atmospheric hydrologic cycle over the Arctic Basin from reanalyses. Part I: Comparison with observations and previous studies, *J. Climate*, **13**, 923-937.
- Curry, J. A., 1983: On the formation of continental polar air, *J. Atmos. Sc.*, **40**, 2278-2292.
- Curry, J. A., 1987: The contribution of radiative cooling to the formation of cold-core anticyclones, *J. Atmos. Sc.*, **44**, 2575-2592.
- Deardorff, J. W., 1978: Efficient prediction of ground surface temperature and moisture with inclusion of a layer of vegetation, *J. Geophys. Res.*, **83**, 1889-1904.

-
- DeGaetano, 2000: Climatic perspective and impacts of the 1998 northern New York and New England ice storm, *Bull. Amer. Meteorol. Soc.*, **81**(2), 237-254.
- Déry, S. J. and Taylor, P. A., 1996: Some aspects of the interaction of blowing snow with the atmospheric boundary layer, *Hydrol. Proc.*, **10**, 1345-1358.
- Déry, S. J., Taylor, P. A., and Xiao, J., 1998: The thermodynamic effects of sublimating, blowing snow in the atmospheric boundary layer, *Bound.-Layer Meteorol.*, **89**, 251-283.
- Déry, S. J. and Yau, M. K., 1999a: A climatology of adverse winter-type weather events, *J. Geophys. Res.*, **104**(D14), 16,657-16,672.
- Déry, S. J. and Yau, M. K., 1999b: A bulk blowing snow model, *Bound.-Layer Meteorol.*, **93**, 237-251.
- Déry, S. J. and Yau, M. K., 2001a: The large-scale mass balance effects of blowing snow and surface sublimation, submitted to *J. Geophys. Res.*
- Déry, S. J. and Yau, M. K., 2001b: Simulation of blowing snow in the Canadian Arctic using a double-moment model, *Bound.-Layer Meteorol.*, in press.
- Dickson, B., 1999: All change in the Arctic, *Nature*, **397**, 389-391.
- Douville, H., Royer, J.-F., and Mahfouf, J.-F., 1995: A new snow parameterization for the Météo-France climate model, Part I: Validation in stand-alone experiments, *Climate Dyn.*, **12**, 21-35.
- Eagleman, J. R., 1990: *Severe and Unusual Weather*, 2nd ed., Van Nostrand Reinhold, 372 pp.
- Endoh, T., Yamanouchi, T., Ishikawa, T., Kakegaw, H., and Kawaguchi, S., 1997: Dark streams observed on NOAA satellite images over the katabatic wind zone, Antarctica, *Ant. Record*, **41**(1), 447-457.
- Environment Canada, 1984: *Principal Station Data*, vol. 34, Yellowknife A, Atmos. Env. Ser., 48 pp.
- Environment Canada, 1993: *Canadian Climate Normals, 1961-1990*, vol. 3, The North: Yukon and Northwest Territories, Atmos. Env. Ser., 58 pp.
- Essery, R., Li, L., and Pomeroy, J. W., 1999: A distributed model of blowing snow over

-
- complex terrain, *Hydrol. Proc.*, **13**, 2423-2438.
- Gallée, H., 1998: Simulation of blowing snow over the Antarctic ice sheet, *Ann. Glaciol.*, **26**, 203-206.
- Gallée, H. and Pettré, P., 1998: Dynamical constraints on katabatic wind cessation in Adélie Land, Antarctica, *J. Atmos. Sci.*, **55**, 1755-1770.
- Garratt, J. R., 1992: *The Atmospheric Boundary Layer*, Cambridge University Press, Cambridge, 316 pp.
- Gibson, J. K., Kållberg, P., Uppala, S., Hernandez, A., Nomura, A., and Serrano, E., 1997: *ERA Description*, ECMWF Re-Analysis Project Report Series, 1, 72 pp.
- Giovinetto, M. B., Bromwich, D. H., and Wendler, G., 1992: Atmospheric net transport of water vapor and latent heat across 70°S, *J. Geophys. Res.*, **97**, 917-930.
- Graff, J. V. and Strub, J. H., 1975: The Great Upper Plains blizzard of January 1975, *Weatherwise*, **28**, 66-69.
- Grumm, R. H. and Gyakum, J. R., 1986: Systematic surface anticyclone errors in NMC's limited area fine mesh and spectral models during the winter of 1981/82, *Mon. Weather Rev.*, **114**, 2329-2343.
- Hanesiak, J. M., Stewart, R. E, Szeto, K. K., Hudak, D. R., and Leighton, H. G., 1997: The structure, water budget, and radiational features of a high-latitude warm front, *J. Atmos. Sci.*, **54**, 1553-1573.
- Harrington, J. Y., Meyers, M. P., Walko, R. L., and Cotton, W. R., 1995: Parameterization of ice crystal conversion process due to vapor deposition for mesoscale models using double-moment basin functions. Part I: Basic formulation and parcel model results, *J. Atmos. Sci.*, **52**, 4344-4366.
- Holtstag, A. A. M., de Bruijn, E. I. F., and Pan, H.-L., 1990: A high resolution air mass transformation model for short-range weather forecasting, *Mon. Weather Rev.*, **118**, 1561-1575.
- Hoode, E., Williams, M., and Cline, D., 1999: Sublimation from a seasonal snowpack at a continental, mid-latitude alpine site, *Hydrol. Proc.*, **13**, 1781-1797.

-
- Huo, Z., Zhang, D.-L., Gyakum, J., and Staniforth, A., 1995: A diagnostic analysis of the Superstorm of March 1993, *Mon. Weather Rev.*, **123**(6), 1740-1761.
- Källberg, P., 1997: *Aspects of the Re-Analysed Climate*, ECMWF Re-Analysis Project Report Series, 2, 89 pp.
- Kind, R. J., 1976: A critical examination of the requirements for model simulation of wind-induced erosion/deposition phenomena such as drifting snow, *Atmos. Env.*, **10**, 219-227.
- Kind, R. J., 1981: Snowdrifting, in Gray, D. M. and Male, D. H. (Eds.), *Handbook of Snow - Principles, Processes, Management & Use*, Pergamon Press, pp. 338-359.
- King, J. C. and Anderson, P. S., 1999: A humidity climatology for Halley, Antarctica based on hygrometer measurements, *Antarctic Sc.*, **11**, 100-104.
- King, J. C., Anderson, P. S., Smith, M. C., and Mobbs, S. D., 1996: The surface energy and mass balance at Halley, Antarctica during winter, *J. Geophys. Res.*, **101**, 19,119-19,128.
- King, J. C. and Turner, J., 1997: *Antarctic Meteorology and Climatology*, Cambridge University Press, 409 pp.
- Klein, P. M., Harr, P. A., and Elsberry, R. L., 2000: Extratropical transition of western north Pacific tropical cyclones: An overview and conceptual model of the transformation stage, *Wea. Forecasting*, **15**, 373-395.
- Kocin, P. J. and Uccellini, L. W., 1990: *Snowstorms along the Northeastern Coast of the United States: 1955 to 1985*, Meteor. Monogr. No. 44, Amer. Meteorol. Soc., 280 pp.
- Kong, F. and Yau, M. K., 1997: An explicit approach to microphysics in the MC2, *Atmos.-Ocean*, **35**, 257-291.
- Kosović, B. and Curry, J. A., 2000: A large eddy simulation of a quasi-steady, stably stratified atmospheric boundary layer, *J. Atmos. Sci.*, **57**, 1052-1068.
- Lackmann, G. M. and Gyakum, J. R., 1996: The synoptic- and planetary-scale signatures of precipitating systems over the Mackenzie River Basin, *Atmos.-Ocean*, **34**(4), 647-674.
- Lackmann, G. M., Gyakum, J. R., and Benoit, R., 1998: Moisture transport diagnosis of a wintertime precipitation event in the Mackenzie River Basin, *Mon. Weather Rev.*,

126, 668-691.

- Lander, M. A., Trehubenko, E. J., and Guard, C. P., 1999: Eastern hemisphere tropical cyclones of 1996, *Mon. Weather Rev.*, **127**, 1274-1300.
- Lawford, R. G., 1993: The role of ice in the global water cycle, in Wilkinson, W. B. (Ed.), *Macroscale Modelling of the Hydrosphere*, IAHS Publ. No. 214, Wallingford, pp. 151-161.
- Lawford, R. G., 1994: Knowns and unknowns in the hydroclimatology of the Mackenzie River Basin, in Cohen, S. J. (Ed.), *Mackenzie Basin Impact Study (MBIS)*, Interim Report #2, Yellowknife, NWT, pp. 173-195.
- Lawson, B., 1987: *The Climatology of Blizzards in Western Canada 1953-1986*, Central Region Report CAES 88-1, Atmos. Env. Ser., Environment Canada, Winnipeg, Man.
- Lee, L. W., 1975: *Sublimation of Snow in Turbulent Atmosphere*, Ph.D. Thesis, Dept. of Mechanical Engineering, University of Wyoming, Laramie WY, 82070, 162 pp.
- Li, L. and Pomeroy, J. W., 1997: Estimates of threshold wind speeds for snow transport using meteorological data, *J. Appl. Meteorol.*, **36**, 205-213.
- Liston, G. E. and Sturm, M., 1998: A snow-transport model for complex terrain, *J. Glaciol.*, **44**, 498-516.
- Lydolph, P. E., 1977: *Climates of the Soviet Union*, World Survey of Climatology, vol. 7, Elsevier, 443 pp.
- Mailhot, J. and Benoit, R., 1982: A finite-element model of the atmospheric boundary layer suitable for use with numerical weather prediction models, *J. Atmos. Sci.*, **39**, 2249-2266.
- Makkonen, L., 1996: Comments on "A method for rescaling humidity sensors at temperatures well below freezing", *J. Atmos. Oceanic Tech.*, **13**, 911-912.
- Male, D. H., 1980: The seasonal snowcover, in Colbeck, S. D. (Ed.), *Dynamics of Snow and Ice Masses*, Academic Press, 305-395.
- Mann, G. W., Anderson, P. S., and Mobbs, S. D., 2000: Profile measurements of blowing snow at Halley, Antarctica, *J. Geophys. Res.*, **105**(19), 24,491-24,508.

-
- Maxwell, J. B., 1980: *The Climate of the Canadian Arctic Islands and Adjacent Waters*, vol. 1, Climatol. Studies No. 30, Atmos. Env. Ser., Environment Canada, 532 pp.
- Mikhel', V. M., Rudneva, A. V., and Lipovskaya, V. I., 1971: *Snowfall and Snow Transport During Snowstorms over the USSR*, Main Admin. of the Hydrometeorological Service of the Council of Ministers of the USSR, Leningrad, 174 pp., [translated from Russian].
- Milbrandt, J. and Yau, M. K., 2001: A mesoscale modeling study of the 1996 Saguenay flood, *Mon. Weather Rev.*, in press.
- Misra, V., Yau, M. K., and Badrinath, N., 2000: Atmospheric water species budget in mesoscale simulations of lee cyclones over the Mackenzie River Basin, *Tellus*, **52A**, 140-161.
- Mobbs, S. D. and Dover, S. E., 1993: Numerical modelling of blowing snow, in *Antarctic Special Topic*, British Antarctic Survey, Cambridge, pp. 55-63.
- Noilhan, J. and Planton, S., 1989: A simple parameterization of land surface processes for meteorological models, *Mon. Weather Rev.*, **117**, 536-549.
- Ohtake, T., Jayaweera, K., and Sakurai, K.-I., 1982: Observation of ice crystal formation in lower Arctic atmosphere, *J. Atmos. Sci.*, **39**, 2898-2904.
- Oke, T. R., 1987: *Boundary Layer Climates*, 2nd ed., Methuen, 435 pp.
- Oke, T. R., 1997: Surface climate processes, in Bailey, W. G., Oke, T. R., and Rouse, W. R. (Eds.), *Surface Climates of Canada*, McGill Queen's Press, 21-43.
- Phillips, D., 1990: *Climates of Canada*, Environment Canada, 176 pp.
- Pomeroy, J. W., 1988: *Wind Transport of Snow*, Ph.D. Thesis, Division of Hydrology, University of Saskatchewan, Saskatoon, 226 pp.
- Pomeroy, J. W. and Essery, R. L. H., 1999: Turbulent fluxes during blowing snow: Field tests of model sublimation predictions, *Hydrol. Proc.*, **13**, 2963-2975.
- Pomeroy, J. W. and Goodison, B. E., 1997: Winter and snow, in Bailey, W. G., Oke, T. R., and Rouse, W. R. (Eds.), *Surface Climates of Canada*, McGill Queen's Press, 68-100.
- Pomeroy, J. W. and Gray, D. M., 1990: Saltation of snow, *Water Resources Res.*, **26**,

1583-1594.

- Pomeroy, J. W. and Gray, D. M., 1995: *Snowcover Accumulation, Relocation and Measurement*, NHRI Sci. Rep. 7, Environment Canada, Saskatoon, 144 pp.
- Pomeroy, J. W., Gray, D. M., and Landine, P. G., 1993: The Prairie Blowing Snow Model: Characteristics, validation, operation, *J. Hydrol.*, **144**, 165-192.
- Pomeroy, J. W. and Male, D. H., 1992: Steady-state suspension of snow, *J. Hydrol.*, **136**, 275-301.
- Pomeroy, J. W., Marsh, P., and Gray, D. M., 1997: Application of a distributed blowing snow model to the Arctic, *Hydrol. Proc.*, **11**, 1451-1464.
- Pruppacher, H. R. and Klett, J. D., 1997: *Microphysics of Clouds and Precipitation*, 2nd ed., Kluwer Academic Publishers, Dordrecht, 954 pp.
- Reisner, J., Rasmussen, R. M., and Bruintjes, R. T., 1998: Explicit forecasting of super-cooled liquid water in winter storms using the MM5 mesoscale model, *Q. J. R. Meteorol. Soc.*, **124**, 1071-1107.
- Rogers, R. R. and Yau, M. K., 1989: *A Short Course in Cloud Physics*, 3rd ed., Pergamon Press, 293 pp.
- Rothrock, D. A., Yu, Y., and Maykut, G. A., 1999: Thinning of the Arctic sea-ice cover, *Geophys. Res. Lett.*, **23**, 3469-3472.
- Rouault, R. R., Mestayer, P. G., and Schiestel, R., 1991: A model of evaporating spray droplet dispersion, *J. Geophys. Res.*, **96**(C4), 7181-7200.
- Rouse, W. R., 2000: Progress in hydrological research in the Mackenzie GEWEX Study, *Hydrol. Proc.*, **14**, 1667-1685.
- Salmon, E. M. and Smith, P. J., 1980: A synoptic analysis of the 25-26 January 1978 blizzard cyclone in the Central United States, *Bull. Am. Meteorol. Soc.*, **61**, 453-460.
- Schmidt, R. A., 1972: *Sublimation of Wind-Transported Snow - A Model*, USDA Res. Paper RM-90, USDA Forestry Service, Rocky Mountain Forest and Range Experimental Station, Fort Collins, Colorado, 24 pp.
- Schmidt, R. A., 1980: Threshold wind-speeds and elastic impact in snow transport, *J.*

-
- Glaciol.*, **26**, 453-467.
- Schmidt, R. A., 1982: Vertical profiles of wind speed, snow concentrations, and humidity in blowing snow, *Bound.-Layer Meteorol.*, **23**, 223-246.
- Schmidt, R. A., 1991: Sublimation of snow intercepted by an artificial conifer, *Agri. and Forest Meteorol.*, **54**, 1-27.
- Schwerdtfeger, W., 1970: The climate of the Antarctic, in Orvig, S. (Ed.), *Climate of the Polar Regions*, World Survey of Climatology, vol. 7, Elsevier, pp. 253-355.
- Schwerdtfeger, W., 1984: *Climate of the Antarctic*, Developments in Atmospheric Science 15, Elsevier, 261 pp.
- Serreze M., 1995: Climatological aspects of cyclone development and decay in the Arctic, *Atmos.-Ocean*, **33**, 1-23.
- Serreze, M. C., Walsh, J. E., Chapin III, F. S., Osterkamp, T., Dyurgerov, M., Romanovsky, V., Oechel, W. C., Morison, J., Zhang, T., and Barry, R. G., 2000: Observational evidence of recent change in the northern high-latitude environment, *Clim. Change*, **46**, 159-207.
- Siple, P. A. and Passel, C. F., 1945: Measurements of dry atmospheric cooling in sub-freezing temperatures, *Proc. Amer. Phil. Soc.*, **89**, 177-199.
- Slingo, A., Pamment, J. A., and Webb, M. J., 1998: A 15-year simulation of the clear-sky greenhouse effect using the ECMWF reanalyses: fluxes and comparisons with ERBE, *J. Climate*, **11**, 690-708.
- Smirnov, V. V. and Moore, G. W. K., 1999: Spatial and temporal structure of atmospheric water vapor transport in the Mackenzie River Basin, *J. Climate*, **12**(3), 681-696.
- Sommerfeld, R. and Businger, J. A., 1965: The density profile of blown snow, *J. Geophys. Res.*, **70**, 3303-3306.
- Steadman, R. G., 1971: Indices of windchill of clothed persons, *J. Appl. Meteorol.*, **10**, 674-683.
- Stewart, R. E., 1991: Canadian Atlantic Storms Program: Progress and plans of the meteorological component, *Bull. Amer. Meteorol. Soc.*, **72**, 364-371.

-
- Stewart, R. E., Yiu, D. T., Chung, K. K., Hudak, D. R., Lozowski, E. P., Oleski, M., Sheppard, B. E., and Szeto, K. K., 1995a: Weather conditions associated with the passage of precipitation type transition regions over Eastern Newfoundland, *Atmos.-Ocean*, **33**, 25-53.
- Stewart, R. E., Bachan, D., Dunkley, R. R., Giles, A. C., Lawson, B., Legal, L., Miller, S. T., Murphy, B. P., Parker, M. N., Paruk, B. J., and Yau, M. K., 1995b: Winter storms over Canada, *Atmos.-Ocean*, **33**, 223-247.
- Stewart, R. E., Leighton, H. G., Marsh, P., Moore, G. W. K., Rouse, W. R., Soulis, S. D., Strong, G. S., Crawford, R. W., and Kochtubajda, B., 1998: The Mackenzie GEWEX Study: The water and energy cycles of a major North American river basin, *Bull. Am. Meteorol. Soc.*, **79**, 2665-2683.
- Stewart, R. E., Burford, J. E., and Crawford, R. W., 2000: On the meteorological characteristics of the water cycle of the Mackenzie River Basin, *Contr. Atmos. Phys.*, **9**, 103-110.
- Stull, R. B., 1988: *An Introduction to Boundary Layer Meteorology*, Kluwer Academic Press, Dordrecht, 666 pp.
- Szeto, K. K. and Stewart, R. E., 1997: Cloud model simulations of surface weather elements associated with warm frontal regions of winter storms, *Atmos. Res.*, **44**, 243-269.
- Szeto, K. K., Stewart, R. E., and Hanesiak, J. M., 1997: High latitude cold season frontal cloud systems and their precipitation efficiency, *Tellus*, **49**, 439-454.
- Szeto, K. K., Tremblay, A., Guan, H., Hudak, D. R., Stewart, R. E., and Cao, Z., 1999: The mesoscale dynamics of freezing rain storms over Eastern Canada, *J. Atmos. Sci.*, **56**(10), 1261-1281.
- Tabler, R. D. and Schmidt, R. A., 1972: Weather conditions that determine snow transport distances at a site in Wyoming, *UNESCO/WMO Symposia on the Role of Snow and Ice in Hydrology*, 118-127.
- Tabler, R. D., 1975: Estimating the transport and evaporation of blowing snow, *Proc. Symposium on Snow Management on the Great Plains*, Great Plains Agricultural Coun-

-
- cil Publ. 73, 85-104.
- Tabler, R. D., 1979: Visibility in blowing snow and applications in traffic operations, *Snow Removal and Ice Control Research*, Special Rep. 185, Proc. Second International Symp., Hanover, N.H., 15-19 May 1978, National Academy of Science, Washington, D. C., 208-214.
- Thorpe, A. D. and Mason, B. J., 1966: The evaporation of ice spheres and ice crystals, *Brit. J. Appl. Phys.* **17**, 541-548.
- Turner, J., Connolley, W. M., Leonard, S., Marshall, G. J., and Vaughan, G., 1999: Spatial and temporal variability of net snow accumulation over the Antarctic from ECMWF Re-Analysis project data, *Int. J. Climatol.*, **19**, 697-724.
- van den Broeke, M. R., 1997: Spatial and temporal variation of sublimation on Antarctica: Results of a high-resolution general circulation model, *J. Geophys. Res.*, **102**(D25), 29,765-29,777.
- Verge, R. W. and Williams, G. P., 1981: Drift control, in Gray, D. M. and Male, D. H. (Eds.), *Handbook of Snow - Principles, Processes, Management & Use*, Pergamon Press, pp. 630-647.
- Vowinckel, E. and Orvig, S. 1970: The climate of the North Polar Basin, in Orvig, S. (Ed.), *Climate of the Polar Regions*, World Survey of Climatology, vol. 7, Elsevier, pp. 129-252.
- Walsh, J. E., Zhou, X., Portis, D., and Serreze, M. C., 1994: Atmospheric contribution to hydrologic variations in the Arctic, *Atmos.-Ocean*, **32**, 733-755.
- Walsh, J. E., Kattsov, V., Portis, D., and Meleshko, V., 1998: Arctic precipitation and evaporation: Model results and observational estimates, *J. Climate*, **11**, 72-87.
- Wild, R., 1995: Definition of the British blizzard, *Weather*, **50**, 327-328.
- Wild, R., O'Hare, G., and Wilby, R., 1996: A historical record of blizzards/major snow events in the British Isles, 1880-1989, *Weather*, **51**, 82-91.
- Wilks, D. S., 1995: *Statistical Methods in the Atmospheric Sciences*, Academic Press, 467 pp.

- Wintels, W. and Gyakum, J. R., 2000: Synoptic climatology of Northern Hemisphere available potential energy collapses, *Tellus*, **52A**, 347-364.
- Woo, M.-K. and Ohmura, A., 1997: The Arctic Islands, in Bailey, W. G., Oke, T. R., and Rouse, W. R. (Eds.), *Surface Climates of Canada*, McGill Queen's Press, pp. 172-197.
- Woo, M.-K., Heron, R., Marsh, P., and Steer, P., 1983: Comparison of weather station snowfall with winter snow accumulation in high Arctic basins, *Atmos.-Ocean*, **21**, 312-325.
- Xiao, J., Bintanja, R., Déry, S. J., Mann, G. W., Taylor, P. A., 2000: An intercomparison among four models of blowing snow, *Bound.-Layer Meteorol.*, **97**(1), 109-135.
- Zishka, K. M. and Smith, P. J., 1980: The climatology of cyclones and anticyclones over North America and surrounding ocean environs for January and July 1955-77, *Mon. Weather Rev.*, **108**, 387-401.